Distributed Road Grade Estimation for Heavy Duty Vehicles

PER SAHLHOLM

KTH Electrical Engineering

Doctoral Thesis in Automatic Control
Stockholm, Sweden 2011

KTH Electrical Engineering

Distributed Road Grade Estimation for Heavy Duty Vehicles

PER SAHLHOLM

Doctoral Thesis
Stockholm, Sweden 2011

KTH School of Electrical Engineering
Automatic Control Lab
SE-100 44 Stockholm
SWEDEN

TRITA-EE 2011:008
ISSN 1653-5146
ISBN 978-91-7415-869-4

Akademisk avhandling som med tillstånd av Kungliga Tekniska högskolan framlägges till offentlig granskning för avläggande av teknologie doktorsexamen i reglerteknik fredagen den 29 april 2011 klockan 10.15 i sal Q2 Kungliga Tekniska högskolan, Osquldas väg 10, Stockholm.

Tryck: Universitetsservice US AB

Abstract

An increasing need for goods and passenger transportation drives continued worldwide growth in traffic. As traffic increases environmental concerns, traffic safety, and cost efficiency become ever more important. Advancements in microelectronics open the possibility to address these issues through new advanced driver assistance systems. Applications such as predictive cruise control, automated gearbox control, predictive front lighting control, and hybrid vehicle state-of-charge control decrease the energy consumption of vehicles and increase the safety. These control systems can benefit significantly from preview road grade information. This information is currently obtained using specialized survey vehicles, and is not widely available. This thesis proposes new methods to obtain road grade information using on-board sensors. The task of creating road grade maps is addressed by the proposal of a framework where vehicles using a road network collect the necessary data for estimating the road grade. The estimation can then be carried out locally in the vehicle, or in the presence of a communication link to the infrastructure, centrally. In either case the accuracy of the map increases over time, and costly road surveys can be avoided.

This thesis presents a new distributed method for creating accurate road grade maps for vehicle control applications. Standard heavy duty vehicles in normal operation are used to collect measurements. Estimates from multiple passes along a road segment are merged to form a road grade map, which improves each time a vehicle retraces a route. The design and implementation of the road grade estimator are described, and the performance is experimentally evaluated using real vehicles.

Three different grade estimation methods, based on different assumption on the road grade signal, are proposed and compared. They all use data from sensors that are standard equipment in heavy duty vehicles. Measurements of the vehicle speed and the engine torque are combined with observations of the road altitude from a GPS receiver, using vehicle and road models. The operation of the estimators is adjusted during gearshifts, braking, and poor satellite coverage, to account for variations in sensor and model reliability. The estimated error covariances of the road grade estimates are used together with their absolute positions to update a stored road grade map.

Highway driving trials show that the proposed estimators produce accurate road grade data. The estimation performance improves as the number of road segment traces increases. A vehicle equipped with the proposed system will rapidly develop a road grade map for its area of operation. Simulations show that collaborative generation of the third dimension for a pre-existing large area two-dimensional map is feasible. The experimental results indicate that road grade estimates from the proposed methods are accurate enough to be used in predictive vehicle control systems to enhance safety, efficiency, and driver comfort in heavy duty vehicles. The grade estimators may also be used for on-line validation of road grade information from other sources. This is important in on-board applications, since the envisioned control applications can degrade vehicle performance if inaccurate data are used.

To my family

Acknowledgements

First, I would like to thank my advisor Karl Henrik Johansson for his competent guidance and contagious enthusiasm and energy. Thanks also go to my co-advisors Henrik Jansson and Ather Gattami for their respective contributions in the beginning and end of the project. At Scania, I have had three managers since the start of this work. I thank Michael Blackenfelt for hiring me as an engineer and then letting me switch jobs within the group shortly thereafter to begin this project. I thank Nils-Gunnar Vågstedt for his optimism when taking over the lead. Many thanks also go to my current manager Tony Sandberg for helping me focus on the research and the creation of this dissertation.

Thanks to Maria Ivarsson for the cooperation we have had in this project, proofreading parts of the manuscript, and all the invaluable help you and Erik Hellström gave when collecting experimental data. I thank Assad Alam, Phoebus Chen, Nils-Gunnar Vågstedt, and Jim Weimer for proofreading and commenting on various parts of the manuscript. Assad Alam has also been an important ally both as a Master's student and a fellow PhD candidate at Scania and the Control department. I have enjoyed our discussions immensely.

Thanks also go to all of you who have participated in the steering committee, and attended the reference group meetings, thereby supporting the project. Thanks to all the Master's thesis students I have supervised for your fresh ideas and all the fruitful discussions. All my colleagues at both Scania and KTH deserve great thanks for providing such an inspiring and positive work environment, you are far too many to name individually.

The research presented in this thesis has been financed by the Intelligent Vehicle Safety Systems (IVSS) programme, the Strategic Vehicle Research and Innovation partnership (FFI), and by Scania CV AB. The financial support is appreciated, hopefully it will lead to better products for the customers and increased tax income for the government.

Writing this thesis has been an absorbing activity. Thanks to all of you who have helped by caring for Vilgot while I've been working; Brita, Ben, Joel, Sten, and Carin. Finally, extra special thanks to my wife Anna, my son Vilgot, my parents Brita and Ewert, and my brother Erik, for always being there.

Per Sahlholm
Stockholm, March 2011.

Contents

Chapter 1

Introduction

"*Wir müssen wissen*
wir werden wissen."

David Hilbert, in an address to the Society of German Scientists and Physicians, Königsberg, 1930.

Road vehicles have seen a rapid growth in on-board processing power and digital storage capacity during the last few decades. Recently, wireless communication capabilities have been added, enabling both real-time updates to the information digitally stored in the vehicle and a return path from the vehicle to the outside world. The combination of this information path from the vehicle and the rich variety of sensors available in modern vehicles enable an entirely new set of applications, where vehicles share information with each other and the infrastructure. Vehicles in normal operation can now provide sensor data for many transport related applications. Vehicle-to-vehicle and vehicle-to-infrastructure communication and applications are currently very active research areas.

Satellite based navigation with digital maps has become popular among motorists. The maps that power these systems constantly evolve. What has traditionally been a replacement for a road atlas is quickly turning into a digital description of every feature of interest, static or dynamic, in the vicinity of the vehicle. This development is made possible by replacing quarterly physical media updates to the navigation system by live communication links to other vehicles and the infrastructure. In many of the electronic safety and comfort systems developed today, data from local sensors are merged with a variety of other information sources into an overall digital description of the surroundings.

This thesis proposes a method for road grade estimation that uses vehicle sensor data to generate digital maps. The performance of three versions of the method is investigated, when they are applied to real measurements. The method is evaluated experimentally using the three types of Heavy Duty Vehicles (HDVs) shown in Figure 1.1. The convergence of the road grade estimate when many measurements are available is studied through simulations.

Figure 1.1: The proposed road grade estimation method has been tested on highway E4 between Södertälje and Nyköping, using three types of HDVs. (Photographs courtesy of Scania CV AB)

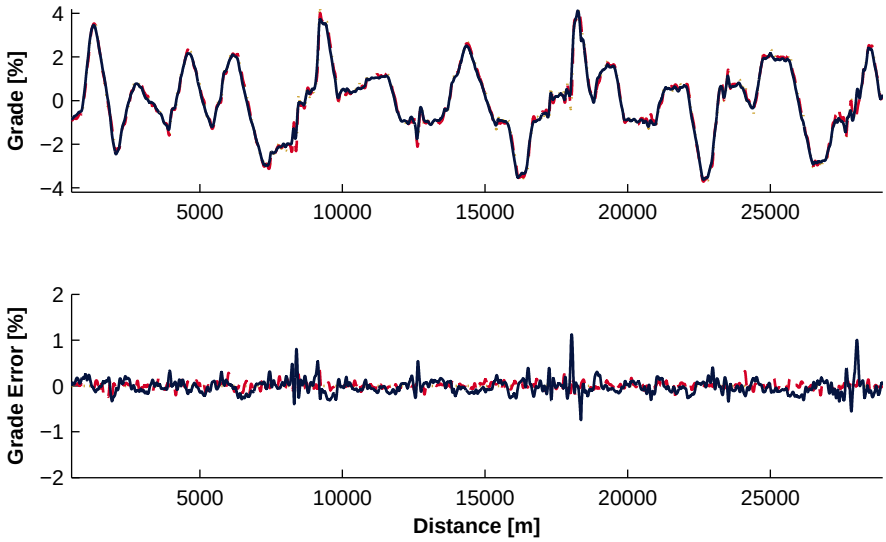

Figure 1.2: The top graph shows the estimated road grade profile for the Southbound direction on highway E4 south of Södertälje, based on the conducted experiments. The bottom graph illustrates the deviation from the reference profile for each data set. The results from the constant estimator (solid blue), are shown together with the measured reference road grade (dotted gold), and sample data from a commercial provider of road grade map data (dashed red).

The final grade estimate created by the method, based on six experiments on a 15 km test segment of the southbound highway E4 south of Södertälje, is shown together with reference road grade data in Figure 1.2. Using the proposed method, the road grade in the experiments can be estimated with a bias of −0.04 % grade, with an approximately normal error distribution with a mean standard deviation around the bias of 0.13 % grade. The convergence of the road grade estimate to the reference road grade is illustrated in Figure 1.3, for two example road sections.

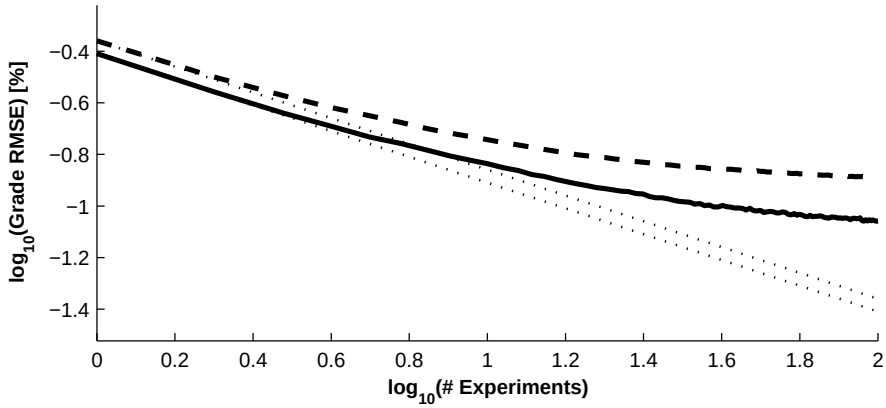

Figure 1.3: The road grade errors quickly decrease when several estimates are combined. Initially the rate is close to the $1/\sqrt{N}$ to be expected for white noise errors. As more experiments are added, the decay rate decreases. The figure shows the decrease in the log of the estimation error versus the log of the number of experiments used, based on simulations for the southbound segment of the test site (solid), and a part of highway E44 between Koblenz and Trier (dashed). Lines starting at the error after one experiment, and decreasing at a rate of $1/\sqrt{N}$, are shown for each data set (dotted).

The first section of this chapter introduces the ideas of using standard vehicles for road grade mapping. This is followed by a motivation for the thesis through a description of look-ahead vehicle control. The next section gives the problem statement for the thesis. This is followed by descriptions of the main thesis contributions. The introduction is concluded by a description of the publications forming the basis for the thesis and an outline of the rest of the thesis.

1.1 Distributed Road Grade Estimation

Current in-vehicle navigation systems primarily provide information such as turn-by-turn directions and hazard warnings to the driver. In the future, this will likely shift so that the navigation system also provides information to automated vehicle functions, such as an automated speed control, electronic stability system, or anti-rollover system. Digital maps are increasingly being seen as a source of information that can complement the vehicle sensors, and the information about the vehicle surroundings obtained from the map is commonly referred to as the ADAS (Advanced Driver Assistance Systems) horizon. An example of such a horizon is shown in Figure 1.4. A standardized protocol for transmitting ADAS horizon information from a map database control unit to other systems in vehicles has recently been developed. Early products using such systems are now entering the market.

The road geometry information in digital maps has traditionally been obtained

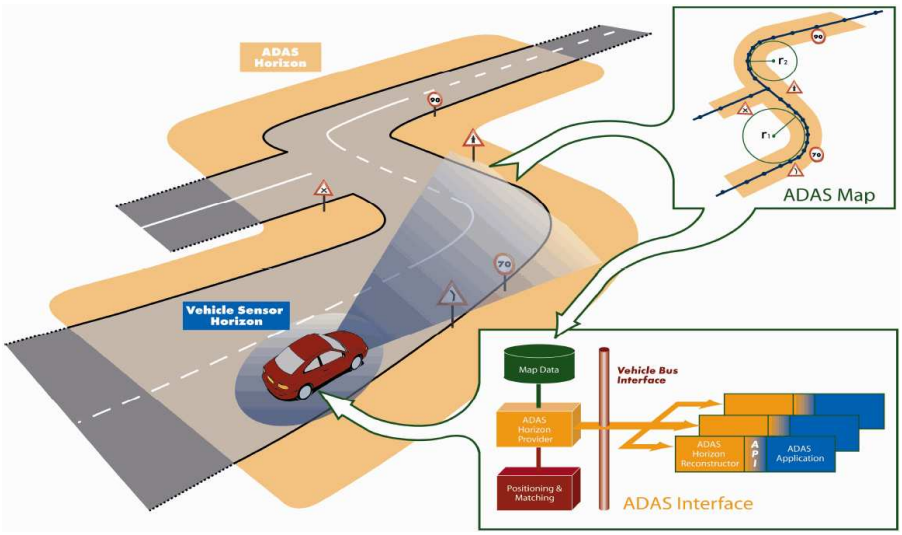

Figure 1.4: Illustration of an ADAS horizon with a number of physical and legal attributes. (Illustration courtesy of the PReVENT project)

by specialized survey vehicles, operated by mapping companies. The update frequency of the map data has been limited by the number of survey vehicles operating in a region. The availability of affordable Global Positioning System (GPS) receivers with logging capabilities has spurred interest in amateur mapping. This interest has been captured by the major mapping companies through features that allow users to send corrections back to the companies. The generation of map data has expanded from a centralized process controlled by the mapping companies to a distributed effort by the users together with the mapping company.

The new possibilities to record accurate position information have also led to the emergence of an alternative map. There is now a free and open map database available online, the OpenStreetMap (OSM). It has been created by volunteers as a community effort. Reporting an error in a commercial navigation device using the provided tool is usually very easy. Mapping your neighborhood for OSM requires significantly more skills, but there are thousands who have both the desire to do so and the technical know-how.

Until recently, only rather inexact two-dimensional road geometry information was recorded by the mapping companies. Growing automotive industry interest in map based control applications has led to the emergence of new products providing accurate information on the geometry, including the third dimension. However, the user-generated road maps currently available are still almost exclusively restricted to two dimensions. The system described in this thesis could be used to obtain highly accurate information about highway road grades, by using the principles

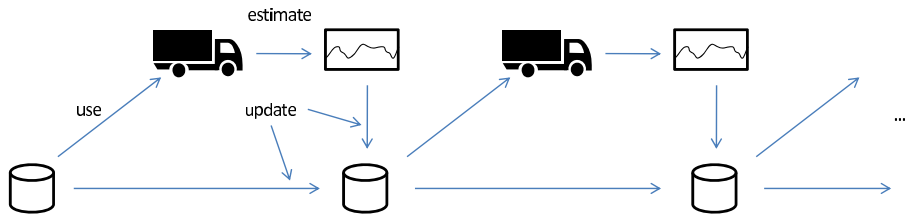

Figure 1.5: Sensor data from each drive along a road segment is used to estimate a road grade profile. This profile is then processed together with the existing road grade map database to give an updated database. The new database is used for control applications the next time the vehicle returns to the same road segment. If a communication link is available the database may be centralized. All vehicles connected to the system may then benefit from the estimates generated by all other vehicles.

of user generated content and crowdsourcing[1]. The principle of operation for the proposed system is illustrated in Figure 1.5. Road grade data are both collected and used by vehicles in normal operation.

Autonomous road map creation, without any prior knowledge, is very hard. Adding information to an existing map is much easier. By combining the currently available user generated two-dimensional map with this new method, a three-dimensional road map, which can potentially be used in on-board control systems, can be created. The methods described in this thesis have been designed to operate with sensors that are already standard equipment in HDVs. If the methods were to be implemented in series production, tens of thousands of road grade probes would be estimating the road grade of hundreds of millions of miles of roadway annually, within a few years.

1.2 Motivation

Resource scarcity generates demand for increased efficiency in all aspects of society. The longitudinal dynamics of an HDV traveling on a highway is considerably affected by the road grade. In uphill sections a fully loaded vehicle is likely to lose speed, and in downhill sections braking must be done properly to maintain safety. Compared to a regular cruise controller, predictive cruise control, where the vehicle speed is adapted ahead of upcoming changes in the road grade, has the potential to significantly reduce the energy consumption. If there is information about an upcoming obstacle or speed restriction on the road, coasting from the proper distance can save energy as well. These and many other future vehicle control systems that

[1] Wikipedia defines crowdsourcing as the act of outsourcing tasks, traditionally performed by an employee or contractor, to an undefined, large group of people or community (a “crowd”), through an open call.

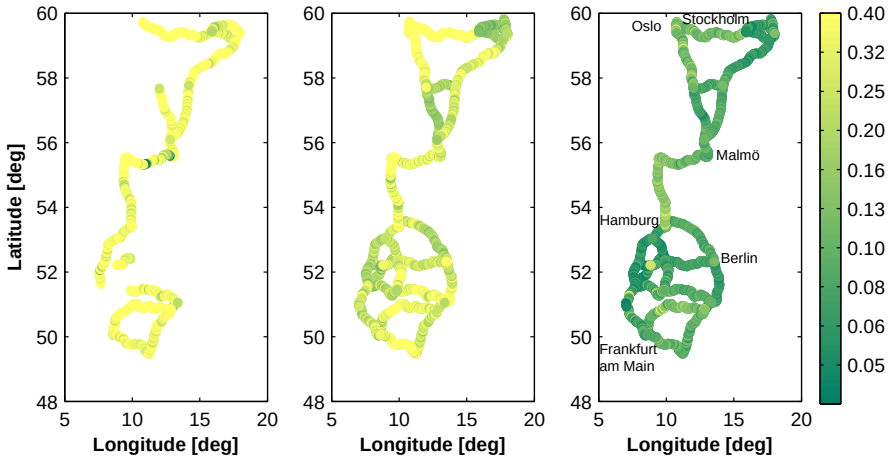

Figure 1.6: A large fleet of vehicles will quickly produce an accurate estimate of the major highways in an area. The figures show the predicted RMS grade estimation error for major European roads in southern Sweden, Denmark, and northern Germany after data from (starting from the left) $N = 10, 100, 1\,000$ trips, of 50–500 km each, have been recorded and used in the proposed estimation scheme. Darker segments have lower estimation errors

have a potential to increase the energy efficiency, comfort, and safety, rely on high quality information about the road grade ahead of the vehicle.

The road grade maps that are available have limited geographical coverage, and require a license fee to be paid to the supplier. Currently available sensors in HDVs can be used to estimate the road grade, e.g., through models for the driving resistance and Newton's second law. Thus, alternative road grade maps may potentially be created using standard vehicles. It is however hard to achieve the accuracy required by emerging control applications with a single measurement, collected with the sensors present in production vehicles. By recording estimates in a map as the truck drives along, it is possible to predict the road grade the next time the same road is driven. In general, HDVs frequently drive along a limited set of roads. By merging estimates from many trips in the map, the desired accuracy can be achieved.

The problem of obtaining road grade information for HDV applications can be solved using vehicles in normal operation. Signal noise from the standard mounted sensors in the vehicle make determining the road grade after only one trip along a road section hard. Using a combination of an iterative road grade estimation algorithm with a map that can be used to store estimates, accurate information about future road grades can be created based on many trips. The truck will have a better map each time it returns to a particular road. Figure 1.6 shows the road grade accuracy for a map generated with the proposed method, based on a simulation

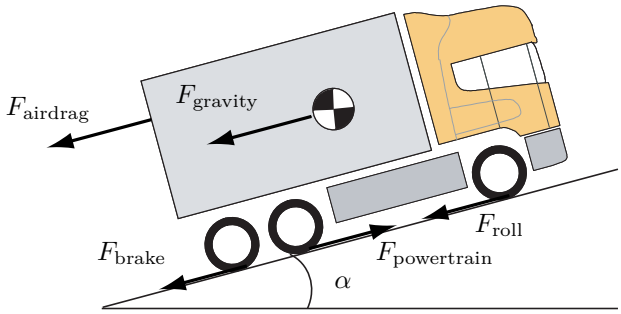

Figure 1.7: An HDV traveling on a road is affected by forces from its powertrain, rolling resistance, air resistance, gravity, and possibly its brake system. The influence of gravity depends on the road grade α.

study. By combining local map-building with communications technologies and a global community, large amounts of estimates become available in a short time. Most vehicles will then also have access to a good map already on the first trip along a road.

1.3 Problem formulation

The problem studied in this thesis is how to estimate the road grade of roads that are frequently traveled by HDVs, based on sensors that are part of the standard vehicle equipment. Due to sensor signal noise and model mismatch during some driving events, the required accuracy of the estimates cannot be achieved using only one measurement. It is thus necessary to use data from multiple passes over each road segment.

An HDV climbing a hill with a road grade α, and the most important forces affecting the vehicle, are shown in Figure 1.7. The vehicle is described by a dynamic model f_v for its longitudinal movement, which links the road grade to the engine torque and the absolute altitude. The road is modeled with one state for the altitude, whose dynamics is described by f_z, and one for the road grade. Two different road grade models f_α, are investigated. One is based on the fact that the road grade changes slowly compared to the other signals, the other one is based on highway design principles. The total system model is

$$\begin{aligned} \frac{dv}{ds} &= f_v(v, \alpha, T_{\text{e}}) \\ \frac{dz}{ds} &= f_z(\alpha) \\ \frac{d\alpha}{ds} &= f_\alpha(s) \end{aligned} \tag{1.1}$$

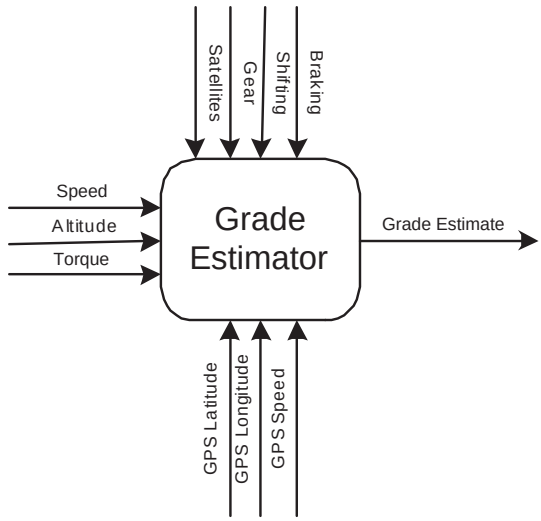

Figure 1.8: The proposed grade estimation methods use sensor information from a standard HDV. The estimators depend on two directly measured states; the vehicle speed and road altitude. The engine torque is treated as a measured input signal in the vehicle model. The estimators also rely on auxiliary information about when braking and gearshifts occur, the currently engaged gear, and the number of tracked GPS satellites. The current two-dimensional position of the vehicle is used to locate the vehicle in the map.

where s is the distance along the road, v is the vehicle speed, α is the road grade, T_{e} is the engine torque, and z is the absolute altitude of the vehicle.

The vehicle speed and engine torque are available from the vehicle control network. The altitude can be determined from a GPS receiver. The GPS receiver also reports the number of tracked satellites. This signal is used to assess the accuracy of the altitude signal. The vehicle dynamics model f_v depends on which gear is engaged, if any. This information is obtained by sensing the current gear and if a gearshift is in progress. When the vehicle is braking the dynamics will be radically different than otherwise. Since the brake force F_{brake} is not available for measurement, the road grade estimation is done with only a status signal indicating if braking is taking place. Since the task is to estimate roads that are traveled frequently, a position log from the GPS is included to enable many estimates of the road grade to be merged. Finally the GPS receiver vehicle speed signal used to calibrate the in-vehicle speed sensor. The system model and sensor information are used together to create the road grade estimator shown in Figure 1.8.

The problem that is solved in this thesis is how to use sensor signals already available in many HDVs to iteratively create road grade maps based on all the sensor information available from many runs along the same roads.

1.4 Main Thesis Contributions

The problem of how to obtain accurate road grade information for HDV control is analyzed and solved through proposed estimators based on standard mounted sensors. Three different estimators are proposed and evaluated.

The first estimator uses a constant road grade model together with a time-varying longitudinal vehicle model to link acceleration, engine torque, and absolute altitude readings to a common road grade estimate. This estimator is referred to as the *constant estimator* throughout the thesis. Logic is developed to adjust the estimator to vehicle operating conditions such as the number of available GPS satellites, and whether gear changing or braking is in progress. A Kalman Filter (KF) is used to process the sensor data based on information about the operating conditions. The estimator is designed to be operated off-line, which enables Rauch-Tung-Striebel (RTS) smoothing to be used to increase the measurement information used and avoid filter lag. The smoothed estimate is used to update a stored map based on the relative reliability of the latest estimate and the already stored data.

The constant road grade model assumption, while being simple to work with, conflicts with the properties of real road grade profiles. In the second estimator, dubbed the *piecewise estimator*, the road grade signal is instead restricted to be a piecewise linear function. The least-squares optimal, piecewise linear road grade approximation is identified from sensor data. For comparison, the reference road grade profile is approximated with a piecewise linear function as well. The analysis shows that while the piecewise linear assumption is certainly more accurate than the constant road grade model, restricting the grade profile to a piecewise linear representation gives larger errors than in the first estimator. The residual error in the piecewise linear approximation of the reference road grade signal is also significant, compared to the total estimation error of the previous method.

In the third estimator, the *spline estimator*, the piecewise linear model is used to extend the first estimator. A linear spline road grade model is identified and used, but the output is not restricted to be piecewise linear. This method yields better grade estimates than the second one, and for large sampling distances it works better than the first estimator.

The three estimators are also compared to the performance obtained by filtering road grade estimates computed directly through the vehicle model or the derivative of the GPS altitude signal. This is referred to as the *nominal estimator*.

Finally, a framework for using the estimated road grade profiles to build a road grade map is developed and tested in simulations. The convergence of the estimates of the constant estimator, when a large number of estimates are available, is analyzed. Two scenarios are studied. In the first, a single vehicle is performing all the estimation on-board. In the second scenario, communication equipment is available and all vehicles in an area are exchanging information with each other. The proposed estimation scheme is predicted to be useable for collecting road grade information that is accurate enough for HDV control applications, both in the non-communicating and communication-enabled scenarios.

1.5 Publications

The work described in this thesis has previously appeared in scientific publications, as outlined below. In parallel with the development of the grade estimators, applications of the data have also been studied. This has been done primarily through supervision of Master's thesis projects. The work has also resulted in a number of patent applications, mainly related to the applications of the road grade data. These are detailed in Section 1.5.1.

The development and evaluation of the constant estimator has been described in four papers. These form the foundation for the modeling of the vehicle and sensors in Chapter 3 and the description of the estimation method in Chapter 4. The experimental setup given in Chapter 5, and the majority of the experimental results for the constant estimator described in Chapter 5, are also included in these papers.

The first paper, presented at the Fifth IFAC Symposium on Advances in Automotive Control in August of 2007, outlines the basic ideas of the methods and initial grade estimation results. Additional experimental results are given in the second paper. The follow up paper, at the 17th IFAC World Congress in July 2008, gives a deeper analysis of the grade estimator. In that paper the possibility of using a linear, instead of a non-linear, vehicle model is also investigated. The results were summarized, and illustrated through additional examples, in the journal publication.

P. Sahlholm, H. Jansson, E. Kozica, and K. H. Johansson. A sensor and data fusion algorithm for road grade estimation. In *Fifth IFAC Symposium on Advances in Automotive Control*. Monterey Coast, CA, USA (2007*b*)

P. Sahlholm, H. Jansson, and K. H. Johansson. Road grade estimation results using sensor and data fusion. In *14th World Congress on Intelligent Transport Systems*. Beijing, China (2007*a*)

P. Sahlholm, H. Jansson, and K. H. Johansson. Road grade estimation for look-ahead vehicle control. In *17th IFAC World Congress*. Seoul, Korea (2008)

P. Sahlholm and K. H. Johansson. Road grade estimation for look-ahead vehicle control using multiple measurement runs. *Control Engineering Practice*, 18(11): 1328 – 1341 (2010*a*). Special Issue on Automotive Control Applications, 2008 IFAC World Congress

From the literature on road design, it is clear that highways should be built with a piecewise linear road grade profile, as is further described in Chapter 3. The contribution to the 2011 SAE World Congress details the effort to identify a piecewise linear road grade profile based on this design principle. The proposed method is described in Chapter 4. While the method does produce optimal piecewise linear estimates, it is computationally intensive and, contrary to the other two developed methods, does not allow for efficient distributed updates. Experimental

results from this work are given in Chapter 5.

P. Sahlholm, A. Gattami, and K. H. Johansson. Piecewise linear road grade estimation. In *SAE 2011 World Congress, accepted for publication.* Detroit, MI, USA (2011)

By requiring that the end of each linear piece of the road grade profile meet with the beginning of the next piece, a linear spline approximation of the profile is obtained. This road grade model was used in the paper presented at CDC 2010, to extend the constant estimator. A three step estimation method is proposed. First, the measured data are used to obtain an initial road grade estimate. Second, linear segments are identified in the road grade signal. Third, the linear segments are used with the measured data to produce a final road grade estimate. The method is described in Chapter 4. The proposed method is implemented and evaluated experimentally, and the results are given in Chapter 5.

In addition to material from the fully peer reviewed publications listed above, the thesis contains results that have not yet been published, and results from the non-fully peer reviewed publications summarized below. These are either Master's thesis reports where the author has supervised the work, or papers presented at conferences that only peer review an extended abstract.

P. Sahlholm and K. H. Johansson. Segmented road grade estimation for fuel efficient heavy duty vehicles. In *49th Conference on Decision and Control.* Atlanta, GA, USA (2010*b*)

A leading motivation for estimating the road grade is the possibility of using a known future grade profile to plan an efficient vehicle speed trajectory. The first Master's thesis presents both a patent survey of control applications using positioning systems, and a test implementation of an optimizing vehicle speed controller based on the future road grade. The implementation part of the work was carried out under the supervision of the author of this thesis. The potential HDV applications of road grade information, and the negative effect of errors in that information, are explored in the first contribution to the 2008 ITS World Congress. A proposed system for adjusting the speed of an HDV based on road grade information, and knowledge of upcoming mandated speed changes, is described in the second paper at the same conference, and the last Master's thesis report.

N. Gustafsson. *The Use of Positioning Systems for Look-Ahead Control in Vehicles.* Master's thesis, Linköpings tekniska högskola (2006)

P. Sahlholm. Improved heavy duty vehicle performance through the use of 3d map data. In *15th World Congress on Intelligent Transport Systems.* New York, NY, USA (2008)

A. Alam and P. Sahlholm. A method for determining an economical speed for heavy vehicles. In *15th World Congress on ITS.* New York, NY, USA (2008)

A. Alam. *Optimally Fuel Efficient Speed Adaptation.* Master's thesis, Royal

Institute of Technology (KTH) (2008)

Further work aimed at analyzing the vehicle sensor data and estimator performance is described in the above publications. The first two are focused on analyzing the difference between GPS based road grade determination based on vertical speed and absolute altitude information. The last report analyzes the influence of modeling and parameter errors in the vehicle model on estimation errors. The work in that project has also contributed to the formulation of the simulation model used in Chapter 6.

K. Wänglund and P. Sahlholm. Comparison of road grade estimation results based on GPS position and velocity data. In *16th World Congress on ITS*. Stockholm, Sweden (2009)

K. Wänglund. *Evaluation of GPS Velocity and Altitude Data used for Road Grade Estimation*. Master's thesis, Royal Institute of Technology (KTH) (2009)

P. Ståhl. *Performance analysis of a road grade estimation method by means of simulation*. Master's thesis, Royal Institute of Technology (KTH) (2011). In preparation

The creation of software capable of turning estimated road grade profiles into content in a road map was done as a Master's thesis project. This software was used to generate the map estimation results presented in Chapter 6.

N. Andersson. *Skapande av karta för fordonsreglering med framförhållning [Map creation for look-ahead vehicle control]*. Master's thesis, Royal Institute of Technology (KTH) (2011). In preparation

1.5.1 Patents

In addition to the academic publications, the work described in this thesis has led to five Swedish patents. Three of these have been published as international patents as well.

The last four Swedish patents are active. The first was approved based on the merits of the invention, but later revoked due to publication of parts of the invention before the submission of the patent application. The first patent is related to the constant estimator while the rest describe methods developed when studying applications of road grade data.

P. Sahlholm, H. Jansson, and E. Kozica. *Metod och anordning för estimering av lutningen för ett underlag på vilket ett fordon färdas [Method and system for esimating the inclination of a surface on which a vehicle is driving]*. Swedish patent SE 530 728 C2 (filed 2006). Revoked: Sep 2, 2010

J. Slettengren, H. Jansson, and P. Sahlholm. *Förfarande och anordning för att stödja en reglerstrategi för framförandet av ett fordon [Method and device for supporting a regulating strategy for the driving of a vehicle]*. Swedish patent SE 531

835 C2 (filed 2007)

A. Alam, J. Andersson, and P. Sahlholm. *Metod, system och datorprogram för automatisk hastighetsreglering av ett motorfordon [Method, system and computer program product for automated vehicle speed control].* Swedish patant SE 531 922 C2 (filed 2008*b*)

A. Alam, J. Andersson, and P. Sahlholm. *Fastställande av accelerationsbeteende [Determination of acceleration behavior].* Swedish patent SE 533 144 C2 (filed 2008*a*)

A. Alam and P. Sahlholm. *Metod och system för reglering av ett fordons hastighet i en kurva [Method and system for vehicle curve speed control].* Swedish patent SE 533 044 C2 (filed 2008)

The three international patents are translated versions of the first three Swedish patents.

J. Slettengren, H. Jansson, and P. Sahlholm. *Method and device for supporting a regulating strategy for the driving of a vehicle.* World patent WO 2009 072965 (filed 2008)

A. Alam, P. Sahlholm, and J. Andersson. *Method, system and computer program product for automated vehicle speed control.* World patent WO 2009 096882 (filed 2009*b*)

A. Alam, J. Andersson, and P. Sahlholm. *Determination of acceleration behaviour.* World patent WO 2010 062242 (filed 2009*a*)

1.6 Outline

The rest of this thesis is organized as follows. Chapter 2 describes applications of road grade information, as well as an overview of the methods for obtaining such information. Data quality requirements and the sensors that are used are also treated. The proposed road grade estimators are based on models for both the road grade signal and the vehicle. A vehicle model is also used in simulations to generate data for the study on the convergence of the estimates. The necessary models are developed in Chapter 3. In Chapter 4, the details of the three different road grade estimators are described. Chapter 5 contains the experimental setup and a comprehensive description of the experimental results for each of the studied road grade estimation algorithms. It ends with a comparison of the performance of the different methods. In Chapter 6, the predicted behavior when using the proposed method with a large number of vehicles is analyzed. Finally, in Chapter 7, the thesis is concluded with a discussion about the usefulness of the proposed methods, and an outlook into the future.

Chapter 2

Background

"*Knowledge is of two kinds. We know a subject ourselves, or we know where we can find information on it.*"

Samuel Johnson, quoted in Boswell's Life of Johnson, 1791.

The demand for accurate digitized information about the road grade has recently increased in the automotive world. This is an effect of the evolution of embedded electronics, which has made HDV control units powerful enough to take such information into account in real-time. When the control algorithms are extended from considering only the local road grade to also include the upcoming grade profile it becomes impractical to sense the data as it is needed. A road grade map is required.

This chapter starts off with a motivating scenario highlighting potential benefits from having road grade information available. This is followed by an account of recent major research projects related to the acquisition and use of such information. Section 2.3 provides an overview of the development and current state of digital road maps. The following sections describes the most important applications of road grade maps, from an HDV point of view, and outlines options for how such maps can be created.

A large number of methods for obtaining road grade information, both on-board vehicles and through surveying, are available in the literature. An overview of the field is given in Section 2.6. This is followed by an analysis of the accuracy requirements on the estimated road grade, based on a predictive speed control application. The chapter is concluded with a description of the sensors used in the experimental study, with a special focus on the GPS, and a summary of the background for the thesis.

2.1 A Vision for Road Traffic

The road transport networks that carry the trade goods and people of the globalized world consume massive amounts of energy in the form of liquid fuel. The rise out of poverty currently happening in large parts of the world drives the demand for ever more transport. Future fuels may provide part of the solution to the energy challenge, but new energy approaches to energy conservation will also be required.

The growth in traffic is not only an energy problem. Traffic is also a leading cause of death and severe injury around the world. A World Health Organization report lists deaths and injury from traffic accidents as the ninth leading cause of disability-adjusted life year health loss, a measure designed to combine years lost from premature death with health lost from injury, globally in 2004 (World Health Organization, 2008, p.51). The same report predicts that traffic accidents will be the third largest cause in 2030.

Significant improvements in vehicle control, to a point where vehicles mainly drive autonomously, can provide the solution to both these problems. Driverless vehicles can have power plants designed to solve only the transport task, replacing the powerful engines, optimized for driveability, found in most vehicles today. Automated vehicles can also be designed to communicate with surrounding vehicles to decrease the overall energy consumption of the transport network. Well designed cooperative control algorithms should also be able to significantly reduce the number of high energy crashes. As a result the passive safety features in vehicles should not need to be as extensive as today, enabling vehicles to be made much smaller, lighter, and thus more energy efficient. The potential of this idea is explored in detail in (Guzzella, 2009). Since the road grade affects the dynamics and energy balance of a vehicle, one of many pre-requisites for crash-free, autonomous, energy optimizing vehicles is a high quality map of the surroundings. Such a map needs to include road grade information. Since there are already many driver support systems in cars that rely on, or can be improved using, road grade information making it available in vehicles can have an important effect on the safety and energy efficiency of the transport network both today and in the future.

2.2 Intelligent Transportation Systems

Modern information and communications technology is being applied around the world to transport more goods and people with higher energy efficiency and fewer accidents than before. Intelligent Transportation Systems (ITS) is a broad area, which covers a large number of technologies and applications. Government agencies have been set up to work within the area in many countries, and regular conferences are held to discuss developments.

In Europe, ITS activities are coordinated by the European Road Transport Telematics Implementation Co-ordination Organisation (ERTICO). Their official definition of ITS, as presented on the organization web page is:

> ITS - Intelligent Transport Systems and Services - is the integration of information and communications technology with transport infrastructure, vehicles and users. By sharing vital information, ITS allows people to get more from transport networks, in greater safety and with less impact on the environment. (ERTICO, 2010)

A number of Swedish, European, and American research projects have been carried out within the ITS field. The most recent and closely related projects are described in the next section.

2.2.1 Research Projects

Research into various ITS related fields has in recent years been carried out in many different contexts worldwide. A large part of the projects focused on digital road maps intended for use by vehicle systems rather than directly by humans have been funded by the EC. These include eCoMove, MAPS&ADAS (PReVENT), ROSATTE, NextMAP, ActMAP, FeedMAP, and EuroRoadS. The Swedish Intelligent Vehicle Safety Systems (IVSS) programme has, in addition to the project "Vehicle control by using preview information —- Look Ahead', which is funding the research reported in this thesis, supported the Safe Operation for Large Vehicles Initiative (SOLVI) project with a similar aim as the ROSATTE project.

eCoMove

The goal of the Cooperative Mobility Systems and Services for Energy Efficiency (eCoMove) project is to combine state of the art vehicle control for energy efficient driving with traffic information, infrastructure management and communications technologies to achieve a 20 % reduction in energy and consumption and CO_2 emissions. The areas that the project aims to improve are indicated in Figure 2.1. The algorithms intended to provide energy efficient speed control rely heavily on accurate road grade information. The project was initiated in 2010 and will run until 2013 (eCoMove, 2010).

MAPS&ADAS

PReVENT was a large integrated project within the EC sixth framework programme. It handled many different aspects of ITS, and one of the sub-projects was MAPS&ADAS. The MAPS&ADAS project was initiated by the Advanced Driver Assistance Systems Interface Specification (ADASIS) forum. The objective of the ADASIS forum is to jointly develop a standardized data model to represent the map data ahead of a vehicle, and a way for applications to access this data. Much of the initial development work on this data model and the associated communication protocol was carried out within MAPS&ADAS. The final report was delivered in January 2008. This effort is described in further detail in Section 2.4.2. The work of the ADASIS forum continues, and the developed standard for transmitting digital

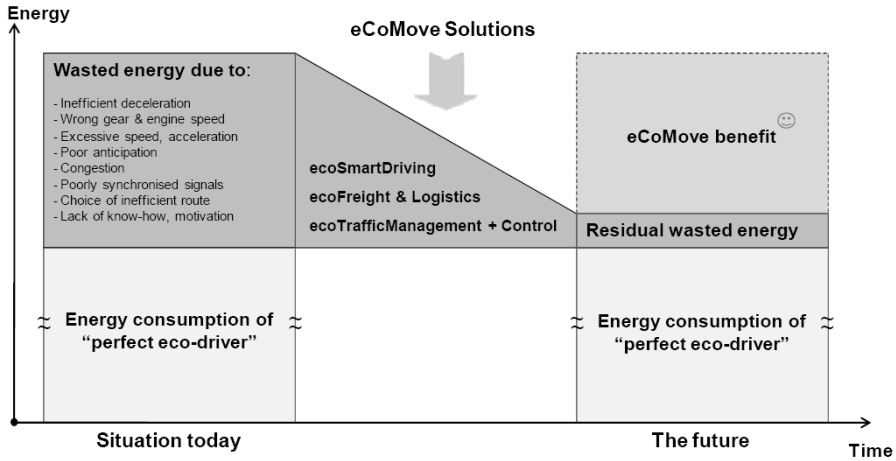

Figure 2.1: Transport energy wasted due to real drivers not behaving like perfect eco-drivers. The recently launched eCoMove projects intends to narrow the gap, partly by using road grade information stored in maps. Source: eCoMove (2010)

horizon information (c.f. Section 2.4.2) on car communication networks is about to be introduced in production vehicles from several manufacturers.

ROSATTE

The challenge of how to transfer of information from the databases of road authorities across Europe, to the companies who supply advanced digital maps to the market was studied in the ROad Safety ATTributes exchange infrastructure in Europe (ROSATTE) project. The availability of reliable road data in general has been seen to be rather low, and where it exists the storage methods differ widely between different authorities. A well functioning data exchange system between map suppliers and road authorities would be a good way to use potentially excellent data from when roads are built. The lack of quality data at the source, specifically road grade data, limits this approach to be a partial solution to obtain European road grade data. This is true even if effective data transfer methods are developed. ROSATTE was the next step after the earlier EuroRoadS project of the 2004–2006 period. ROSATTE ran from 2008 to 2010. The survey of available data and storage formats was published as a public deliverable by the project (ROSATTE, 2008).

SOLVI

The Swedish project SOLVI was also aimed at finding ways to move road network data between providers, distributors, and users. The focus was on safety critical attributes for HDVs e.g., load carrying capacity, overpass height, and dynamic attributes such as road works, traffic congestion, and variable speed limits. Road

grade and road curvature information, and potential sources for it, were also studied. The transferred data was validated in the project, by building demonstrators for the intended applications. The results are described in (Sena, 2008).

NextMAP, ActMAP, FeedMAP

The development of map databases for vehicle navigation application was done in part through EC funded projects. The Geographic Data Files (GDF) standard for storing geographical data is one example of a widely used result of these efforts. As newly developed ITS applications created a demand for more precise maps with new attributes, an update to the format became necessary. In the year 2 000 NextMAP was launched, the first of a series of projects to define, prototype, and evaluate map content for future in-vehicle ITS systems (NextMAP, 2002). NextMAP ran until the end of 2001, and was followed by ActMAP (2002–2004) and FeedMap (2006–2008).

These later projects focused on ways of delivering incremental updates to in-vehicle databases (ActMAP), and provide a return channel for data from the user (FeedMAP). Mapmakers estimate that 10-15,% of the road network changes every year, and this number may be as high as 40,% in high growth areas (Löwenau et al., 2008). Making incremental over-the-air updates instead of replacing the entire map is a way to provide users with more current information. The proposed incremental data update chain from the ActMAP final report is shown in Figure 2.2.

One challenge that map suppliers face is how to determine where the road network has changed, so that those areas can be scheduled for re-survey. The FeedMAP project aimed to investigate methods to collect deviation reports from both vehicles that detect erroneous map attributes (automatically or manually) and public authorities. A framework to validate these reports, and potentially turn them into dynamic updates through the ActMAP chain was developed. Road grade is mentioned (but called slope) in the FeedMAP final specification, as an attribute that can be validated in the system (FeedMAP, 2008). This would be one potential use of the road grade estimation system described in Chapter 3.

2.3 Encoded Road Maps

A key element in ITS is the use of machine readable maps. They are used on every level from simulation for infrastructure planning, to helping a vehicle stay in its lane. Machine readable maps for automotive navigation and route guidance have been used since the first trials with route guidance systems in the early 1900's. Accounts of the history of automobile navigation can be found in (French, 1987), and the introduction chapter of (Zhao, 1997). A more thorough historic account of the use of maps in travel and navigation is available in (Akerman, 2006).

The first systems were mechanical and used a dead reckoning to signal upcoming turns or points of interest to the user. Dead reckoning is a process where a known starting point and a traveled distance, e.g., from an odometer, are used to predict the current position. The map was an encoded set of distances to drive between

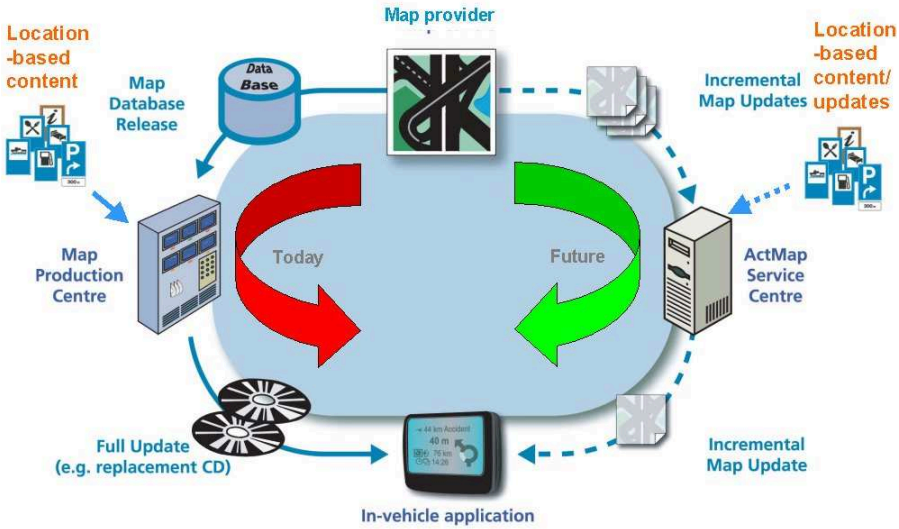

Figure 2.2: The ActMAP chain of incremental map updates. Road network updates are combined with changes to location based content and sent to clients as incremental updates over digital communication channels instead of by replacing or overwriting the entire map. Source: (ActMAP, 2005)

instructions. With better road signage and paper maps interest in the primitive guidance systems declined. During World War II an electromechanical system that could draw a vehicle's course on a map based on the driven distance and a magnetic compass was developed by the U.S. Army. In the late 1960's computer technology had matured to the level where electronic systems started to be developed. These were either based on dead reckoning from a known starting point, or proximity beacons with known positions throughout the road network. In the 1980's map matching algorithms, where a recorded drive path was compared to possible routes in a database, gained popularity. These digital maps contained larger and more complex road networks than in previous systems (French, 1987).

From the launch of the GPS, satellite based positioning enabled devices with digital road maps, aided by different levels of dead reckoning and Inertial Navigation Systems (INS) support, have been the industry standard in navigation aids. Modern solid state storage can easily hold detailed road maps of entire continents. The world market for digital road maps for vehicle navigation is currently dominated by two companies, Navteq and Tele Atlas. They have large fleets of data collection vehicles that measure new roads and verify existing data in the field. The widespread adoption of consumer oriented navigation devices has made collection of detailed data sets covering large parts of the globe economically feasible for these companies. However, despite recent progress, many features are still missing from the maps.

Current business models and technologies also lead to many systems operating with outdated maps. There is still room for significant improvement both in the way data are collected, and distributed to the users.

A key map feature for HDV applications that is still missing from the majority of commercial maps is the road grade. Road grade data can be obtained using suitably equipped survey vehicles. Both Navteq and Tele Atlas have such equipment, but not all roads have been surveyed with the new equipment. The existing road grade data are only included in specialized map products sold to industrial partners at a premium price point. The availability of road grade maps from the major suppliers is likely to increase in the future, and the price difference may decrease. Using the system proposed in Chapter 6, it may become unnecessary to buy the road grade information at all. Standard vehicles operating on the roads may be able to provide the necessary grade data themselves, over time and given that an extensible two-dimensional road map already exists.

2.3.1 OpenStreetMap

The OSM project was started to create and provide free geographic data to anyone who wants it. It is a community driven project largely enabled by the advent of cheap ubiquitous GPS receivers. Contributors record tracks and take notes about their surroundings when taking trips, or go out specifically to record raw data for mapping. They then log in to the OSM database and input their data using one of the many software applications available. The database is then processed to produce street maps in many formats. There are routines to make live online maps as well as printed maps of a specific area. Seeing that the project lives and develops online, the most authoritative and up to date information is found on the Internet, see for example (OpenStreetMap, 2010; OpenCycleMap, 2010). The OSM data are easily accessed and manipulated using free tools, making it ideal for use in research projects.

The project is now mature enough, and has a wide enough user base, that frequently traveled roads, such as major highways, are included with very good coverage. The data quality depends on the skill and equipment used by the person encoding the information, but very bad data points tend to be corrected by someone else rather quickly. Many roads have also been checked versus geographical information, such as satellite and aerial imagery, which has been donated to the project by various rights holders. The current version of OSM is note reliable enough to be used directly in ADAS systems, but it does provide a starting point for automated mapping efforts such as the one described in this thesis. The task of creating a high quality map focused on a particular feature is greatly simplified by starting from the encoded knowledge already present in the street map. As cars become even more connected, it is likely that numerous contributors around the world will start working on implementing algorithms for automatic refinement of the map based on large amounts of trip data. The case study presented in Chapter 5 of this thesis is one early example of such an effort.

The map database is governed by a creative commons share-alike license, with relatively liberal terms for reuse (OpenStreetMap License, 2010). The presence of the basic data set has inspired many extensions. Some display the data of the main database in new ways, essentially adding another graphical layer on top of the basic map. One example is the OpenCycleMap (OpenCycleMap, 2010). The data displayed is part of the regular OSM, but the OpenCycleMap highlights it for the user. Other extensions use additional data sources to create new maps, such as the WikipediaWorld project that places all georeferenced articles of the Wikipedia georeferencing project on a rendition of OSM (Wikipedia, 2010*b*,*a*).

While there is support for both altitudes and road grades in the OSM database, these attributes are not commonly used. Attributes are stored in the database as keys connected to nodes, ways, or relations (groups of nodes or ways). In the European subset of the map the key "highway", which is to be used for all roads and streets, is used on 14 988 523 objects. The key "incline", which is recommended for representing the road grade, is used on 15 304 objects. The "incline" key can have both numerical and text values. The values "up", "down", and "yes" together account for 7 544 of the occurrences. The majority of the rest of the values are numerical. By considering the dominance of integer inclines among the numerical values, it appears that accurate road grades are highly unusual in today's map. All the statistics for the map are current as of November 12, 2010, and extracted from the map using the service (OpenStreetMap tag watch, 2010).

There is also an elevation tag described in the documentation, but it is primarily used to represent the elevation of landmarks such as mountain peaks and train stations. The software infrastructure of the OSM project has been built around editing of two-dimensional maps. The information on the official wiki about elevation and altitude is rather sparse, and there is apparently no established way of incorporating road elevation or road grade into the map database. There has been some discussion in the OSM community on how to improve the altitude content in the maps. The discussions do not seem to be finalized, and whatever content does exist is commonly relative to an unspecified altitude reference system, c.f. Section 2.8.2. The English language documentation of open street map is very sparse when it comes to altitude, but some information is given in the German documentation (OpenStreetMap Altitude, 2011). A proposal for how altitude and road grade information can be added to the map is a part of the contribution of this thesis, it is given in Chapter 6. Some projects based on OSM, for example the OpenCycleMap, use external elevation data from the NASA Shuttle Radar Topography Mission (SRTM) altitude data set. While this is the best global elevation data set currently released into the public domain, the accuracy is far from sufficient for ADAS.

2.4 Applications of Road Grade Maps

Current and future vehicles contain many ADAS designed to improve transport safety and energy efficiency. Sensors, which are a part of many such systems, help

the driver by improving the total perception of the environment. In the case of look-ahead systems, a map with stored information is used to extend the perception horizon beyond what either the driver or conventional on-board sensors can see. Actuators connected to ADAS improve vehicle control by acting in situations where the driver is unable to do so. In map based look-ahead systems the automatic action can be based on information that the driver will only be able to get at a later time.

An increasing number of vehicle control systems now utilize stored information from a map, to aid the driver in piloting the truck in a safe and economical manner. Examples of map attributes that are commonly used are speed restrictions, road class, road curvature, and road grade. Knowledge of the current and future road grade can be used in engine and gearbox control systems to help meet the instantaneous power demand while keeping fuel consumption and environmental impact as low as possible.

2.4.1 Look-Ahead Vehicle Control

The emerging availability of low cost high accuracy GPS receivers together with enhanced computational capabilities of embedded control systems and increased storage capacity has opened up new possibilities in vehicle control. Absolute global positioning combined with a map enables the vehicle to predict where it is going next, and exercise control actions based on this assumption. Many different types of attributes can be utilized in this way to enhance vehicle safety and efficiency, but for HDV the road grade is the most important one.

Vehicle functions that support the driver, by using electronic sensors, actuators and control units, are usually referred to as ADAS. A multitude of such systems that utilize look ahead have been showcased in the last few years, but only a few have yet entered production. This section describes how ADAS benefit from access to electronic maps, and outlines main application areas where look-ahead road grade information improves existing, or enables new, functionality. The systems covered are

- Speed Control for Energy Efficiency
- Hybrid Vehicle Control
- Control of Auxiliary Units
- Gearbox Control
- Adaptive Front Lighting Control
- Overtaking Assistance

There are already many more examples of imaginative ways of using look-ahead road information, and more will undoubtedly follow once such information becomes universally available. The applications described here have been chosen for their relevance to HDVs and dependence on road grade information.

Road grade information is particularly important for HDVs, due to their large mass. To illustrate the road grade sensitivity of a standard long haulage HDV, the maximum grade that can be traversed at a constant speed, using the top gear, is shown in Figure 2.3. The figure is based on the vehicle model developed in Chapter 3, and results are shown for three different vehicle weights. Similarly, the large mass will lead to increased speed in downhill sections. The equilibrium grade at which the vehicle will coast at a constant speed, again using the top gear, is shown in Figure 2.4.

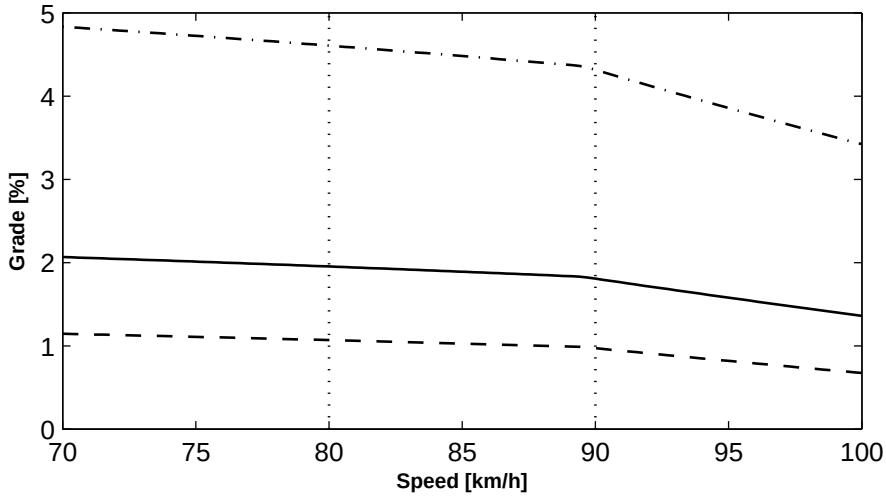

Figure 2.3: HDVs are heavily influenced by the road grade. The maximum uphill grades that can be traversed at constant speed are shown for three different vehicle weights. The weights are 20 t (dash-dotted), 40 t (solid), and 60 t (dashed). A road grade of 1 % is barely noticeable in a passenger vehicle.

The HDV in Figure 2.5 will speed up when going down one hill, and lose speed when climbing the next one. If the road grade for the kilometer or so directly ahead of the vehicle is known, it is possible to automatically adjust the speed in advance of up- and downhill road segments and thus conserve fuel without increasing trip time. The preview road grade information can also be utilized when determining if a gearshift should be performed or the state of some energy buffer changed. Furthermore the brake management system could use the road grade information to determine the highest allowable speed when going down a hill. Thus waste heat generation in excess of the system's ability to release it can be avoided. This in turn ensures that the vehicle retains emergency stopping power, a clear safety benefit.

Road grade maps of sufficient accuracy to support automatic vehicle control systems are currently not widely available. Commercial efforts to create such maps are underway, but access to them will most certainly be associated with some cost.

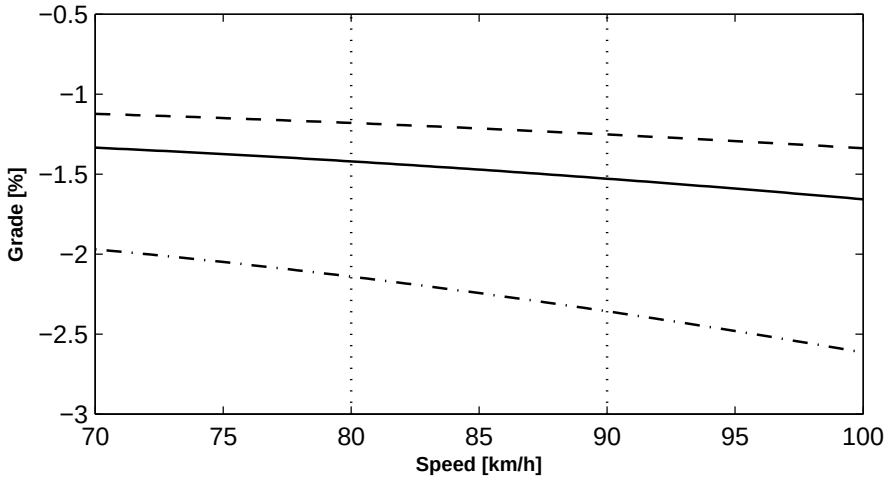

Figure 2.4: Even moderate downhill road grades will lead to large speed increases. The figure shows the road grade required for running at constant speed with no engine power. The lines represent the vehicle weights 20 t (dash-dotted), 40 t (solid), and 60 t (dashed). On long downhill segments steeper than -1.5 % most fully loaded trucks will need to apply some brake system.

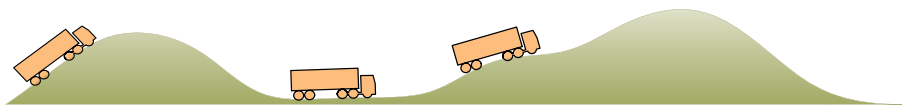

Figure 2.5: HDVs traveling on a hilly road. At the position of the leftmost vehicle, it is advantageous to lower the speed to take full advantage of the upcoming downhill road segment. In the second position the overall fuel economy can be improved by increasing the speed before the steep part of the hill is reached. In the third position it is important to maintain the driving torque, to avoid costly loss of turbo pressure when entering the continued ascent.

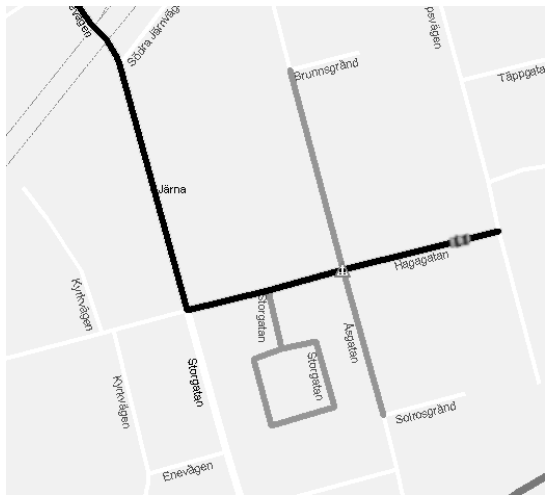

Figure 2.6: The ADAS horizon road network ahead of the car is shown in grey, and its most probable path is shown in black. The vehicle is located in the middle right of the figure, heading left and soon to encounter an intersection, highlighted by a small warning sign. (Illustration courtesy of Navteq)

HDVs commonly travel the same routes frequently, and are thus ideally suited to be their own probes and estimate the road grade for the small subset of all roads that are relevant for a particular vehicle.

2.4.2 ADAS Horizon

A crucial part of a look-ahead control system is the ability to extract the interesting part of a large map. The map is generally kept on a mass storage device, in some format that allows for fast searching based on geographical coordinates. As the vehicle moves a digital model of the surrounding road network with its associated attributes needs to be constructed. This model is commonly referred to as the ADAS horizon. Figure 1.4 shows an example ADAS horizon with both physical and legal attributes. The desired application places varying demands on the selection of ADAS horizon attributes, their accuracy, and the horizon size. In some applications one is only interested in the vehicle's most probable path, in others the entire horizon is taken into account. An example of the most probable path, based on road network attributes such as the road type classification and turn angles, is shown in Figure 2.6.

To enable multiple look-ahead applications in a distributed control system to use a single map data source there needs to be a method for transferring the ADAS horizon to different control units on the vehicle communication network. The ADASIS forum is a joint effort by slightly more than 30 ADAS original equipment manufac-

turers, map suppliers, and vehicle manufacturers to create a common solution for how to accomplish this. The ADASIS forum has developed a proposed standard for both the representation of attributes in the ADAS horizon and the transmission of these attributes over vehicle communication networks. These efforts started in 2001, and there is currently a fully functional proposal available. The most recent results from the forum can be found in (Ress et al., 2008).

2.4.3 Speed Control for Energy Efficiency

When a highway contains segments with an uphill grade so steep that a vehicle cannot maintain the desired speed, or a downhill grade so steep that over speeding will occur unless the brake system is used, there is a potential for decreasing the fuel consumption compared to a standard cruise controller, with unchanged trip time. This has been explored for example in (Huang, 2010; Hellström, 2010; Hellström et al., 2010; Fröberg, 2008; Terwen et al., 2004).

To achieve a reduction in the fuel consumption it is necessary to lower the vehicle speed over hill crests and increase it ahead of steep uphill segments. Thus the number of steep hill segments as well as the traffic load of the road affects the fuel consumption gain that can be achieved.

Furthermore, road grade data of sufficient accuracy must be present for the highways where the vehicle will operate. The quality of the grade data needs to be high, so that the vehicle speed can be predicted over a long enough distance. Field tests have shown that averaged single frequency GPS based measurements from a few runs along the road give sufficient precision to realize fuel savings in actual driving. The most crucial information needed by the optimization algorithm is whether the vehicle will lose speed uphill despite running at full throttle or gain speed without fuel injection when going downhill. Not knowing the exact rate of the speed increase or decrease will reduce the possible savings due to the extra margins needed before action can be taken, but the principle of operation can remain largely unchanged. For typical long haulage HDVs the most interesting range of road grades will be 0 %–2 % either up- or downhill.

2.4.4 Hybrid Vehicle Control

In hybrid electric vehicles one of the most challenging control objectives is to keep the state of the energy buffer from hitting the boundaries of its operating range. To minimize the energy consumption it is necessary to empty the buffer ahead of driving events that will generate surplus energy, such as braking or driving in steep downhill grades. On the other hand, driveability will generally suffer if the energy buffer happens to be empty when an event that requires maximum power output occurs. Since the problem of determining the optimal state of the energy buffer at every point along the route depends on the power demands ahead of, as well as behind, the vehicle it seems natural to use some type of look-ahead information. The road grade is one factor that influences the power demands of a hybrid electric

vehicle, but the speed profile is often of equal or higher importance. Much of the energy consumption gains, using hybrid technology come from regenerative braking in city driving scenarios. Numerous solutions to how to utilize advance knowledge of both the road grade and anticipated speed profile have been proposed in the literature. In (Johannesson, 2006) various predictive control strategies based on stochastic models of the road grade and speed profiles for a hybrid electric passenger car in city traffic are evaluated. The work is extended further in (Johannesson and Egardt, 2007). A current and instructive survey of results obtained by route optimized control of hybrid electric vehicles, both passenger cars and HDVs, can be found in (Gonder, 2008), while a wider survey of the current state of energy buffer management research for hybrid electric vehicles is available in (Salmasi, 2007). A self-learning system that identifies the power demands for various segments of a commuting route through many repeated measurements is described in (Ichikawa et al., 2004). A system using similar ideas to those applied in the previous section is the predictive driveline control system, thoroughly investigated in (Back, 2005).

2.4.5 Control of Auxiliary Units

An HDV contains a number of auxiliary units such as an electric generator, a power steering pump, a water pump, a cooling fan, an air compressor, an oil pump, and sometimes an air conditioning unit. A common trait of these is that they generally operate with some kind of energy buffer. As an example the electric generator charges a battery, and the power steering pump maintains pressure in the power steering system. For short periods of time the battery could potentially be used to power the electric system without the help of the generator, and the power steering pump might not need to run at full throttle when going straight. Advance knowledge of the near-future energy needs of auxiliary systems, combined with state information about their energy buffers, and improved auxiliary units that can be turned on and off enable look-ahead control strategies to be used in pursuit of maximum energy efficiency. Similarly to the speed control case the units can be used to charge the buffers when there is an energy surplus available. The potential for energy savings from using more controllable auxiliaries is explored in (Pettersson and Johansson, 2006).

2.4.6 Gearbox Control

Automatic gearboxes stand to benefit considerably from advance knowledge of the upcoming road grade. Performing a gearshift takes some time, especially with the automated manual gearboxes that are commonplace in HDVs. During this time the turbo pressure is lost in the engine, and the vehicle slows down rapidly due to the absence of a driving torque. If the vehicle is near the top of the hill the gearshift can often be avoided, if the grade profile is known. Unnecessary downshifts near the end of uphill road segments are a well known annoyance to truck drivers using

automatic gearboxes. Additionally, the shifting strategy and choice of starting gear can be improved in many other cases using reliable stored road grade information.

2.4.7 Safety and Comfort Systems

Two examples of look-ahead systems that need road grade information, but focus on safety and driver comfort rather than energy efficiency, are adaptive front lighting control and overtaking assistance. The basic idea of front lighting control is that the center of the light beam should always be where the driver wants to look. In curves the headlamps then have to be angled sideways, and when the road grade changes the beams need to be adjusted up or down. With look-ahead information about the three-dimensional road profile, and full position information about the vehicle, fully controllable headlamps can be directed to center on a specific point on the road, as described in e.g., (Löwenau et al., 2000) and (Lauffenburger et al., 2007).

The more passenger car focused overtaking assistance has been described as a utility to inform the driver of when it is unsafe to pass vehicles in front, and how far it is until the next location where there may be an overtaking opportunity (Löwenau et al., 2006). In this application the road grade is of importance both to judge the visibility distance at any given point, and to determine the maximum relative acceleration available. The acceleration in turn determines the time required to pass the preceding vehicle.

2.5 Map Creation

It is apparent that the idea of using vehicle sensors and a model for the vehicle and road is not new. Solutions based on this idea have been implemented using a number of different methods, to reach various design goals. GPS receivers of varying quality are used in a number of methods for road map generation. What is new in this thesis is the particular method of combining the vehicle sensors and a GPS to create a road grade map based on many runs along a particular road segment.

2.5.1 Enhanced Navigation Maps

The current major suppliers of road maps for navigation devices make up a potential source for digital maps with road grade information. The currently delivered maps do not contain road grade or altitude information accurate enough to be used in vehicle control. However, the major companies in the field already have numerous measurement vehicles in the field, as well as a built up infrastructure for map production based on collected data. Relatively simple equipment upgrades to the measurement vehicles should enable road grade data to be included in the products. Plans to provide a compact low cost navigation system without a user interface, with only map attributes relevant for ADAS have recently been announced by one of the manufacturers (NAVTEQ Press Release, 2008).

At least one of the current navigation map suppliers have been investigating ways to add road grade data to their during the last decade. This is indicated by a patent application filed in filed 2003 and awarded in 2005. The patent describes a system where the road grade is estimated onboard a vehicle using one of a selection of methods from the classes outlined in Section 2.6, and then sent to a data collection facility. The key point of the patent the act of detecting and locating a road grade change point (using a known method) and sending it to a remote data collection facility.

2.5.2 Data Mining

The idea of automatic creation of road maps from GPS traces has been described in a few places. An interesting approach based on position logs from many runs along a road, using consumer grade GPS receivers, is described in (Schroedl et al., 2004). Another automatic road map generation approach, based on more expensive Differential GPS (DGPS) receivers, is detailed in (Brüntrup et al., 2005). The emphasis in this project is on the data mining methods being applied, and on achieving lane-level accuracy in the generated maps. Both these contributions treat two-dimensional maps without road grade information. They also do not explore the possibility to use a vehicle model and on-board sensors to improve accuracy.

A method based on high resolution specialized measuring equipment is also described in (Noyer et al., 2008), where an attempt is made at defining a map production method with curve clothoid identification for a lane-level accurate map. The roads to be mapped have to be driven by the probe vehicle, but there is no need to interfere with the regular flow of traffic, as there is with classical surveying methods. The aim of the method is to produce a map with an accuracy one order of magnitude better than current street maps for navigation purposes, i.e., around one meter. The road grade is currently not treated by this method.

A research group in Germany is developing a self-learning route memory, that records vehicle state and driving events along frequently traveled roads. The system described aims to automatically identify route conditions accurately enough to be used in look-ahead vehicle control applications such as predictive powertrain control for hybrid electric vehicles. The work has recently been described in (Carlsson et al., April 2009), where a prototype implementation of the route memory is detailed. In this work significant attention is directed towards practical issues such as data storage requirements for different attributes, rather than the identification of attribute values, such as the road grade.

2.6 Road Grade Estimation

A large number of methods for estimating road grades have been proposed during the last 40 years of automotive research. As the computational power of the electronic control units has increased, and more advanced sensor technology appeared,

the resolution and accuracy of the methods have improved. Today accurate estimation of dynamic vehicle states is an important pre-requisite for many vehicle safety and driver assistance systems. Some approaches are directly focused on finding the road grade, while others attempt to identify the full vehicle movement with six degrees of freedom (three linear velocities and three angular velocities). Using data from multiple vehicles to build road grade maps increasing accuracy is not explicitly described in any of the previous work.

The term road grade is used in this work to refer to the rate of change in the road surface altitude along the direction of travel for the road. In the mathematical models the road grade is expressed as an angle between the roadway and the horizontal plane, measured in radians. It is common, e.g., on road signs to express road grade in terms of percent. This generally refers to an altitude difference divided by a corresponding traveled distance. It is sometimes ambiguous whether the traveled distance is measured along the incline, or if the distance along a virtual horizontal reference plane should be used. The difference in practice is very small. It does not reach 1 % of the road grade until a grade of approximately 14 %. In this work all road grade results are presented as percent, calculated as the ratio of altitude change divided by the covered distance in the horizontal plane. A 100 % road grade thus corresponds to an angle of 45 deg The road grade expressed in percent can be determined from the road plane angle relative to the horizontal plane as

$$\alpha_{\%} = 100 \arctan \alpha_{\text{radians}}$$

Expressing changes or intervals of a quantity expressed with the unit % is somewhat delicate. One has to make the distinction between a 5 % change from a grade of 2.0 % to 2.1 % and a 5 percentage points change from 2.0 % to 7.0 %. When the distinction is not obvious due to the context the term "% grade" will be used as shorthand when the intended meaning is a change denoted as percentage points of road grade.

The previous research within the field is classified by the method that is used to estimate the road grade. Some proposals include more than one method, and are then mentioned in multiple categories. Much of the work in the area is done by car manufacturers or automotive OEMs. Therefore many methods first, or only, appear in patent applications. The estimation methods are based on the following:

- *Road grade sensors:* Several ideas for sensors that directly convert the current road grade into an electric signal have been proposed.
- *Dynamic state estimation:* Many methods intended to provide information on the movement of the vehicle give road grade information as an additional output.
- *Linear and vectorized acceleration:* When the vehicle is not driving horizontally there is a difference between the speed change and the acceleration detected by an inertial sensor.

- *Driving force and acceleration:* The road grade affects the amount of driving force required to achieve a particular acceleration.
- *Absolute position:* If the absolute position of the vehicle can be determined exactly the road grade can be found as the derivative of the altitude.
- *Survey methods:* Survey engineering is dedicated to accurately determining absolute positions. This is an accurate but costly way of finding road grades.
- *Imaging:* By studying the road ahead with an imaging device the relative road grade compared to the present location can be tracked.

2.6.1 Road Grade Sensors

One common approach for estimation of the instantaneous road grade is to use a sensor to directly measure the grade. A direct road grade sensor for automotive use is described in a patent application filed as early as 1971 by (Gaeke, filed 1971).

2.6.2 Dynamic State Estimation

A current survey of vehicle dynamic state estimation methods, focused on sensors and methods common in automotive practice or research is given by Tin Leung et al. (2010). Some of the methods produce road grade information as a part of the estimation result. The authors propose to divide current methods into seven classes depending on the sensors and estimation methodology applied, as illustrated in Figure 2.7. The methods developed in this thesis fall into the proposed category five. Some analysis on the performance differences compared to reduced methods belonging in categories two and three is also provided.

Vehicle dynamic state estimation using GPS receivers is described in (Bae et al., 2001). The paper compares a grade estimation method based on a GPS receiver with three-dimensional velocity output to one using a two-antenna GPS. The three-dimensional velocity signal is used to calculate the grade as the ratio of the vertical and horizontal velocities, while the two antenna solution directly gives the grade as the height difference between the measurement points. The GPS receiver employed is a high performance model, and satellite reception is flawless during the entire test segment. Thanks to the high quality grade estimate a precise determination of the vehicle mass is possible through the use of a driving force estimate and a vehicle model similar to the one used in this thesis.

2.6.3 Linear and Vectorized Acceleration

If an accelerometer oriented in the longitudinal direction is available in a vehicle this will give an output that is a combination of the acceleration of the vehicle along the road and the component of the gravitational acceleration parallel to the road surface. If the acceleration along the road surface can also be found, e.g., through

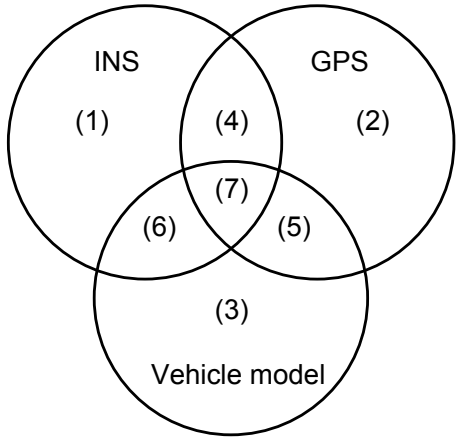

Figure 2.7: Ground vehicle dynamic state estimation categories proposed by (Tin Leung et al., 2010). The categories are (1) numerical integration of INS/sensors measurements; (2) direct measurements from GPS device; (3) direct determination from a vehicle model; (4) estimation via GPS/INS without considering forces in a vehicle model; (5) estimation via GPS and vehicle model considering forces; (6) estimation via INS and vehicle model considering forces; (7) estimation via GPS/INS and vehicle model

derivation of a speed signal from a wheel speed sensor, these two may be subtracted to find the road grade. The road grade α, with a small angle approximation, is given by

$$\alpha \approx \sin \alpha = \frac{a_{\text{acc}} - a_{\text{wheel}}}{g} \tag{2.1}$$

where a_{acc} is the acceleration sensed by the longitudinal accelerometer, a_{wheel} is the acceleration from the wheel speed sensors, and g is the gravitational acceleration. A brief experimental comparison of this method, with a driving force and wheel speed based acceleration determination method is given in Ohnishi et al. (2000). The method is also described and evaluated through experiments in (Kiencke and Nielsen, 2003, pp. 403–404).

2.6.4 Driving Force and Acceleration

The idea of using vehicle sensor information in combination with a longitudinal road model to find the road grade has been explored in (Lingman and Schmidtbauer, 2001), where a KF is used to process a measured or estimated propulsion force or estimated retardation force and a measured speed into a road grade estimate. Another approach, based on a longitudinal vehicle model, where the grade and mass are estimated using a "recursive least squares" method has been suggested in (Vahidi et al., 2005, 2003). The idea is further developed in (McIntyre et al., 2009). There, a two stage process where the mass is estimated first is used in lieu

of the recursive method. In Bassho et al. (2005) a model based linear observer design using pole placement and essentially the same sensors and vehicle model is described. The estimator is evaluated in a single short steep hill and appears to be tuned for city driving with a passenger car. Another method, together with a survey of similar approaches, can be found in (Fathy et al., 2008).

On-line road grade estimation based on accelerometers, calculated driveline torque and a vehicle model, or other on board sensors is state-of-the-art in today's vehicles. A large number of patents describe variations of the idea. These methods have the advantage of not needing any external signal, such as the GPS, but hence don't provide the extra bias compensation or easy inclusion of data from multiple runs along the road. They are generally used to obtain data to support automatic gearboxes and other systems that currently use road grade information. In a patent to Yamada and Ishiguro (filed 1999) a measured driving torque, vehicle driving resistance model, and measured acceleration are used to estimate both the road grade and the vehicle weight. The vehicle weight is separated from the influence of the road grade by only estimating the former at gearshifts from low to second gear, where a large difference in driving torque, on what can be assumed to be an almost constant road grade, can be observed. In a patent to Nelles (filed 2002) a similar vehicle model and driving torque based approach is used with a KF. Here the mass is separated from the road grade by modeling the former as slow changing and the latter as fast changing through the adopted process noise covariances.

A novel related idea is described in a patent to Kawasaki (filed 2002). There, no engine force estimate is used, instead the wheel speeds of four wheels are measured. The acceleration is continually calculated as a moving average based on the wheel speeds and the wheel slip ratio of the driving wheels compared to the non-driving wheels is determined when the acceleration is close to zero. The magnitude of the wheel slip ratio then indicates the required propulsion force at zero acceleration, which is in turn related to the road grade. Corrections are made for the air resistance as a function of speed and for the rolling resistance. A road grade estimate can then be calculated. Similar, but not as elaborate, solutions are described in two earlier patents (Aminpour and Reiner, filed 1995; Gramann et al., filed 1993). All vehicles with an anti-lock brake system already have the required sensors, making this a very low cost alternative that may work well as long as the weather is constant and the tires are not worn or changed. However, most such vehicles would also be able to estimate the engine torque from fuel injection times or throttle opening angle and operating point. The latter, a more standard approach, is believed to give a more accurate driving force estimate with fewer parameters that may change after calibration.

2.6.5 Absolute Position

A barometer may be used to obtain an absolute or relative altitude measurement. A major problem with this sensor is its sensitivity to weather variations as well as changes in the local conditions at the sensor location. With expensive hardware and

proper calibration accurate readings may be obtained, but with the budget available in automotive mass production the accuracy is limited, and there is generally no reliable weather dependent pressure information available. The vehicles used for testing in Chapter 5 were equipped with barometers, but based on results from an earlier study (Johansson, 2005) it was decided not to use that signal.

The altitude component of the position estimate from a GPS receiver can also be used to determine the road, but it is too noisy to be used without being combined with some other sensor. It could potentially be average over a large number of journeys to provide good enough information on its own.

A variety of methods for combining a barometer or other altimeter with GPS data to determine the current altitude are proposed in a patent to McBurney and Braisted (filed 1997). A common trait of the methods is that they aim to minimize the effect of the bias in the barometer or altimeter by using many GPS readings taken during good signal conditions, e.g., by switching between calibration and usage of the barometer or altimeter. Prior art include a patent to Masumoto (filed 1992) where a barometer is only used to obtain relative altitude readings when a three-dimensional GPS position fix is not possible.

2.6.6 Survey Methods

To determine the road grade accurately from absolute position estimates high accuracy data are necessary, since the road grade is approximated by the difference of two altitude measurements of similar magnitude divided by the horizontal distance between the measurements. Most consumer grade GPS receiver outputs an altitude estimate, if at least four satellites are tracked. This information is too noisy to determine a useful road grade estimate based on only one pass along a road section.

Geographical coordinates can be measured with very high precision using current GPS based geodetic measurement equipment. With the right sensor and sufficient time, finding the road grade locally is not a hard problem. It becomes much harder when the problem is scaled to finding the road grade at millions of points along vast stretches of roadway. When the sensor budget is also reduced to zero the problem studied in this thesis arises.

The main problem with methods from the survey engineering field is that they are slow, and therefore costly to apply on a large scale. To obtain the highest accuracy results, meaning errors on the order of a few millimeters, it is necessary to use a base station and a mobile rover sensor. The base station is fixed for the entire measurement and the rover is moved between measurement points. The occupation time at each point can vary between 20 minutes and a few hours depending on the circumstances. The local base station is normally placed within a few dozen kilometers, and its position has to be known with very high precision. The base station may for example be placed in the area ahead of time such that any error can be averaged out, or be placed on a pre-surveyed point. Positioning fixes from this type of survey are generally calculated off-line at the office, using the recorded sensor data. There are numerous surveying methods that are variations on this

theme, adapted for different usage scenarios. By sacrificing some of the accuracy the procedure can be relaxed somewhat. Many methods require a considerable initialization time before reliable measurements can be obtained. In some methods significantly shortened occupancy times at each location may be used, and if a live data link is available between the base station and the rover sensor positions may be obtained in the field, without post-processing (El-Rabbany, 2006).

A road grade mapping effort based on high precision GPS equipment is described in (Han and Rizos, 1999), where a road in Australia has been surveyed using moving geodesy GPS receivers in live contact with stationary base stations for improved accuracy. A spatial KF with height and road grade states is used to post-process the data.

Using a network of fixed base stations and correction information broadcast over satellite or terrestrial radio link it is possible to obtain position fixes accurate to within less than ten centimeters 95 % of the time with only one moving sensor. A commercial service that provides this level of accuracy is the OmniSTAR HP satellite based service provided by OmniSTAR Inc (OmniSTAR, 2011). This type of system does away with the local base station requirement, allowing continuous measurements along long roads. The two remaining problems are cost and coverage. While the accuracy of the absolute position fixes is suitable for vehicle control applications the sensors that can receive these signals currently cost tens of thousands of dollars, with annual subscription fees for the correction service of thousands of dollars. These systems also depend on uninterrupted line of sight contact with the satellites. If obstructions like trees or overpasses are present, the accuracy is degraded until a full lock in the signal can be re-acquired (El-Rabbany, 2006). If the GPS receiver is combined with a high quality INS the output data rate can be increased, and stability of the position signal can be improved, giving better relative accuracy between adjacent data points. A GPS/INS system that uses the corrections described above has been used to record the reference road grade profile in this work, as described in Section 5.1.5. Similar systems are currently being applied when the major map database providers are out collecting new data for ADAS maps (Barrett, 2008). An effort at creating a low-cost GPS/INS road geometry identification system, aided by the wheel speed sensors already mounted in standard vehicles, is described in (Ogonda, 2009). The work is related to the estimators proposed herein due to assumptions on the geometric properties of the true road, and the cost limitation on sensors. The implementations do however differ in that Ogonda uses an external IMU, and focuses on full three-dimensional road reconstruction at low driving speeds. The system is also described as a surveying aid rather than an autonomous system.

A common method for surveying large areas is to use an airplane with a radar or Light Detection And Ranging (LIDAR) device aimed at the ground. By keeping accurate track of the position of the airplane, the range measurements can be used to build a ground altitude model. Several challenges exist, such as detecting and compensating for trees and buildings hit by the radar, but the method can yield an accurate three-dimensional terrain model. If this model is combined

with a two-dimensional road network map, road grades can be obtained. This technique for obtaining road grade maps is described in e.g. (Hatger and Brenner, 2003; Zhang and Frey, 2005). Data collected using these techniques are marketed commercially by e.g. Intermap (Intermap, 2011). If an area has already been surveyed, finding road grades in this manner can be cost efficient. There are however issues with coverage of areas where no air survey has been conducted, and with updates. Re-surveying by airplane to update a few roads is not feasible, so supplementary surveying techniques need to be employed when updating the data.

Survey grade data can provide the accuracy required for producing road grade maps for ADAS applications, but obtaining it is very costly. Equipment with this level of accuracy will not be used in production vehicles for a long time. The data are nevertheless important as a tool for analyzing what accuracy can be achieved using more cost efficient estimation methods.

2.6.7 Imaging Sensor Based Methods

One way to estimate road grades is to use an imaging sensor to depict the environment including the road, and then process the signal. This approach is described in the literature primarily in association with the robotics problem of Simultaneous Localization and Mapping (SLAM). In autonomous vehicle research and robotics laser range scanners are commonly used to obtain high quality range and angle information about surrounding objects. One method of using such data to identify planar surfaces is described in (Weingarten et al., 2004). The authors use recorded point clouds to find an optimally fitting plane. This could be extended into a road grade estimation system by identification of the relative angle between planes taken from the road surface ahead of the vehicle. As the vehicle drives along and new planes are added in sequence. Assuming that the vehicle enters the previously identified road planes, a continuous road grade profile can be built from the measurements. Such a method would suffer from drift and a lack of global reference for the true road grade magnitude. Laser scanners are however currently very expensive, and a vehicle that would include this type of system would most likely also contains other sensors that could be fused with the laser ranged estimate.

A similar method can be applied using cameras that identify the movement of points in an image between frames due to the relative movement of the camera and the recorded scene. This movement is called the optical flow. By using the geometry of the vehicle, road, and camera, it is possible to identify the relative location and orientation of a planar surface based on the optical flow of its constituent points. The resulting successively identified planes can be used in the same way as discussed in the laser ranger example above. A vehicle motion and orientation detection method capable of estimating, among other things, the relative road grade of a road segment ahead of a vehicle is described in (Suzuki and Kanada, 1999). Front-facing cameras are becoming common in modern vehicles, but precise optical flow identification is still a difficult and computationally demanding task. For the purpose of road grade estimation other sensors provide a more cost efficient solution, but the connection

between the detected image and the road grade may still be of importance. A known future road grade (and possibly other road properties) may be used in image based object detection algorithms to improve performance and robustness.

2.7 Road Grade Requirements

The road grade information available in the vehicle will of course never be completely accurate. The effects of errors in the road grade depend on the system where the information is used. An optimal speed controller is used as an example of how road grade errors affect control performance. If the actual road grade profile does not match the assumed profile when an optimal speed profile is calculated the control action that results will not remain optimal. To illustrate the effect of moderate errors in the road grade on optimal speed control a Monte Carlo simulation is made for a slightly perturbed simple road profile where the optimal speed trajectory is known for the nominal case. The results described in this section have previously appeared in (Sahlholm, 2008).

The road grade error model used is based on a filtered White Gaussian Noise (WGN) signal. A second order low-pass filter has been applied to the white noise sequence to obtain a time varying error signal with zero mean but mainly low frequency components. The resulting vertical error around the critical point of the nominal road profile is essentially zero mean normally distributed with $\sigma = 0.66\,\mathrm{m}$. The resulting road profiles are shown in Figure 2.8.

The resulting energy consumption for two different speed profiles is calculated in the analysis. The reference speed profile is the one that would result from a standard vehicle cruise controller. This means that as long as a torque contribution from the engine is required, in order to maintain a speed of at least 85 km/h, the appropriate torque is applied. If gravity accelerates the vehicle above this speed, fueling is cut and the vehicle is allowed to accelerate. The brake system is used to ensure that the vehicle never exceeds 90 km/h. The cruise controller speed strategy results, when it is applied to the test roads, are shown as a solid line in Figure 2.9.

The second speed profile is based on the optimality results in (Fröberg, 2008). The allowable speed range is between 80 km/h and 90 km/h, with a set speed for level road segments of 85 km/h. There is also a requirement that fuel must not be saved by lowering the average speed. To achieve this, an extra cost corresponding to the energy required to make up any lost time after the downhill segment is added to the end result. The resulting strategy involves cutting off fueling at the exact moment that will give a speed of 80 km/h when the vehicle reaches the point on the hill where it will start to accelerate solely under the influence of gravity. This point will be referred to as the *critical point*. The results of the second speed strategy, applied to the perturbed roads, are shown Figure 2.9. On level road the coasting deceleration distance for the test vehicle from 85 km/h to 80 km/h is about 170 m. On a gradually steeper hill the distance can be much longer, on the nominal test road it is 320 m.

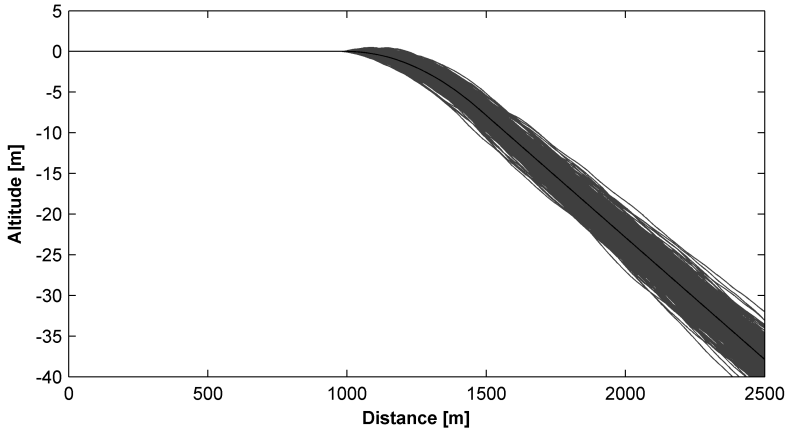

Figure 2.8: Road altitude as a function of distance for the 500 test road profiles (gray, solid) generated by application of a disturbance generated from filtered WGN to the nominal road grade from the point (983 m) where the two speed strategies start to differ. The nominal altitude profile is also shown (black, solid).

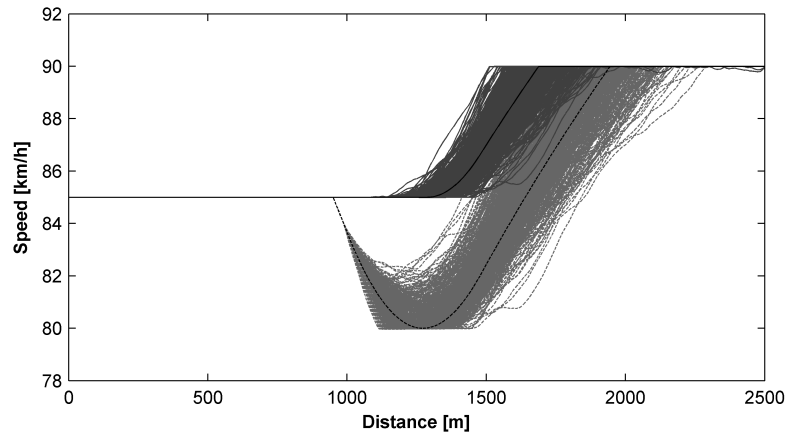

Figure 2.9: Speed profiles resulting from the randomly disturbed road grade profiles. Results from the cruise control (dark gray, solid) are shown together with results from the optimal control (light gray, dashed). The speed profiles based on the nominal altitude profiles are included as black lines.

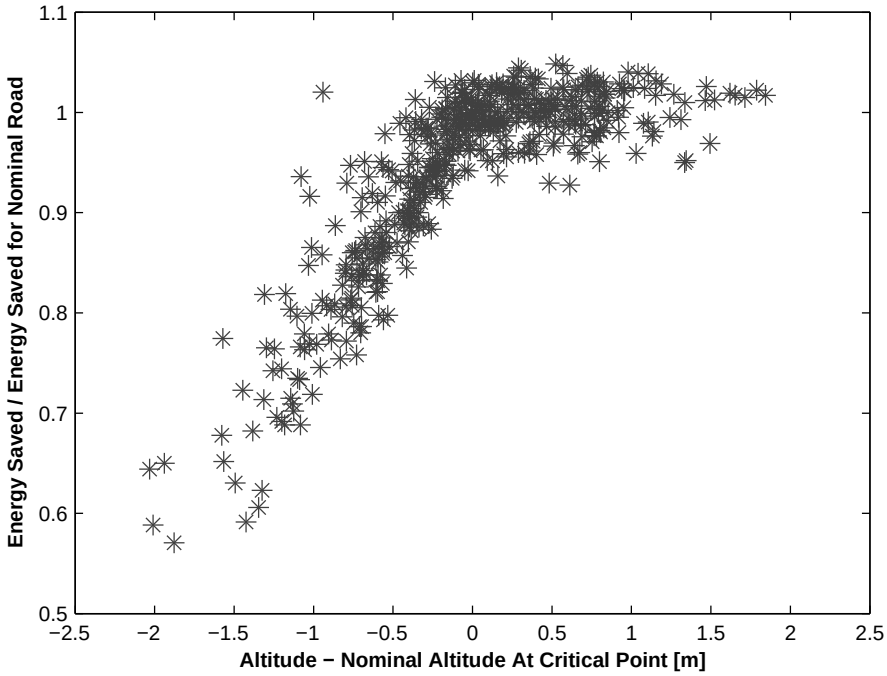

Figure 2.10: Results from the random process grade bias experiment. The ratio of energy saved when driving a modified road to energy saved when driving the reference road is shown against the magnitude of the altitude error at the nominal critical point. A negative altitude error causes the mean realizable energy savings to decrease almost linearly to about 60 % for an error of −1.6 m. Positive altitude errors have no mean effect on the energy savings, the average ratio is close to 1 for the investigated range of positive errors.

The realized energy savings for each disturbed road profile divided by the nominal energy savings were investigated based on the vertical error at the critical point of the nominal road profile. The results are shown in Figure 2.10. The ratio of realized to potential energy savings is essentially 1 for small vertical errors. For negative errors (the disturbed road has descended further than the reference road) the realized energy savings decreases almost linearly. When the disturbance causes a vertical error of −1 m approximately 75 % of the nominal energy savings are realized. This effect can intuitively be attributed to the fact that the vehicle does not slow down enough to take full advantage of the downhill grade.

For positive errors (the disturbed road has descended less than the reference road) the effects are less severe. The realized energy savings are essentially identical to the optimal case. In these cases the vehicle slows down to 80 km/h before the critical point, and then maintains that speed using the engine. The lost time penalty applied is not severe enough to cause an increase in the total energy cost.

2.8 Measurements

An important property of the presented road grade estimation method is that it only relies on sensors that are commonplace in HDVs, and that will most certainly be available in vehicles that are to be equipped with map based predictive control. It is thus suitable for deployment in a large number of vehicles, without significant hardware costs, given that the computational and data storage requirements can be met by the vehicle platform. The restriction of creating a method based on existing mass market sensors limit the accuracy that can be expected from the input data. The grade estimator is thus constructed to use many measurements from the same location in the map creation process.

2.8.1 Driveline Sensors

The method relies on two continuous signals to be sensed in the vehicle driveline; the engine torque and the vehicle speed. Information is also required about the current gear, when gearshifts occur, and when any of the braking systems present in the vehicle are activated.

Modern HDVs generally feature a distributed control system, with a number of interconnected electronic control units. These control units communicate in a network, usually an implementation of the Controller Area Network (CAN) described in the ISO standard (ISO 11898-1:2003, 2003). The vehicles used in this study broadcast all the needed signals on their CAN buses.

The speed sensor is a part of the anti-locking brake system. This system monitors the speed of each individual wheel, to avoid lock-ups during braking. The speed is determined by counting the number of teeth on a gear passing by a pickup during a unit of time. The average of the speed sensed on the front wheels is used as the vehicle speed. The front wheels are generally not driven, except on all-wheel drive vehicles, and are as such preferable from a slip perspective.

The current gear and gearshift signals are broadcast by the gearbox control unit. If the vehicle is equipped with a manual gearbox, it does not have such a unit. In that case the signals can be recreated by using the engine speed and wheel speed signals that are still present. The ratio between these speeds will either be consistent with a particular gear, in which case the conclusion is drawn that the indicated gear is engaged. If the ratio varies or is inconsistent with any gear a gearshift is signaled.

The engine torque is calculated and broadcast by the engine control unit. It is determined by the engine state, and how much fuel is injected during each cycle. The amount of injected fuel is in turn governed by how long the fuel injectors stay open. The opening times required to come as close as possible to providing the torque requested by the driver are calculated by the control unit before each injection. The expected engine torque is sent on the communication bus as a percentage of the maximum torque for the engine.

2.8.2 Satellite Based Positioning

Satellite based positioning systems are rapidly becoming ubiquitous not only as personal navigation devices, but also as parts in many more complex products. In the near future it is anticipated that the majority of HDVs being sold will have at least one satellite based positioning device built in. These devices will not necessarily provide navigation services to the driver, but rather support other functions integrated into the vehicle. Various fleet management and remote surveillance services are quickly becoming essential for the operation of a modern and competitive transportation network. A basic set of such services may include periodical status updates on position, speed, and fuel consumption from a vehicle to the traffic office, an alert system that triggers if a vehicle leaves its normal operating area and status updates about the vehicle condition to the function responsible for vehicle maintenance. This information stream from the vehicle enables more efficient resource utilization in fleets, increases safety, and lets the operator schedule maintenance when it is needed instead of with specific time or distance intervals.

Access to the absolute vehicle position also opens up the possibility of repeated measurement of a particular road segment using vehicle sensors. In this work we utilize this to update a road grade estimate each time the vehicle has been driven along a certain road segment. A GPS device is used both as a sensor in the road grade estimator, and as the means of synchronizing data sets from multiple runs along a road.

While there are several, regional, and global, satellite navigation systems available or entering service, only the GPS system has been used in this project. It is understood that any such system could be used instead, but only the term GPS will be used henceforth. Future systems will most certainly improve performance and introduce new features that can improve the performance of the proposed grade estimator.

The GPS works by measuring the time it takes for radio signals to travel from satellites to a receiver on the ground. Knowing the speed that the radio signal propagates at, it is possible to determine the distance to each of the satellites. The positions of the satellites themselves are transmitted to the receiver at the same time as the propagation time is identified, and it is thus possible to determine the position of the receiver as well. In general the receiver does not have access to a calibrated time signal, so the current time has to be determined from the satellite signals as well. To determine the three-dimensional position of the receiver a total of four unknowns (latitude, longitude, altitude, and time) have to be determined. This calculation requires four satellites to be visible. A more thorough description of the satellite navigation systems is beyond the scope of this work, but a good starting point for a general overview without too much mathematics is (El-Rabbany, 2006). A thorough treatment of the subject, including the relevant equations, is given in (Misra and Enge, 2006).

As the European Galileo navigation satellite system becomes operational, in 2014 according to the planned schedule, both the accuracy and reliability of satel-

lite based positioning will increase (EC, 2010). This does not however change the fundamental limitations that satellite based positioning systems face. Vehicle based sensor signals will still play an important role in providing a high quality road grade estimate in as few passes over the terrain as possible.

GPS Measurement Errors

By their nature GPS receivers output absolute position fixes, with an error that does not grow over time. This makes well suited to compensate for modeling and parameter errors that cause static errors. On average, over very long time periods, the GPS will be very precise. The short term errors of a consumer grade GPS receiver however, often exhibit large sudden jumps and subsequent slow drifts due to the internal filtering logic applied.

The accuracy of the position given by the GPS is very important for the correct functioning of the grade estimator. The error in the vertical position reported by the GPS will directly influence the estimated road grade, and the horizontal positioning error will cause grade estimates from different points on the road to be merged together. Since the proposed system is designed for use in a cost-sensitive environment a standard low-cost single channel GPS receiver will have to suffice. Such a receiver delivers what is called a standard positioning service, and has a typical 10 m horizontal and 15 m vertical accuracy. The accuracy figure is given as the 95th percentile of the error distribution (Misra and Enge, 2006, page 49). The error at any given time is dependent on the receiver used as well as the atmospherical conditions, the receiver surroundings, and the satellite geometry. The satellite geometry portion of the error is commonly described by a Dilution Of Precision (DOP) number. This is broadcast by many receivers as an aid to the user in determining the quality of a given position estimate.

A particularly troublesome error source is multipath effects, that occur when both reflected and direct signals from a satellite reaches the receiver antenna. The receiver will then process the sum of all the signals, and may obtain a satellite range measurement with a large error. As the vehicle moves the reflections will change quickly. This can lead to severe noise in the delivered position. Many large reflective sources, such as mountains and buildings, are stationary and are likely to cause trouble every time the vehicle passes them.

The major error sources, except multipath, in the GPS system are slow varying, which means that measurements taken over short time intervals likely will have a bias as the major error component. Over long periods of time the GPS position estimates are bias free and the error approximately normally distributed. In our grade estimation application this means that adjacent GPS measurement points will likely have a slow varying bias, with a period of several hours. Grade estimates for a specific location however, will be based on uncorrelated normally distributed measurements. This is a prime motivation for developing a method for fusion of many measurements spread over time into one road grade estimate. In the proposed estimators the GPS signal is averaged over many measurements, to provide

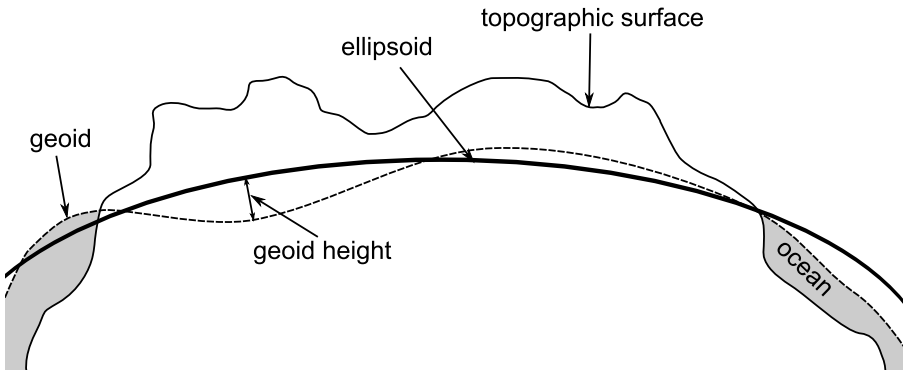

Figure 2.11: The ellipsoid, geoid, and topographic surface of the earth are illustrated. The mean sea level, without effects of wind and tides, is equal to the geoid.

vehicle model bias compensation. Over short time periods the vehicle model derived estimates are generally more reliable.

Measuring Altitude Using GPS

The altitude component of the position obtained by calculating distances from GPS satellites is not related to gravity. It represents the distance from the rotational center of the earth, minus the distance from that center to an ellipsoid. The ellipsoid major and minor axes have been chosen to give the ellipsoid surface a distance from the sea level that is zero on average. The force of gravity though, is not perfectly evenly distributed around the earth. Therefore the local sea level at many locations does not match the zero level of the ellipsoid.

To obtain an altitude measurement relative to the local sea level the ellipsoidal altitude must be adjusted by the geoid height. The different earth models and are illustrated, and the height measures defined, in Figures 2.11 and 2.12. To determine the local geoid height N, with high accuracy, based on a geoid model, requires extensive computations and is not suitable for a handheld battery powered device. Instead, a lookup table with a grid of correction values is generally used. This table is not necessarily identical between receivers of different makes and models, although EGM96 is a commonly used geoid model when generating it.

Due to the changes in geoid height, one may travel horizontally at the same ellipsoidal height h, but still go up or down in the gravitational field. The road grade of interest for vehicle control is the angle relative to the gravitational field, since the effect of gravity is generally the cause for the interest in the road grade. An implementation of a road grade estimation system using GPS should thus use orthometric heights rather than ellipsoidal ones. In practice the difference between an ellipsoid approximation of the earth and the geoid changes very slowly compared to the changes in the road altitude profile.

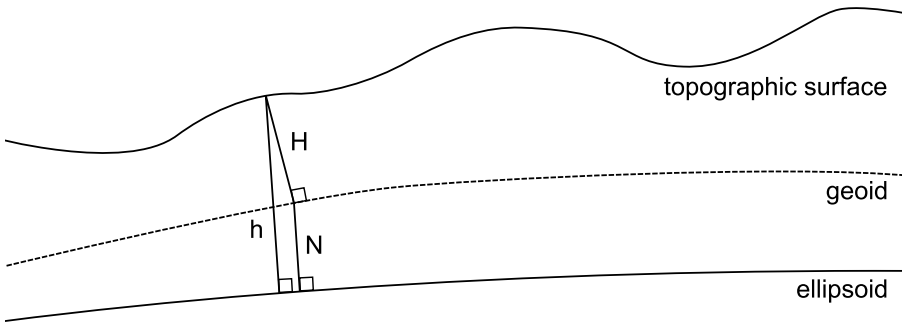

Figure 2.12: The ellipsoidal height from the GPS h, can be used to obtain the orthometric height H, if the geoid height N, is known.

2.9 Summary

There is a growing need for accurate road grade maps due to advances in vehicle control technology. Vehicle efficiency and safety, as well as driver comfort, can be improved in a number of ways using stored road grade information. The use and distribution of advance digital maps is an active research area, with several recent European research projects. There is as of yet no standard solution to how these maps shall be obtained, even though a number of proposals for how the road grade can be estimated have already been made. Systems for estimating the instantaneous road grade have been used in vehicles for some time, but these cannot directly provide the preview information required by the emerging control systems. Maps created automatically by vehicles, or hand edited maps enhanced by automated estimation of features, is one potential way of getting good coverage and accuracy at a low cost.

Many different vehicle control applications that will clearly benefit from access to accurate road grade maps have been proposed. Due to the large potential for saving energy, predictive cruise control is anticipated to be an early application of preview road grade information in HDVs. This application was therefore chosen for an analysis of the effects of errors in the road grade data. The results indicate that 75 % of the potential gain remains with an altitude error of 1 m after a distance of 320 m.

An important feature of the proposed method is that only standard truck sensors are used in the road grade estimators. This opens up the possibility of mass deployment of the system, without significant hardware cost. The sensors already available in vehicles give the signals necessary for the operation of the proposed estimators, but the accuracy is not sufficient to produce road grade profiles for predictive control based on only one experiment. The use of a GPS sensor is crucial, since it gives a stationary, although noisy, absolute altitude measurement. The ve-

hicle model based estimates will always show some bias, but appropriate use of the GPS can minimize its effect. Related works contain many of the components used in the proposed estimators, but the combination of using a vehicle model, driving event detection, GPS, and many experiments, to create an iteratively improved road grade map is novel.

Chapter 3

Modeling

> "*A mathematical model does not have to be exact; it just has to be close enough to provide better results than can be obtained by common sense.*"
>
> Herbert A. Simon

The first step in developing the methods for road grade estimation investigated in this thesis is to obtain a model that links the observable signals vehicle speed v, altitude z, and engine torque T_{e}, to the road grade α. This chapter starts with a description of how a vehicle model is derived from a representation of the longitudinal dynamics of an HDV as a function of time. In order to implement the estimator we also need a model for how the road grade signal develops, which is provided in Section 3.2. To facilitate merging of measurement data from multiple runs along the road, the vehicle model is then transformed into the spatial domain and discretized. Next, the two sub-models are put together into a complete description of the road-vehicle system, to be used in the road grade estimators. A simulation study has been conducted to complement the experiments. The simulation models are described in Section 3.4. A summary of the modeling efforts concludes the chapter.

The total system description is given by the state space representation in (3.1).

$$\begin{aligned} \frac{dv}{ds} &= f_v(v, \alpha, T_{\mathrm{e}}) \\ \frac{dz}{ds} &= f_z(\alpha) \\ \frac{d\alpha}{ds} &= f_\alpha(s) \end{aligned} \tag{3.1}$$

The states are vehicle speed v, the road altitude z, and the road grade α. The independent variable s, in the final model, is the distance along the road.

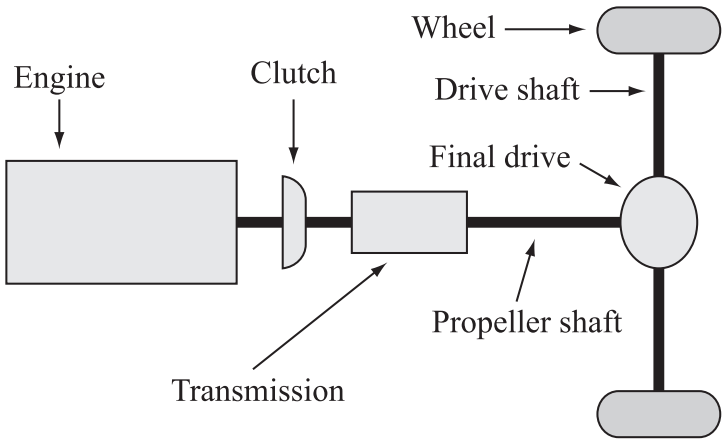

Figure 3.1: Powertrain components for a rear-driven diesel powered truck.

3.1 Vehicle Models

A basic vehicle model that describes one-dimensional longitudinal movement and links engine torque, vehicle speed, and road grade is sufficient to support the road grade estimation. Only the relatively low frequency dynamics of the vehicle itself is of interest. Higher frequency phenomena such as driveline oscillations and torsional vibration in the propeller and drive shafts can thus be ignored. The model is developed based on straightforward mechanical relations and Newton's laws of motion. The development of the vehicle model is done in continuous time. This section provides an overview of the components included in the vehicle model, and how they are represented. More details on the various subsystems and their representation can be found in (Kiencke and Nielsen, 2003).

3.1.1 Powertrain Models

The powertrain of the vehicle includes the engine and a system to transfer power to the road surface over a broad range of vehicle velocities, while maintaining a restricted range of possible engine speeds. A powertrain for a rear-wheel–driven vehicle consisting of engine and a driveline is shown in Figure 3.1. The various parts of the powertrain are described individually before they are put together to form a complete model. The notation for torques and angles used in the model is given in Figure 3.2.

Engine

A typical truck engine runs on diesel fuel and has an operating range of 500–1900 rpm. Most of the thermodynamic processes of the engine are not important in

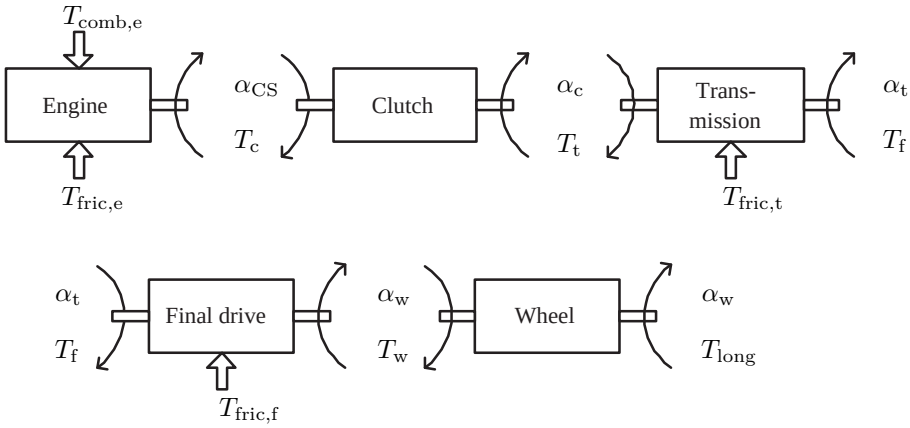

Figure 3.2: Subsystems and notation for the torques and angles used in the powertrain model.

our model, so it will be considered as a black box that generates torque. The one part of the engine operation that we do care about is how much torque it generates. An estimate of the generated torque is continually broadcast by the engine management system, as described in Section 2.8.1. The engine dynamics is the net result of torque generated from the internal combustion ($T_{\text{comb,e}}$), engine friction and pumping losses ($T_{\text{fric,e}}$), and the external load from the clutch (T_{c}). From Newton's second law of motion, using dot notation to indicate derivatives with respect to time, the model becomes

$$J_{\text{e}}\ddot{\alpha}_{\text{cs}} = T_{\text{e}} - T_{\text{c}} \tag{3.2}$$

where J_{e} is the mass moment of inertia of the engine including the flywheel. α_{cs} is the crankshaft angle and $\ddot{\alpha}_{\text{cs}}$ is the crankshaft acceleration. The quantity

$$T_{\text{e}} = T_{\text{comb,e}} - T_{\text{fric,e}} \tag{3.3}$$

is available as a measurement reported on the vehicle CAN bus, and will be used as an input signal in the model.

Clutch

A vehicle equipped with a manual gearbox generally has a friction clutch, which is used to disengage the engine from the rest of the driveline while idling without moving to neutral and when changing gears. In the current model idling with the clutch depressed is not distinguished from running in neutral gear, and gearshifts are considered to be instantaneous. The clutch can thus be considered as a solid massless shaft, and the torque and angular velocity do not change. This gives the

model

$$\dot{\alpha}_{\mathrm{cs}} = \dot{\alpha}_{\mathrm{c}} \tag{3.4}$$

$$T_{\mathrm{c}} = T_{\mathrm{t}} \tag{3.5}$$

Transmission and Final Drive

The task of the transmission and the final drive is to match the engine speed to the wheel speed. The gear ratio in the transmission can be varied by shifting gears, while the ratio in the final drive is fixed for a particular vehicle. In each engagement of gears there is a small transmission loss incurred as power is transferred. For our purposes the loss can be modeled as a percentage of the output torque. The transmission and final drive are considered stiff, and their respective inertias are neglected. For the transmission we get an expression for the friction loss torque

$$T_{\mathrm{fric,t}} = (1 - \eta_{\mathrm{t}}) i_{\mathrm{t}} T_{\mathrm{t}} \tag{3.6}$$

where i_{t} is the current transmission gear ratio and η_{t} is the torque transfer efficiency for the current gear. Using this loss model the transmission model can be written as

$$\dot{\alpha}_{\mathrm{c}} = \dot{\alpha}_{\mathrm{t}} i_{\mathrm{t}} \tag{3.7}$$

$$T_{\mathrm{t}} i_{\mathrm{t}} - T_{\mathrm{fric,t}} = \eta_{\mathrm{t}} T_{\mathrm{t}} i_{\mathrm{t}} = T_{\mathrm{f}} \tag{3.8}$$

It is important to consider the angular velocity of the transmission rather than the angle. Otherwise, there will be an error when switching gears (changing i_{t} when $\alpha_{\mathrm{t}} \neq 0$).

Between the transmission and the final drive there is a propeller shaft that is considered stiff. The final drive is described in the same way as the transmission, but the gear ratio will never change. The friction losses in the final drive are labeled $T_{\mathrm{fric,f}}$, and calculated from the efficiency η_{f}. The final drive model becomes

$$\dot{\alpha}_{\mathrm{t}} = \dot{\alpha}_{\mathrm{w}} i_{\mathrm{f}} \tag{3.9}$$

$$T_{\mathrm{f}} i_{\mathrm{f}} - T_{\mathrm{fric,f}} = \eta_{\mathrm{f}} T_{\mathrm{f}} i_{\mathrm{f}} = T_{\mathrm{w}} \tag{3.10}$$

where α_{w} is the wheel rotation angle and T_{w} is the wheel torque.

The transmission ratio used in the simulation model is chosen based on the active gear. Neutral gear and open clutch situations require special care, since there is no fixed ratio between the input and output speeds in the transmission during these times. Gearshifts without clutch depression are considered to be instantaneous switches between transmission ratios. Manual gearshifts with the clutch depressed are treated as a move from the original gear into neutral, and then from neutral into the new gear. The neutral gear is represented by a zero torque transfer between the engine and the rest of the driveline.

Wheels

The driven wheels constitute the contact point where power can be transferred between the powertrain and the road. Rotation and torque in the powertrain are linked to longitudinal movement and forces acting on the vehicle through the wheels. A vehicle model including the effects of both torques and forces acting in the direction of travel can be created by transforming the powertrain torque into a longitudinal force. Under the assumption of a rolling condition (no slippage in the contact point between the tires and the ground)

$$\dot{\alpha}_{\mathrm{w}} = \frac{v}{r_{\mathrm{w}}} \tag{3.11}$$

the transformation is straightforward. Here r_w is the effective wheel radius, $\dot{\alpha}_{\mathrm{w}}$ is the wheel speed, and v is the vehicle speed.

When the vehicle speed changes, the moment of inertia of all the wheels has to be overcome. For a passenger car the number of wheels is generally four. For HDVs it can vary between six and twenty, or even more. The rotational dynamics of all the wheels are given by

$$J_{\mathrm{w}}\ddot{\alpha}_{\mathrm{w}} = T_{\mathrm{w}} - T_{\mathrm{long}} \tag{3.12}$$

where J_{w} is the total wheel moment of inertia, and T_{long} is the torque induced by the resisting forces and longitudinal mass inertia of the vehicle. The longitudinal force F_{long}, from the powertrain is related to the torque through

$$F_{\mathrm{long}} = \frac{T_{\mathrm{long}}}{r_{\mathrm{w}}} \tag{3.13}$$

Flexibilities and Backlash

The forces affecting an HDV driveline are large, and quite capable of twisting the driveshafts and the propeller shaft considerably. It is in fact quite possible to break the drive shafts by accelerating hard in a low gear with a heavy load. Consequently, an accurate representation of the driveline dynamics would require flexible components rather than stiff. This would allow for the representation of the energy stored in twisted shafts. The driveline flexibilities are however mainly of importance during quick changes in the transferred torque, and give rise primarily to high frequency oscillations. The road grade generally changes much more slowly, as seen in Section 3.2, and we are thus content with excluding these factors.

Play between different parts of the driveline can give rise to backlash effects when the torque changes rapidly. This also causes high frequency oscillations in the driveline. Backlash oscillations are ignored, on the same grounds as the torsional effects of the shafts.

3.1.2 External Forces Acting on the Vehicle

In addition to the influence of the powertrain, the external environment affects the vehicle in a number of ways. Air drag generates a resisting force, and so does wheel

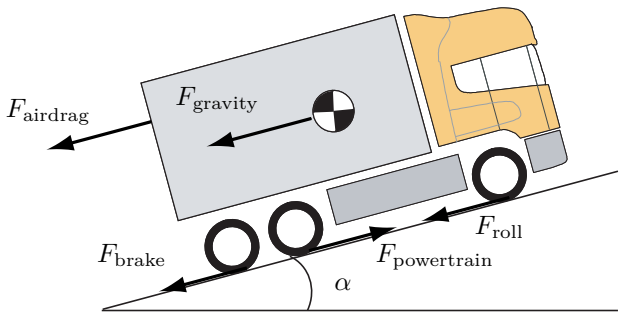

Figure 3.3: Longitudinal forces acting on the vehicle.

roll friction. The road topology can give rise to either a resisting or assisting force. If the brakes are applied this is regarded as a longitudinal resisting force, even though it might just as well have been included with the powertrain torques and considered as a resisting torque on the wheels.

The most important forces affecting the vehicle and the sign conventions used are shown in Figure 3.3. The forces are generally time varying; time has been left out of the equations for clarity of notation. $F_{\text{powertrain}}$ has been described above.

At highway speeds the air drag can be quite considerable. For the 39 t tractor and semitrailer combination used in the experiments the air drag accounts for 41 % of the total modeled resistive force when traveling at 80 km/h on a flat road. The force

$$F_{\text{airdrag}} = \frac{1}{2} c_{\text{d}} A_{\text{a}} \rho_{\text{a}} v^2 \tag{3.14}$$

is calculated based on the measured vehicle speed v, and the vehicle model parameters, air drag coefficient c_{d}, vehicle frontal area A_{a}, and air density ρ_{a}. The true air density varies with meteorological conditions and the altitude. In this work the air density is described by a constant, whose value is chosen to be representative for the test site temperature and altitude ranges.

A first order model and small angle assumption for the road grade α gives the rolling resistance

$$F_{\text{roll}} = mgc_{\text{r}} \cos\alpha \approx mgc_{\text{r}} \tag{3.15}$$

where the vehicle mass is m, gravity g, and c_{r} the coefficient of rolling resistance. Being proportional to the vehicle weight the rolling resistance becomes large for a fully loaded vehicle. For a very heavy or streamlined vehicle, it will exceed the air drag at many speeds. For the example vehicle above the rolling resistance accounts for the remaining 59 % of the resistive force when traveling at a constant speed of 80 km/h on a flat road.

The road grade α is included in the model through the gravity induced force

$$F_{\text{gravity}} = mg \sin\alpha \tag{3.16}$$

Even a small road grade generates a considerable force, for our example tractor and trailer combination, an 1 % uphill grade increases the total resistive force by 84 %, if the speed is unchanged.

The brake force F_{brake} is excluded from the model since it is generally unknown in a standard HDV. Its effects are considered at a later stage, as described in Section 4.1.3.

3.1.3 Vehicle Motion

The measured quantities related to the longitudinal vehicle motion are the engine torque and the vehicle speed. The powertrain equations and the resisting forces are combined in the model in such a way that the acceleration $\dot{v}$, is expressed as a function of the current vehicle speed v, the net engine torque T_{e}, and the vehicle parameters. By combining the rotational moments of inertia in the powertrain with the longitudinal mass inertia into a total inertial mass through the gear ratios and efficiencies already described, the longitudinal force from the powertrain F_{long} can be treated as an external powertrain force $F_{\text{powertrain}}$, given by

$$F_{\text{powertrain}} = \frac{i_{\text{t}} i_{\text{f}} \eta_{\text{t}} \eta_{\text{f}}}{r_{\text{w}}} T_{\text{e}} \tag{3.17}$$

The total inertial mass m_{t} for the vehicle is given by

$$m_{\text{t}} = m + \frac{J_{\text{w}}}{r_{\text{w}}^2} + \frac{i_{\text{t}}^2 i_{\text{f}}^2 \eta_{\text{t}} \eta_{\text{f}} J_{\text{e}}}{r_{\text{w}}^2} \tag{3.18}$$

By using Newton's second law of motion and the forces described above we get a time domain model for the changes in the longitudinal vehicle speed, expressed as

$$\dot{v}(t) = \frac{1}{m_{\text{t}}} (F_{\text{powertrain}} - F_{\text{airdrag}} - F_{\text{roll}} - F_{\text{gravity}}) \tag{3.19}$$

This model, expressed with distance as the independent variable, provides an implementation of $dv/ds = f_v(v, \alpha, T_{\text{e}})$ in the state space model (3.1).

3.2 Road Models

In order to estimate the road grade, a model for it is developed. Since roads are fixed in space, but may be traversed at any speed it is natural to express the road model in spatial coordinates, i.e., with the distance along the road as the independent variable. Roads are built according to specifications determined by construction engineers. For every type of road and legislative region there are regulations that transcribes into requirements for the design. An efficient way of determining the road grade could be to request it from the authority that approved the design. With knowledge of the quality requirements for the constructions process, and the planned road layout it should, in theory, be possible to get a road grade estimate

Table 3.4: Maximum allowable road grade α for various road quality classes in Sweden. Excerpt of table 13-1 in (Swedish Road Authorities, 2004)

	High Standard	Medium Standard	Low Standard
Countryside	6 %	7 %	8 %
Urban, main road	6 %	7 %	8 %
Urban, intersection	2.5 %	3.5 %	9 %

within a known error interval. Unfortunately reality does not agree with theory in this case and construction data are rarely readily available. Some benefits can nevertheless be had from studying road building specifications, since they give a basic idea of what type of dynamics might be expected in the road grade signal.

The specifications for Swedish roads give a good starting point for a model to describe highway road grades. The Swedish road authority has published a document, "Vägars och gators utformning" (Swedish Road Authorities, 2004), that lists requirements and guidelines for all current road construction. Some existing roads may not fully comply with these guidelines, but they will nevertheless serve as a starting point for our road model. The road grade estimation method described in this work is focused on estimating highway grades. As seen in Table 3.4 the requirements state that a highway should preferably have a road grade below 6 %. The grade may only exceed 8 % during short periods and due to exceptional circumstances (Swedish Road Authorities, 2004, p. 102). The desired road quality has to be chosen at design time, and is related to the expected traffic load. These numbers may be higher for highways in other countries, as the topography of for example the Alps would most certainly be regarded as exceptional circumstances by Swedish standards.

Furthermore, the document states that vertical road profile should be made up from segments with constant grade and vertical curves. The vertical curves are to be carried out as linear transitions, i.e., the altitude profile should be described by a parabola where the vertical offset is proportional to the square of the distance. The same model for vertical curves is also used in the guidelines for highway construction in the United States (AASHTO, 2001, p. 270). Mathematically, concave curves going into more uphill gradients, are described by the parabola

$$\Delta z(l) = \frac{l^2}{2R} \tag{3.20}$$

where $\Delta z(l)$ is the relative altitude, and l is a horizontal distance, measured relative to the lowest point of the parabola, and R is a design parameter. A vertical transition curve from a flat road to a constant uphill grade is illustrated in Figure 3.5. For the magnitudes of l used in this application the parameter R essentially repre-

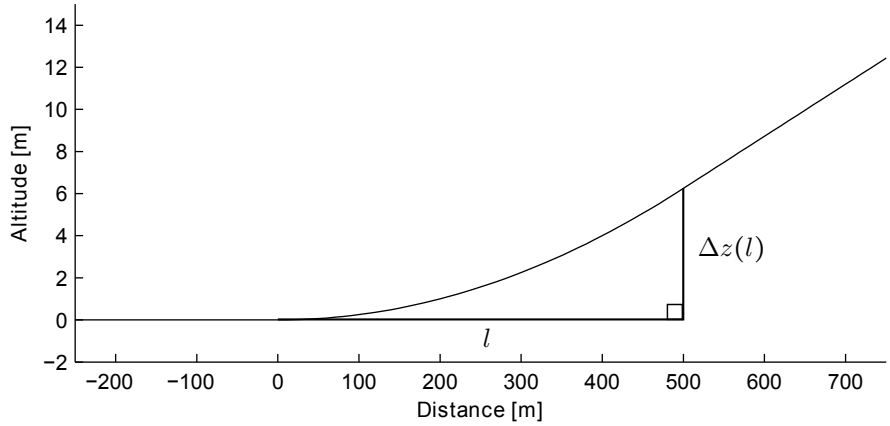

Figure 3.5: Road design guidelines state that vertical curves are to be laid out as parabolas. The figure shows the altitude of a road section with a transition from a grade of 0 % to a constant uphill grade of 2.5 %, with a radius parameter of $R = 20\,000$.

sents the radius of a circular arc similar to the specified parabola. The part of the parabola to use is determined by the road grades at the start and end of the vertical curve. For convex vertical curves, i.e., hilltops, the parabola is flipped upside down.

The designed sizes of the parabolas depend on a number of factors such as traffic safety, driving dynamics, visibility conditions, terrain, and esthetics. The chosen vertical arc length and radius parameter have to match the surrounding terrain, and provide sufficient visibility for drivers to be able to stop before unexpected obstacles. This is particularly an issue for convex vertical curves, i.e., hilltops. For a major highway to be considered to have a good visibility standard when designed for a speed of 110 km/h the minimum radius, as listed in Table 3.6, is $R = 16\,000$ m. If the arc length is so short that it does not limit visibility the limiting requirement becomes comfort, and the limit is $R = 2\,200$ m. There are also regulations in place requiring a certain density of overtaking opportunities. To provide enough sight distance for overtaking on a convex vertical curve, a radius on the order of $R = 100\,000$ m is required.

For concave vertical curves the constraint on minimum radius for arc lengths long enough to limit visibility is $R = 6\,500$ m on major highway with a high visibility standard. If the maximum speed is restricted to 90 km/h it is allowed to design with $R = 4\,500$ m for high visibility standard, and $R = 3\,500$ m for low visibility standard. These limitations are based on requirements for headlamps and their illumination cone. A potential obstacle in a vertical curve must be illuminated in time for the driver to have a chance to stop before impact. For short arc lengths, which do not limit visibility, the limits are the same as for convex curves.

Based on the assumption that the vertical road profile can only consist of seg-

Table 3.6: Minimum convex vertical curve radius R for roads with at least two lanes with regard to sight distance for passenger cars. High, medium, and low refers to the chosen visibility standard for the road. Excerpt of table 11-1 in (Swedish Road Authorities, 2004)

v_{ref} [km/h]	Environment	High [m]	Medium [m]	Low [m]
50	Urban, main road	1 200	400	300
70	Countryside	3 000	1 800	1 200
70	Countryside	3 000	1 200	1 800
90	Countryside	7 000	6 000	5 000
110	Countryside	16 000	13 000	9 000

ments with constant road grade, or parabolic segments as described above we obtain a road model with the distance along the road as the independent variable. For the road grade magnitudes of interest a small angle approximation can be made for arctan. Letting the altitude of the lowest/highest point of a vertical curve parabola be given by $z_0 = z(0)$ gives an expression for the road grade (in radians) as

$$\begin{aligned}\alpha(l) &= \arctan\left(\frac{d}{dl}(z_0 \pm \Delta z(l))\right) \\ &= \arctan\left(\pm\frac{d}{dl}\frac{l^2}{2R}\right) \\ &\approx \pm\frac{d}{dl}\frac{l^2}{2R} = \pm\frac{l}{R}\end{aligned} \tag{3.21}$$

The change in the road grade α can thus be approximated as

$$\frac{d\alpha}{dl} \approx \pm\frac{1}{R} \tag{3.22}$$

Since the approximation of $d\alpha/dl$ does not depend on l, the distance from the start of a local parabola l, can be replaced by s, the distance along the road. The model indexed by s is still only valid locally. Dividing the road into N segments we then have local models

$$\frac{d\alpha_i}{ds} = \pm\frac{1}{R_i} = c_i,\ \ i = 1, \ldots, N \tag{3.23}$$

for convex and concave vertical curves between the segment end points. At the junction between two segments different assumptions will be made for different estimation methods. The methods and associated road model assumptions are described in Sections 4.2.2 and 4.2.3.

Since the true road grade model, assuming the road has been built as prescribed by today's standards, varies with distance, the task of choosing a suitable representation becomes a delicate one. Using a road grade model that includes a piecewise linear change in the road grade, with unknown knot points between the linear segments, would introduce the difficulty of finding the knot points in addition to the grade itself. This would lead to a hybrid continuous/discrete estimation problem. The change in the true road grade signal is physically limited to be slow, an alternative model is thus to adopt a simpler model

$$\frac{d\alpha}{ds} = 0 \tag{3.24}$$

and account for the change in the road grade through a noise term. Both approaches have been investigated, as described in Chapter 4 and evaluated in Chapter 5. Equations (3.23) and (3.24) provide two alternative implementations for the third state equation, $d\alpha/ds = f_\alpha(s)$ in the state space model (3.1).

The sensors assumed to be available for this project include a GPS receiver capable of measuring the absolute altitude. A model for the change in altitude is adopted to relate the sensed altitude to the other measured signals. From the trigonometric relationship between the road grade angle α, the altitude z, and the traveled distance s, the model becomes

$$\frac{dz}{ds} = \sin\alpha(s) \tag{3.25}$$

This implementation of the second state equation $dz/ds = f_z(\alpha)$ completes the description of the components of the state space model (3.1).

3.3 Estimation Models

The vehicle and road models of Sections 3.1 and 3.2 need to be combined to relate all measured signals to the road grade. In this section a complete vehicle and road model is developed, for use in the road grade estimator.

3.3.1 Spatially Sampled Models

To easily obtain estimates at specific spatial locations rather than time instants a spatially sampled version of the vehicle model expressed in the time domain is derived. This is a prerequisite for effortlessly merging road grade estimates from multiple runs along a road.

After the change of independent variable the model is discretized using the sample distance Δs. By resampling measurement data from different runs along the road to represent common spatial coordinates a consistent merge can be performed. Successful resampling relies on accurate time stamps in the input signal, as well as a high quality record of the vehicle position as a function of time. The process used

for resampling time domain measurements obtained in the experiments is described in Section 5.1.4.

The vehicle longitudinal motion model given in (3.19), expressed with distance as the independent variable becomes

$$\frac{dv}{ds} = \frac{1}{vm_{\mathrm{t}}}(F_{\mathrm{powertrain}} - F_{\mathrm{airdrag}} - F_{\mathrm{roll}} - F_{\mathrm{gravity}}) \tag{3.26}$$

Discretizing the model with the sample distance Δs, and a one step forward difference approximation for the derivative, yields

$$\frac{v(s+\Delta s) - v(s)}{\Delta s} = \frac{1}{vm_{\mathrm{t}}}(F_{\mathrm{powertrain}} - F_{\mathrm{airdrag}} - F_{\mathrm{roll}} - F_{\mathrm{gravity}}) \tag{3.27}$$

where the function characteristic of all the quantities on the right hand side has been omitted. The variables v, m_{t}, $F_{\mathrm{powertrain}}$, F_{airdrag}, and F_{gravity} are all functions of the location along the road and the state of the vehicle, as described earlier.

To yield an equation suitable for determining the road grade from measurements the road grade α is isolated in the vehicle model. Using the vehicle sensors and the one step forward speed difference approximation for the acceleration, the road grade $\alpha_{\mathrm{driveline}}$ can be calculated as

$$\begin{aligned}\alpha_{\mathrm{driveline}}(s) = \arcsin\Bigg[\frac{1}{mg}\Bigg(&\frac{i_{\mathrm{t}}(s)i_{\mathrm{f}}(s)\eta_{\mathrm{t}}(s)\eta_{\mathrm{f}}(s)}{r_w}T_{\mathrm{e}}(s) \\ &- m_{\mathrm{t}}(s)v(s)\frac{v(s+\Delta s) - v(s)}{\Delta s} - \frac{1}{2}c_{\mathrm{w}}A_{\mathrm{a}}\rho_{\mathrm{a}}v(s)^2 - mgc_{\mathrm{r}}\Bigg)\Bigg]\end{aligned} \tag{3.28}$$

In all of the proposed estimation methods the vehicle model based road grade estimate is further filtered, therefore a one step difference approximation is chosen over alternatives using more estimates to either side of the current position.

A road grade estimate can also be determined directly from the GPS. This method gives a very noisy signal for all but very long sample distances. It is therefore only for illustration and as an average over a long road section. The road grade estimates obtained by directly differentiating the GPS altitude signal are shown in Figure 5.30. A central difference approximation is used to obtain a small amount of filtering. The GPS altitude based road grade estimate α_{GPS}, can be computed as

$$\alpha_{\mathrm{GPS}}(s) = \frac{z(s+\Delta s) - z(s-\Delta s)}{2\Delta s} \tag{3.29}$$

The use of the averaged GPS altitude derivative is described further in Section 4.2.2.

3.3.2 Combining the Road and Vehicle Models

Two of the proposed road grade estimation methods use a KF to estimate the states. The vehicle speed, altitude, and road grade models are therefore combined into a

non-linear state-space system model with process noise. One white noise process is added to each of the model states.

We define a discrete state vector indexed by k

$$x_k = \begin{bmatrix} v_k \\ z_k \\ \alpha_k \end{bmatrix} \tag{3.30}$$

containing the vehicle speed v, the road altitude z, and the road slope α. With the simplified, constant, road grade model (3.24) the discretized model becomes

$$\underbrace{\begin{bmatrix} v_{k+1} \\ z_{k+1} \\ \alpha_{k+1} \end{bmatrix}}_{x_{k+1}} = \underbrace{\begin{bmatrix} v_k + \Delta s \frac{dv_k}{ds} \\ z_k + \Delta s \sin \alpha_k \\ \alpha_k \end{bmatrix}}_{f_k(x_k, u_k)} + \underbrace{\begin{bmatrix} w_k^v \\ w_k^z \\ w_k^\alpha \end{bmatrix}}_{w_k} \tag{3.31}$$

where the state evolution depends on the previous state and the control signal $u_k = T_{\mathrm{e}k}$. The control signal is the engine torque, which is assumed to be measured or otherwise known. Unmodeled changes in the state variables are accounted for through the process noise w_k.

With the piecewise linear road grade model (3.23), the discretized system model becomes

$$\underbrace{\begin{bmatrix} v_{k+1} \\ z_{k+1} \\ \alpha_{k+1} \end{bmatrix}}_{x_{k+1}} = \underbrace{\begin{bmatrix} v_k + \Delta s \frac{dv_k}{ds} \\ z_k + \Delta s \sin \alpha_k \\ \alpha_k + \Delta s c_i \end{bmatrix}}_{f_k(x_k, u_k)} + \underbrace{\begin{bmatrix} w_k^v \\ w_k^z \\ w_k^\alpha \end{bmatrix}}_{w_k} \tag{3.32}$$

where the value of c_i corresponds to the linear segment that data point k belongs to.

In both (3.31) and (3.32) the rate of change in speed is determined based on (3.27), which with all model parameters inserted yields

$$\frac{dv_k}{ds} = \frac{i_{\mathrm{t}} i_{\mathrm{f}} \eta_{\mathrm{t}} \eta_{\mathrm{f}}}{r_{\mathrm{w}} m_{\mathrm{t}}} \frac{T_{\mathrm{e}k}}{v_k} - \frac{\frac{1}{2} c_{\mathrm{d}} A_{\mathrm{a}} \rho_{\mathrm{a}}}{m_{\mathrm{t}}} v_k - \frac{mg}{m_{\mathrm{t}}} \frac{1}{v_k} \left(c_{\mathrm{r}} + \sin \alpha_k \right) \tag{3.33}$$

Since the transmission ratio and associated efficiency are dependent on the engaged gear the model changes discretely at gear changes. Additionally, since the driveline friction always causes an energy loss in the direction energy is flowing, the efficiencies η_{t} and η_{f} depend on whether the net engine torque T_{e} is positive or negative. Whenever the power flow from the engine to the wheels is negative, the efficiencies become the inverse of their nominal values, causing a discrete switch in the system model. Thus, equations (3.31) and (3.32) are both time-varying discrete models with traveled distance along the road as the independent variable.

3.3.3 Linearized Model

To evaluate the influence of the nonlinearity in the vehicle model a piecewise constant linear version of the model (3.31) is also derived. The linear model is changed at gear changes and when the direction of power flow in the driveline changes. Each gear and power flow direction will lead to a different mode, denoted by an index p, added to the relevant variables. For each mode a specific torque is required to maintain a constant speed, and equilibrium in the model. The linearization point thus changes as well, when the model parameters change. The linear discretized model around the equilibrium x_p is given by the system transition matrix F_p and the input matrix G_p according to

$$\tilde{x}_k = F_p \tilde{x}_{k-1} + G_p \tilde{u}_k + w_k \tag{3.34}$$

where $\tilde{x} = x - x_p$ is the state relative to the linearization point and $\tilde{u} = T_\mathrm{e} - T_{\mathrm{e}p}$ is the engine torque difference from the equilibrium torque. The transition matrix is given by $F_p = I + J_f(x)|_{x_p,u_p}\,\Delta s$, where $J_f(x)|_{x_p,u_p}$ is the first three columns of the Jacobian for the nonlinear system transfer function. We also have $G_p = J_f(u)|_{x_p,u_p}$, where $J_f(u)|_{x_p,u_p}$ is the fourth column of the Jacobian. Using the model the system transfer function based on the constant road grade model, F_p and G_p become

$$F_p = \begin{bmatrix} 1 + \frac{\partial f_v}{\partial v}\big|_{x_p,u_p}\Delta s & 0 & -\frac{mg}{m_{\mathrm{t}p} v_p}\cos\alpha_p \Delta s \\ 0 & 1 & \cos\alpha_p \Delta s \\ 0 & 0 & 1 \end{bmatrix} \tag{3.35}$$

$$G_p = \begin{bmatrix} \frac{i_{\mathrm{t}p} i_\mathrm{f} \eta_{\mathrm{t}p} \eta_{\mathrm{f}p}}{r_\mathrm{w} m_{\mathrm{t}p} v_p}\Delta s \\ 0 \\ 0 \end{bmatrix} \tag{3.36}$$

where

$$\frac{\partial f_v}{\partial v}\bigg|_{x_p,u_p} = -\frac{i_{\mathrm{t}p} i_\mathrm{f} \eta_{\mathrm{t}p} \eta_{\mathrm{f}p}}{r_\mathrm{w} m_{\mathrm{t}p}} \frac{T_{\mathrm{e}p}}{v_p^2} - \frac{\frac{1}{2} c_\mathrm{d} A_\mathrm{a} \rho_\mathrm{a}}{m_{\mathrm{t}p}} + \frac{mg}{m_{\mathrm{t}p} v_p^2}(c_r + \sin\alpha_p)$$

The equilibrium point x_p for the most common mode, cruising under engine power on the top gear, is obtained by choosing $v_p = 80\,\mathrm{km/h}$, $z_p = 0\,\mathrm{m}$, $\alpha_p = 0\,\%$ grade, and the nominal vehicle specific values for i_{tp}, η_{tp}, and η_{fp}. The driveline efficiencies and transmission gear ratio will also directly give $m_{\mathrm{t}p}$. We can now compute the input torque equilibrium by inserting the equilibrium values into (3.33), setting the speed change to zero, and solving for T_e. We get

$$T_{\mathrm{e}p} = \frac{r_\mathrm{w} \frac{1}{2} c_\mathrm{d} A_\mathrm{a} \rho_\mathrm{a} v_p^2 + r_\mathrm{w} mg(c_\mathrm{r} + \sin\alpha_p)}{i_{\mathrm{t}p} i_\mathrm{f} \eta_{\mathrm{t}p} \eta_{\mathrm{f}p}} \tag{3.37}$$

for each mode of the linear system.

3.3.4 Measurement Equation

When the described vehicle and road models are used in a KF, a measurement equation is needed. Two measured states and the input signal engine torque T_e, are available for estimation of the system model state. The measured states are the vehicle speed v, and the altitude z. This leads to a linear measurement equation

$$y_k = \underbrace{\begin{bmatrix} 1 & 0 & 0 \\ 0 & 1 & 0 \end{bmatrix}}_{H_k} \underbrace{\begin{bmatrix} v_k \\ z_k \\ \alpha_k \end{bmatrix}}_{x_k} + \underbrace{\begin{bmatrix} e_k^{\mathrm{v}} \\ e_k^{\mathrm{z}} \end{bmatrix}}_{e_k} \tag{3.38}$$

which is used with both the linear and non-linear models. The measurement noise for the two states is described by the white noise processes e_k^{v} and e_k^{z} respectively.

3.4 Simulation Models

The proposed estimation methods have been evaluated in field experiments and computer simulations. This section describes the simulation models, including the method for calculating the control signals and the sensor models. The main aim of the simulations has been to predict the performance of the proposed road grade estimation scheme when a large body of measurements becomes available. Since only eleven on-road experiments, with a total of three trucks, are available, many parameters and statistical properties of the model are uncertain. Model validation has been performed by estimating parameters based on the six southbound experiments, and then comparing the results to the five northbound experiments. For the prediction of the estimation performance based on a large number of experiments, all available data were used to estimate the model parameters.

3.4.1 Vehicle Models for Simulation

The vehicle model used in the simulations is based on the vehicle model described in Section 3.1. It has been adapted to provide the necessary sensor signals, by the addition of speed and brake controllers, and sensor models.

Vehicle Speed Model

The simulated vehicle speed is calculated using the same expression as in the estimation models (3.33), with the addition of a brake term. The brake force is not included in the estimation, but it is necessary in the simulation to avoid unrealistic overspeed on long downhill road sections. The engine and brake torque's are determined by PI-controllers, designed to let the vehicle track a reference speed

trajectory. The simulation model becomes

$$v_{k+1} = v_k + \Delta s \left(\frac{i_\mathrm{t} i_\mathrm{f} \eta_\mathrm{t} \eta_\mathrm{f}}{r_\mathrm{w} m_\mathrm{t}} \frac{T_{\mathrm{e}k}}{v_k} - \frac{\frac{1}{2} c_\mathrm{d} A_\mathrm{a} \rho_\mathrm{a}}{m_\mathrm{t}} v_k - \frac{mg}{m_\mathrm{t}} \frac{1}{v_k} \left(c_\mathrm{r} + \sin \alpha_k \right) - \frac{1}{r_w m_\mathrm{t}} \frac{T_\mathrm{b}}{v_k} \right) + w_k^v \tag{3.39}$$

where the notation agrees with the estimation models, and the brake force has been included with the appropriate sign. The brake force is calculated based on the total brake torque T_b applied at the center of the wheels, which gives

$$F_{\mathrm{brake}k} = \frac{T_\mathrm{b}}{r_\mathrm{w}} \tag{3.40}$$

as the brake model discretized in the distance along the road. A process noise term w_k^v has also been included in the simulation model.

Vehicle Speed Control

To follow a particular reference speed profile it is necessary to control the simulated engine and brake torque. Discrete PI-controllers were used for both tasks. The parameters of the controllers were adjusted to give response characteristics similar to those observed in the logged data. A constant speed reference signal of 80 km/h has been used, unless otherwise noted when a simulation experiment is described. The controllers used are similar to those applied as engine and brake cruise controllers in real vehicles.

The engine controller is limited by the torque output available from the engine, and is often saturated in uphill segments. The brake controller is limited by the brake torque available at the wheels. Since the speed reference is generally constant, the brakes are only used to avoid overspeed on long steep downhill segments. The brake controller was set to prevent speeds above 89 km/h. Anti-windup was used for both controllers, and no instability issues were observed.

Gearshift Control

A gearshift controller has been implemented for the simulation model, based on the general behavior of automated manual transmissions in HDVs. The gear selection logic attempts to keep the engine operating between 1 000 and 1 550 rpm. In some occasions the gear is changed two steps at once, to ensure that the current speed can be maintained at the new gear. The implemented controller logic is illustrated in Figure 3.7. A gear change is modeled as one discrete simulation step with no connection between the engine and the wheels (no torque transfer).

Driveline Sensor Models

The most important driveline signals, for the road grade estimation, are the vehicle speed and the engine torque. The high frequency content in the road grade error

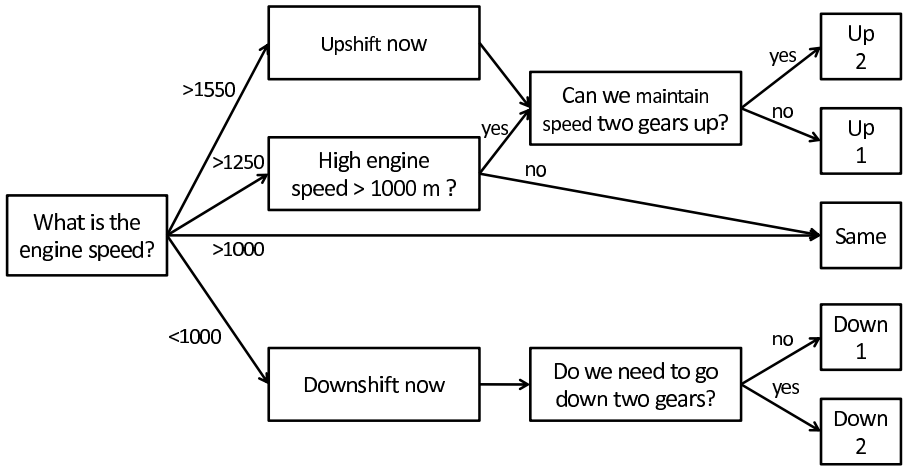

Figure 3.7: The engine speed and the ability to maintain vehicle speed at various gears are evaluated at each step of the simulation. These factors decide if a gear change should take place.

signal heavily depends on the random errors in the vehicle speed signal. This is due to the connection between the vehicle model derived grade estimate and the acceleration of the vehicle. The road grade estimate depends on the derivative of the speed, and is thus very sensitive to noise in the speed signal. The one step difference approximation of the derivative in the discrete representation also contributes to the sensitivity to speed signal noise.

Analysis of the speed signal from the experiment vehicles indicate that there is a difference between the vehicles with respect to the filtering applied by the brake system, before the signal is reported on the CAN bus. In the simulations the true vehicle speed signal has been corrupted by WGN, with zero mean and an intensity σ_v, that yields a noise level in the estimated road grade similar to the one observed in the experiments. The simulated speed signal recorded for use in the estimation is given by

$$v_k^{\text{sim}} = v_k \cdot (1 + \varepsilon_k^v), \ \varepsilon_k^v \sim N(0, \sigma_v) \tag{3.41}$$

were v_k is the true speed of the simulated vehicle, and ε_k^v is the speed sensor error.

The engine torque signal errors are difficult to model, since there is no good reference signal available in the experiments. Based on interviews with experts in the field the random parts of the engine torque error have been neglected. Instead a multiplicative error, which is constant for each vehicle, has been applied. The error generated for each vehicle is given by

$$\varepsilon_{T_e} \sim N(0, \sigma_{T_e}) \tag{3.42}$$

where σ_{T_e} is the standard deviation of the error. This is used to account for the

uncertainty in the maximum actual engine torque. The simulated torque signal is described by

$$T_{\mathrm{e}}^{\mathrm{sim}}{}_k = T_{\mathrm{e}k} \cdot (1 + \varepsilon_{T_{\mathrm{e}}}) \tag{3.43}$$

where T_{e} is determined by the PI-controller used in the simulation and $T_{\mathrm{e}}^{\mathrm{sim}}$ is the torque actually applied.

Parameter Values

The vehicle parameters used in the model are based on nominal values for the type of vehicle considered. Variations in the detailed configuration of a particular vehicle, as well as the weather and road surface conditions at a particular time can greatly affect the true parameter values. A commonly quoted engineering estimate of the accuracy for each parameter is around 10 %. In order to investigate the behavior of the grade estimator as many measurements are added, reasonable guesses have been made as to the distribution of errors in the individual parameters, as described further in Section 6.2.

3.4.2 GPS Signal Models

The modeling of the GPS signal properties is very important for the behavior of the estimation algorithm. The main benefit of using the GPS as an altitude sensor is its stability over long time periods. Its main drawback is the large changes in the altitude error over short time periods. The distribution of GPS errors is approximately normal over long time periods, but there is significant correlation between errors in samples taken at short intervals. A simulation model for the GPS signal has to accurately reproduce all these aspects of the error. Based on suggestions in the literature, a first order discrete Markov chain model was chosen to represent the GPS errors (Allerton, 2009, p. 276). The model was identified based on the difference between the sensed values and the reference values for the experiments described in Chapter 5. Two different models were identified, one for the altitude signal, and one for the latitude and longitude signals. Different models were also used for the simulations with sample distances 10 and 20 m respectively.

Upon analysis of the differences between the measurements and the reference altitude profile it was observed that errors outside the range $[-8, 8]$ m were uncommon. These outlier errors corresponded to less than 0.4 % of the altitude data, and less than 0.8 % of the latitude and longitude data. After the outliers had been removed, the remaining data points for each model were divided into $m = 50$ equally sized bins. This process yielded a total of 11 state sequences $\{X_p^n,\ n = 1, \ldots, n_p\}$ for $p = 1, \ldots, 11$, with as many entries n_p, as the number of data points in each of the experiments, minus the number of outliers. These state sequences were then used to identify a Markov chain process models for the GPS errors. The observed errors include both the raw GPS error and any effect added by the processing carried out to match corresponding data points of the different experiments and the reference to each other.

The Markov chain process model identification was carried out as follows. Consider a stochastic process

$$\{X^n, n = 0, 1, 2, \ldots\} \tag{3.44}$$

that takes on a finite or countable set M. Let the state space M be $\{0, 1, 2, \ldots\}$.

Definition 3.4.1. *Suppose there is a fixed probability P_{ij} independent of time such that*

$$P(X^{n+1} = j | X^n = i, X^{n-1} = i_{n-1}, \ldots, X^0 = i_0) = P_{ij} \;\; n \geq 0 \tag{3.45}$$

where $i_0, i_1, \ldots, i_{n-1}, i, j \in M$. Then this is called a Markov chain process.

To identify a model from the data, the observed state sequences $\{X_p^n,\ n = 1, \ldots, n_p\}$ for $p = 1, \ldots, 11$, constructed from the binned differences between the reference and the measurements, were used to find the one step transition frequencies F_{ij}. This was done by counting the number of transitions in one step from state i to state j in the sequences. The one step transition matrix was then constructed as follows:

$$F = \begin{bmatrix} F_{11} & F_{12} & \cdots & F_{1m} \\ F_{21} & F_{22} & \cdots & F_{2m} \\ \vdots & \vdots & & \vdots \\ F_{m1} & F_{m2} & \cdots & F_{mm} \end{bmatrix} \tag{3.46}$$

From F the one step transition probability matrix P was constructed through estimation of the individual elements based on the samples as

$$P = \begin{bmatrix} P_{11} & P_{12} & \cdots & P_{1m} \\ P_{21} & P_{22} & \cdots & P_{2m} \\ \vdots & \vdots & & \vdots \\ P_{m1} & P_{m2} & \cdots & P_{mm} \end{bmatrix} \tag{3.47}$$

where

$$P = \begin{cases} \frac{F_{ij}}{\sum_{j=1}^{m} F_{ij}} & \text{if } \sum_{j=1}^{m} F_{ij} > 0 \\ 0 & \text{if } \sum_{j=1}^{m} F_{ij} = 0 \end{cases}$$

Further details on Markov chain processes, and the estimation method applied can be found in (Ching and Ng, 2005).

3.4.3 Road Models

The vehicle model has been used for simulations both on short synthetic road sections, to illustrate the behavior of various vehicles to various road grades, and on real roads. The majority of the simulations have been carried out using reference measurements from real roads as the input road grade. These measurements do not perfectly correspond to either of the road grade models presented in Section 3.2, but they should provide a good representation of true highway road grade signals.

For the map generation study presented in Section 6.1.3, artificial road grade profiles generated from terrain altitude data were used. As a result of the process by which these profiles were generated they have less high frequency content than the reference road grade profiles. Effects of this are discussed in Section 7.1.

3.5 Summary

Discrete spatially sampled nonlinear models for the combined system made up of an HDV on a road have been derived, based on two different road models. The vehicle model is based on the longitudinal motion of a vehicle with a stiff driveline as obtained from Newton's laws of motion. The first road grade model describes the signal as constant, since the magnitude of deterministic change in the road grade over one sample distance is very small, even for the sharpest vertical bends allowed on a highway. The second model is based on highway design guidelines, and describes the road grade as being a piecewise linear signal. The road altitude is described as a primitive function for the road grade. A linearized version of the system model with a constant road grade model is also derived. It is later used to assess the effect of the nonlinearity in the original model for the data collected in the field test. Finally a simulation model is developed, which will later be used to predict the performance of the proposed road grade estimation scheme to a large fleet of vehicles.

Chapter 4

Estimating the Road Grade

"*Practical sciences proceed by building up; theoretical sciences by resolving into components.*"

Saint Thomas Aquinas, Commentary on the Nicomachean Ethics, 1271.

The models described in Chapter 3 have been used to develop three road grade estimators. In the first estimator, the *constant estimator* described in Section 4.1, logic based on vehicle sensor signals is used to determine vehicle model parameters and associated signal uncertainty measures for a KF. The vehicle model, driveline sensor data, and GPS data are then used to compute an estimated road grade and an associated error covariance. The estimate and uncertainty information are then used together with auxiliary information on the location of the data to create or update a road grade map. In this part the same constant road grade model is applied for the whole data set.

The other two estimators use the piecewise linear road grade model developed based on road design guidelines, and are detailed in Section 4.2. The first of the two, the *piecewise estimator*, uses the measurements and vehicle model directly to identify a Root Mean Square Error (RMSE) optimal piecewise linear road grade estimate. The last estimator, the *spline estimator*, uses a combination of the constant estimator and identification of linear segments. These parts are combined in a three step process to find the road grade. The three developed estimators are compared to directly filtering the measurements; this is referred to as the *nominal estimator*. The chapter concludes with a section that describes the performance criterions used in evaluating road grade estimates, and a summary.

4.1 Constant Estimator

The road grade is iteratively estimated from sensor signals available on the communication bus in the vehicle. Messages from the engine management system, gearbox

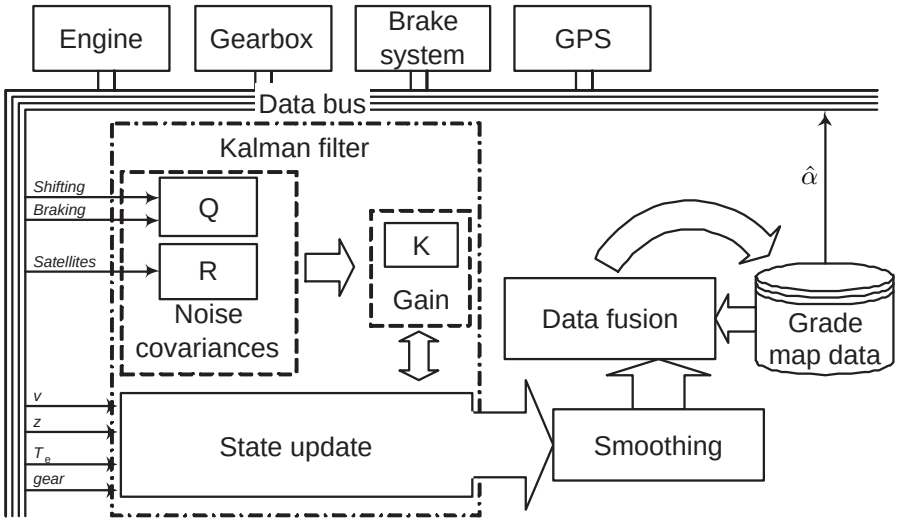

Figure 4.1: Overview of the data filtering, smoothing, and fusion of the proposed road grade estimation method.

management system, brake system, and the vehicle GPS receiver are parsed to extract the necessary measurements. These are used in the filtering logic to compute road grade and variance estimates, based on the vehicle and constant grade road models developed in Chapter 3. Since the estimator is designed for batch processing, after a complete segment has been measured, filter lag can be avoided, by using an additional filter applied backwards from the end of the data. This is referred to as the smoothing step in the method. The smoothed estimates are used together with the existing map to create a new version of the map for the segment. On the next trip along the same road segment, the updated road grade estimate is broadcast on the communication bus, and used for vehicle control. Once the next trip is complete, the estimation process starts over.

Figure 4.1 shows a schematic view of how the available sensor signals are used together with previously stored road grade information to generate an updated map. Three signals, the vehicle speed v, the absolute altitude from the GPS z, and the engine torque T_e are used directly with the model and KF to produce road grade estimates. The selected gear signal is used to choose appropriate values for the time-varying parameters in the system model. The KF also needs the error covariance matrices Q and R to be set. These are adjusted based on the number of available satellites, if the vehicle is shifting gears, or whether the brakes are applied. The exact choice of Q and R in each situation is detailed in Section 4.1.3.

Once a complete system state trajectory estimate for a road segment has been computed in the KF, the segment is processed in the smoothing step. This ensures

that all recorded sensor information is used for the estimation at each distance index. The smoothed grade and altitude estimates are then fused with any existing data for the road segment, based on the estimated relative accuracy of the new estimate and the current map. Finally, the new road grade map segment is stored in the database. In addition to the road grade, the covariance and location information from the estimator is needed when processing an estimate. For simplicity of notation all this information is referred to as a road grade estimate.

4.1.1 Kalman Filtering

Two different KFs are used in the estimator to determine the road grade and other model states. The non-linear vehicle and road model (3.31) is used together with an Extended Kalman Filter (EKF), and the linearized model (3.34) with a standard KF. Using the notation of the previous chapter, the vehicle model to be used in the filtering with the EKF is given by

$$\begin{aligned} x_k &= f(x_{k-1}, u_k) + w_k \\ y_k &= Hx_k + e_k \end{aligned} \tag{4.1}$$

Only the state update is non-linear, the output model simply indicates that two of the states are directly measurable.

In the EKF the non-linear model is linearized around the current state at every time step. The obtained transition matrix F_k is then used to complete the steps of the standard KF recursions. These recursions are described by two update steps: a time update, or prediction, step and a measurement update. In the time update the system model is used to predict the future state of the system. Using the notation $\hat{x}_{k|k-1}$ to denote the quantity $\hat{x}$ at time k based on information available up to time $k-1$ the time update is done according to

$$\begin{aligned} \hat{x}_{k|k-1} &= f(\hat{x}_{k-1|k-1}, u_k) \\ P_{k|k-1} &= F_k P_{k-1|k-1} F_k^T + Q_k \end{aligned} \tag{4.2}$$

Similarly to F_m in the piecewise linear model the transition matrix F_k is defined to be the Jacobian $F_k = \frac{\partial f}{\partial x}(\hat{x}_{k-1|k-1}, u_k)$. $P_{k|k-1}$ is the estimated error covariance, and $Q_k = E[w_k^2]$ is the process noise covariance. After the time update the measurement at time k is used in a measurement update to improve the estimate. The measurement update is described by

$$\begin{aligned} K_k &= P_{k|k-1} H^T (H P_{k|k-1} H^T + R_k)^{-1} \\ \hat{x}_{k|k} &= \hat{x}_{k|k-1} + K_k (y_k - H\hat{x}_{k|k-1}) \\ P_{k|k} &= (I - K_k H) P_{k|k-1} \end{aligned} \tag{4.3}$$

Here K_k is the Kalman gain, and $R_k = E[e_k^2]$ is the measurement noise covariance.

The piecewise constant linear model is used with a standard KF. At each mode change between different linearizations of the model the final state of the old filter is used to initialize the new filter. The linear system model in each mode is

$$\begin{aligned} \tilde{x}_k &= F_m \tilde{x}_{k-1} + G\tilde{u}_k + w_k \\ \tilde{y}_k &= H\tilde{x}_k + e_k \end{aligned} \tag{4.4}$$

where $\tilde{y}_k = y_k - Hx_m$. This leads to the KF time update equations

$$\begin{aligned} \hat{x}_{k|k-1} &= F_m \hat{x}_{k-1|k-1} + Gu_k \\ P_{k|k-1} &= F_m P_{k-1|k-1} F_m^T + Q_k \end{aligned} \tag{4.5}$$

The measurement equations are identical to the EKF case.

Smoothing

By carrying out the road grade estimation off-line, when a complete road segment has already been recorded, it is possible to use smoothing to compensate for the filtering delay and include later measurements in the estimate for each data point. The RTS fixed point smoothing algorithm, introduced in (Rauch et al., 1965), is used to find $\hat{x}_{k|N}$ where N is the total number of data points collected during one run along the road segment. These are the best available estimates at each position based not only on the measurements up to that position, but on all estimates collected on the road segment. The smoothing is performed backwards along the road segment, and uses quantities generated by the KF.

The predicted quantities at the last position of the road segment, where $k = N$, are used to initialize the recursion. This gives access to $P_{N+1|N}$ and $\hat{x}_{N+1|N}$ in the first step of the smoothing recursion. P_k^s denotes the smoothed error covariance, $\hat{x}_k^s$ is the smoothed state estimate, and K_k^s is the smoothing gain. The smoothing backwards recursion is given by

$$\begin{aligned} K_k^s &= P_{k|k} F_k^T P_{k+1|k}^{-1} \\ \hat{x}_{k|N}^s &= \hat{x}_{k|k} + K_k^s (\hat{x}_{k+1|N}^s - \hat{x}_{k+1|k}) \\ P_{k|N}^s &= P_{k|k} + K_k^s (P_{k+1|N}^s - P_{k+1|k}) K_k^{sT} \end{aligned} \tag{4.6}$$

4.1.2 Data Fusion

To merge data from many runs along the same road segment a distributed data fusion method is used. The distributed approach has the important advantage that the amount of road data that has to be stored does not increase as additional estimates from known road segments are incorporated into the map. For each road segment, the map consists of the road related states (altitude z, and grade α) and the associated estimated error covariance estimates for those states. The vehicle speed is not of any interest in the map, since it is not a road property. Based on the

estimated error covariances stored in the map and the estimated error covariances of a new smoothed estimate an updated map is created each time a new estimate of a road segment becomes available.

Assuming that the errors in estimates from each run along the road are entirely uncorrelated, the quantities for the new map can be calculated as follows

$$\begin{aligned} P_k^f &= ((P_k^1)^{-1} + (P_k^2)^{-1})^{-1} \\ \hat{x}_k^f &= P_k^f((P_k^1)^{-1}\hat{x}_k^1 + (P_k^2)^{-1}\hat{x}_k^2) \end{aligned} \tag{4.7}$$

where P_k^f is the resulting error covariance, $\hat{x}_k^f$ is the new state estimate for the map. The quantities P_k^1, P_k^2, $\hat{x}_k^1$, and $\hat{x}_k^2$ are the source estimates and estimated error covariances. This data fusion method is described in more detail in e.g., (Gustafsson, 2010, p. 30).

The assumption in (4.7) that estimation errors in the two source samples are uncorrelated is troublesome. Since the estimates are based on repeated measurements using the same method, and of the same realization of a road grade signal, it is unlikely that this is fully satisfied. This discrepancy will lead to an underestimate of the state error covariances in P_k^f. Over time this will lead to new estimates having little influence on the already stored data. In practice it may very well be desirable to have the opposite behavior. Roads are occasionally modified, so it may be good practice to eventually forget very old data, i.e., weight the new estimate higher than what would be indicated by P_k^f.

Another important caveat is that in practice covariance terms between the altitude and road grade states, represented by the off-diagonal terms of the source matrices P_k^1 and P_k^2 actually degrade the merged result. Uncertainties in the estimation of these quantities in the KF and smoothing steps occasionally cause the weighting factors to give a combined estimate that is not in the interval $[\hat{x}_k^1, \hat{x}_k^2]$. Currently this problem is solved by only using the diagonal elements of P_k^1 and P_k^2 in the fusion. The result is that only the estimated covariance of each of the states will affect how much weight the measurement of that state has in the merge, the estimated cross correlation between altitude and road grade errors will be ignored.

When a map is first created based on estimates from two runs along the road both the source sets are smoothed results from individual runs, after that one source will be the map (based on all previous measurements), and one will be the new estimate to be incorporated.

4.1.3 Selection of Q and R

One of the main challenges in using the grade estimation method on real data is that the true noise covariances Q and R are not known. In the estimator they are instead used as design variables to tune the grade estimation filter to generate an accurate and reliable estimate, when compared to training data.

To simplify the choice of these design parameters the noise covariance matrices were chosen to be diagonal. For the measurement noise this seems reasonable since

the vehicle speed and GPS altitude are obtained through independent sensors measuring different quantities, whose measurement error can be assumed independent. For the process noise the situation is more complicated. Unmodeled changes in the road grade are likely to show up also in the running sum of the road grade multiplied by the sample distance, i.e., the altitude. It is also likely that a road grade error would have an effect on the speed error as well, since the road grade used in the speed prediction is then faulty. The magnitudes of these effects are hard to estimate beforehand, since they depend on the magnitudes of the model errors themselves. In this work the results when using a diagonal Q matrix are investigated, evaluation of possible improvements with a full matrix is left as future work.

For normal driving at a fixed gear the process noise covariance matrix Q is tuned to be as small as possible while still allowing the road grade estimate to follow the reference road grade closely during unmodeled transitions between flat road and constant grade inclines, as discussed in Section 3.2. Driving events such as gearshifts and braking affect the vehicle in ways that are not covered by the relatively simple vehicle model given in Chapter 3. To account for this the process variance for the speed state is increased when such events occur. During braking no useable torque estimate is generally available, so the action taken in the filter is to reduce the reliance on speed predictions. During gearshifts it can be assumed that the engine torque that comes through the driveline and affects the vehicle will be low. With a manual gearbox this is true since the clutch will be depressed during shifting. With an automated manual gearbox the same holds since the gearbox controller will take over engine control to achieve matching input and output transmission speeds as well as zero torque transfer in order to switch gears without clutch engagement. Driveline oscillations as well as drive and propeller shaft torsion can cause considerable torques, but the average value of these on the time scale of interest is limited. The net engine torque during braking is assumed to be zero in the model, regardless of the value reported from the vehicle.

The measurement noise covariance matrix R is adjusted depending on the number of GPS satellites available. While other GPS-system related factors also affect the GPS position accuracy, the number of satellites is the only relevant signal that is available from the satellite receiver used. When satellite coverage was lost, a very high variance was set for the altitude measurement. This causes the grade estimate only to depend on vehicle signals. Even during ideal conditions the noise in the GPS altitude signal can be considerable, so the error covariance was chosen to be relatively high all the time. It should be noted that the chosen noise covariance during nominal conditions for the GPS altitude measurement is large enough to essentially saturate the influence through the filter equations that it can have on the estimated grade error covariance $[P_k]_{3,3}$. Thus, the estimated error covariance for the grade state does not increase noticeably when satellite loss occurs. With the covariance levels used for the GPS sensor its main influence is on the long-term average of the road grade estimate. This causes a decoupling effect, where the vehicle model is mainly used to detect relatively high frequency road grade signal content. The main influence of the GPS is to compensate for bias errors in the road grade

model estimates.

4.1.4 Optimality of the Kalman Filter and Smoothing

The KF in the estimator is known to produce an optimal state estimate in the minimum mean square error sense, given that the system is linear and, that the measurement and process noises are truly WGN and have the assumed covariances. Since we have a non-linear system, with model and sensor errors that most likely yield somewhat colored process and sensor noises, the estimates will not be optimal. Furthermore, the KF may not converge to the true value. The RTS smoothing similarly provides minimum mean square error estimates of the state at each position based on all the collected measurements, for systems that fulfill the same assumptions as for the KF. As we are using our EKF results as input to the smoothing recursion, suboptimal and biased estimates may be obtained. A version of the estimator using a linear vehicle model has also been developed, but this merely moves the non-compliance with assumptions about the model to the assumptions about the noises. In this case not only the previously existing model errors, but also linearization errors contribute to coloring the noise.

Optimal estimation based on all available experiments would yield a very large KF that includes two states to describe the road, and one speed state for each experiment. By only fusing the road states based on their estimated error covariances, the requirement to include models for all the vehicles in the filter is avoided. As a consequence the estimate will no longer be optimal. The applied fusion method includes the assumption that the different experiments observe the system with different realizations of the process noise. In our case this is not true, since the road realization is the same each time the vehicle passes over it. When the process noise is correlated between experiments, the distributed fusion will underestimate the error covariance matrix. As noted in Section 4.1.2 issues with the estimated cross-correlation between the altitude and slope states further moves the implemented method away from the theoretical optimum.

4.1.5 Prediction Error

Using a constant road grade model in a KF intended for estimation of a varying road grade will introduce errors. The influence of the road model, in the road grade estimator described above, on the final estimation error depends on the sample distance employed, and the assumptions on the process and noise variance models. Assuming a smaller variance for the process noise increases the effect of the road model. Increasing the distance between samples also increases the effect of road grade model assumptions, as the prediction is carried out over a longer distance. The grade of a true road with the same rate of change in the road grade will thus have changed more when the next sample arrives, and the ratio of samples per unit of prediction error decreases. The effect of the prediction error from the road grade model is illustrated in Example 4.1.

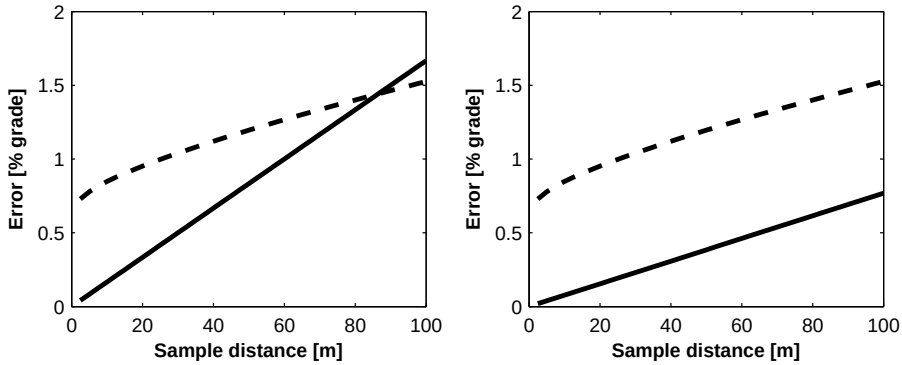

Figure 4.2: The prediction error resulting from adopting the model $d\alpha/ds = 0$ when the true model is $d\alpha/ds = 1/R = 1/6\,000$ (left) or $d\alpha/ds = 1/R = 1/13\,000$ (right) is shown as a function of the sample distance (solid). Also included is the expected standard deviation of the one step ahead prediction error for the KF used for state estimation in Section 4.1 (dashed). The importance of the model choice increases for larger sample distances.

Example 4.1. The prediction error from the simplified constant road grade model (3.24) is compared to the expected prediction standard deviation of the proposed road grade estimation method. The computation is based on the combined vehicle and road model given in Section 3.3.2, when the vehicle operates at a constant speed of 80 km/h.

Figure 4.2 shows the prediction error that will result from adopting the model given by Equation (3.24), in which the road grade doesn't change, when the real road has a vertical curve radius R designed according to the SRA guidelines in Table 3.6, for the reference speeds 90 km/h (left figure) and 110 km/h (right figure). The true road is described by

$$\frac{d\alpha}{ds} = \pm\frac{1}{R} \tag{4.8}$$

where $R = 6\,000$ m in the left figure, and $R = 13\,000$ m in the right figure.

For longer sampling times the modeling error becomes increasingly large compared to the expected prediction standard deviation. The practical influence of the prediction error on the estimation performance is however limited by the fact that large parts of the test road have very small changes in the road grade. Using a second order road grade derivative approximation 15 % of the reference data points on the highway section used for experiments has a vertical curve radius $R < 13\,000$ m. Only 1 % of the data points have a vertical curve radius $R < 6\,000$ m. The full distribution of vertical curve radii is shown in Figure 4.3. When the road grade changes slowly

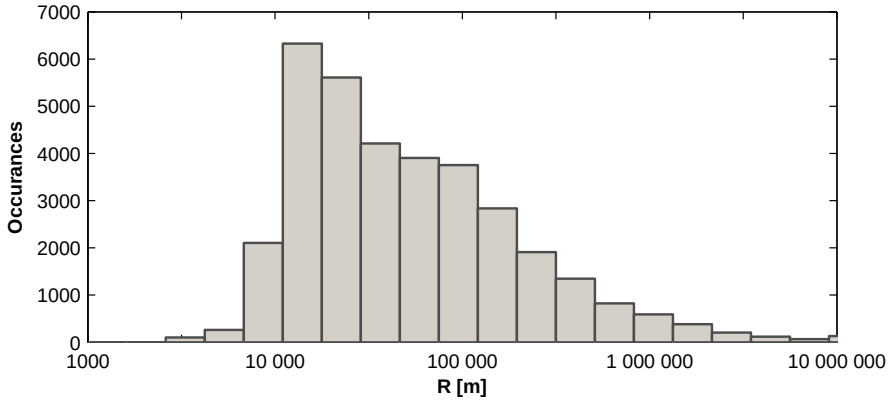

Figure 4.3: The vertical curve radii for most data points on the highway section used for experiments are rather large. The figure shows a histogram for the vertical curve radius R, with logarithmic bin sizes.

the assumption $d\alpha/ds = 0$ is quite accurate. The vertical curve radius calculation is sensitive to noise and the result should only be regarded as rough estimate.

4.2 Piecewise Estimators

Based on the background knowledge on road design principles described in Section 3.2, and the piecewise linear road grade model (3.23), it is warranted to investigate if an assumption on piecewise linearity of the road grade signal can be used to increase estimation performance. Two different methods, which take the background knowledge into account in the estimation, have been developed and tested experimentally. The method first described yields a globally optimal piecewise linear approximation of the road grade. This method results in a road grade profile with separate linear descriptions in each segment, and no limit on the magnitude of the difference between the estimated grade at one data point, at the end of one segment, and the next data point, at the beginning of the next segment. Additionally, the experimental data show that the real road has features not captured fully by the piecewise linear model. Therefore another method is developed, where a linear spline is identified and used as the basis for estimating the road grade. The methods and their respective implementations are described below; the experimental validation is detailed in Chapter 5.

4.2.1 Estimation of Piecewise Linear Functions

In the estimators described in Sections 4.2.2 and 4.2.3, two different methods of estimating a piecewise linear function are used. They differ in the conditions applied

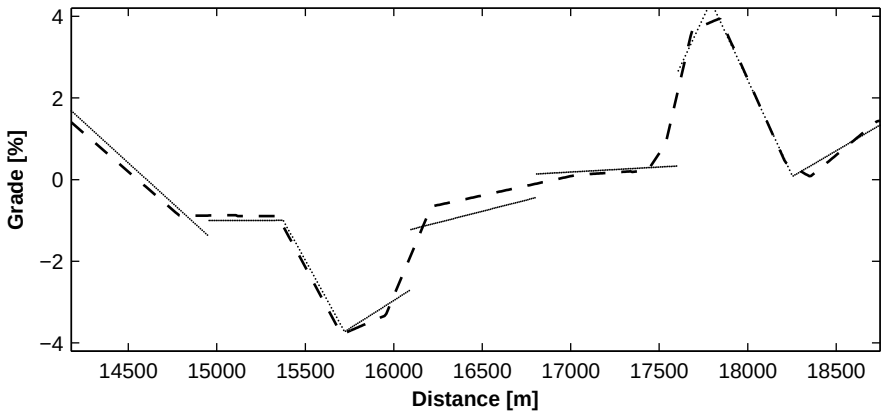

Figure 4.4: The difference between a spline (dashed) and piecewise linear (dotted) approximation of the road grade for a part of the southbound profile. The spline approximation is continuous, but the piecewise linear one isn't.

at the end of the segments. The method used in the piecewise estimator, described in Section 4.2.2, produces a series of disconnected linear segments. The method used in the spline estimator, described in Section 4.2.3, relies on identification of a linear spline. The difference between the two is illustrated in Figure 4.4, and both types of piecewise linear functions are formally defined below. Many estimation methods exist for each type, each with their own merits and shortcomings. A thorough treatment of the subject is beyond the scope of this thesis, but a few comments on the implemented methods and possible alternative approaches are given below.

A piecewise polynomial function with disconnected segments is defined as follows. A piecewise polynomial function $P(d)$ of the distance d with q segments, has $q+1$ locations where the describing polynomial changes (including the start and the end). Given the $q+1$ distinct change points d_i such that

$$d_0 < d_1 < \cdots < d_{q-1} < d_q \tag{4.9}$$

a piecewise polynomial function with q segments is defined by

$$P(d) = \begin{cases} P_0(d) & d \in [d_0, d_1) \\ P_1(d) & d \in [d_1, d_2) \\ \vdots & \vdots \\ P_{q-1}(d) & d \in [d_{q-1}, d_q] \end{cases} \tag{4.10}$$

where each $P_i(d)$ is a polynomial of degree n. When a piecewise polynomial function is fitted to a set of discrete data points, the value of each of the constituent polynomials outside the last data points included in the fitting is not considered in

the cost function. It is thus necessary to be careful if a piecewise polynomial function, that is fitted to discrete data points, is to be interpolated. Interpolation in the area between data points belonging to different segments, using the polynomials of either segment, suffers the same uncertainty as is normally associated with extrapolation. All piecewise polynomial functions used in this work have degree $n = 1$, i.e., are piecewise linear.

A spline requires the values at the corresponding ends of each pair of segments to match. These transition points are called knots, and a spline $L(d)$ with q segments has the $q+1$ distinct knots d_i such that (4.9) still holds. The knot points have knot values y_i and the spline function of degree q is given by

$$L(d) = \begin{cases} L_0(d) & d \in [d_0, d_1] \\ L_1(d) & d \in [d_1, d_2] \\ \vdots & \vdots \\ L_{q-1}(d) & d \in [d_{q-1}, d_q] \end{cases} \tag{4.11}$$

where each $L_i(d)$ is a polynomial of degree n. When a spline approximation of a continuous function is determined, knot points are generally chosen on the function, i.e., once d_i is fixed, so is y_i. When fitting a spline to a set of discrete data points there is generally no requirement for the knot points to coincide with data points. The knot locations d_i can be chosen arbitrarily, and the values y_i are often determined by minimization of a, possibly weighted, least squares criterion. The possible knot locations can thus not be enumerated. Instead, a continuous cost function must be minimized even for a discrete data set. There are numerous publications suggesting methods to find suitable knot locations and spline approximations with a known or unknown number of polynomial segments.

The linear spline method described in Section 4.2.3 is straightforward and generates reasonable results from an engineering intuition point of view. It is however suboptimal both due to a possibility of ending up in local minima in the cost function, and due to the sub-division of the road. Its main merit is that it provides a piecewise linear road grade profile with knots instead of the "jumps" produced by the optimization method described in Section 4.2.2. The absence of jumps is a desirable quality since the road grade design specification is violated by too large jumps (larger than $1/R \cdot \Delta s$) between the end of one linear segment and the start of the next. Limiting the jump between two linear segments in the optimal method is nontrivial, since necessary properties for reducing the computational complexity would be lost. Finding the optimal linear spline for a road segment is hard due to the complexity growth.

The chosen spline estimation method doesn't limit the slope, i.e., the derivative of the estimated road grade profile, of any segment. It may thus also produce estimates that violate the road design principles. Experimentally this has however been seen to be less of an issue, since it occurs much less frequently than large jumps between linear segments. The practice of merging closely spaced knot points also reduces the occurrence of spline segments with slopes in excess of $1/R$.

Alternative Approaches

The field of piecewise linear model identification for discrete data sets is very large. There are numerous alternative methods that could have been chosen instead of the ones that were implemented. A survey of different approaches is given in (Keogh et al., 2004). The main motivation for the method described in Section 4.2.2 is that it finds the optimal piecewise linear approximation in a least squares sense, in a computationally efficient manner. The spline identification method, described in Section 4.2.2, relies on numerical optimization of a cost function based on the knot locations. Its main merits are that it is very simple to implement and provides a relatively fast way to find a spline approximation. The results will generally not be optimal, but compared to the other road grade estimation methods it performs well for the experimental data.

One alternative way of finding disconnected linear segments would be to use generalized principal component analysis to cluster the measurements, and find the best linear representation in each cluster. This method does not only account for the error in the dependent variable (road grade), but also accounts for the possibility that there may be an error in the independent variable (position). This method is described in (Vidal et al., 2005).

In the spline case one alternative would be to use l_1 trend filtering, as described in (Kim et al., 2009). The computational complexity of this method grows linearly with the number of samples, making it efficient for large data sets. Another advantage is that it only requires one parameter to be set, which makes it easy to use. The end result is a linear spline with knot points that vary in number and placement with the input parameter.

For both types of linear segmentation various top-down methods for splitting the data set into smaller parts until some criterion is met are popular. Alternatively, a bottom-up approach may be used. In that case the largest possible number of segments is used as a starting point. These small segments are then merged, until the chosen criterion is satisfied. A performance comparison between popular methods can be found in (Keogh et al., 2004).

To define criterions for what is the best method of estimating piecewise linear functions for this applications is left as future work. Two methods with different strong and weak points have been tested, with the main aim of investigating under what conditions there is a potential for improved road grade estimation performance from using a piecewise linear road grade model. The experimental results indicate that the main conclusions from the work would not be affected by a different choice of methods for the linear segmentation.

4.2.2 Piecewise Estimator

Given the road model developed in Section 3.2, the road grade profile of a properly engineered road should consist of linear segments. It is thus natural to attempt to estimate the road grade as a set of piecewise linear functions, based on measured

data. By using only the measurements that belong to a particular segment when trying to find a linear representation, it is possible to formulate the estimation problem in such a way that optimal linear segments for a feasibly long road section can be found, using dynamic programming.

Estimation Method

The road grade data can be regarded as a time series, although the independent variable in this case represents distance along the road instead of time. Formally the road grade profile consists of a sequence of N points

$$(s_0, \alpha_0), \ldots, (s_{N-1}, \alpha_{N-1}) \tag{4.12}$$

where s, the distance values, are ordered such that $s_i > s_{i-1}$. A segmentation of the profile is defined as the sorted set of $q+1$ segmentation indices $z_0, \ldots, z_q$ such that $z_0 = 0$ and $z_q = N$. The profile is divided by the segmentation points into intervals $S_0, \ldots, S_{q-1}$ defined by the segmentation indices as

$$S_j = \{(s_i, \alpha_i) | z_j \leq i < z_{j+1}\} \tag{4.13}$$

For each interval $S_0, \ldots, S_{q-1}$, there is an associated linear model $P_j(s) = a_j s + b_j$ defined by a_j, b_j. The total segmentation error is computed from

$$\sum_{j=0}^{q-1} V(S_j) \tag{4.14}$$

where V is the total squared error between the piecewise linear approximation and the measured data. The squared error V is given by

$$V(S_j) = \min_{(a_j, b_j)} \sum_{r=z_j}^{z_{j+1}-1} (a_j s_r + b_j - \alpha_r)^2 \tag{4.15}$$

Other measures than the squared error, such as the l_∞-norm (maximum error) are also possible in the same framework, by replacing the $\sum$ operators by max operators. The RMSE e for the piecewise linear estimate is calculated as

$$e(q, N) = \sqrt{\sum_{j=0}^{q-1} V(S_j)/N} \tag{4.16}$$

Finding linear segments in time series data is a problem that arises in many different fields and that has been extensively studied. When the number of segments in the data as well as their start and end positions are unknown, finding the optimal piecewise linear approximation is computationally intensive. Straight on evaluation of all $\binom{N-1}{q-1}$ possible segmentations of N data points into q subintervals is not

feasible, even a short data set with $N = 200$ can be divided into $q = 6$ segments in over $2 \cdot 10^9$ different ways. Fortunately, there are more efficient algorithms available.

Using a dynamic programming algorithm where the cost function is partially precomputed, as presented in (Lemire, 2007) the optimal segmentation and associated linear segments can be found with computational complexity $\mathcal{O}(N^2 q)$. With this algorithm, the optimal segmentation can be found for data sets large enough to provide insights into the performance of piecewise linear road grade estimation within a few hours of computation time, on a standard office PC. Experiments with $N = 1\,200$ and $q = 40$ were used, which gave execution times of 8–10 hours on a ≈ 2 GHz desktop CPU. The piecewise linear approximations used in this paper have been determined using a Matlab implementation of the algorithm proposed in (Lemire, 2007), available through the homepage of the author.

In a large scale implementation of the method, significant performance gains can be achieved by dividing the road into sections of approximately 10 km. The resulting piecewise linear road grade profile for the entire road will not be globally optimal for the chosen number of segments, but the approximation within each section will. At the cost of an, arguably small, deviation from the optimal solution the computation complexity for estimating M such sections of X km with q_X segments and N_X samples each can be reduced from $\mathcal{O}(M^3 N_X^2 q_X)$ to $\mathcal{O}(M N_X^2 q_X)$. On a 100 km road, this gives a solution in only 1 % of the original computation time.

Implementation

As described in Chapter 3 the measured signals yield information about the road grade in two ways. The vehicle model gives one input, and the altitude measured by the GPS gives another. As noted in Section 3.3.1 the numerical differentiation of the GPS altitude signal gives a very noisy signal. It was discovered that this noise caused problems with the identification of linear segments. The adopted solution was to average the derivative of the GPS altitude signal over the entire measurement, and to only use the altitude input to reduce the effect of the bias that was present in the estimates from the vehicle model. Thus, the input road grade estimate for the optimal linear segmentation algorithm was calculated using Equation (3.28). After the piecewise linear estimate $\hat{\alpha}^{\mathrm{v}}$ was computed, it was adjusted by the average GPS altitude derivative obtained from Equation (3.29) according to

$$\hat{\alpha}^{\mathrm{p}}_k = \hat{\alpha}^{\mathrm{v}}_k - \frac{1}{N} \sum_{k=0}^{N-1} {\alpha^{\mathrm{GPS}}}_k, \;\; k = 0, \ldots, N-1 \tag{4.17}$$

to arrive at the final piecewise linear road grade estimate $\hat{\alpha}^{\mathrm{p}}$.

4.2.3 Spline Estimator

By studying road grade profiles obtained by high accuracy measurement devices it becomes evident that the assumption that road grade profiles are always described by piecewise linear functions does not hold fully in practice. To combine the benefits

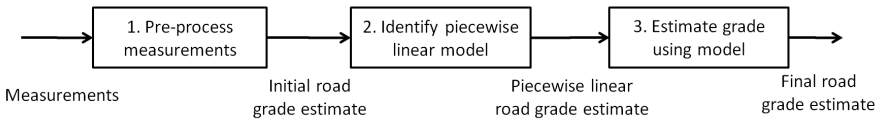

Figure 4.5: In step 1 measurements from a road section are used to generate a first road grade estimate. In step 2, a piecewise linear road grade model is identified from the initial estimate. The estimation method in step 3 uses the piecewise linear model $\alpha_{k+1} = \alpha_k + c_i$ and measured data to produce a final estimate.

of a more accurate road model than the no-change assumption $\alpha_{k+1} = \alpha_k$, with the flexibility of the KF used in the constant estimator, described in Section 4.1, a three step estimation method is proposed. This method exploits the piecewise linear road grade model (3.23), while still allowing the estimated profile to deviate from that model if the measurements indicate that to be the case. The method is described on an abstract level in Section 4.2.3. The method has also been implemented and evaluated experimentally, the implementation is detailed in Section 4.2.3, and the experimental validation in Section 5.6.

Method Overview

The idea behind the proposed method is to use the background knowledge on road design described in Section 3.2, while allowing for local deviations from that assumption. The method is most easily motivated backwards, from the final road grade estimate. In the final step a piecewise linear road grade model is combined with the measured data. A trade-off is made between trusting the road grade model assumption of using nothing but linear segments and the actual measurements. The final profile is not restricted to be piecewise linear. To perform this trade-off both a linear piecewise linear road grade model and raw measurement data are needed.

Thus, before the final step a piecewise linear road grade model is created. The model can be created using one of a large number of methods for estimating piecewise linear models without knowledge of the segment end points, for example the method described in Section 4.2.2. Since no direct measurement of the road grade is available, this step relies on some form of pre-processing of the measurements into individual road grade estimates.

The pre-processing of measurements into road grade estimates useable for finding the piecewise linear road grade model is the first step of the proposed method. Depending on the sensors available this step could be carried out in a large number of ways, as described in Section 2.6.

In summary, a road grade estimation method that exploits the piecewise linear nature of the road grade signal without restricting the output to be piecewise linear, through a three step process, is proposed. The method is illustrated in the block diagram in Figure 4.5.

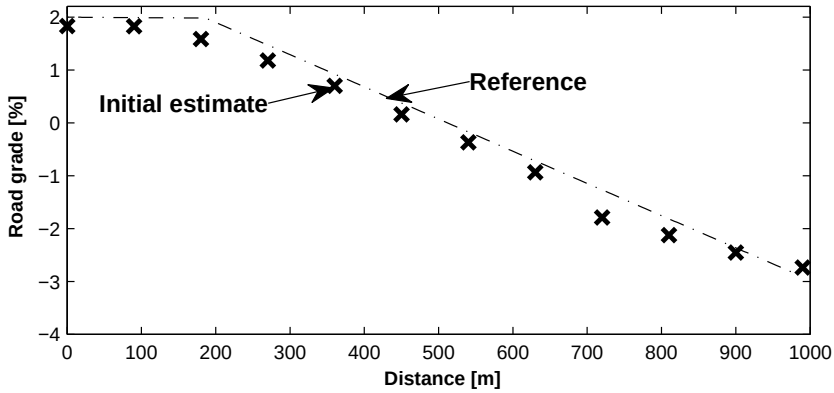

Figure 4.6: The estimated road grade after the first step in the spline estimator has been completed is shown for a short road segment (×). The reference road grade profile is shown as well (dash-dotted).

Implementation

In order to evaluate the potential of the proposed method each of the steps illustrated in Figure 4.5 have been implemented and tested in experiments. There are numerous other choices of methods available for each of the steps. The choices made are motivated as follows. The implementation of the first and third step was made as similar to the already described constant estimator as possible. For the linear segmentation step a method which produces a linear spline was chosen, as a contrast to the method used in Section 4.2.2 above. The spline method imposes a restriction on the road grade jumps between linear sections, by joining the linear segments in knot points rather than identifying them independently of each other, as is further explained in Section 4.2.1. Optimal spline estimation, with unknown knot points is not computationally feasible; therefore a sub-optimal method was chosen.

The first step, creating a first road grade estimate on which to base the identification of a piecewise linear model, is carried out by applying the constant estimator described in Section 4.1. The simple road grade model given in (3.24), without parameters that need to be identified, is used. In discretized form the model becomes

$$\alpha_{k+1} = \alpha_k \tag{4.18}$$

This gives the combined road and vehicle model (3.31). The results obtained for an example road section are shown in Figure 4.6

In the second step of the method, the first estimate of the road grade is used to identify a piecewise linear model. This is completed through optimization of the knot point locations of a linear spline. The optimization is carried out by minimizing the

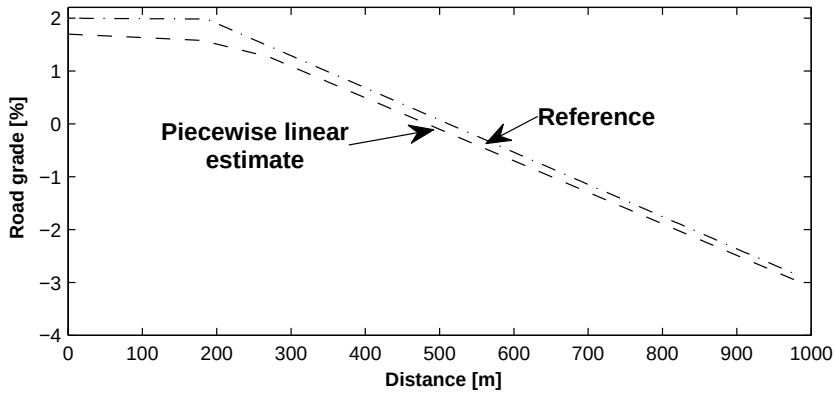

Figure 4.7: In the second step a piecewise linear spline approximation of the road grade is identified based on the initial road grade estimate shown in Figure 4.6. The piecewise linear estimate (dashed) is shown together with the reference road grade profile (dash-dotted).

least squares cost of the difference between the linear spline and the measurements, as a function of the placement of the knot points. The knot point locations are not limited to be sample instances, and the linear spline is a continuous function, being observed at the sample instances.

Unfortunately this is a non-convex constrained optimization problem, with as many degrees of freedom as knot points between the edges. Distretizing the knot point locations and performing an exhaustive search of all possible combinations of knot placements is impossible due to the computational cost, even for rather short road segments. The solution was instead obtained by dividing the road into shorter sub-sections, which were each given a maximum number of allowed linear spline segments. Constrained multivariable non-linear numerical minimization was then used to find a knot placement within each section. If two knot points ended up being very close together they were merged into one point. The resulting linear spline was used as a road grade model. An example result after the second step is shown in Figure 4.7.

In the third step, the linear spline model is used to find a final road grade estimate. The implementation is very similar to the one in the first step of the method, with the difference that the combined road and vehicle model is given by Equation 3.31. The final result for the example road section is shown in Figure 4.8. The experimentally determined measurement and process noise covariance matrices Q and R were modified to reflect added trust in the more accurate road grade model employed. The results obtained from experimental validation of the method are described in Section 5.6.

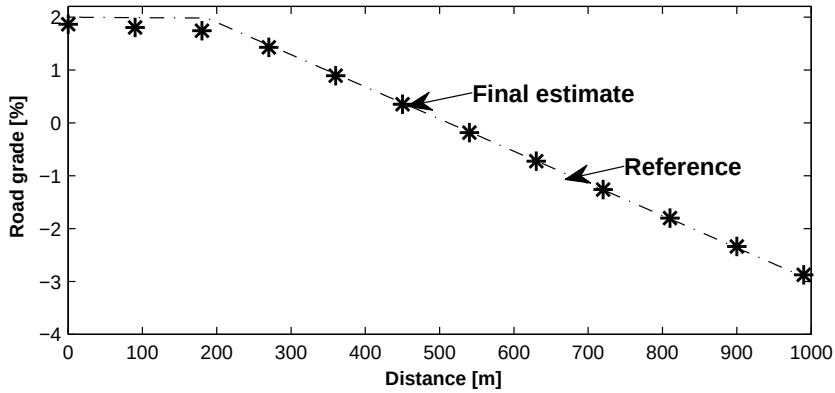

Figure 4.8: In the third step of the estimation process the linear spline model is used in the filter based estimation method to obtain a final estimate ($*$), shown together with the reference road grade profile (dash-dotted).

4.3 Performance Metrics

In order to quantify the estimation results for the proposed road grade estimators some performance metric is required. The basic metric applied to evaluate the road grade estimates $\hat{\alpha}$ is the RMSE

$$RMSE = \sqrt{E((\hat{\alpha} - \alpha)^2)} \tag{4.19}$$

where the expected value is computed as the mean over the N available samples

$$E((\hat{\alpha} - \alpha)^2) = \frac{1}{N} \sum_{i=1}^{N} (\hat{\alpha} - \alpha)^2 \tag{4.20}$$

Figures showing actual errors as a function of time for various estimation schemes are also employed in the analysis of the estimation performance.

The main focus of this work is on developing and analyzing a method to obtain road grade information for control, from vehicles in regular service. For each control application that is going to use the data it is necessary to determine the accuracy requirements that will need to be satisfied for the particular application. A large class of applications relies on predictive speed calculations, e.g., energy efficient highway cruise control, automatic lowering of the speed ahead of changes in the legal speed limit, and energy efficient stopping at intersections and traffic lights. The predicted speed is often calculated in open loop, with the engine fueling being either zero or the maximum possible value. Therefore the error in predicted speed at a future location that will arise from the error in the road grade profile, if all other truck and environment parameters are correctly identified and modeled, is of

interest. This quantity primarily depends on the error between the predicted relative altitude and the actual relative altitude of a future point on the road versus the current vehicle position. The relative altitude errors at locations between the point where the prediction is made and the current point also affect the predicted speed error, but in a much less significant way, as is illustrated in Examples 4.2 and 4.3.

The relative altitude of a future point, m sample distances ahead of position index k on the discretized road is determined by

$$\Delta z_k(m) = \Delta s \sum_{p=1}^{m} \sin \alpha_k \tag{4.21}$$

Denoting the thus calculated relative altitude of the reference road grade profile $\Delta z_k(m)$ and the corresponding relative altitude for the estimated road grade profile $\Delta \hat{z}_k(m)$ the error in the predicted relative altitude at index k, $e_k^{\Delta z}(m)$, can be calculated as

$$e_k^{\Delta z}(m) = \Delta z_k(m) - \Delta \hat{z}_k(m) \tag{4.22}$$

This altitude error will lead to different errors in the predicted vehicle speed depending on vehicle parameters and vehicle speed.

Example 4.2. The error in the predicted speed and altitude at a future location is determined through simulation, based on two flawed road grade estimates, for a coasting vehicle traveling on a flat road. The first estimated road grade profile has a bias of 0.1 % grade, giving a relative altitude error of 1.0 m after 1 000 m. The second estimated profile has a sinusoidal road grade error with a period of 500 m, and an amplitude of 0.3 % grade. The prediction is carried out up to 1 000 m ahead of the vehicle. The vehicle used is the one described by Table 6.3, and the initial conditions are cruising at 85 km/h on the top gear. The results are shown in Figure 4.9.

Example 4.3. The same vehicle, initial conditions, and estimation errors as in Example 4.2 are used, but the road profile is changed. The true road grade is now a vertical curve with $R = 20\,000$ into a downhill section with a constant −1.5 % grade. The results are shown in Figure 4.10. The altitude prediction error is unchanged, but the speed prediction error decreases slightly. The potential energy of the 1 m altitude error corresponds to a smaller speed difference at the higher final speed, compared to the previous example.

The examples clearly illustrate that a bias in the estimated road grade affects the predicted speed of the vehicle much more than a sinusoidal zero-mean error. The road grade RMSE of the bias was only 0.10 % grade, while it was 0.21 % grade for the sinusoidal error. For applications that rely on speed predictions low-bias road grade estimates are very important.

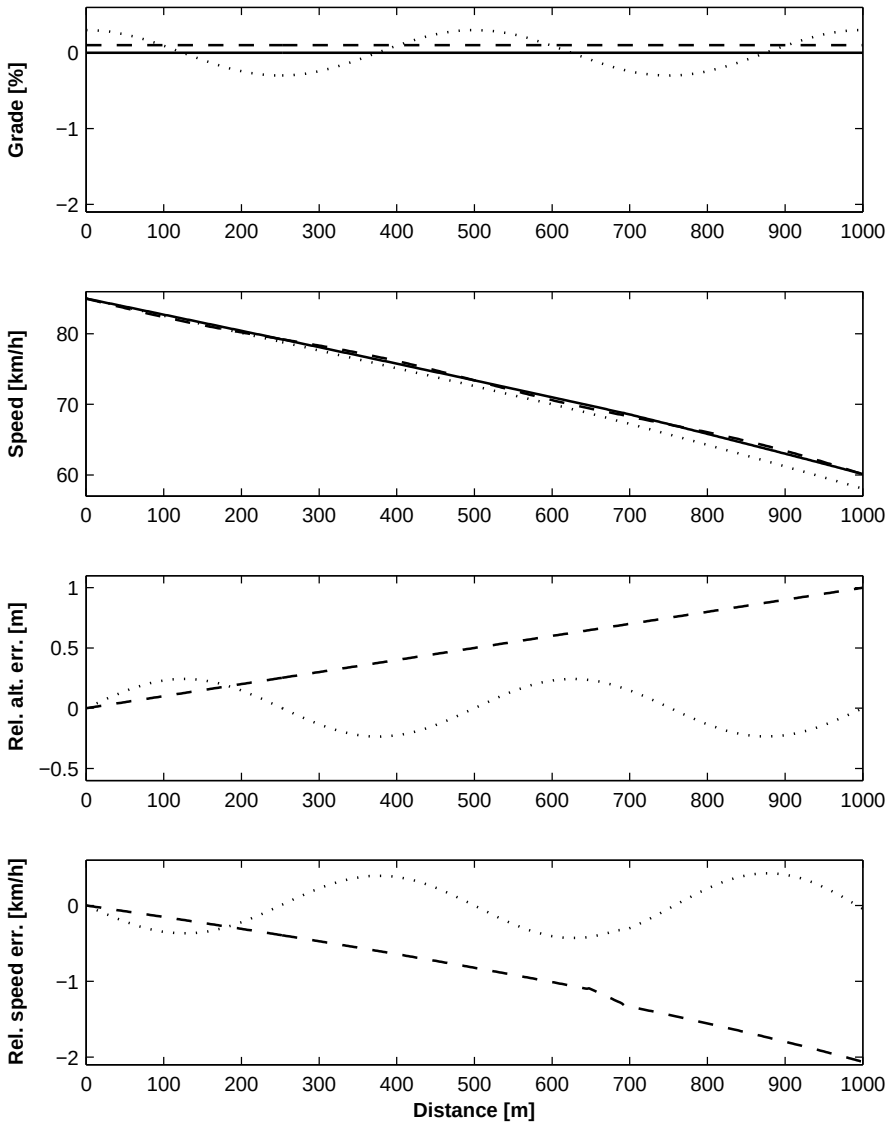

Figure 4.9: Illustration of the effect of a bias error in the estimated road grade. When coasting for 1 000 m on a flat road, the vehicle speed drops from 85 km/h to about 60 km/h. The results for the true road are shown (solid) together with the results based on the biased road grade profile (dashed), and the profile with a sinusoidal error (dotted). The first part of the figure shows the road grade, and the second the vehicle speed. The third part illustrates the altitude prediction error made by relying on each of the estimated profiles. The final part shows the resulting speed prediction error.

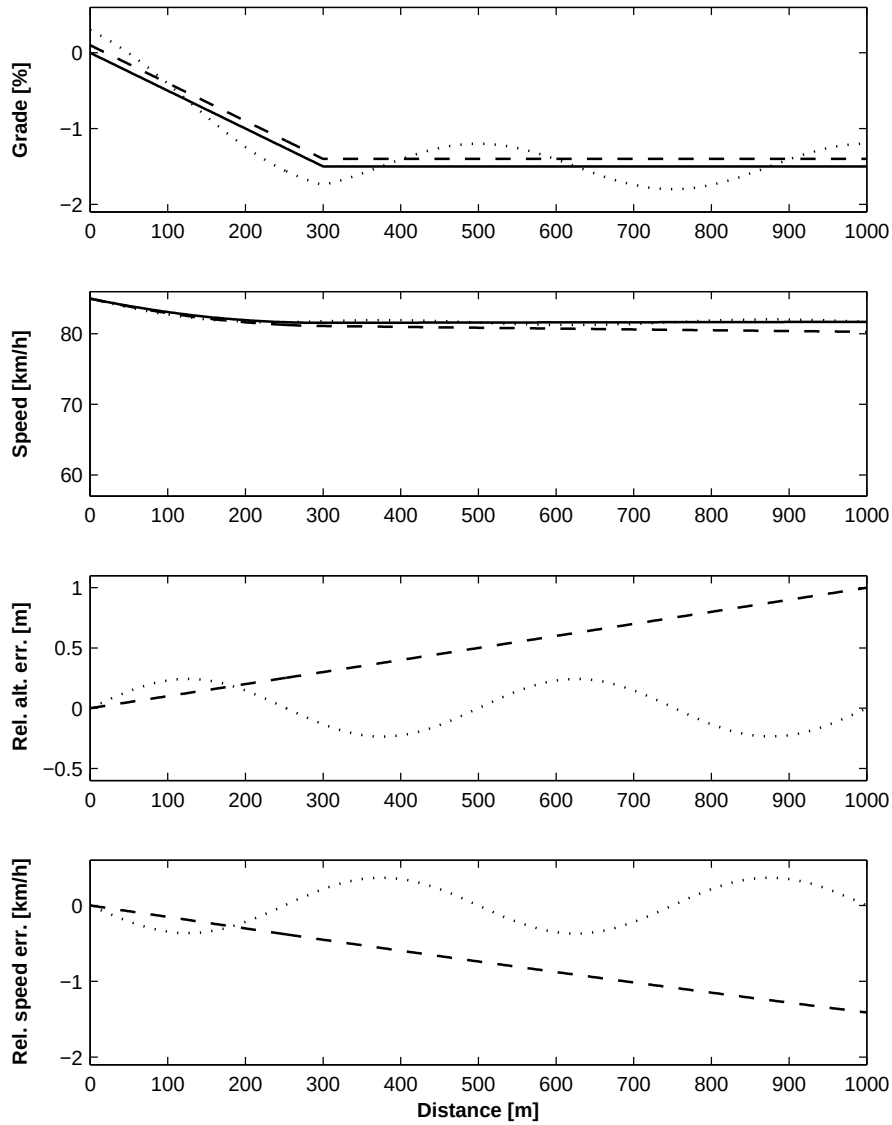

Figure 4.10: Illustration of the effect of a bias error in the estimated road grade. Coasting for 1 000 m when going into the downhill section leads to an initial speed loss, followed by an almost constant speed. The results for the true road are shown (solid) together with the results based on the biased road grade profile (dashed), and the profile with a sinusoidal error (dotted). The first part of the figure shows the road grade, and the second the vehicle speed. The third part illustrates the altitude prediction error made by relying on each of the estimated profiles. The final part shows the resulting speed prediction error.

4.4 Summary

Three different road grade estimators based on standard HDV sensors have been developed. The first estimator, called the constant estimator, uses a model that assumes the road grade to be constant, while the other two are based on the assumption that the road grade is described by a piecewise linear function. The constant estimator is illustrated in Figure 4.1. It adapts the internal weighting of different sensors and the vehicle model predictions to driving events, detected through sensor signals and decision logic. Estimation is carried out after a run along one road segment has been completed and smoothing can thus be used to improve accuracy and avoid time-lag issues. The estimator produces spatially sampled estimates that are fused together with the aggregate of previous estimates of the road grade at that location.

The second estimator, designated the piecewise estimator, computes an optimal piecewise linear representation for the road grade profile based on driveline sensors and the vehicle models developed in Section 3.1. Biases in the vehicle model data are then compensated for using averaged GPS altitude derivatives. Despite being efficiently implemented through dynamic programming this method is still computationally intensive, and does not allow easy updates to a map when new measurements become available.

The third estimator, the spline estimator, combines the constant estimator with a piecewise linear road grade model. This is achieved through a three step process, where the first step provides merged input data, from the driveline sensors and GPS, to the piecewise linear model identification. In the second step a linear spline road grade model is found, which is finally used in a modified version of the first estimator to find a final grade estimate. While being significantly more computationally intensive than the first estimator, this method also allows for efficient updates to a map when new data arrives. It also has the same ability to adapt the estimator to different driving events that affect the quality of the available sensor signals.

For the constant estimator and the spline estimator, the use of data from more than one experiment, with one or multiple vehicles, is part of the design of the methods. In the piecewise estimator, inclusion of data from more than one experiment is more challenging. The chosen approach is to average all measurements mapped to the same discrete road position, before the road grade estimate is computed. While this method works for a fixed set of experiments, updates to the estimated road grade cannot be made if the original data has been discarded. The computation time for an update also grows with the number of experiments available.

Chapter 5

Experiments

> "*No one believes an hypothesis except its originator but everyone believes an experiment except the experimenter. Most people are ready to believe something based on experiment but the experimenter knows the many little things that could have gone wrong in the experiment. For this reason the discoverer of a new fact seldom feels quite so confident of it as others do. On the other hand other people are usually critical of an hypothesis, whereas the originator identifies himself with it and is liable to become devoted to it.*"
>
> W. I. B. Beveridge, The Art of Scientific Investigation, 1950.

The proposed road grade estimation algorithms have been tested using experimental data collected by HDVs driving on a Swedish highway. The road tests verify the applicability of the estimators, and highlight strong and weak points of each method. This chapter describes the experiments and the obtained results. The first section details the experimental setup, including the test road and the vehicles. Experimental results are given in Section 5.2. This is followed by results for the nominal estimator in Section 5.3. Results for the constant estimator are given in Section 5.4. The estimators using the piecewise linear road grade model are evaluated in the following two sections. Results for the piecewise estimator are given in Section 5.5. Finally, the experimental results with the spline estimator are detailed in Section 5.6. The results from the individual estimators are followed by a discussion on the results from the different vehicles and methods. Finally, the chapter is concluded with a summary of the main results and conclusions.

5.1 Experimental Setup

The results from the same on-road experiments have been used in three different road grade estimators, and compared to the nominal case. This section details the test site, vehicles used, and data gathered. A description of the data processing

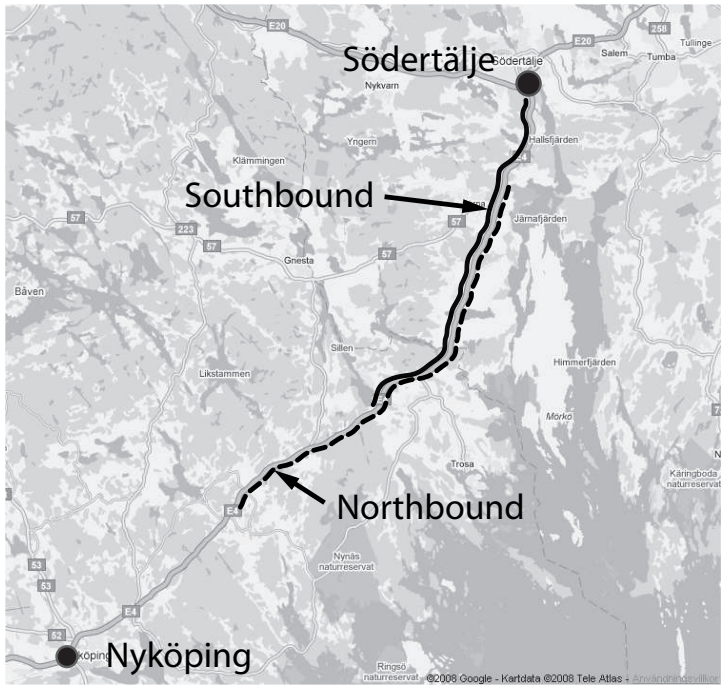

Figure 5.1: Map of the test area. Experiments were conducted on highway E4 between Södertälje and Nyköping. (Image courtesy of Google)

applied to transform the logged data into equidistantly sampled signals, useable in the estimators, is also included.

5.1.1 Road Tests

Road tests to gather data for the proposed grade estimation algorithms were carried out on a part of highway E4 from Södertälje to Nyköping, as shown in Figure 5.1. The test road contains a mix of hills with road grades between −4 % and 4 % and flat segments. This gives an opportunity to study how the estimation algorithms handle various situations such as hill climbing using maximum engine torque, hill descent with no brakes applied, hill descent while using the brakes, and steady state driving on relatively flat road.

To illustrate details in the behavior of the road grade estimators results are presented for the 29 km southbound, and 38 km northbound road segments, as well as short segments that represent different driving scenarios. Segments have also been extracted to illustrate the behavior of each estimator in more detail. To effectively evaluate the obtained road grade estimates a reference grade profile is required. The reference profile used in this work was obtained from a high quality trajectory

Figure 5.2: Test vehicles used for road tests of the grade estimation algorithms. Three vehicle configurations were used. Starting from the left they were a tractor-semitrailer combination (A), tractor only (B), and rigid truck (C). (Photographs courtesy of Scania CV AB)

Table 5.3: Key properties and specifications for the test vehicles used to collect experimental data. The total vehicle weight is given in tons. The last column indicates in what experiments the vehicle was used.

Vehicle	Type	Configuration	Weight [t]	Exp.
A	P310LA4x2MNA	Tractor & semi-trailer	39	1,2,3
B	R420LA4x2MNA	Tractor	12	4,5
C	R420LB6x2*4MNB	Rigid truck	21	6

measurement system capable of recording movements in three dimensions, based on a tightly coupled GPS and INS, as described in Section 5.1.5.

5.1.2 Test Vehicles

The configuration and important parameters of an HDV can vary substantially. Therefore, three different vehicles were used to verify the applicability of the grade estimation methods in each case. The types of test vehicles used are illustrated in Figure 5.2.

The weight of an HDV in Sweden typically varies between 8 t for a small empty truck and 60 t for a fully loaded large vehicle combination. On most European markets the maximum allowable weight is 40 t. The test vehicles weighed from 12 t to 39 t and had between 2 and 5 axles. Important properties for the test vehicles are listed in Table 5.3.

The modeled external forces described in Section 3.1.2 depend heavily on the vehicle parameters used in the equations. Getting reasonable values for these can be a challenge, especially when they are supposed to describe a vehicle in day to day operations rather than in a laboratory setting. In this work the vehicle parameters were chosen as representative values for the vehicle types that were used. They represent sensible values for the vehicle configurations used, on the day of the

experiment, but have not been tuned using the experimental data.

A total of six round-trip experiments were conducted on the test road. The measurement equipment failed on the last northbound experiment. Therefore a total of six southbound and five northbound sets of data are analyzed. The vehicles used in each of the experiments are indicated in Table 5.3. The total vehicle weight in each experiment is assumed to be known in the road grade estimator, so it was measured using a scale. The different vehicles were driven on different days and under varying weather conditions, but a nominal air density figure was still used for all experiments. The experiments with vehicle A were conducted during testing of a look-ahead vehicle speed controller. This represents a very likely scenario for a recursive road grade estimation application, since a truck equipped with a look-ahead speed controller with a self-learning map engine can be assumed to operate with the controller enabled. There are currently not enough directly comparable measurements to conclude if estimation while operating with this speed controller yields results that significantly differ from for example a constant speed controller. However, the overall accuracy of the estimation results when using the look-ahead speed controller is likely to be somewhat higher due to the reduction in braking and gearshifting.

5.1.3 Measurements

The proposed road grade estimation algorithms depend on measurements of a number of vehicle state variables, and share a common abstract representation, as shown in Figure 5.4. The vehicle speed v, the current altitude z, and the instantaneous engine torque T_e, shown on the left side in Figure 5.4, are all used directly in the road grade estimation. They are treated further in Section 5.1.3. In addition to these a number of signals are needed for proper adaptation of the grade estimators to changes in the vehicle and the environment, these are shown entering the grade estimator from the top, and are described in Section 5.1.3. Finally GPS position information is used during data processing to synchronize the data from different experiments. The GPS speed signal is used for vehicle speed sensor calibration. These signals enter the grade estimator from below in the figure, and are further described in Section 5.1.3. At this level of abstraction the grade estimators have only one output, the road grade.

Experimental data were collected while the test vehicles were being driven at normal cruising speed along the highway. A laptop computer with a controller area network (CAN) bus interface card was used to log both vehicle signals and GPS data. The setup is illustrated in Figure 5.5.

Grade Estimator Inputs

The vehicle speed measurements are obtained from standard CAN messages transmitted on the vehicle data bus. The measurements originate from the brake system and represent the mean speed of the wheels on the front axle. The engine torque

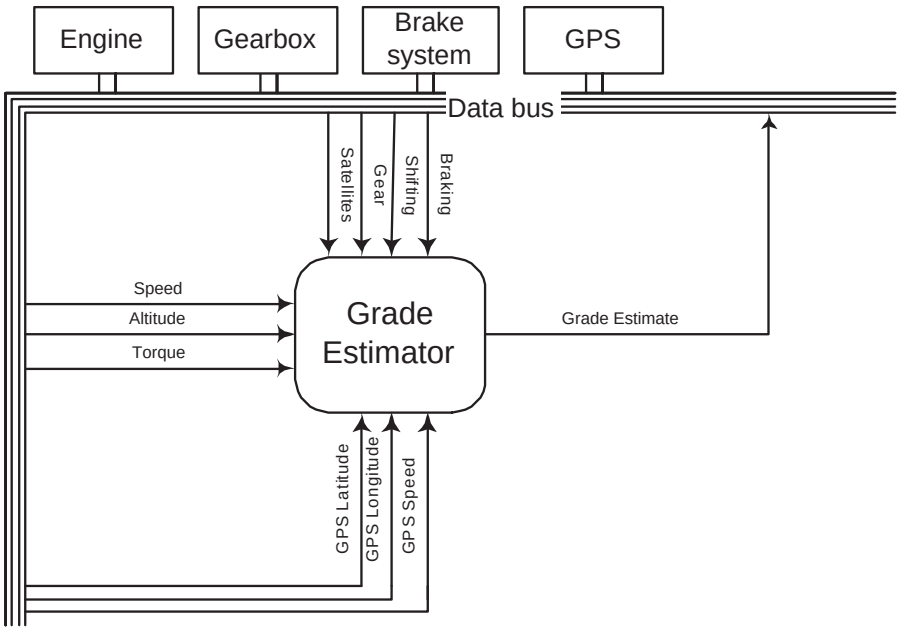

Figure 5.4: The grade estimators described in Chapter 5 depend on two directly measured states, the speed and the altitude. The engine torque is treated as a measured input signal. The estimators also rely on auxiliary information about when braking and gearshifts occur, the currently engaged gear, and the number of tracked GPS satellites. Finally, additional GPS signals are recorded to enable fusion of road grade estimates from multiple runs along a road.

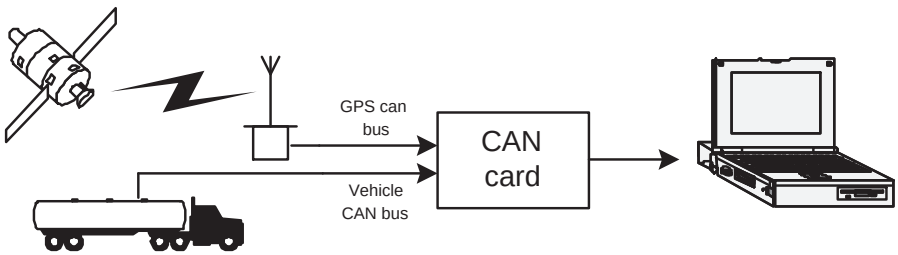

Figure 5.5: During the road tests measurement data were collected using a laptop computer with a dual channel CAN interface card. Vehicle data were logged through one of the channels, and the other one was used to collect GPS messages.

information is sent on the vehicle CAN bus by the engine control unit. It is calculated based on the control signal governing the opening time of the diesel injectors and the current engine state. The quality of this signal is usually reasonable, although variations between individual engines and over the life of a single engine are present. All CAN messages were logged using a Vector CANCardXL (Vector Informatik, 2010) connected as shown in Figure 5.4.

Each CAN message is time stamped by the receiver board upon arrival. This timestamp has been used to synchronize all the signals during data post processing. No special consideration has been given to possibly varying latencies in the different sensors and processing units that supply the signals.

The altitude measurement comes from a single frequency (L1) GPS receiver without differential corrections. While there are higher precision GPS options available, the choice of GPS receiver technology was motivated by the belief that the accuracy would match what will soon be implemented as standard equipment in vehicles. The GPS altitude signal contains a considerable amount of noise that varies with the satellite reception conditions, as previously discussed in Section 2.8.2. For the road tests a Racelogic VBOX receiver was connected to its own channel on the CAN logger used to record the vehicle CAN signals. The chosen receiver has three-dimensional velocity measurement capabilities beyond those of regular low-cost GPS units, but those velocity outputs have not been used in this work. The specified horizontal error for the receiver is 3 m 95 % Circle Error Probable (CEP) and the vertical error specification is 6 m 95 % CEP. 95 % CEP is defined as 95 % of the measurements being within a circle of the given diameter. This absolute positioning accuracy is comparable to single channel consumer grade GPS receivers in general. The setup used does not provide any dilution of precision information from the receiver. As an effect position quality is judged only from the number of tracked satellites, as described in Section 5.1.3. Detailed information on the GPS receiver can be found in the user's manual (Racelogic Limited, 2009).

System Mode Inputs

The road grade estimators with KF are tuned to different operating modes of the vehicle by adjustments to the assumed measurement and process noise covariances as discussed in Section 4.1.3. The noise covariances are determined based on the four signals entering from the top in Figure 5.4.

When the vehicle is braking there is no accurate estimate of the torque transmitted through the wheels. The process noise for the vehicle prediction is then increased, to reduce the effects of a wrongly predicted speed on the estimated grade.

During manual gearshifts the gearbox is briefly put into neutral and the engine is disconnected from the drive wheels. This makes our vehicle model invalid, since the reported engine torque never reaches the driving wheels. During gearshifts with an automated manual gearbox the engine is controlled to give zero torque transfer through the transmission, and the new gear is selected without using the clutch. Due to imperfections in the control during the gearshift there are often transient

effects in the driveline associated with the shift, so in either case the same action with regard to the filter covariances is taken as during braking. The experiments 1–5 were carried out using a vehicle with an automated manual gearbox, and experiment 6 was done with a regular manual gearbox. The vehicle model is updated to operate based on the newly selected gear once the gearshift is complete.

The number of tracked satellites is used together with a look-up table to determine an appropriate measurement noise covariance for the measured altitude signal.

Data Fusion Inputs

In order to synchronize state estimates from several runs along a road, the latitude and longitude of the current position are recorded along with each altitude value. The GPS derived speed signal is also recorded and used to calibrate the front wheel based vehicle speed. The speed measurement calibration almost completely removes wheel radius scale factor errors from the speed signal. This in turn makes merging of data from vehicles with different stock scale factor errors much more precise. The number of satellites used to determine each position fix is saved for the measurement noise variance selection.

5.1.4 Data Processing

The recorded sensor data from the experiments have time stamps, added by the measurement equipment. These time stamps are used to synchronize the various signals. To apply the road grade estimators it is necessary to resample all the data with a common sample distance. The average values of the speed recorded from the GPS and the front wheel sensors, at all times where the difference between them is small, are used to calibrate the front wheel sensors in each experiment. After this the average front wheel speed signal is integrated, to obtain a time-distance connection. In the next step start and end points for the southbound and northbound experiments are determined in the reference road grade profile. The closest points to these locations in each experiment are then chosen as the start and end points for that experiment. To improve the matching within an experiment, additional points are chosen in the reference profile every 10 km, and the best matches in all experiments found. The distance vectors between the synchronization points, for each experiment, are adjusted by a scale factor such that the driven distance between all synchronization points is the same in all experiments. The now obtained distance vectors are used to resample all signals to a common distance index vector with a sample distance of 2.5 m. This data set is used to compute the experimental results for each estimation method.

5.1.5 Reference Road Grade

In order to evaluate the performance of the proposed road grade estimators, a reference road grade profile is needed. The profile used was collected by measuring the road grade with a high accuracy combined GPS and INS measurement unit. The equipment used was an Oxford RT3040 unit, with a specified road grade estimate standard deviation of 0.05 % (Oxford Technical Solutions Limited, 2010). A single experiment was used to compute the reference road grade used for the evaluation of the constant estimator and spline estimator. The instrument yields a signal sampled at 100 Hz, which was resampled with a sample distance of 2.5 m. It was also low-pass filtered, using a third-order Butterworth filter with a cut-off frequency corresponding to a wavelength of 111 m.

The road was later measured additional times using the high accuracy instrument. The extra measurements were used to validate the reference profile. An average of all GPS/INS measurements of the test roads was also used directly to evaluate the piecewise estimator. The five measured reference profiles available for a section of the southbound test segment, and the difference between them, are shown in Figure 5.6. The Root Mean Square (RMS) differences in grade, between the measurement used as a reference profile and the other measurements, were 0.03 %, 0.04 %, 0.06 %, and 0.05 %. The accuracy given in the specifications for the instrument appears to be achieved.

To further validate the measurements, the reference road grade profile for the southbound test segment is compared to a road grade profile obtained from Navteq. A section of the two profiles, and the difference signal, are shown in Figure 5.7. The RMS difference between the signals was 0.07 %. In both comparison between both the measured signals and the externally sourced signal the differences between them grow when the grade changes rapidly. This indicates that errors in the positioning of data points are likely to result in road grade errors.

The differences between all the measurements, and between the reference signal used and the independent estimate obtain from Navteq are small compared to the estimation errors in the experiments. It is therefore reasonable to use the reference signal to analyze the performance of the grade estimators.

5.2 Experimental Results

Example sensor data recorded on a 12 km segment of the southbound test road are used to illustrate the different input signals used by the state estimators. For clarity the figures only contain data from one run along the road for each of the three test vehicles. The chosen experiments are numbers two (solid line, vehicle A), four (dashed line, vehicle B), and six (dotted line, vehicle C). The grade estimator inputs are treated in Section 5.2.1, and the system mode inputs are described in Section 5.2.2.

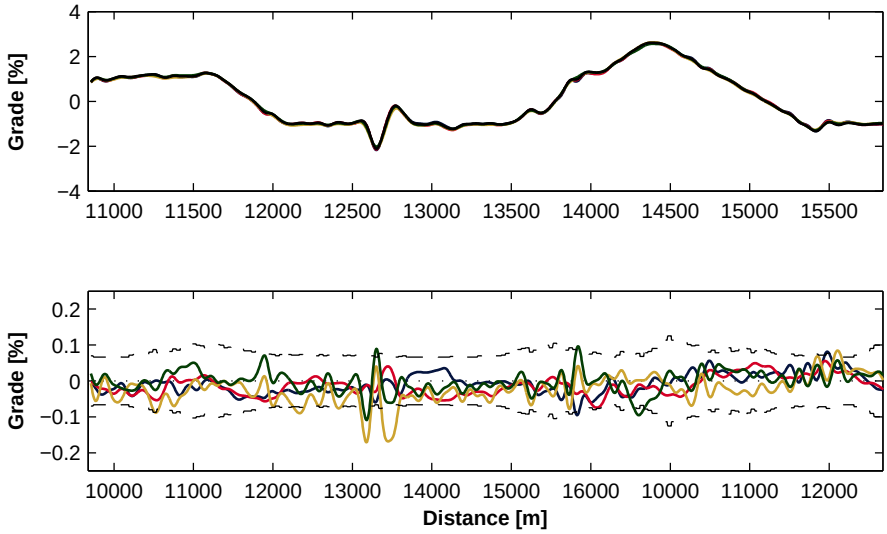

Figure 5.6: The reference road grade for a section of the southbound test road is shown in the top figure, together with four other measurements using the same equipment. The reference profile (solid, black) agrees very well with the other measurements (solid, colored blue, red, gold, and green). To illustrate the differences a magnified view of the difference between the reference and the other measurements is shown in the bottom figure. The measurements are shown as solid lines with the same colors as above. The estimated standard deviation from the instrument used, during the measurement of the reference road grade profile is indicated by dashed black lines.

5.2.1 Grade Estimator Inputs

Figure 5.8 shows the recorded mean front wheel speed, GPS altitude, and engine torque.

Speed

Vehicle A is heavy in relation to its engine power, and has a typical speed profile for an economically driven HDV. The driver (or in this case the look-ahead cruise control) has ordered the speed to be lowered ahead of long downhill segments, thus reducing the amount of braking necessary. This can be seen at 15 km and 25–26 km. At 23 km the algorithm for some reason does not predict the vehicle behavior correctly, and braking becomes necessary even though the speed could have been decreased ahead of time without hitting the lower speed bound (80 km/h in this case). Vehicle B is very light, more powerful than vehicle A, and was operated with a constant cruise control system enabled. The speed profile is very flat with no speed loss in uphill segments, and no run-out in downhill segments. Vehicle C

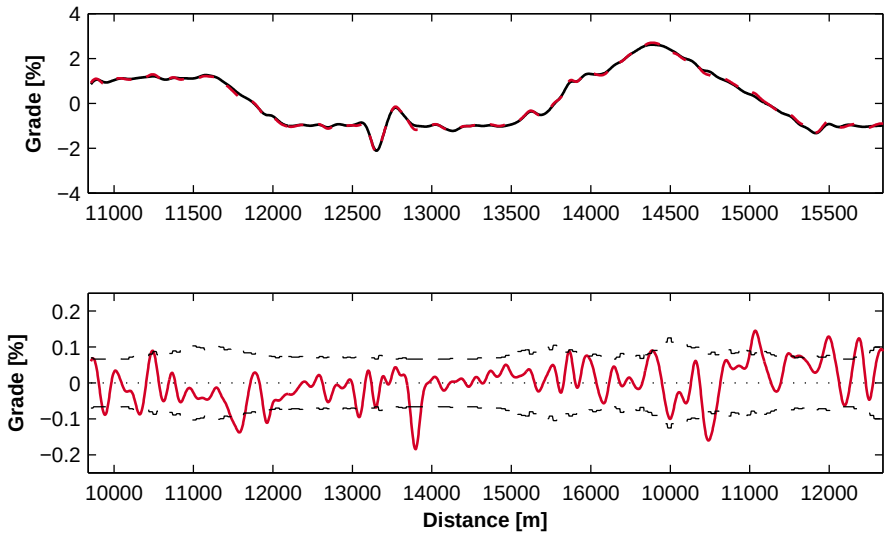

Figure 5.7: The top figure shows the reference grade profile (solid, black) and the profile obtained from Navteq (dashed, red) in the same way as in Figure 5.6. In the bottom figure the difference between the profiles (solid, red) is shown, together with the standard deviation of the grade estimate indicated by the GPS/INS equiment (dashed, black). The differences between the Navteq data and the reference is larger than the differences between the measurements obtained from the GPS/INS equipment, but still smaller than the differences between the estimates from the investigated methods and the reference profile.

is heavy enough to gain some extra speed in downhill segment, but was following slower moving traffic for part of the drive. At 18–19 km there was a roadwork in one of the lanes, with an associated mandated speed decrease. The speed of vehicle C was controlled manually. All vehicles are electronically speed limited, and thus unable to accelerate above 89 km/h by the means of their engine.

Altitude

The effects of loss of satellite coverage can be seen clearly around 24–26 km in the altitude trace for vehicle B, but short signal loss also occurs with vehicles A and C. Note the large almost static difference between the altitudes reported by vehicles B and C, and the one from vehicle A. This difference of approximately 10 m is common for a GPS system without differential corrections applied. The data is collected on different days, with variations in atmospheric conditions as well as the visible satellite constellation. The key advantageous properties of the GPS altitude signal are that the error changes very slowly, and that its mean is zeros over very

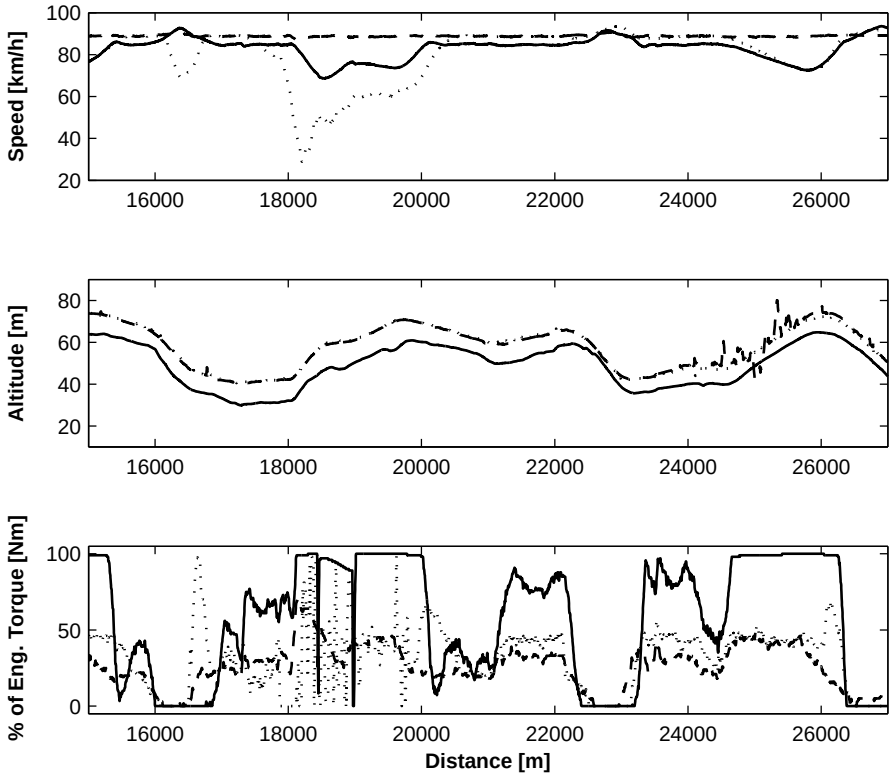

Figure 5.8: The measured states of the road grade estimators are the vehicle speed and the GPS altitude. The engine torque in the third sub-figure is treated as a known input to the vehicle model in the estimators. It is measured as a fraction of the maximum available torque for a particular engine, and then multiplied by the maximum torque. Data are shown for three runs along a road segment ranging from 15 km to 27 km in the southbound data set. The solid line represents experiment 2 (vehicle A), the dashed line is experiment 4 (vehicle B) and the dotted line is experiment 6 (vehicle C).

long time periods.

Engine Torque

The engine torque reported by the engine management system is used as an input to the longitudinal movement models for the trucks. This signal changes rapidly and is given as a percentage of the maximum torque for a given engine. It can be seen in the figure that vehicle A uses its maximum power for long periods of time in the uphill segment, and applies no engine power in a number of downhill segments. The almost empty vehicle B never utilizes the full engine power, and rarely has zero utilization. Vehicle C has to work slightly harder on average than vehicle B, but also shows a number of gear changes and peak power utilizations during acceleration. Gear changes can be seen in the torque data as short spikes towards zero.

5.2.2 System Mode Inputs

The signals described above, and shown in Figure 5.8, are used directly in the grade estimators. In addition to these, a number of auxiliary signals are used to adjust the parameters of the vehicle model, and the process and noise covariances, as described in Section 4.1.3. Figure 5.9 shows examples of these signals.

In addition to the signals in Figures 5.8 and 5.9, the absolute position and vehicle speed are recorded from the GPS for each data point. This information is not used directly for the grade estimator, but it is necessary in order to synchronize several source data sets, as described in Section 5.1.4.

Number of Satellites

The number of available satellites is very important to the functioning of the GPS receiver, and for the equipment used in the experiments this is the best indicator of GPS altitude signal quality that is available. The number of tracked satellites by the same receiver can vary substantially, on the same road, due to the constant movement of the satellites and change in atmospheric conditions. This can be clearly seen in the first part of Figure 5.9, where the conditions during experiment 2 (solid line) were significantly worse than during the other two.

Current Gear and Shifting

Not too many gearshifts are available in the test data set. The predictive cruise controller that controlled vehicle A was configured to minimize gearshifts to conserve fuel, and it was quite successful in doing so. Vehicles B and C are overpowered in the sense that they didn't need all the available engine power available on the top gear to climb the hills of the test road, and thus had no need for gearshifts. The second plot in Figure 5.9 shows a segment where vehicle A needs to downshift to climb the hill, and vehicle C has to slow down and then accelerate due to the previously mentioned road work. The third plot is closely related to the second

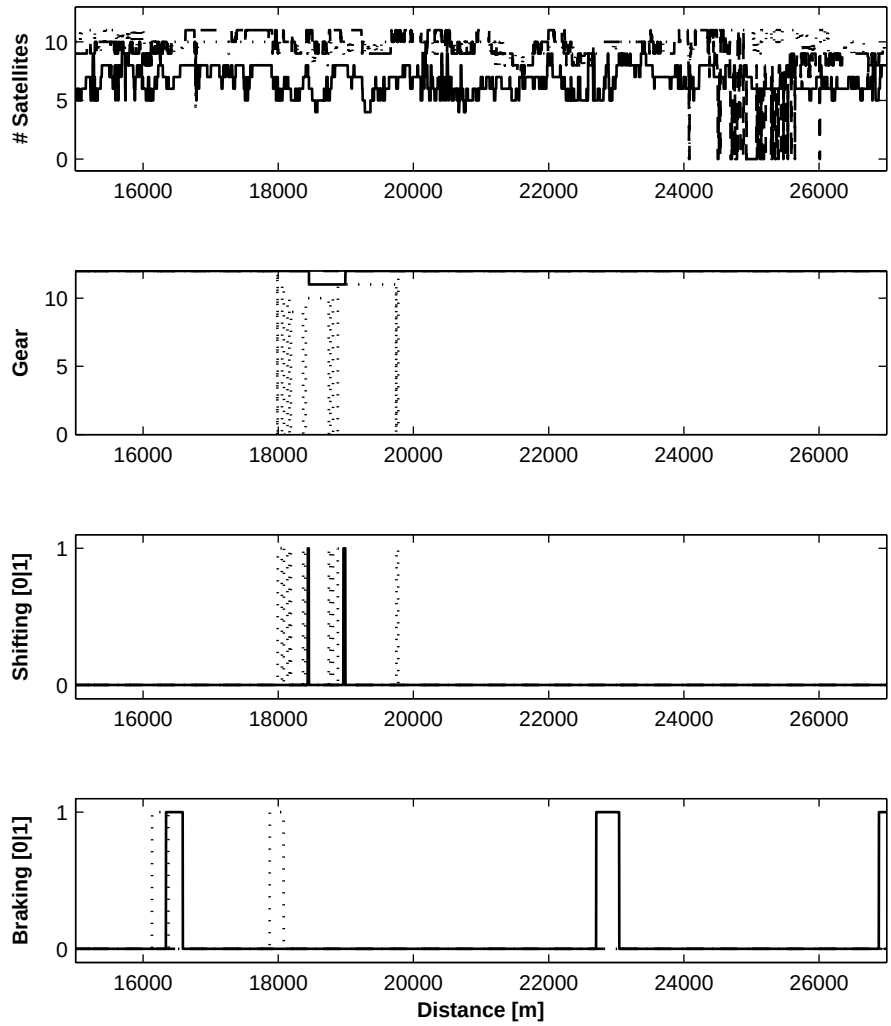

Figure 5.9: Auxiliary variables are recorded to facilitate mode switching in the algorithms based on anticipated signal quality and vehicle behavior. The first plot shows the number of tracked GPS satellites, this signal is correlated with the accuracy of the GPS altitude measurements. The second plot shows the current gear. The chosen gear influences the dynamics of the vehicle model. The third and fourth plots indicate where gearshifting and braking has occurred, these events lead to adjustments in the process noise assumptions. Included are experiments 2 (solid), 4 (dashed), and 6 (dotted).

Table 5.10: Estimation errors for the nominal estimation method, based on averaged data over all experiments, for each road section. The results are given in % grade.

Source	Direction	Unfiltered		Filtered	
		Mean	RMSE	Mean	RMSE
GPS	South	-0.01	0.46	-0.01	0.34
	North	0.01	0.71	0.01	0.38
Vehicle model	South	-0.15	0.39	-0.15	0.31
	North	-0.44	0.57	-0.44	0.50
Combined	South	-0.01	0.37	-0.01	0.28
	North	0.01	0.37	0.01	0.24

one, the shifting signal indicates when the driveline is not operating with a fixed ratio between the engine and the driving wheels. During this time the longitudinal vehicle model becomes void, and actions are taken as described in Section 4.1.3.

Braking

It is important to know when any of the vehicles' brakes are applied, since this leads to an external, unknown, torque entering the equations of motion. The "braking" signal indicates when the longitudinal vehicle model should not be trusted for this reason. Vehicle A applies the brakes to avoid overspeeding, while vehicle C uses them to avoid running into traffic ahead.

5.3 Nominal Estimator

By applying a central difference approximation to calculate the derivative of the GPS altitude signal, or solving for the road grade in the vehicle model, nominal sensor based road grade estimates can be computed. Expressions for the nominal estimates are given in equations (3.28) and (3.29) in Section 3.3.1. These estimates can be seen as virtual sensors, and will contain large random errors, due to the lack of filtering. Low-pass filtering these quantities, forwards and backwards, yields a simple, phase error free, road grade estimate based on each sensor. It is interesting to study how each of the proposed road grade estimators perform compared to this nominal method for obtaining road grade estimates. The RMSE and mean errors for the nominal method, with and without filtering, are given in Table 5.10. The estimates were filtered using the same Butterworth low-pass filter as the reference signal. Small variations of the cut-off frequency produce only marginal changes in the performance, and large deviations from the frequency used significantly degrade performance.

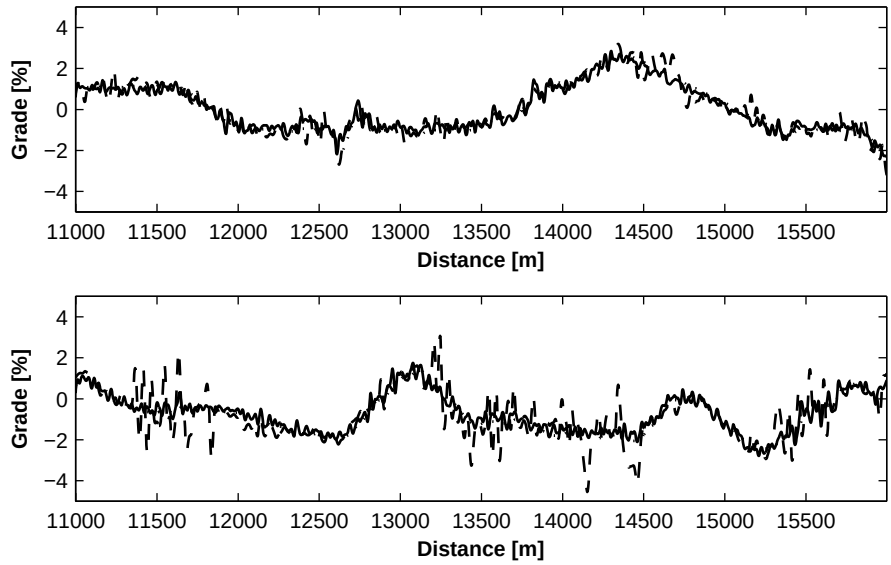

Figure 5.11: The averaged, GPS corrected, and filtered vehicle model based estimate (solid lines) is shown together with the filtered GPS based estimate (dashed lines) and the reference road grade profiles (dotted lines). The top figure shows the southbound profile, and the bottom figure the northbound road grade profile.

As noted earlier, the vehicle model based estimates contain less noise in the frequency band of interest than the GPS, but suffer from bias issues. The GPS derived estimates are noisy, but stable over long time intervals. To combine the two in the nominal method the average value of the vehicle model based estimates were corrected using the average value of all available GPS based estimates. This procedure produces significantly improved estimates compared to both the vehicle model and GPS based methods, the method is referred to as "combined" in Table 5.10. From the nominal estimates it is clear that there is significant high frequency noise in the inputs to the vehicle model that can be removed through low-pass filtering.

The averaged, GPS corrected, and filtered nominal vehicle model based estimates, in each direction, and the reference road grade profiles, are illustrated in Figure 5.11. This road grade profile corresponds to the combined estimator in Table 5.10.

5.4 Constant Estimator

The results from the constant estimator are promising. Even if individual measurements sometimes are far from the true road grade, the merged estimate from few runs along the road comes quite close over most of the distance. The final result

based on only data from the six experiments in the southbound direction and five experiments in the southbound direction, described in Section 5.1, agree very well with a reference road grade profile. Events such as braking and shifting generally decreases the quality of the road grade estimate for that experiment, but most of the time they not occur at the exact same position in all experiments. As a result of the data fusion described in Section 4.1.2, many segments with lower quality data can be identified and suppressed in the final estimate. The main performance criterion used to evaluate the results is the RMSE of the grade estimate compared to the reference road grade for that location, as described in Section 4.3.

This results section starts with an overview of the estimation results for all runs along the road for a representative road segment, with vehicle behavior that adheres to the basic state of the model. This is followed by in-depth studies of how the algorithm performs during more adverse conditions. The cases highlighted are when the vehicle is:

- Braking
- Shifting gears
- Losing satellite coverage

To illustrate the operation of the data fusion step in the estimation algorithm a step by step series of figures is provided. The benefits of a reduced bias in the estimated road grade from using the GPS receiver as an altitude sensor are illustrated by a comparison of estimation results when the altitude signal from the GPS receiver has been excluded from the estimation and the full input case. Finally a comparison is made between real world estimation results based on the EKF algorithm and the linearized system with a regular KF.

5.4.1 Aggregate Results

The overall impression of the constant estimator is that it works well and produces road grade data that should be useable for a number of applications. The estimates are not free of bias, but the inclusion of the GPS makes the results fair even when the vehicle parameters are non-ideal, as seen in Section 5.4.5. On the southbound test road as a whole the RMSE of the estimated road grade was 0.13 % grade, with a bias error of −0.02 % grade. For the northbound direction the RMSE was 0.15 % grade, with a bias of −0.06 % grade. The statistical distributions of estimation errors in the two test roads are illustrated in Figure 5.12, together with normal distributions with the same standard deviations. It can be seen that the errors are roughly normally distributed, with the identified bias.

There is a correlation between the road grade estimation errors and the rate of change in the road grade. When the road grade changes rapidly, the estimation error increases. This is caused by an apparent misalignment of the reference road grade profile by approximately 12 m. The estimated road grade profile changes

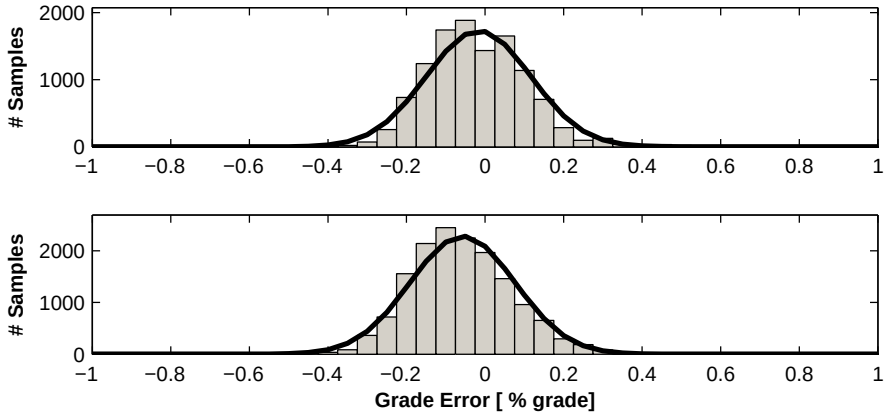

Figure 5.12: The distribution of road grade estimation errors for the southbound (top) and northbound (bottom) test roads. A normal distribution with the observed mean and standard deviation is overlaid for comparison. The observed errors are close to being normally distributed.

at an earlier position along the road than the reference grade profile. This effect may be depend on the way the filtering and smoothing steps of the estimation method works, or on some timing issue in the data processing. The 12 m difference amounts to about 0.5 s at highway speeds. With knowledge of the reference grade, the misalignment can be corrected retroactively by finding the distance offset that minimizes some performance criterion, e.g., the RMSE in the grade estimate. Doing so eliminates the mentioned correlation and reduces the road grade RMSE by approximately 0.02 % grade, but also sacrifices the ability to apply the complete method without access to a road grade reference. It has been opted not to correct the alignment in the analyzed data. It is noted that improved synchronization of the sensors is likely to improve the end results.

To illustrate the magnitude of the obtained estimation errors during nominal driving the numerical standard deviation among the six road experiments on the southbound road is investigated. Figure 5.13 shows the agreement of the final grade estimate with the reference for a 5 km segment of the southbound test road, together with the sample standard deviation for each data point.

5.4.2 Comparison with Nominal Estimator

As an alternative to using the proposed road grade estimator, the GPS signal and the vehicle model could be used directly, as described in Section 5.3. Figure 5.14 shows the performance of such an approach, compared to the proposed constant estimator. Using all available experimental data, the nominal method yields a RMSE that is 115 % higher for the southbound data, and 38 % higher for the northbound

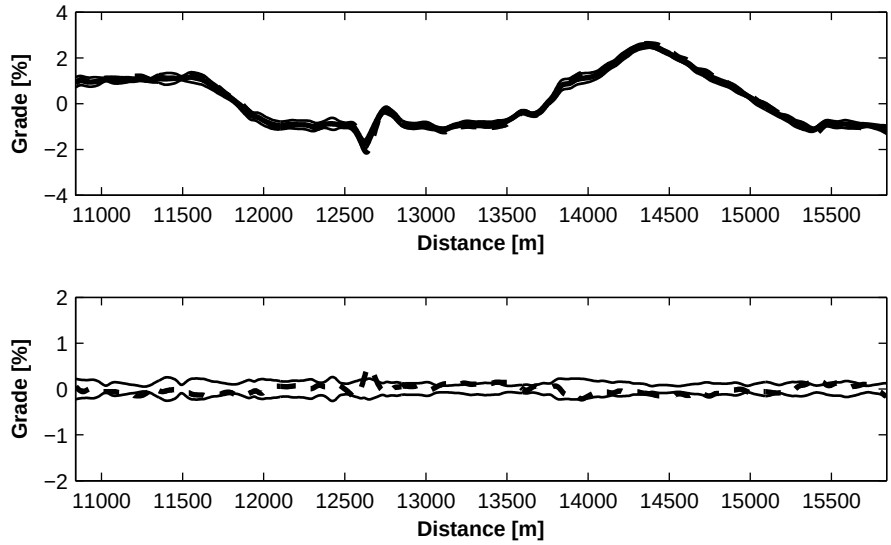

Figure 5.13: The top figure shows the final grade estimate calculated through data fusion based on six experiments (solid). It agrees well with the reference grade profile from a specialized measurement vehicle (dashed). The numerical one standard deviation interval around the final grade estimate at each sample point, based on the six experiments, is also shown (thin lines). The bottom figure shows the difference between the fused grade estimate and the reference profile (dashed), as well as the standard deviation from the top figure (solid).

data. A further comparison of the various estimation methods investigated is given in Section 5.7

5.4.3 Braking

One of the most challenging situations for the grade estimator is when the vehicle applies one of the brake systems. Therefore, we shall study one such occasion in more detail. During braking the engine will generally report a negative net torque from internal friction when fueling is cut off. This means that the vehicle model based prediction in the grade estimator will be computed using only the engine friction as its driveline input, even though there is a braking force present as well. The roll resistance and air drag will still be correctly modeled. The missing brake force will then be attributed to the gravity component, aka the road grade. This should lead to a road grade estimate that is too high (more uphill than in real life). To avoid this effect, and at the same time raise a flag to the data fusion algorithm that this data deserves lower trust than the norm, the process noise covariance for the speed state is increased. This causes the estimator to rely less on the vehicle

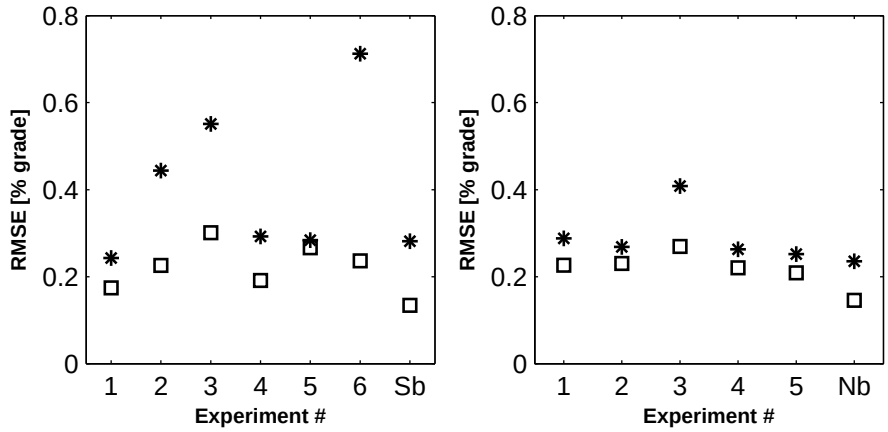

Figure 5.14: The road grade RMSE for the nominal estimator (∗), is compared to the performance of the proposed constant estimator (□). The proposed estimator has better performance for all experiments, and the relative difference is particularly large when using all data available from a particular road section (denoted by Sb and Nb).

model, and more on past road grade estimates and the GPS measurements. At the same time the estimated error covariance of the output increases.

The example segment shown in Figure 5.15 represents a comparatively steep downhill segment, where the heavy vehicle A needs to apply the brakes to avoid exceeding its set maximum allowed speed. Data are shown for experiments 2 (solid, vehicle A), 3 (dashed, vehicle A), and 6 (dotted, vehicle C). Vehicle C does not apply the brakes in this segment. Figure 5.15 shows the key signals of interest during braking. The first two sub-figures show the speed profiles and GPS altitude measurements, below that comes the reported engine torque and braking signal. Vehicle A is pulled down the hill by its weight, and does not need to utilize the engine until the very end of the segment. Vehicle C, at 21 t, can only coast at a constant speed for a few hundred meters, and then needs to use engine power to maintain speed. Braking is required by vehicle A for a total of almost 1 km in each of the experiments. The resulting road grade error in the fifth part of the figure shows that experiment 2 yields an overestimate of the grade during the first brake application, an underestimate during the second, and no visible additional error during the third application. Experiment 3 yields no significant additional error during the first application and overestimates of the grade during the second. The final part of the figure shows the estimated grade error covariance after the smoothing step in the grade estimator. The estimated error variance almost doubles during the segments where the brakes are applied.

Somewhat surprisingly the experimental data does not indicate that the investigated periods of braking severely affect the overall merged road grade estimate.

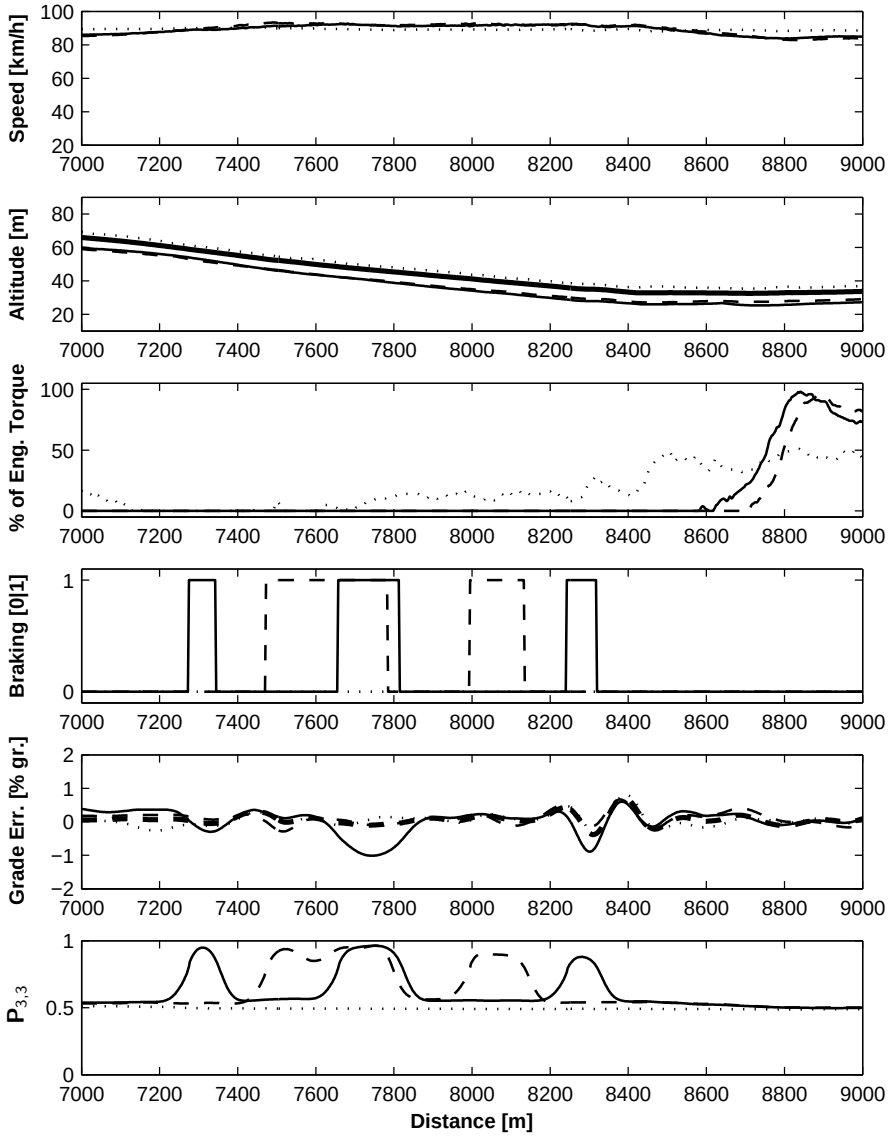

Figure 5.15: Signals of interest during braking for a segment of the southbound test road. Data are shown for experiments 2 (solid), 3 (dashed), and 6 (dotted). In the fifth part the road grade error of the merged final estimate is shown as well (thick solid).

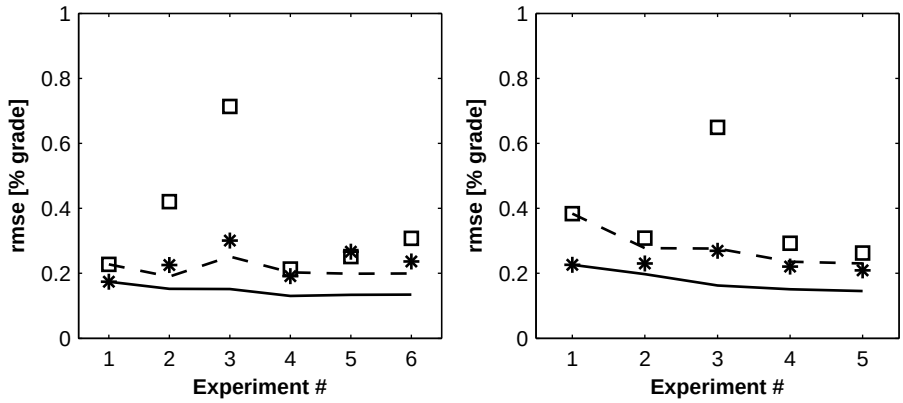

Figure 5.16: Estimation results during braking. The road grade estimate RMSE is shown for the southbound (left figure) and northbound (right figure) test segments. The value for the entire road segment, based on the experiments up to and including the index on the x-axis, is shown (solid line) together with the value when only the sample points where braking occurs in at least one experiment are included (dashed line). The values for the individual experiments are shown with stars for the entire segment and squares for the sample points corresponding to the dashed line.

Figure 5.16 shows the RMSE values for the road grade for each experiment, as well as for the map based on an increasing amount of data. The road grade RMSE of the entire segment is compared to the RMSE for only those sample points where the vehicle was braking in at least one of the experiments. Braking occurred primarily in vehicle A. This led to an increased estimation error for most of the corresponding experiments. The worst effects were seen in experiment three, with vehicle A. This was also the experiment that showed the highest errors over the entire segment, out of those done with vehicle A, as indicated by the third star in the figures. Given that the same vehicle was used for experiments 1–3 this indicates that the weather conditions were less in agreement with the parameters used on the day of the third experiment that for the previous two. A brake system was engaged in at least one of the experiments in the southbound data set for a total of 2518 m. For these parts of the road the RMSE in the road grade estimate was the same as the total average of 0.14 % grade. In the northbound direction the effect was more noticeable. A brake system was used in some vehicle for a total of 1568 m. At these times the RMSE increased from 0.15 % grade for the entire road segment, to 0.24 % grade.

In the current implementation of the grade estimator there is no way of assessing the amount of brake torque being applied. If the driver uses the retarder or engine brake as opposed to the wheel brakes there is a possibility to have some additional information on the magnitude of the force.

5.4.4 Shifting Gears

During gearshifts the engine is disconnected from the rest of the driveline, and the model for the influence of the engine torque becomes void. This is handled by setting the engine torque input in the grade estimator to 0 while the status signal "Shifting" is active. The friction losses from the driving wheels to the disconnected gearbox are assumed to be negligible. After the gearshift the estimation continues, with a vehicle model suitable for the newly chosen gear. A shift of gears introduces quite a lot of non-linear and oscillatory behavior in the driveline that is not captured by the model used. To attempt reduce the negative impact of these effects in the merged estimate the process variance for the speed prediction is increased during the gearshift in the same way as during braking.

Example data for a segment with many gearshifts is shown in Figure 5.17. The segment chosen to illustrate the behavior during gearshifts contains a 2 km long uphill segment that is steep enough to require downshifting in vehicle A. During the experiments with vehicle C there was a road work set up at this location, leading to slow moving traffic, as seen in the first part of the figure. The third and fourth parts of the figure show the shifting signal and the current gear. The gearshifts in the two experiments with vehicle A occur close to each other, but do not overlap. The fifth part of the figure shows the road grade estimation error for the three studied experiments, as well as for the final grade estimate. It can be seen that the estimation error generally increases somewhat during the gearshifts. Right before the 19 km mark the estimation error increases significantly during the upshifts for vehicle A. This can be explained by a large error in the derivative of the GPS altitude measurement at that location, as seen parts four and five of Figure 5.18. As the process variance of the vehicle model is increased during the gearshift, the influence of the GPS signal grows. There are a fair number of satellites being tracked at the location, and thus the GPS altitude derivative affects the estimation results.

The large error in all the estimates, and the merged result, around 18 km is due to the algorithm finding the start of the uphill segment at an earlier position than it occurs in the reference profile, as seen in part two of Figure 5.18. The drop in the base level of $P_{3,3}$ in the fifth part of Figure 5.17 for vehicle C is explained by a drop in the measurement innovations at that time. The Q and R matrices are only adjusted during the shift events.

Overall gearshifts, or the driving conditions where gearshifts are performed, yielded mixed grade estimation results. Figure 5.19 shows the RMSE values for the road grade for each experiment, as well as for the map based on an increasing amount of data. The road grade RMSE of the entire segment is compared to the RMSE for only those sample points where the vehicle was shifting gears in at least one of the experiments. The road segments where shifting occurred in some of the experiments generally gave worse estimation results than the test road as a whole. Again, in the same way as during braking, the third experiment was particularly severely affected. However, gearshifts took place in experiments 1, 2, and 6 as well, so gearshifting does not always yield bad grade estimates. In the southbound data

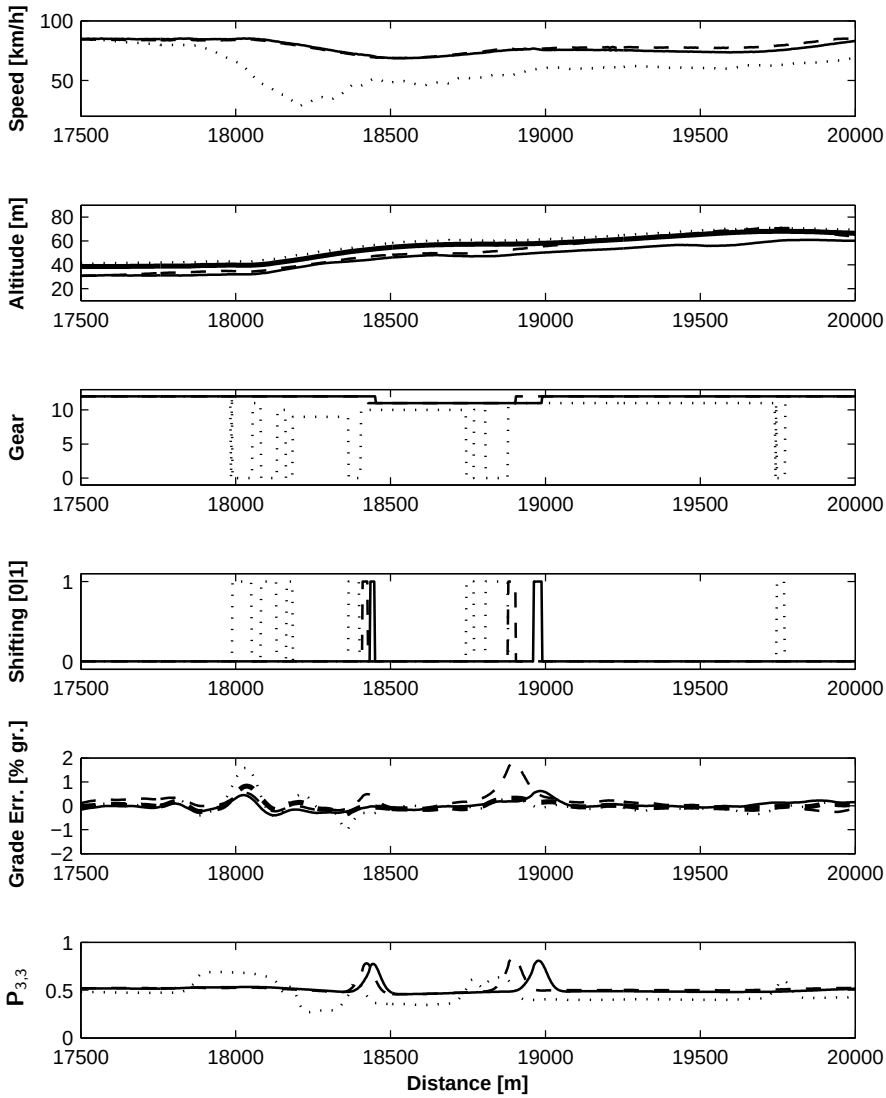

Figure 5.17: Road grade estimation results during gearshifts. Data are shown for experiments 2 (solid), 3 (dashed), and 6 (dotted). In the second part the reference altitude is also included (thick dashed), and in the fifth part the road grade error of the merged final estimate is shown (thick solid).

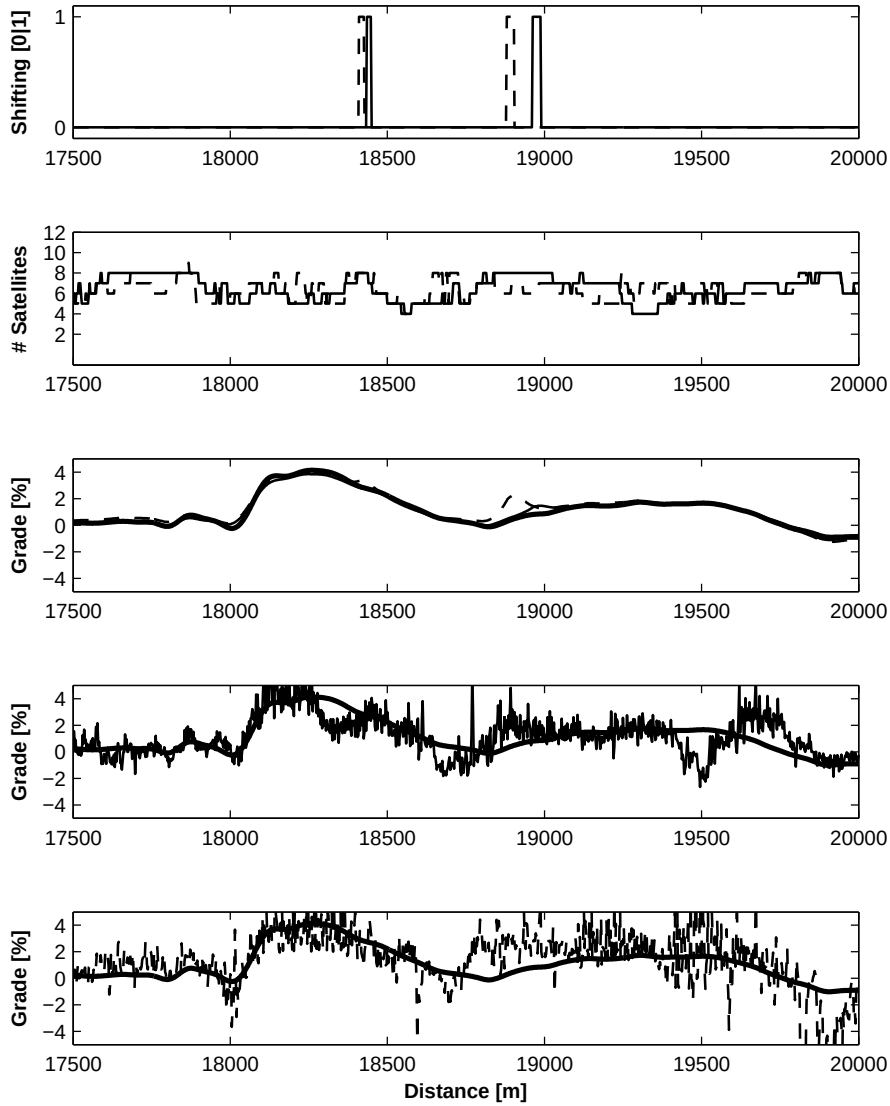

Figure 5.18: The shift signal and GPS data are shown for experiments 2 (solid) and 3 (dashed). The reference grade (thick solid) is included in parts three-five. Parts four and five show the numerical derivative of the GPS altitude for experiments 2 and 3 respectively. The altitude derivative has a significant difference to the reference road grade during the second gearshifts before the 19 km mark.

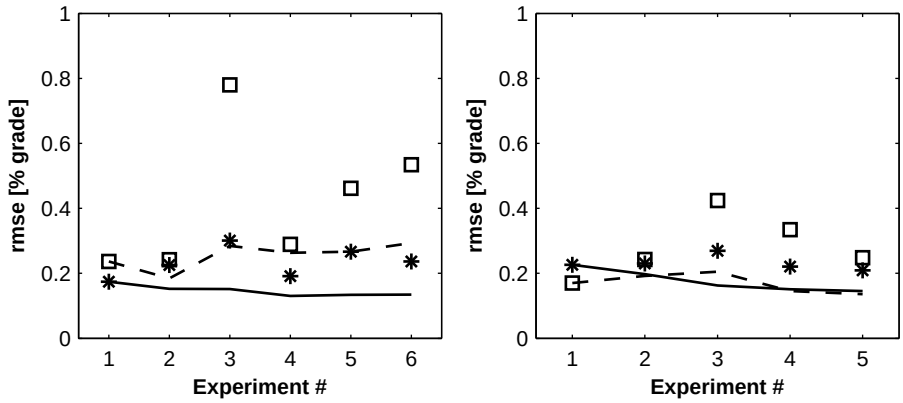

Figure 5.19: Estimation results during gearshifts. The road grade estimate RMSE is shown for the southbound (left figure) and northbound (right figure) test segments. The value for the entire road segment, based on the experiments up to and including the index on the x-axis, is shown (solid line) together with the value when only the sample points where shifting occurs in at least one experiment are included (dashed line). The values for the individual experiments are shown with stars for the entire segment and squares for the sample points corresponding to the dashed line.

set at least one of the vehicles indicated shifting status for a total of 595 m. During this time the road grade RMSE rose to 0.26 % grade, from the 0.13 % grade result for the entire segment. In the northbound direction shifting was indicated for only 218 m. This lead to a road grade RMSE of 0.15 % grade, identical to the error for the entire data set.

5.4.5 Vehicle Model Bias

Without the GPS altitude measurements the vehicle model and measured signals give an estimated grade that has a bias due to modeling errors. The bias is reduced when the GPS altitude measurement is introduced as a vehicle independent low frequency correction in the filter. Depending on the vehicle parameters the magnitude of the drift varies. Figure 5.20 shows the estimated grade and altitude when the grade estimator has been operated without GPS input data. Table 5.21 shows the mean grade biases observed in each of the experiments when compared with the road grade reference. The grade biases range from negligible for vehicle A (experiments 1–3), when using the GPS, to severe for vehicle B (experiments 4–5). It is evident that results could be improved if the parameters for vehicles B and C were better calibrated to match the vehicles and environmental conditions they are supposed to describe.

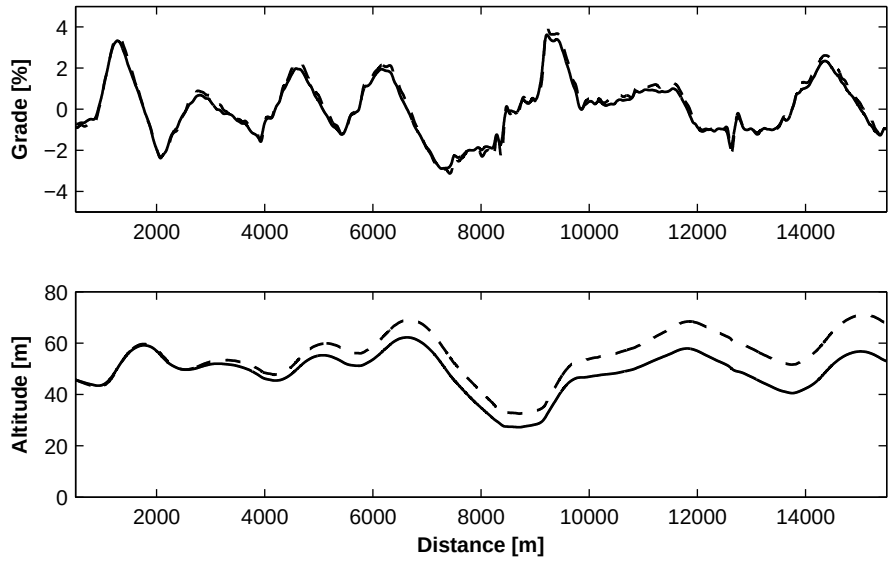

Figure 5.20: The top part of the figure shows the estimated road grade without the GPS input (solid). This signal lies below the reference profile (dashed). As a result the altitude estimate has a noticeable drift. Since there is no absolute altitude measurement available in the filter it was initialized to the same starting value as the reference profile.

5.4.6 Linear System Model

The results from using the piecewise constant linear model instead of the time-varying non-linear model indicated only marginal changes in the estimated road grade. A comparison of road grade estimates obtained with the two methods is shown in Figure 5.22. The main non-linearity in the vehicle model, for the magnitude of road grades considered, is in the speed. The linear model is only valid for vehicle speeds close to the linearization point of 80 km/h. During most of the experiments the speed of the measuring vehicle was close to this value. The proposed method is primarily suited for highway estimation, and it would probably be wise to reject any data sets with large speed deviations, regardless of whether the linear or non-linear model is used. As noted in the discussion in Chapter 7, the possible extension of the proposed methods to estimation of city streets remains future work.

5.4.7 Low Satellite Coverage

While there are very few occasions in the test data where the GPS satellite reception is completely blocked, there are a few instances where signal blockage and multipath

Table 5.21: Observed mean bias in estimated road grade, with and without GPS input, for the south- and northbound test roads. The road grade figures are given in % grade.

Direction	Meas.	Vehicle	Mean bias w. GPS	Mean bias w/o GPS
South	1	A	0.02	0.11
South	2	A	-0.00	0.10
South	3	A	0.00	-0.03
South	4	B	-0.02	-0.17
South	5	B	-0.09	-0.62
South	6	C	-0.01	-0.03
South	Merged		-0.02	-0.12
North	1	A	-0.05	-0.27
North	2	A	-0.06	-0.31
North	3	A	-0.03	-0.29
North	4	B	-0.07	-0.59
North	5	B	-0.07	-0.58
North	Merged		-0.06	-0.41

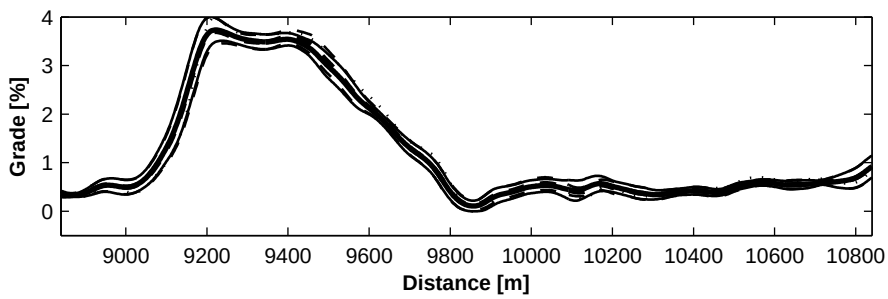

Figure 5.22: The final grade estimate based on the non-linear vehicle and road model (solid) with confidence interval (thin lines) is shown together with the one based on the piecewise constant linearized vehicle and road model (dashed). The reference grade is also shown (dotted thin line). The differences between the two methods are slight, and significantly smaller than the deviation from the reference grade.

effects causes significant degradation of the altitude data accuracy. The effects can be seen in the GPS altitude data on the road segment shown in Figure 5.23. The 1.5 km segment contains a hilltop where the GPS signal is obstructed in several of the experiments. In part two of the figure it is evident that the GPS altitude signal for experiments 2 and 5 contains an unusually large error component. Looking at the number of tracked satellites we note that very few satellites are being tracked in both experiments 2 and 3, yet experiment 3 seems to be much less adversely affected. When three or fewer satellites are tracked the GPS altitude data are disregarded entirely, four or five tracked satellites lead to a very low trust in the data. The number of tracked signals in experiment 5 should be adequate for a reliable three-dimensional position fix, yet the altitude signal is very noisy. From the observation data it seems likely that there are severe multipath problems with reflected signals in this segment. This indicates that it would be desirable to use more diagnostic data about the GPS receiver state in addition to the number of tracked satellites. The raw GPS altitude is treated by a simple outlier detection scheme the maximum change between two consecutive measurements is restricted to 1 m (corresponds to a road grade of 40 %) before it is fed into the road grade estimation.

To make the estimation task even harder, experiment 2 includes gearshifts during the satellite signal outages around 1 600 m and 1 900 m, as seen in part four. During the gearshifts there is no trustworthy data coming from either of the sensors, this immediately leads to large grade estimation errors. These errors are somewhat mediated in the data fusion step, since the gearshifts lead to raised estimated grade error covariances. However, the GPS altitude noise in experiment 5 also leads to a high error in this grade estimate. Since there are many satellites being tracked this error is not detected and flagged in the R matrix. As noted in 4.1.3 increases in GPS altitude measurement noise does not influence the estimated error covariance for the road grade state by any noticeable amount, due to saturation. This explains the lack of variation of $P_{3,3}$ in the sixth part of Figure 5.23.

The experimental data only contains short segments of total loss of satellite coverage, in the northbound direction it only occurred in at least one experiment for 313 m. For those grade estimates the satellite signal is effectively left out of the filter, and it consequently does not matter if the signal is very noisy. Figure 5.24 shows the RMSE values for the road grade for each experiment, as well as for the map based on an increasing amount of data in the same way as for the braking and shifting events. The road grade RMSE of the entire segment is compared to the RMSE for only those sample points where satellite coverage was lost in at least one of the experiments. There is no indication that the total grade estimate on the average should be any worse where there are problems with the satellite reception. This is reasonable since the main effect of the altitude signal, at least while the vehicle model operates normally, is to provide bias compensation. During short outages the grade bias component does not have time to grow enough to cause a noticeable degradation of the estimates. In the southbound data set at least one of the vehicles indicated loss of satellite coverage for a total of 1328 m. During this time the road grade RMSE increased to 0.17 % grade, compared to the 0.13 % grade

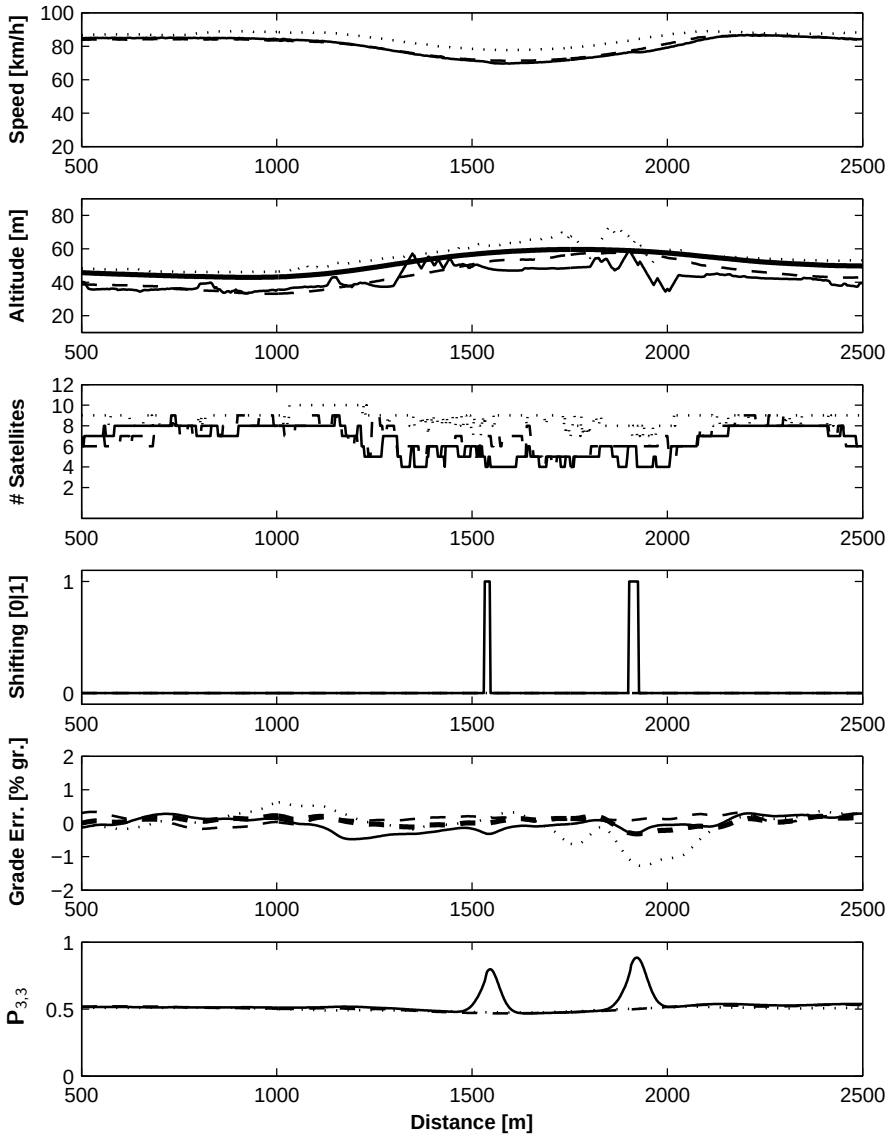

Figure 5.23: Road grade estimation performance during loss of satellite coverage. Several of the experiments show unusually high GPS altitude noise in this segment. Data are from experiments 2 (solid), 3 (dashed), and 5 (dotted). In part two the altitude reference is included (thick solid), and in part five the merged road grade error is shown (thick dashed).

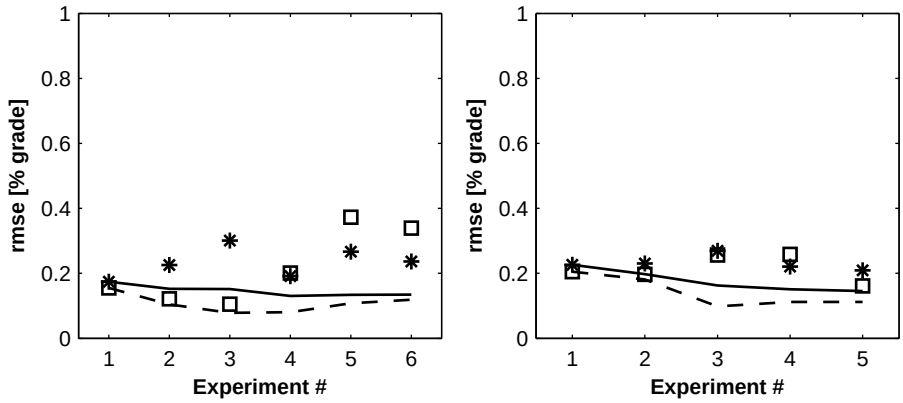

Figure 5.24: Estimation results during loss of satellite coverage. The road grade estimate RMSE is shown for the southbound (left figure) and northbound (right figure) test segments. The value for the entire road segment, based on the experiments up to and including the index on the x-axis, is shown (solid line) together with the value when only the sample points where there is no satellite coverage in at least one experiment are included (dashed line). The values for the individual experiments are shown with stars for the entire segment and squares for the sample points corresponding to the dashed line.

result for the entire segment. In the northbound direction loss of coverage was indicated for 313 m. This lead to a road grade RMSE of 0.13 % grade, compared to 0.15 % grade for the entire data set.

5.4.8 Merged Results

Using data from more than one run along the road and more than one vehicle improves the reliability of the final grade estimate. The downhill segment from $s = 22150$ m to $s = 23150$ m is one of the hardest parts of the test road to estimate accurately, it is therefore used as an example of how the data fusion step improves the quality of the final grade estimate. The grade maps resulting from the progressive inclusion of data from the six experiments can be seen in Figure 5.25. As more data are added the road grade map is improved. The mean value of all included grade estimates at each sample point is also shown, to highlight the effect of the data fusion step. Each figure shows the latest experiment (dashed), the road grade map based on all experiments added so far (solid) and the reference road grade (dotted).

Figure 5.26 shows a comparison of the smoothed estimates from all six southbound experiments with the final grade estimate and the reference grade profile.

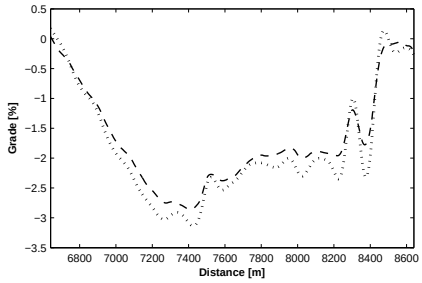

(a) The first experiment forms a road grade map by itself. Estimation errors cause it to differ from the reference road grade.

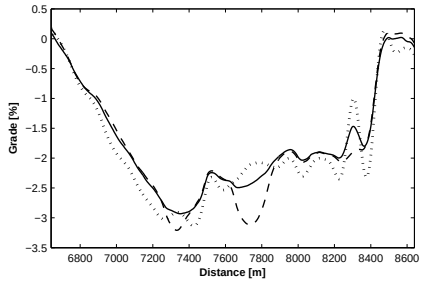

(b) When a second experiment is added to the one in (a) a new road grade map is obtained. The large disturbance in experiment two at s = 22100 m has high uncertainty and thus a low weight in the data fusion.

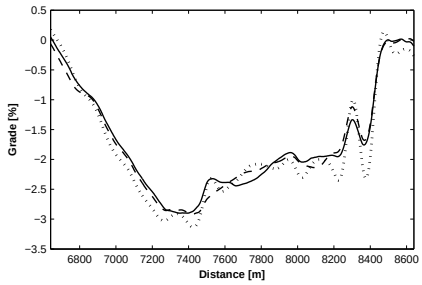

(c) The third estimate from vehicle A does not differ much from the map based on the previous two runs along the road.

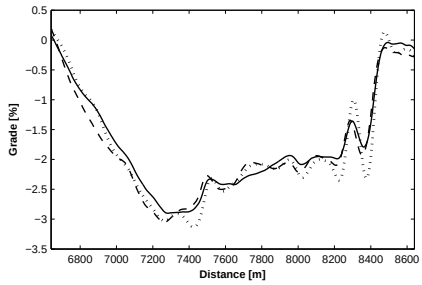

(d) The larger difference in the fourth estimate is probably due to different model parameter errors in relation to vehicle B.

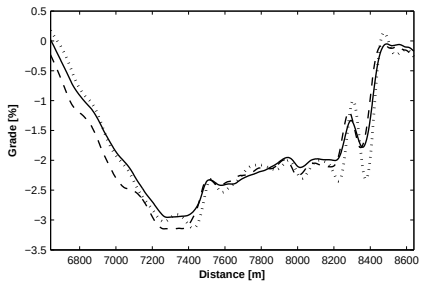

(e) Estimate five is based on vehicle B, just like the one in (d).

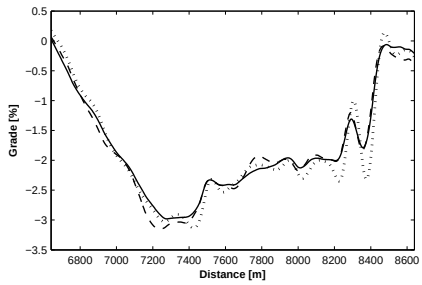

(f) When the sixth estimate, recorded with vehicle C, has been added the map is complete.

Figure 5.25: Iterative road grade estimation results after each iteration. In each figure the most recently added experiment (dashed), is shown together with the reference road grade profile (dotted) and the merged estimate based on all experiments added so far (solid).

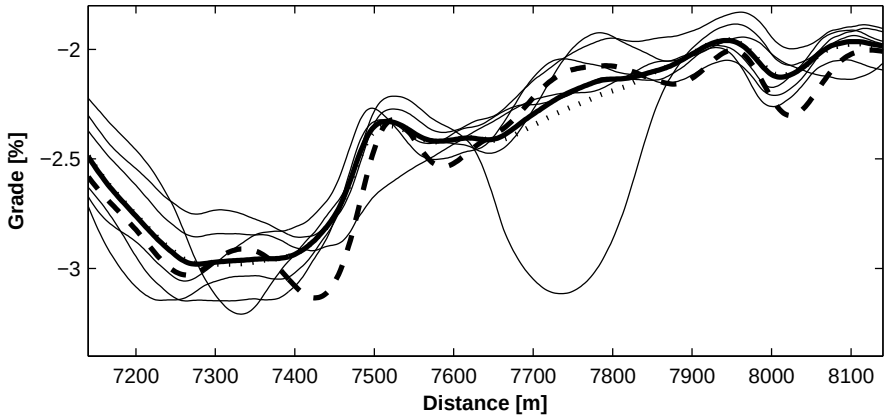

Figure 5.26: The final merged road grade estimate (solid) is shown with the reference grade profile (dashed) and the mean value of all smoothed estimates (dotted). The estimates from the individual experiments are also included (thin lines). This is a magnification of the most challenging part of the test road. The estimate based on experiment two is particularly at odds with the rest at 22750 m. This is due to a combination of poor satellite coverage and the effect of the braking. The detrimental effect on the fused estimate is smaller than on the mean.

5.4.9 Discussion

The road grade estimates based on the constant road grade model have been compared to a reference road grade profile obtained using specialized equipment. Overall the performance of the proposed method is promising, even though vehicle model or parameter errors cause a slight bias in the estimated grade. The estimation error increases during braking, but the error in the final estimate based on experiments where braking takes place at different locations is not affected as much. The analysis of estimation performance during gearshifts yielded mixed results. Data points where gearshifts occur in at least one experiment showed higher than average errors, but this did not seem to be entirely due to the gearshifts. Temporary loss of satellite coverage did not cause any consistent effects on the road grade estimate. Finally it was noted that the GPS receiver is vital to bias rejection, some experiments showed considerable bias in the estimated road grade when the estimation was carried out without it. Grade estimates based on the linearized model showed comparable results to those obtained with the nonlinear model.

5.5 Piecewise Estimator

To test the assumption that road grade profiles are piecewise linear by design, the piecewise estimator, presented in Section 4.2.2, has been evaluated experimentally.

The results of the piecewise estimator have been investigated on 15 km subsets, in both directions, of the experimental data from highway E4. These shorter segments were used since the dynamic programming optimal segmentation algorithm is computationally heavy, despite being significantly more efficient than a straight on optimization for every break point combination. The recorded data were resampled to one data point every 12.5 m, for the same reason. All the results in this section are based on the 12.5 m sample distance and indicated subset of the measurements. The chapter is concluded with an evaluation of a piecewise linear profile for the entire E4 test road, computed by dividing the road into three parts, and finding the optimal segmentation of each part.

The presentation of the results is divided into three parts. First the piecewise linear assumption is analyzed based on the reference road grade profile used for evaluating the proposed method. Next, the recorded sensor signals are analyzed, to provide a baseline for the performance of the estimation method. The estimation results are illustrated using two of the experiments, in addition to aggregate results for the whole data set. Finally, the tradeoff between storage requirements and road grade profile accuracy is treated briefly. The estimation results are evaluated mainly based on the RMSE in the estimated road grade.

5.5.1 Characterizing the Reference

To evaluate the accuracy of the road grade estimation a reference road grade profile was obtained using a high quality combination INS and GPS receiver. The equipment used to collect the reference was the same as described in Section 5.1.5, but instead of the using the low-pass filtering described there, more than one measurement from each location was averaged. The northbound reference profile is based on three passes over the road section, and the southbound profile is based on five passes. The differences in the reference profiles result in calculated performance measures for the piecewise estimator to not be directly comparable to those that refer to the filtered version of the reference road grade profile. The computed RMSE is likely to be higher using the averaged reference, while the mean error should be nearly identical for both profiles.

To investigate the hypothesis that the true road grade can accurately be described as a piecewise linear function, an optimal piecewise linear representation was determined, with an increasing number of segments. The RMSE between the segmented representations and the measured reference road grade profile, as a function of the number of linear segments used, is shown in Figure 5.27.

It is clearly seen in Figure 5.27 that the additional improvement for each new segment decreases with an increasing number of segments. Choosing the best number of segments to use is often referred to as a model order selection problem. There literature contains a large number of methods to choose from for such problems. A simple method would be to assign a weight w, to the number of segments k, used to represent N_0 data points, and minimize a summation cost function including the RMSE $e(k, N_0)$, on the form $\min_k C(k) = e(k, N_0) + w \cdot k$. Here we are satis-

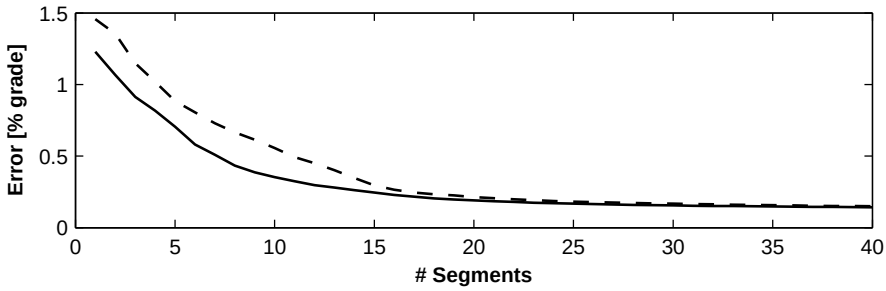

Figure 5.27: Difference (RMSE) between the reference road grade measurement and its piecewise linear approximation. Results for both the northbound (solid line) and southbound (dashed line) test roads are shown.

fied by noting that $k = 20$ segments is enough to get an RMSE compared to the measurement of approximately 0.2 % grade, or 3 % of the range of the road grade signal. Adding a 21 st segment decreases the RMSE by less than 4 % in both the experiments. The measured reference road grade for both the north- and southbound directions, as well as different piecewise linear approximations and resulting errors, are shown in Figure 5.28. It can be seen in the RMSE error plots in the lower part of Figure 5.28 that using only 15 linear segments leads to rather large errors locally, where there are not enough segments to represent the behavior of the signal. With 20 segments the situation improves, and the RMSE is 0.19 % grade in the northbound direction and 0.21 % grade in the southbound direction. Looking at all the measured reference profiles it becomes clear that this deviation from the piecewise linear representation is predominantly due to the real road profile not being exactly described by its piecewise linear model. In this context it should be noted that strict adherence to the simplified road grade model, i.e., no change in the road grade, would yield the mean of the reference profile as the estimate. The RMSE would be 1.46 % in the southbound, and 1.24 % in the northbound direction.

The error between the piecewise linear approximation and the reference profile itself forms a baseline for the estimation of a piecewise affine road grade profile based on measured data, as it would be impossible to find a profile with 20 segments that has a lower estimation error.

5.5.2 Comparison with Nominal Estimator

To relate the performance of the proposed method to the quality of the measurements the measured signals are analyzed in relation to the nominal estimator. Virtual sensors based on the vehicle model and the GPS altitude signal are used, as described in Section 5.3. The road grade RMS and mean errors compared to the reference road grade profile, for each of the virtual sensors and conducted experiments, are shown in Figure 5.29. From the figure it is clear that the virtual sensor

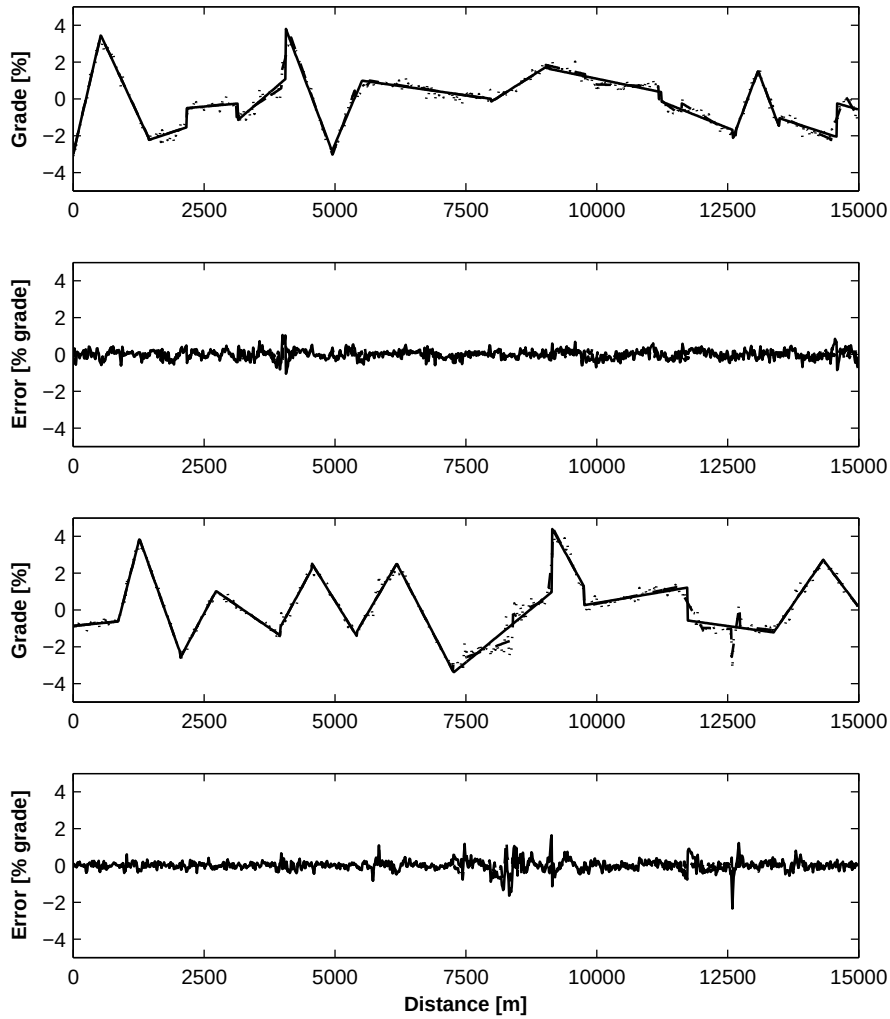

Figure 5.28: The top figures show the reference road grade profile for the northbound (left) and southbound (right) test road sections (dotted) together with the optimal piecewise linear approximation with 15 segments (solid) and 20 segments (dashed). The bottom figures show the RMSE for the approximation with 15 segments (solid) and 20 segments (dashed).

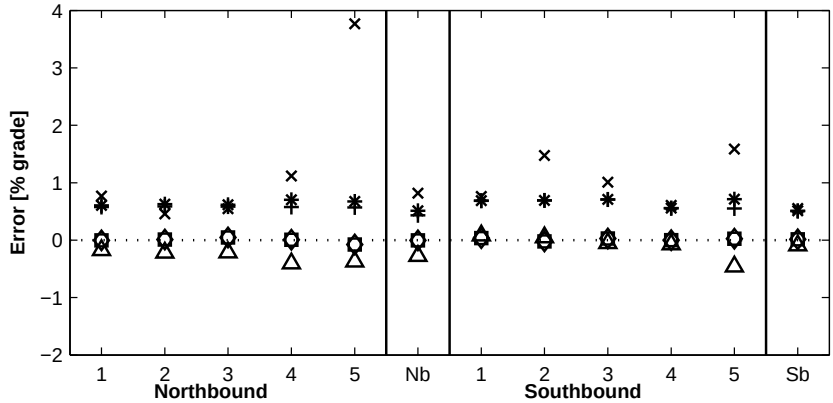

Figure 5.29: The error characteristics of the virtual road grade sensors in the nominal estimator are shown for each of the ten experiments, five in the northbound direction, and five in the southbound direction. To the right of each experiment series the results from averaging all measurements in each data point are shown. The vehicle model based RMSE is indicated by ($*$), and the mean error by ($\triangle$). The GPS based RMSE is denoted by ($\times$) and the mean error by ($\square$). The RMSE of the vehicle model based sensor, with its mean updated to match the GPS based virtual sensor is denoted by ($+$). The mean of this combined signal of course coincides with the mean of the GPS based signal, and is denoted by ($\diamond$).

based on the GPS data has a mean error close to zero, while the RMSE is similar or worse than for the vehicle model based virtual sensor. The mean grade of the virtual sensor based on the vehicle model has therefore been shifted to match the mean road grade of the GPS based sensor. The RMS and mean errors of this third signal have also been included in Figure 5.29.

An illustration of each of the virtual sensor signals for two different experiments are shown in Figure 5.30. In the first example, representing experiment 4 in the northbound direction, the vehicle model based sensor signal shows a clear bias. The measured road grade stays noticeably below both the reference grade and the average of the GPS based sensor signal. This confirms what could be seen in Figure 5.29. When comparing the two examples it is apparent that the random noise in the GPS signal was much worse during experiment 4 in the northbound direction than during experiment 1 in the southbound direction. The large variations in the random GPS noise between experiments, which can also be seen clearly in the large differences in RMSE in Figure 5.29, were dealt with by only considering the average value of the GPS sensor during each experiment, as described in Section 4.2.2.

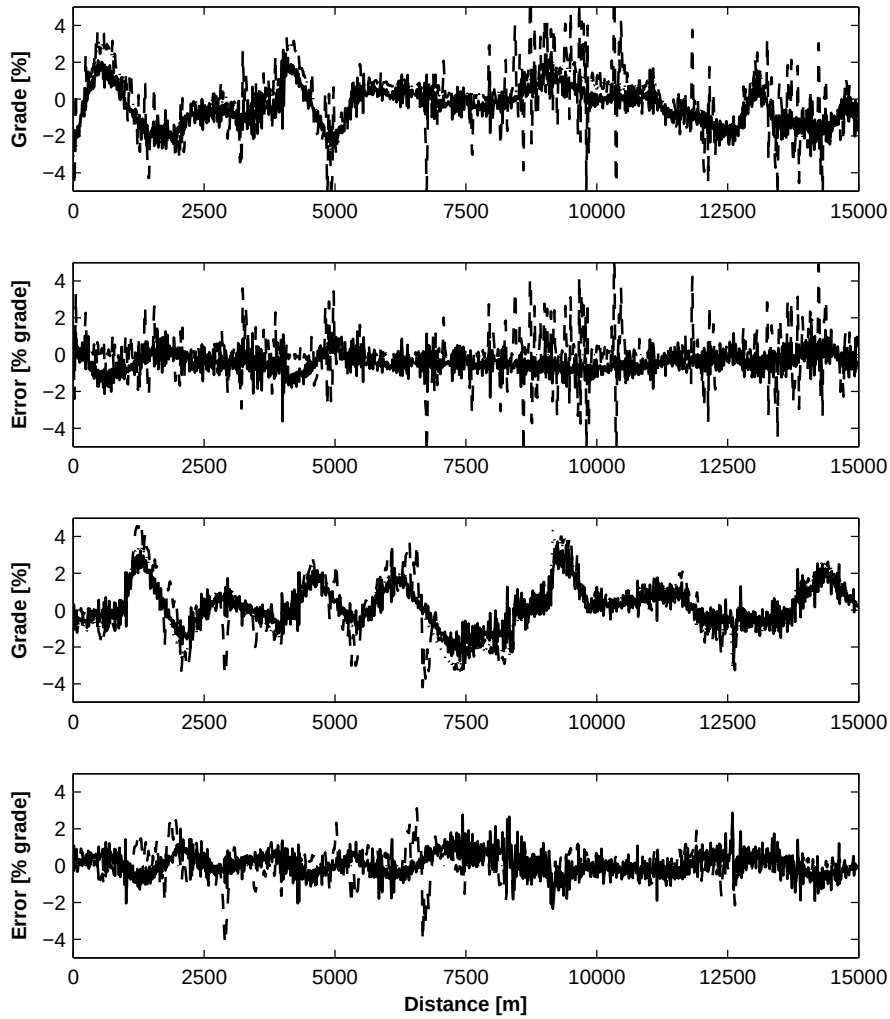

Figure 5.30: Recorded road grade sensor data are shown for experiment 4 in the northbound direction (left figure) and for experiment 1 in the southbound direction (right figure). The virtual sensor based on GPS data (dashed) is illustrated together with the virtual sensor based on the vehicle model (solid). The top parts of the figures show the road grade, and include the reference road grade (dotted). The bottom parts of the figures show the deviation of each sample from the reference profile. It can be clearly seen that the signal quality varies between experiments, and that there is a noticeable bias in the vehicle model based signal in the left figure.

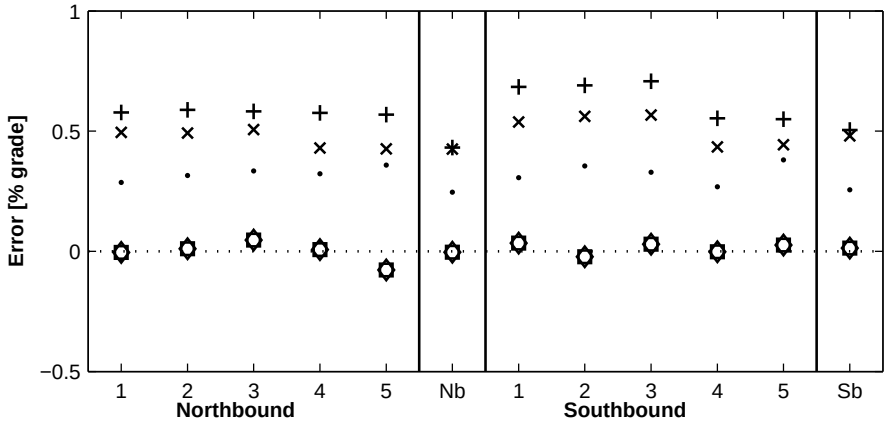

Figure 5.31: Estimation RMSE and mean error for source data (+) and estimate (×). After the five experiments in each direction the results based on averaging all five measurements at each data point is shown The mean error for the piecewise linear estimate (□) and the source data (⋄) are almost identical The RMSE for each experiment, and using all available measurements, for the comparison estimation method described in the text is denoted by (•). Note that the vertical scale of this figure is different from that of Figure 5.29, to more clearly illustrate the results.

5.5.3 Estimation results

The proposed estimation method generates a piecewise linear approximation that can be described by only a few dozen parameters instead of the 1200 original data points, and has a lower RMSE relative to the reference grade profile than the source vehicle model based road grade virtual sensor, for all the conducted experiments. The residual error is higher than for the spline estimator, evaluated in Section 5.6, applied to the same input data. The spline estimator however, only uses the piecewise linear model internally, and does not produce a piecewise linear output. Based on the analysis of the reference road grade above, the majority of results have been computed for a piecewise linearization using 20 segments. When measurement data from all five experiments in each direction are averaged at each position before the linear segment identification, the RMSE of the linear profile is only marginally better than that of the averaged source data. The RMS errors for the source data and estimated piecewise linear road grade profile for each of the experiments are shown in Figure 5.31 together with results for the comparison method, the spline estimator.

The estimated piecewise affine road grade profiles for the two example experiments discussed above are shown in Figure 5.32. The figure also contains the road grade estimate obtained from the spline estimator. When comparing the residual error to the error in the vehicle model based source signal it is apparent that while

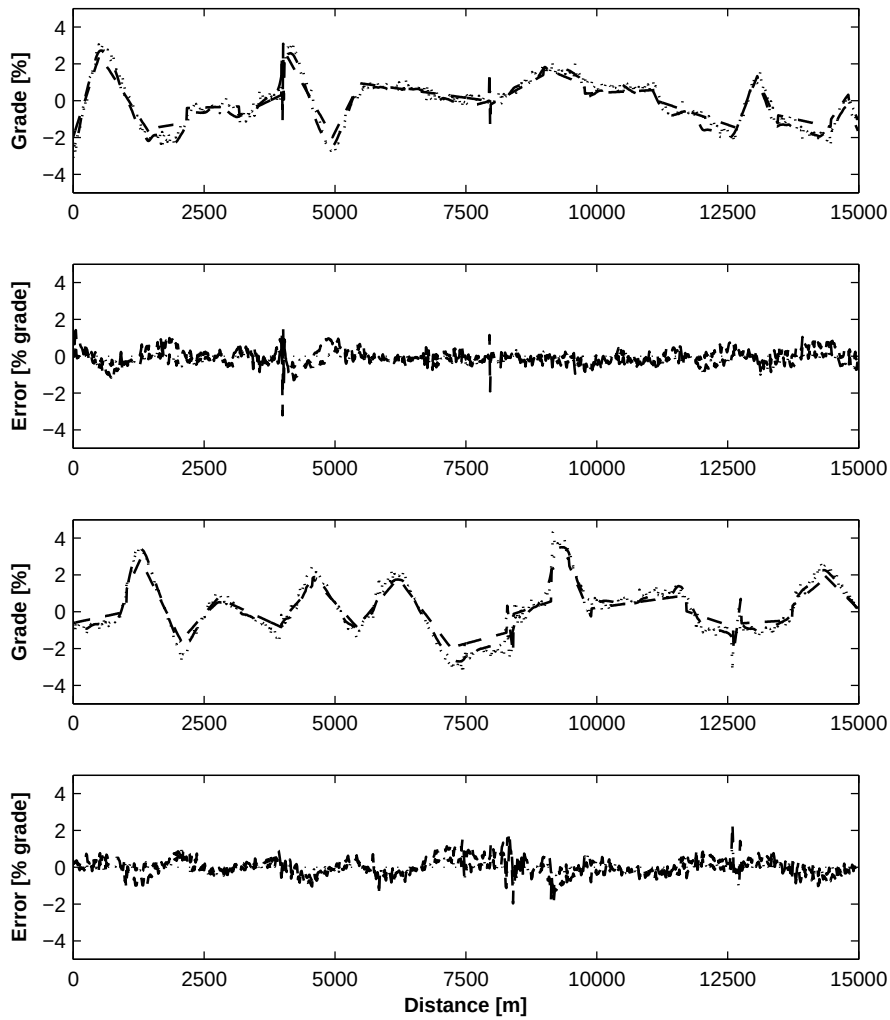

Figure 5.32: Estimation results for the same experiments as sensor data are presented for above (dashed), compared with reference road grade (dotted) and the result from the comparison method (dash-dotted). The northbound direction is shown in to the left, and the southbound to the right. The usage of the GPS signal throughout the estimation in the comparison method has a positive effect. In particular around 8 000 m in the right figure the linear representation is clearly sub-optimal. The left figure shows some examples of over-fitting linear segments to noise in the input signal.

most of the bias has been removed by the use of the averaged GPS based signal, a significant low frequency error component still remains. This error is not observed in the residual obtained when the reference signal is linearized, which leads to the conclusion that it comes from the source data rather than from difficulties representing the true road grade profile as a piecewise affine signal. The comparison method uses the GPS signal throughout the estimation, not just to counteract the vehicle model bias. The results indicate that despite the noisy character of the GPS signal it contains more useful information than just the average road grade over 15 km.

The piecewise linearization based on the averaged input data is only a marginally better approximation of the reference road grade data than the averaged sensor data itself. For the southbound experiments the estimated profiles from experiments four and five are better than the profile based on averaged input data, indicating significant differences in the measurement noise between experiments. The estimated road grade profile, and associated residual error, presented in the same manner as in Figure 5.32, are shown in Figure 5.33.

It can be expected that increasing the number of linear segments used when fitting the experimental data would improve the agreement with the reference road grade profile. This is true up to a certain point, after which additional linear segments end up being fitted to measurement noise rather than true road features. The experiments showed that the RMS road grade error decreased significantly when new segments were added up to about 15 linear segments. Additional segments would not give any significant change to the RMSE for the complete profile. Additional segments do however sometimes increase the error locally, where lines previously fitted to a reasonable average of the underlying road grade signal are split and adjusted to fit measurement errors. The number of linear segments required before the estimation quality levels out depends on the actual road profile, and given the relatively modest error increases from choosing too many segments care should be taken not to use too few segments. The obtained RMSE as a function of the number of piecewise linear segments used, for each of the ten experiments, and by using the average of all five measurements at each measurement point, are shown in Figure 5.34. The piecewise linear segment estimation method does not show significantly improved results when using input data averaged over multiple experiments, the results with averaged data are similar to the best individual experiments. In contrast the comparison method produces averaged results that are better than when data from only one experiment is used.

While the fit compared to the reference road grade does not improve when using an increasing number of segments above 15, the fit to the data itself naturally does. The internal fit to the measurement data were significantly better when all experiments were averaged before the identification of linear segments. The local fit for both the investigated road sections, based on averaged data, was 0.24 % grade. This is only about 25 % worse than the local fit of the reference road grade profile. It can thus be concluded that, on the average, the measured data are almost as well approximated by a piecewise linear function as the reference data. This is illustrated in Figure 5.35. Due to modeling and measurement errors there is however a notable

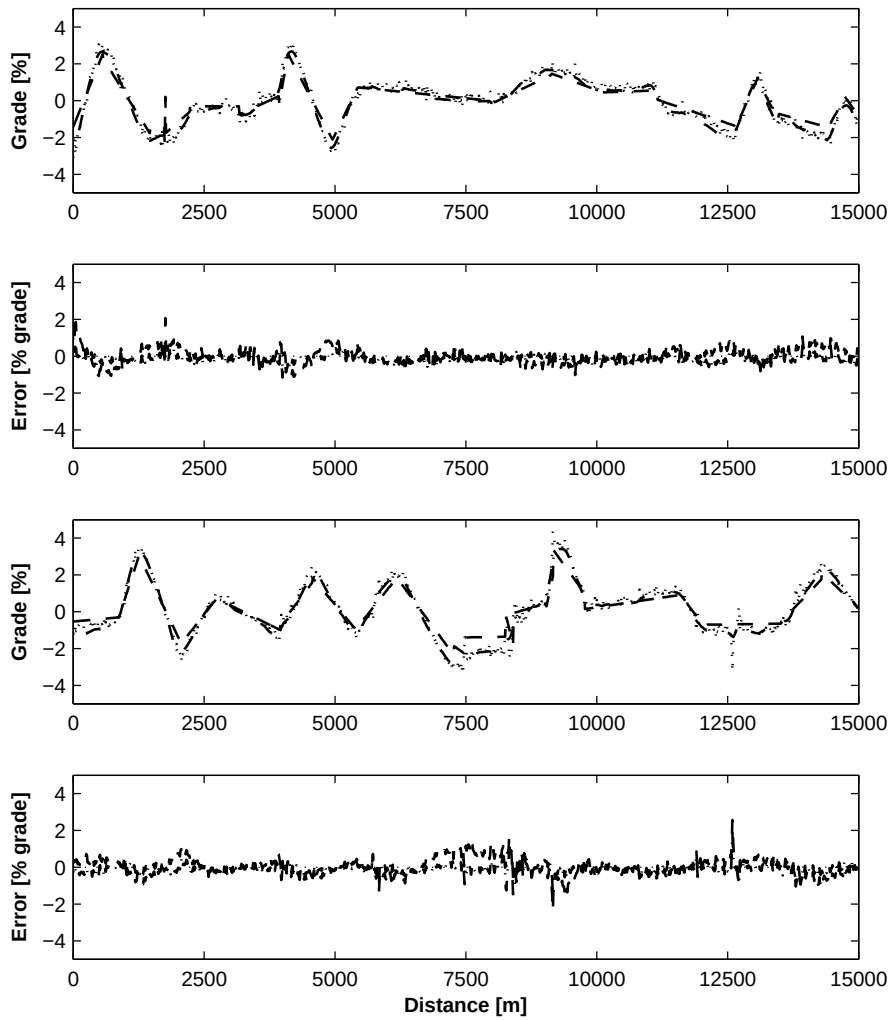

Figure 5.33: Piecewise linear estimation results based on the average of the five measurements for each direction, northbound to the left, and southbound to the right. The piecewise linear profile (dashed) is based on the average sensor value at each position in the five experiments. The reference road grade (dotted) and result from the comparison method (dash-dotted) are also included. The results for the northbound direction show signs of fitting linear segments to measurement noise around 2000 m, indicating that the optimal number of segments may be lower than 20.

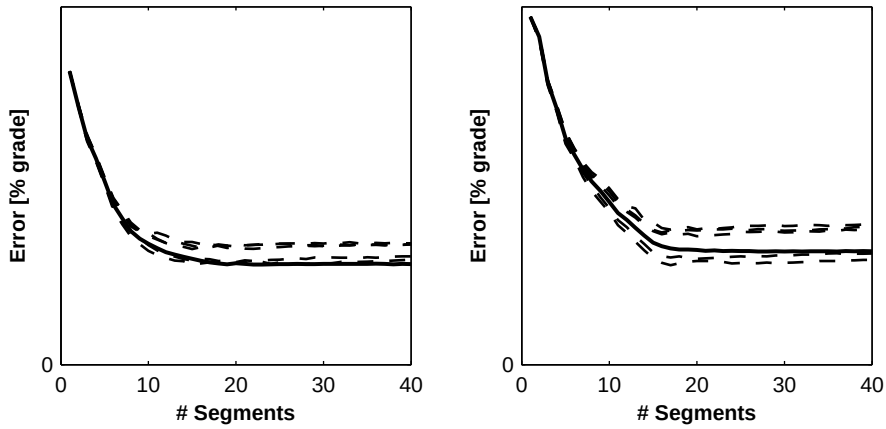

Figure 5.34: Error compared to the reference profile, as a function of the number of segments used. The northbound experiment is shown on the left, and the southbound on the right. The results based on averaged input data are shown (solid line) together with the individual experiments (thin dashed lines). The values in this figure, when using 20 segments, correspond to those in Figure 5.31. The individual experiments yield different final errors, but all indicate that slightly less than 20 linear segments is probably ideal for these road sections and this method.

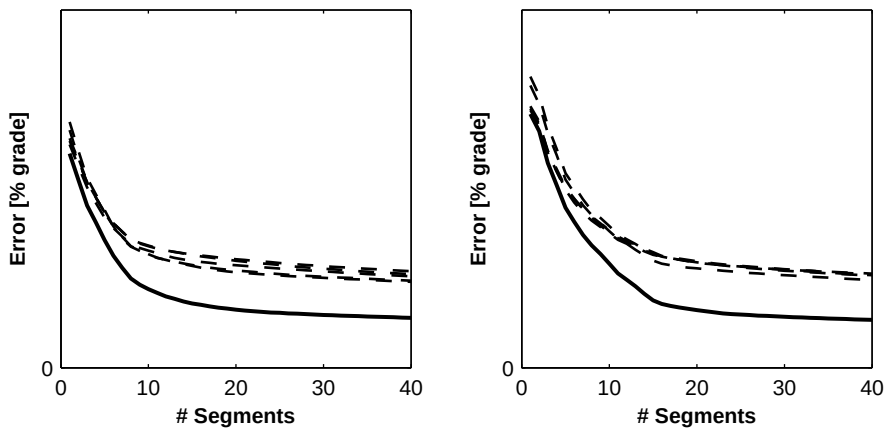

Figure 5.35: Fit error between each piecewise affine estimate and the actual data points used in that estimate. Northbound experiments (left figure) and southbound experiments (right figure) are shown, and the results based on averaged input data (solid line) are compared with the individual experiments (thin dashed lines). Note that the piecewise linear fit to the averaged data is significantly better than the fit in any of the individual experiments.

difference between the identified piecewise linear functions.

The road grade profile obtained from the comparison method consists of 1200 data points that all need to be stored in a map to represent the profile. The piecewise linear profile with 20 segments only requires the storage of 40 line parameters, and 20 segment start positions. If the comparison method result is downsampled such that it is represented by 60 equidistantly spaced data points, and then restored using linear interpolation the resulting RMSE for the northbound profile is 0.39 % grade. The corresponding error for the southbound profile is 0.37 % grade. The proposed method based on averaged measurements from all experiments, the most directly comparable result, yields an RMSE of 0.42 % grade in the northbound direction, and 0.48 % grade in the southbound direction. The comparison method still performs better, but the difference is much smaller than when ignoring storage requirements. The remaining performance gap is likely due to a combination of better utilization of the GPS signal and the added freedom of not being limited to a piecewise linear representation.

5.5.4 Discussion

An estimation method representing the road grade signal as a piecewise linear signal, as suggested by road design guidelines, has been evaluated through experiments. The validity of the piecewise affine assumption has been verified by analyzing reference road grade data. The proposed method was able to estimate the road grade of two 15 km test road sections with RMS errors of 0.42 % grade and 0.48 % grade respectively. The proposed method represents road grade profiles in a compact way, as parameters describing a piecewise linear function. While both the reference data and the averaged experimental data can be well described by piecewise linear functions, the estimation error for the proposed method is larger than that of a comparison method, which does not require its output to be piecewise linear, using the same input data. A challenge in the design of the proposed method has been the use of the GPS signal. While it provides vital bias compensation for the vehicle model, it is at times very noisy. It was therefore only included as an average over an entire experiment. It may well be possible to improve the results by adding the GPS data directly to the estimation of linear segments, after suitable and possibly adaptive pre-filtering. The number of linear segments used to represent a road section must be selected a priori, or determined through some model order selection method. In the conducted experiments, choosing the number of segments too large only produces a small increase in the estimation error while choosing to use too few segments yielded a large increase. The presented method is computationally intensive, but it is useable if computations can be carried out off-line without real-time constraints, and the road is divided into approximately 10 km sections before estimation is carried out.

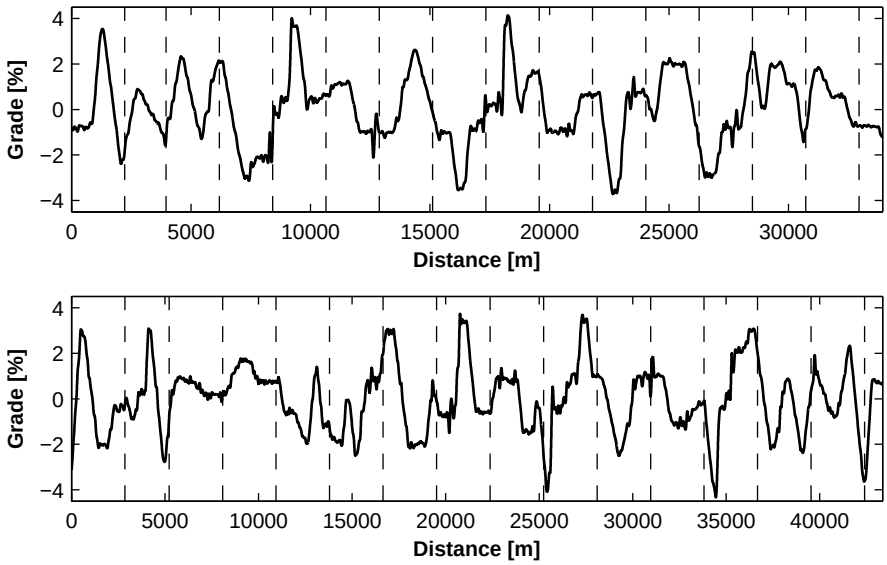

Figure 5.36: The spline estimator was evaluated on the same road as the constant estimator, but data were divided in 30 segments for the analysis. The 15 segments in each of the directions of travel are shown on the reference road grade profile. The top part shows the southbound profile, and the bottom part shows the northbound profile.

5.6 Spline Estimator

The spline estimator described in Section 4.2.3 has been evaluated using the same experimental data as the other two methods. The estimation results obtained by using the described implementation of the three step spline estimator are presented in this section. To use the method the test road had to be divided into sections for processing. The test sections used for evaluating this method are shown in Figure 5.36.

The end result of the proposed method, applied to data from multiple experiments, is an estimated road grade based on all the measurements collected from a specific road section, at all occasions the vehicle has been driven along that specific section. As an example the final estimated road grade for a short section is shown in Figure 5.37. The spline estimator is compared to the constant estimator, described in Section 4.1. These two methods will in this section be referred to as the proposed and previous methods. For the evaluated segments and sample distances, the proposed method generally performs better than the previous method, with an average reduction in the RMSE in the estimation of 6–15 % depending on the sample distance. Since five measurements are available at each location along the

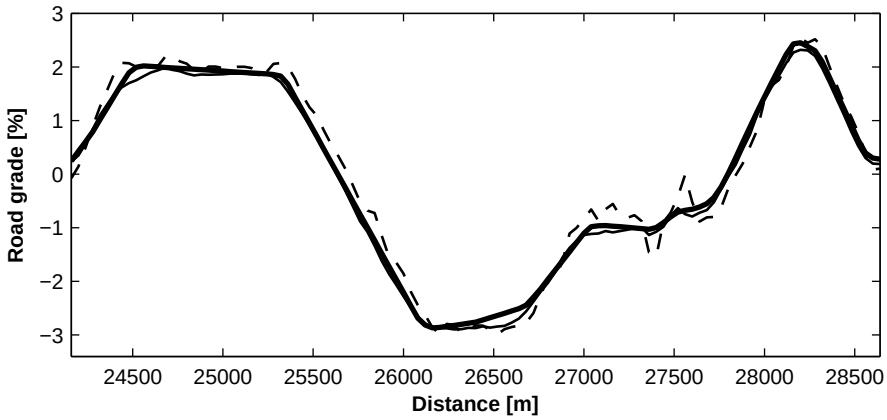

Figure 5.37: A road grade estimate from the proposed method (solid) is shown together with an estimate based the previous method (thin solid) and a reference road grade measurement (thin dashed). The performance improvement with the new proposed method is a 16 % reduction in the RMSE compared to the reference for the left half of the section, and a 1 % reduction in the average RMSE for the right half. The proposed method is generally better than, or at worst, equal to the previous method in estimation performance, for the evaluated segments.

road, the estimation performance both for each experiment individually, and when all available data are used, is analyzed.

5.6.1 Sample Distance

The distance between samples used when estimating the grade affects many factors that influence the quality of the road grade estimate. An increased sample distance will for example decrease the influence of the altitude measurement noise in the GPS on the numerical derivative. As discussed in Section 4.1.5, increasing the sample distance also makes vehicle and road grade model errors more important, since the ratio of samples per unit of prediction error decreases. Finally, the error from the zero-order hold assumption when sampling data for the model based predictions also increases with increased sample distance. The experimental results have therefore been evaluated both with a sample distance corresponding approximately to the rate sensor data is reported by the logging system, and at lower sample rates. The input data were logged at 10 Hz, which at 90 km/h gives one sample every 2.5 m. Results have been computed at increasing sample distances up to 100 m. Input data for a sample distance of $2.5 \cdot n$ m have been obtained by simply keeping only every n:th measurement. Since a total of 30525 sample points have been used for 76 km of road the random estimation performance differences obtained by using different samples for different sample distances should be minor.

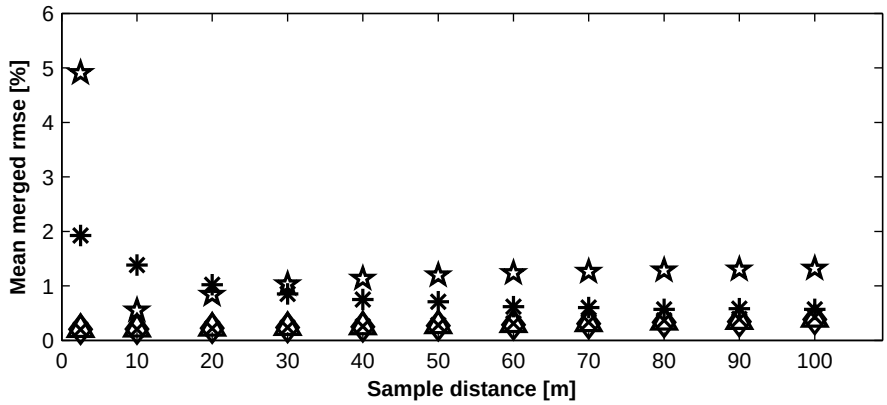

Figure 5.38: The proposed road grade estimation method is compared to nominal estimator. Since five measurements are available at each location along the road, the nominal results are averaged before the average RMSE for all the studied sections along the test road is calculated as a function of the sample distance. The resulting RMSE from the GPS measurements is denoted by ($*$). The measurement noise from the GPS causes large errors in the numerical derivative for short sample distances. For very large sample distances the estimate is quite good. Direct results from the vehicle model are denoted by ($\star$). Due to measurement noise the estimate is bad for the smallest sample distance. For large sample distances the zero-order hold discretization error causes bad performance. The results after each of the steps of the proposed method are similar on the scale of this figure. The results of the previous method, which is identical to step one of the proposed method, are denoted by ($\times$). The RMSE of the linear model obtained in step two is denoted by ($\triangle$). The final result of the proposed new method is denoted by ($\diamond$).

5.6.2 Comparison with Nominal Estimator

The performance of the proposed method has been compared to the quality of the measurements. The two unfiltered nominal estimates described in Section 5.3 are used, but here they are evaluated for a range of discretization sample distances. The absolute road grade RMS errors after each of the three steps of the proposed estimation method have been completed are shown in Figure 5.38, together with the RMS errors for the two estimates directly based on the data at each consecutive pair of sample points. It is clear that a major improvement occurs in the first step for all sample distances. Using the piecewise linear nature of the road grade signal by applying steps two and three further improves the estimate, particularly for the larger sample distances. This can be seen more clearly in Figure 5.39.

5.6.3 Estimation Results

The experiments show that the proposed method generally decreases the RMS errors relative to the previous method. As predicted above the improvement grows with increasing sample distance, and for the smallest studied sample distances the improvement in this study is small, or in a few cases even negative. The performance of the spline estimator, compared to that of the constant estimator, as a function of sample distance, is shown in Figure 5.39.

The results also show that the performance of the piecewise linear model identification varies considerably between sections of the test road. Figure 5.40 shows the performance change with the proposed method for each analyzed section. This result can be explained by the deviations from the assumed model in the reference road grade profile. In some sections there are obvious features in the reference profile that are not captured by the linear segmentation of measurement data. Since the piecewise linear model carries a higher trust in the KF than the model predicting no change used in the previous method, larger errors result when short term peaks that are not included in the piecewise linear model occur.

5.6.4 Discussion

This study gives an indication that it may be worthwhile to investigate methods to automatically segment a road to obtain a piecewise linear model before making the final road grade estimation. Due to the performance differences between the experiments and sample distances, and the increased computational load from the segmentation, the application has to be carefully evaluated in order to make a choice between the spline estimator and the constant estimator.

5.7 Comparison and Discussion

In this section the proposed estimation methods are compared under the same experimental conditions. Due to the differences in the methods, their performance varies with the situation in which they are applied. In the comparison the sample distance $\Delta s = 10\,\mathrm{m}$ was used for all methods.

5.7.1 Road Grade Estimation

The entire estimated road grade profiles, for the southbound and northbound test segments, and each of the three proposed methods, are shown in Figures 5.41 and 5.42. Numerical grade error results for the methods are given in Table 5.43, and predicted relative altitude errors results are given in Table 5.44.

For the chosen sample distance the constant estimator yields the best estimates. This is followed by the spline estimator. Restricting the road grade to only be represented by piecewise linear segments, as in the piecewise estimator, yields the worst result.

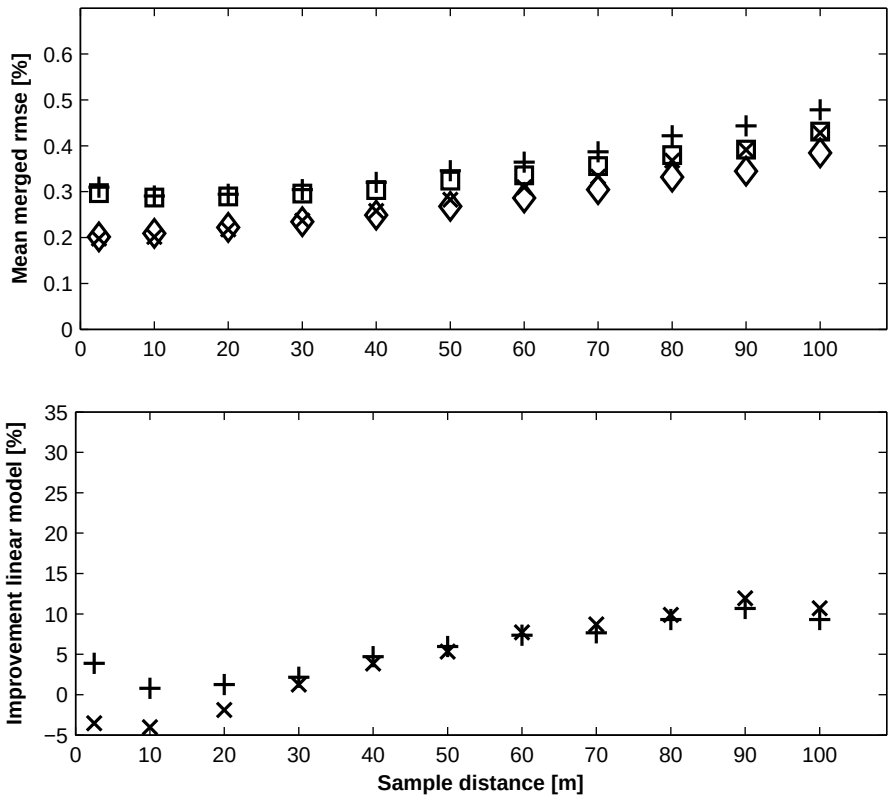

Figure 5.39: A larger distance between sample points increases the model induced error when the road grade changes quickly. This can be seen as an increase in the performance gain for larger sample distances when the piecewise linear road grade model is used. The average road grade RMSE's for the investigated sample distances for the previous method (+) and the new method (□) are shown together with the road grade RMSE's for the fused estimates. The fused error is denoted by (×) for the previous method and (◇) for the new method with the linear model (top figure). The relative improvement in percent, as an average for the individual experiments and for the fused estimates is also shown as a function of the sample distance. The average improvement for the individual experiments is denoted by (+), and the improvement in the fused estimate by (×) (bottom figure).

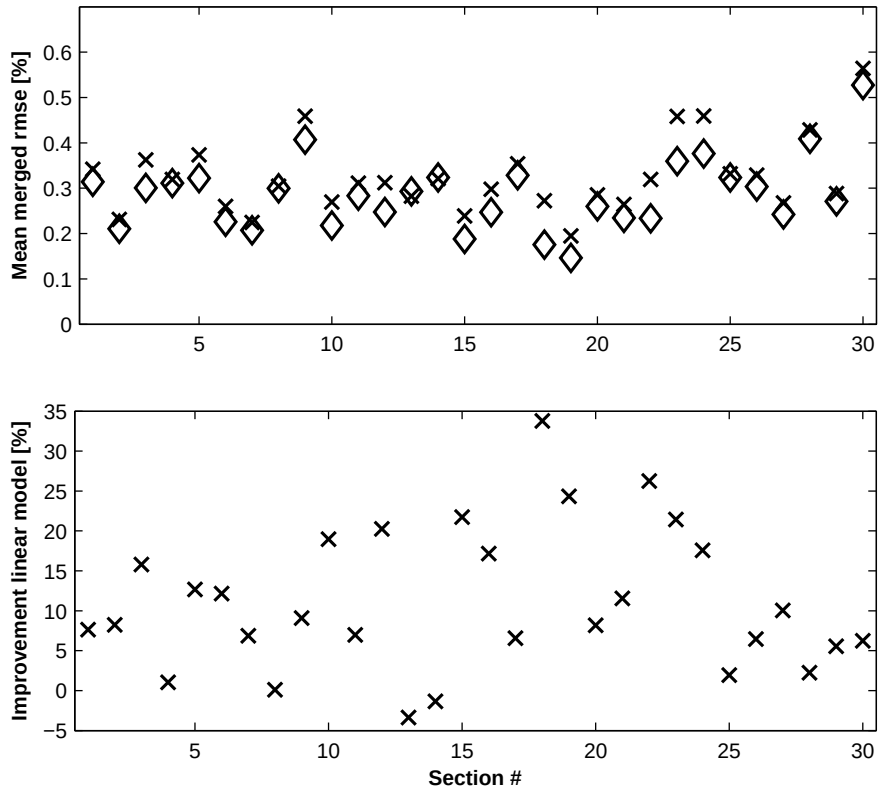

Figure 5.40: The road grade RMSE for the fused estimate for each road section based on all experiments is denoted by (×) for the previous method and (◇) for the proposed method (top figure). The relative RMSE decrease in percent from applying the new method is denoted by (×) (bottom figure).

5.7.2 Relative Altitude Prediction

The mean error in relative altitude is closely related to the mean error. The relative altitude prediction errors 1 000 m ahead of the vehicle, for each method, are illustrated in Figure 5.45. The performance ordering of the methods is unchanged when considering the altitude prediction. In Section 2.7 it was seen that at least 75 % of the potential savings of an optimal speed control algorithm can be realized, for the example profile, with a vertical error of 1 m. The experimental results indicate that the constant estimator can be used to obtain road grade profiles useable for map based predictive speed control.

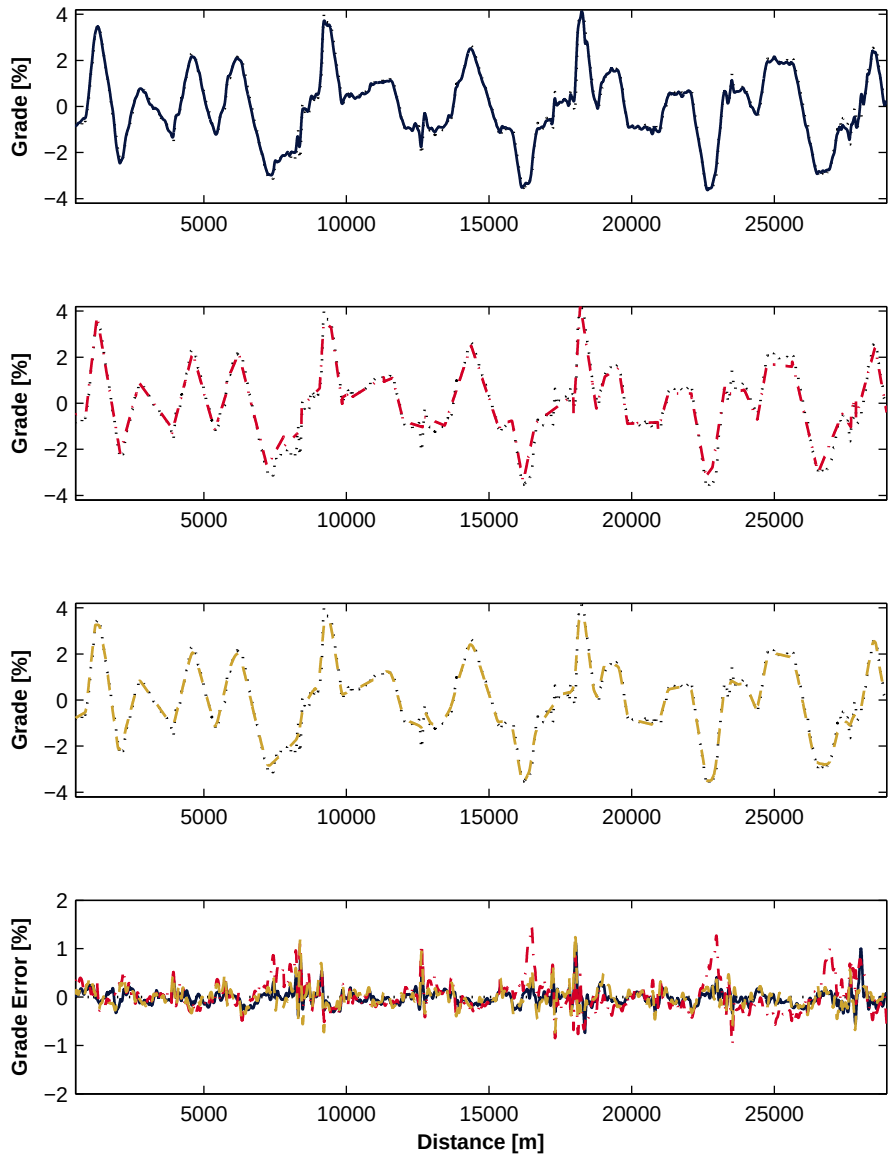

Figure 5.41: Each of the three top figures show the result, from the southbound test segment, of one of the proposed estimators, together with the reference road grade (black, dotted). From the top the estimators are the constant estimator (blue, solid), the piecewise estimator (red, dash-dotted), and the spline estimator (gold, dashed). The bottom figure shows the estimation error for each estimator, using the same line characteristics as in the top three figures. It is clear that the constant estimator is able to capture features in the true road grade that are not described by the piecewise linear model.

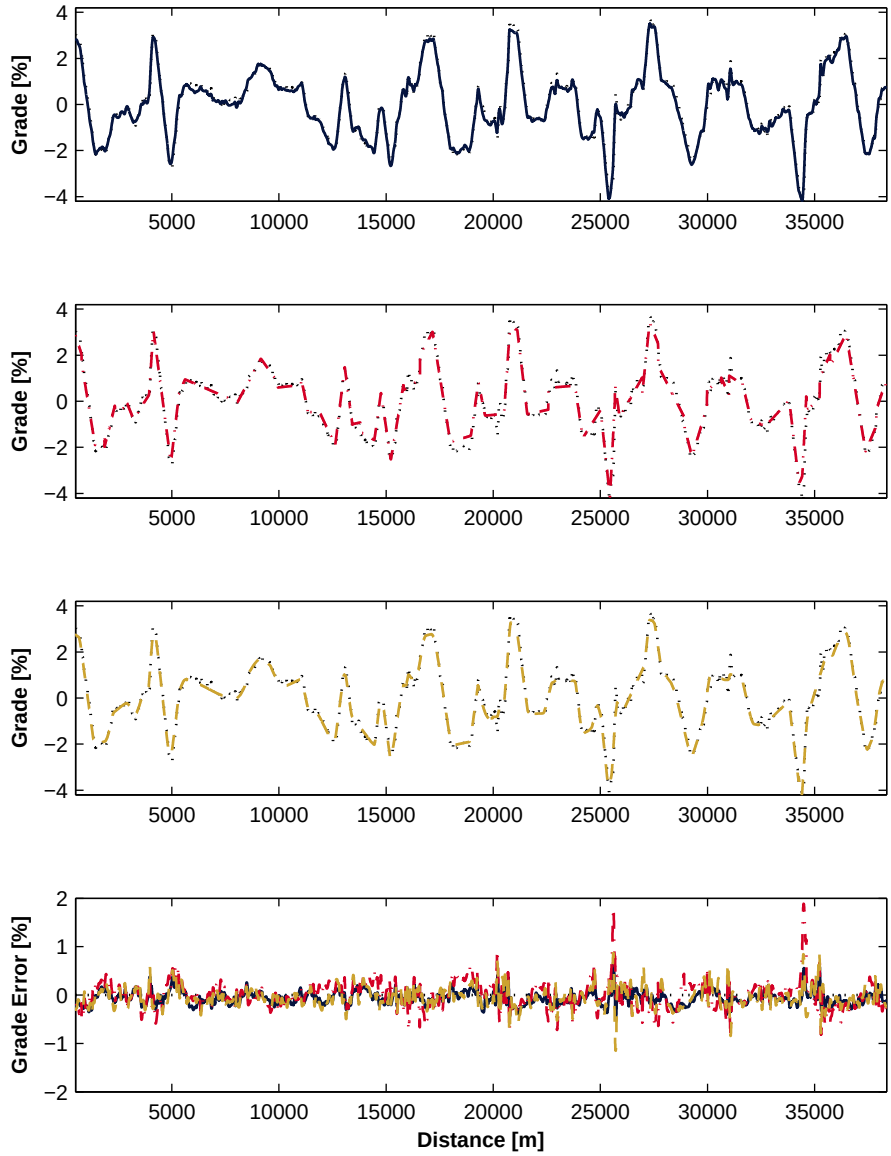

Figure 5.42: Results from the northbound test segment are shown using the same conventions as in Figure 5.42. From the top the estimators are the constant estimator (blue, solid), the piecewise estimator (red, dash-dotted), and the spline estimator (gold, dashed). The bottom figure shows the estimation error for each estimator, using the same line characteristics as in the top three figures. The piecewise estimator shows large errors locally, due to overfitting of linear segments to measurement noise. Choosing the right number of segments to use, without access to the true road grade, is hard.

Table 5.43: Performance comparison for the four studied road grade estimators. The road grade α estimate errors in % grade are shown for each estimator and test segment.

Estimator	Direction	Grade	
		Mean	RMSE
Nominal	South	-0.01	0.28
	North	0.01	0.24
Constant	South	-0.01	0.16
	North	-0.06	0.15
Piecewise	South	0.03	0.32
	North	0.00	0.28
Spline	South	-0.01	0.21
	North	-0.05	0.21

Table 5.44: Performance comparison for the four studied road grade estimators. The predicted relative altitude error results 320 m and 1000 m ahead of the vehicle are shown.

Estimator	Direction	Alt. pred 320 m		Alt. pred 1000 m	
		Mean [m]	RMSE [m]	Mean [m]	RMSE [m]
Nominal	South	0.08	0.87	0.25	2.50
	North	0.03	0.71	0.09	1.91
Constant	South	-0.05	0.47	-0.14	1.13
	North	-0.19	0.46	-0.57	1.24
Piecewise	South	0.09	0.97	0.28	2.75
	North	0.01	0.83	0.05	2.26
Spline	South	-0.03	0.60	-0.10	1.37
	North	-0.16	0.61	-0.50	1.46

5.7.3 Piecewise Linear Road Grade

A piecewise linear function is generally much better than a constant value, as an approximation of a road grade profile. Yet, the constant estimator performs better than the other methods. For the piecewise estimator this is explained by the fact that the deviation between the actual road grade profile and a piecewise linear function is much larger than the error made from making the constant road grade model assumption. In the case of the spline estimator the trust in the piecewise

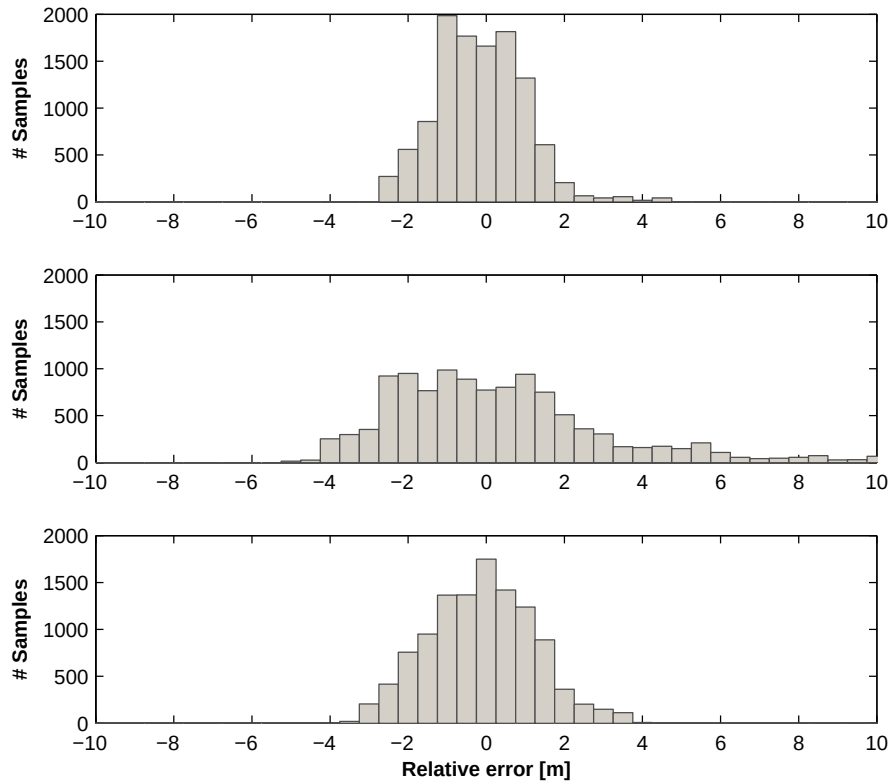

Figure 5.45: An important application of the estimated road grade data for HDV control is to predict the altitude a certain distance ahead of the vehicle. The error in the predicted altitude 1 km ahead is shown for each of the estimators. The first figure shows the constant estimator performance, the middle figure is generated from piecewise estimator data, and the bottom figure represents the spline estimator. While the filtering based estimators show similar performance, the piecewise estimator exhibits very large errors in some cases.

linear model, in the third step of the method, is a design parameter. If the trust is set to be low, the performance is indistinguishable from that of the constant estimator. Theoretically there should be some gain from using the more accurate method, but it is apparently too small to be detected. Increasing the trust in the model does yield improved results when only very few data points are available. In that case neither of the methods is able to capture the higher frequency content of the true signal. The gain from making better predictions in the filter then leads to better overall results.

If a longer sample distance is chosen the effect of the better road grade model in the piecewise and spline estimators would decrease the difference. For very long sample distances the ordering of the methods would change, but then the accuracy will be rather low.

5.7.4 Implementation

The constant estimator would be the easiest to implement with limited computational resources. Even with a desktop computer CPU at disposal both the piecewise linear methods were applied to parts of the test roads at a time. The computed estimates were then joined into on complete profile. This practice introduced some additional errors, but it was required due to the computational complexity of the methods. In a production setting the currently used methods for identification of linear segments are probably too inefficient. Faster sub-optimal methods need to be used.

5.8 Summary

Experimental data have been collected in a total of eleven experiments using three HDVs on a Swedish freeway. Six data sets from the southbound segment and five from the northbound segment have used to evaluate three different road grade estimators. The road grade estimates have been compared to a reference road grade profile obtained using specialized equipment. Overall the performance is promising, and particularly the constant estimator can likely be used to obtain road grade information suitable for vehicle control applications.

The constant estimator has been studied in a number of specific driving situations. The estimation error increases during braking, but the error in the final estimate based on experiments where braking takes place at different locations is not affected as much. The analysis of estimation performance during gearshifts yielded mixed results. Data points where gearshifts occur in at least one experiment showed higher than average errors, but this did not seem to be entirely due to the gearshifts. Temporary loss of satellite coverage did not cause any consistent effects on the road grade estimate. Grade estimates based on a linearized model showed comparable results to those obtained with the nonlinear model.

The estimators based on the more accurate piecewise linear road grade model failed to improve on the results of the estimator with the simplified road grade model

for short sample distances. The results indicate that there is a performance gain to be had for very long sample distances, or if a very compact data representation is needed. At high sample rates there is so much sensor data available that deviations from the piecewise linear model can be detected, using the constant road grade model.

From the discussion on performance criterions in Section 4.3 it is clear that the mean error in the estimated relative altitude a significant distance ahead of the vehicle is an important concern. This is closely related to the mean error, or bias, in the road grade estimates. The inclusion of the GPS signal in the estimation significantly reduces the error due to vehicle or environment parameter errors, making it vital to obtaining good altitude predictions.

Chapter 6

Estimation through Multiple Vehicles

> "*You could have a community capability where you took the GPS data of people driving around and started to see, oh, there's a new road that we don't have, a new route ... And so that data eventually should just come from the community with the right software infrastructure.*"
>
> Bill Gates, quoted by the OpenStreetMap community.

Road grade estimation through vehicles in normal operation, using standard sensors, reduces the need for data collection with survey vehicles. The methods presented in previous chapters do however rely on more than one estimate from each road segment to be available, in order to produce accurate results. For one vehicle, this can be achieved over time, if the number of distinct roads being driven is not too large. Using mobile communications technology, estimates gathered from many vehicles can be transferred to a central location. This enables gathering of a large number of estimates from a wide area. A comprehensive map can then be generated and transferred back to the vehicles. Road grade estimation based on a large number of independent standard vehicles is similar to the crowdsourcing appearing in many other domains. The data collection and estimation work is distributed among the users, instead of being performed by employees.

This chapter presents a simulation study outlining the potential performance of a road grade estimation system using distributed data collection and estimation. Predictions are made about the estimation performance of an isolated vehicle versus a system of connected vehicles. A prototype system for generating a road grade map from estimated road grade profiles is also presented.

6.1 An Architecture for Multiple Vehicle Road Grade Estimation

In the simplest implementation of the proposed road grade estimation algorithm a single vehicle records sensor data, and computes road grade estimates based only on

its own information. Over time the estimates for frequently traveled routes become rather good, but when using a new road any predictive control systems, based on the map data, would be unable to operate. When using only one vehicle the estimation performance is also limited by the single realization of parameter errors available, i.e., all road grade estimates are influenced by the same errors in the vehicle specific model parameters.

By adding two-way communication capabilities to the vehicle, it can be made a part of a collaborative mapping system, where estimates or measured data are shared with other vehicles. This can either be done through a centralized server, or through data sharing with other similarly equipped vehicles in the vicinity. If estimates or measurements are uploaded to a central server, and used to improve a common map, a range of model parameter errors will be represented. This approach both increases the number of estimates available for each road, and decreases the residual error due to parameter biases. The centralized server is a key component in such a system, which might be economically feasible if the users are charged a fee for data transfers, and for access to the server's data.

If vehicle-to-vehicle communication is used, data may be shared between the databases of vehicles within communication range of each other. The amount of data that can be shared while in range of another vehicle is likely to be limited. Some system for determining what data to share, and whether to trust the information from the other vehicle is needed. This type of system has similarities with the P2P technologies on the Internet, with the important difference that there is no one master version anywhere of the file, or road database, being shared. Instead, each vehicle has a subset of the whole information of the system, but no one has the full data set.

Simulations have been used to study two issues related to extending road grade estimation to a fleet of probe vehicles. First, the convergence of the road grade estimates from the constant estimator is analyzed, under a set of assumptions regarding the distribution of the parameter errors and measurement noise. The rate of convergence, and final error after inclusion of a large number of experiments, are evaluated for two scenarios. In the first scenario data from only one vehicle is used. In the second scenario communication facilities are assumed to be available, and each data set is taken from a distinct vehicle.

In the second study a prototype implementation of a road grade map estimation scheme, based on freely available two-dimensional map data and road grade estimates from probe vehicles, is developed and tested. Simulated vehicles are driven on a network of 62 highway sections between cities in southern Sweden, Denmark, and northern Germany.

6.1.1 Inter-Vehicle Communication Requirements

When evaluating the potential for estimation through multiple vehicle the data transfer requirements are important. Depending on whether the estimation is done locally in the vehicles, or at a central processing server, the data that need to

Table 6.1: Communication requirements from the vehicle to the server for each estimated data point, for distributed and centralized road grade estimation.

	Distributed [bits]	Centralized [bits]
Longitude	32	32
Latitude	32	32
Altitude	16	16
Road grade	16	-
Grade variance	16	-
Speed	-	16
Engine torque	-	8
Current gear	-	4
Brake in process	-	1
Shift in process	-	1
Satellites	-	4
GPS DOP	-	8
$\sum$	112	122

be transferred vary. Table 6.1 lists the required variables, and estimated size of each variable for both alternatives. The requirements for each variable are rough estimates. The distributed scheme appears to require slightly less data to be transferred, but the difference is not significant. The possible decrease in data transfers has to be weighed against the potential cost for extra computational power in the vehicles.

In the most costly scheme, the centralized one, 122 bits are used for each data point. Restricting ourselves to whole bytes, 16 bytes of information need to be transferred for each data point. This estimate assumes no compression is applied, which is conservative. Using differential position and altitude coding, combined with non-destructive data compression, less than half of that will actually be needed. On the other hand, no protocol overhead is considered either, so 16 bytes per sample will be the number used. With a sample distance of $\Delta s = 20\,\text{m}$, as is used in the map building simulation study below, this leads to a need to transfer 0.8 bytes per meter traveled. A standard long haulage HDV travels around 250 000 km per year, giving a total yearly need to transfer

$$0.8 \cdot 2.5 \cdot 10^8 \text{ bytes} = 200\,\text{MB} \tag{6.1}$$

of data. With current mobile technologies this should not pose a technological problem, the cost of the data transfer will however need to be taken into account in a system design. With local computation of the road grade estimates, and efficient

data coding, the communication requirements for each vehicle can likely be reduced significantly from the 200 MB stated above. It should be noted that this estimate only covers the uplink data.

6.1.2 Estimator Convergence

As measurement data from an increasing number of trips along a road section become available, and are included in the road grade estimate, the associated estimation errors should intuitively decrease. When assuming unbiased normally distributed uncorrelated estimates with known variances, the variance of the result formed by weighted averaging can easily be computed. In practice the errors in the road grade estimates are however not entirely uncorrelated, normal, or unbiased. This is true in both the simulations and on-road experiments. The convergence of the constant estimator, described in Section 4.1, has therefore been studied through a large number of simulations experiments.

The reference road grade profiles used in the simulations contain some relatively high frequency content that cannot be detected using the proposed method, and will contribute to a common error in all estimates. This is particularly true for the reference road profiles obtained by driving down the roads with a high accuracy GPS and INS system, as described in Section 5.1.5. In other words, the filtering of the reference signal influences the performance results. Whether the difference between the true profile and the estimated one is of any importance depends on the application where the estimates are to be used. Here, that difference will add a correlated error to the estimated road grade signal in all experiments, which cannot be removed by averaging. The magnitude of the error depends on the filter parameters used in the estimator. By increasing the sensitivity to the measurements, the cut-off frequency can be increased at the expense of higher random errors and slower convergence.

If only one vehicle is used to collect data, parameter biases will contribute to similar biases in all estimates. This effect is included in the simulation study. In on-road experiments factors such as multi-path GPS errors due to reflections from large buildings or features in the environment may also cause correlated errors. Multi-path effects are very hard to model correctly, and no attempt has been made to include such errors in the simulation model.

Hilly road sections where braking and gear changing is required are likely to be affected by larger errors than flatter sections. Since the brake force is always ignored in the estimation model, braking produces correlated errors in estimates from all experiments where it occurs. In the constant estimator such data points are weighted less than ones without braking, but they will still have some effect on the result.

6.1.3 Creating a Road Grade Map

To be able to retrieve estimated road grades when returning to a road, they need to be stored a map. The work so far has focused on creating road grade estimates as a sequence of distance-value pairs. Along with each estimated road grade data point the latitudinal and longitudinal position are also recorded, from the GPS. This information has previously been used to synchronize multiple measurements in the experiments. Below, the location information is instead used in a prototype map creation system.

When a vehicle equipped with one of the proposed estimators is driven, in real life or in a simulation, road grade estimates are generated at equidistant points along the road. Estimated latitude and longitude values are saved together with each data point. After the estimation has been completed for a particular section, the location information is used to add the data to a map.

Autonomously building a road map from scratch is hard, and outside the scope of this thesis c.f. (Schroedl et al., 2004; Brüntrup et al., 2005). Instead, an existing two-dimensional road map has been used, and road grade information added. For this project, the freely available OSM database has been used as the source of both the map data model and actual two-dimensional road data (OpenStreetMap, 2010). OSM data for 62 one-way highway segments in southern Sweden, Denmark, and northern Germany was exported and used in the study. Other databases may be used in a similar fashion, as long as they provide a sufficiently rich interface that allows extraction of road geometries programmatically.

Adding a Third Dimension

One of the main challenges in adding the estimated road grade data to a map is to decide where a particular data point should be placed. In OSM terminology the map consists of *nodes*, *ways*, and *relations*. Nodes are the basic building block, and streets and highways are represented by joining many nodes in a way. Ways may then be joined by relations. The nodes are placed by the creators of the map, where they are needed in order to represent the continuous two-dimensional road profile with desired accuracy. On straight sections of large highways the nodes may be several hundred meters apart. In this work the existing OSM data was processed to generate nodes every 20 m along the original road profiles. In a production environment, an event based sampling scheme where nodes are only added where there is an actual change in the road grade is likely to be much more storage efficient.

The matching of measured data points to nodes in the map was accomplished by comparing the estimated location of the data points, and the direction of travel, with nearby nodes and ways. This method worked very well for the reduced set of roads available in the prototype. A number of map matching methods of varying complexity are available in the literature, and given that the matching of data points for inclusion in the map can be completed off-line, solving the matching problem in a full map implementation shouldn't be too hard.

Once a particular estimate had been tied to an existing map node, the road grade data for that node was updated using the inverse variance weighted method described in Section 4.1.2.

6.2 Experimental Setup

The potential performance of the constant estimator has been tested through simulations, using many experiments, with one or many vehicles, to generate the results. The simulations are based on a standard European long haulage vehicle configuration, and the simulation model described in Section 3.4.1. The same simulation setup has been used both to directly evaluate the convergence of the estimates from the proposed method under realistic circumstances, and to generate raw data for evaluation of the road grade map generation method described in Section 6.1.3.

The reference road grade changes rather slowly, as can be expected from the road grade model discussed in Section 3.2. The RMSE compared to the original reference grade profile for a downsampled and then interpolated version of the reference road grade is very small. When the profile is downsampled by a factor of four ($\Delta s = 10\,\text{m}$), the reconstruction RMSE for linear interpolation is 0.0016 % grade, for the highway E4 south of Södertälje. When downsampling by a factor of eight ($\Delta s = 20\,\text{m}$) and the reconstruction RMSE for linear interpolation is 0.0060 % grade. Motivated by this, the simulation studies have been performed at sampling distances of $\Delta s = 10\,\text{m}$ for the convergence study, and $\Delta s = 20\,\text{m}$ for the map building study. The reduction in simulation time compared to using $\Delta s = 2.5\,\text{m}$ is significant, and the loss of accuracy is immaterial compared to other uncertainties involved.

6.2.1 Test Roads

The convergence of the output from the constant estimator has been studied for three different road sections.

- A part of highway E4, from Södertälje to Nyköping, Sweden
- A part of highway E44 from Koblenz to Trier, Germany
- A part of highway E25, from Hamburg to Berlin, Germany

The first two reference road grade profiles were collected on-site, as described in Section 5.1.5. The road grade profile for E26 was based on filtered satellite altimetry data, as described in Section 6.2.4. Figure 6.2 shows a map locating the road sections.

The road grade map generation prototype was evaluated on 62 road segments describing major highways between cities in Sweden, Denmark, and Germany. The road network used is shown in Figure 6.7. The process of obtaining reference road information for the roads is described in Section 6.2.4.

Figure 6.2: Map showing the locations of the road segments used in the estimation convergence study. The reference road profiles for the segments Södertälje–Norrköping and Koblenz–Trier are based on experimental data collected on the ground. The Hamburg–Berlin segment reference grade was determined from NASA SRTM data. (Image courtesy of Google)

6.2.2 Test Vehicles

The most commonly used type of vehicle for long haulage freight in Europe is a tractor and semitrailer combination that may be loaded to a maximum weight of 40 t. Such a vehicle combination would typically have an engine that can produce around 400–450 hp. This configuration has been used for most of the simulation experiments and illustrating examples in the thesis. It has also been used in both the road grade estimate convergence and map creation studies. The model parameters used, and their values, are listed in Table 6.3. For a description of the meaning and use of each parameter, see Section 3.1. The gearbox transmission ratio for the simulation vehicle is $i_t = 1$ at gear 12, the highest gear, and $i_t = 11.3$ at the first gear. The gearbox efficiency is $\eta_t = 0.99$ in the highest gear and decreases to $\eta_t = 0.96$ in the first gear.

Table 6.3: Nominal vehicle model parameter values used for simulations in the thesis, unless otherwise noted.

Parameter	Symbol	Value	Unit
Vehicle mass	m	40 000	kg
Wheel inertia	J_{w}	65.8	kg m^2
Wheel radius	r_{w}	0.495	m
Engine inertia	J_{e}	3.5	kg m^2
Engine max. torque	$T_{\mathrm{e}}^{\max}$	2 300	Nm
Final drive ratio	i_{f}	2.71	-
Final drive efficiency	η_{f}	0.97	-
Rolling resistance coefficient	c_{r}	$7 \cdot 10^{-3}$	-
Air drag coefficient	c_{w}	0.6	-
Front area	A_{a}	10.26	m^2
Air density	ρ_{a}	1.29	kg m^{-3}

Parameter Errors

The parameters in the models for the vehicle, its sensors, and its interaction with the environment will not match the nominal values exactly. If proper care is taken in choosing the parameter values one can however reasonably assume that their errors will belong to some random distribution, with zero mean error. If enough experiments are performed, the parameter errors are then likely to essentially average out. The simulation studies have been set up based on this premise. Very little statistical data are available on the reliability of the various parameter estimates. This has led to a significant number of assumptions being made based on interviews with engineers working in the relevant fields.

Some parameters vary mainly between vehicles, while others are largely determined by the weather or other conditions specific to a certain time or place. In some cases both the vehicle used and the environmental conditions affect the same parameters. A key objective of the convergence study has been to determine the amount of influence from using one or many vehicles in the estimation. The parameter errors have therefore been divided into two categories, one that is kept constant for each simulated vehicle, and one that is updated for each experiment. All parameter errors are kept constant within each experiment.

Vehicle Dependent Parameters

Based on a set of nominal vehicle parameters a number of distinct vehicle realizations were created. The parameters have been chosen based on a normally dis-

Table 6.4: Vehicle dependent parameter error standard deviations used in simulations.

Parameter, p	Symbol	Standard deviation σ_p
Vehicle mass	m	0.05
Wheel radius	r_w	0.02
Engine max. torque	$T_\mathrm{e}^\mathrm{max}$	0.05
Rolling resistance coefficient	c_r	0.05
Air drag coefficient	c_w	0.15

tributed random process, with zero mean and a specified variance unique for each type of parameters. The road grade estimation was always carried out using the nominal parameters, but the values used in the simulated vehicles varied. Each realization, used in vehicle m of a vehicle parameter p_m was determined from the nominal value p_0 as

$$p_m = (1 + \varepsilon_m^p) \cdot p_0, \quad \varepsilon_m^p \sim N(0, \sigma_p) \tag{6.2}$$

where ε_m^p is the error coefficient for a particular parameter p and vehicle m, and σ_p is the assumed standard deviation for that parameter among vehicles. The parameters that were modified for each vehicle and their assumed standard deviations are given in Table 6.4.

Since engine torques are recorded and processed as percentages of the maximum torque $T_\mathrm{e}^\mathrm{max}$, an error in $T_\mathrm{e}^\mathrm{max}$ affects all torque values used. For any vehicle parameter not listed in the table we set $p_m = p_0$ for all vehicles. In many cases the errors in different parameters that would affect the vehicle the same way have been brought to only one parameter, and been described by a single normal distribution.

Experiment Dependent Parameters

The experiment dependent parameters q_n used in experiment n were chosen in the same way as the vehicle dependent parameters, but changed for each new experiment. The values q_n in each experiment n were based on the values, p_m, for the particular vehicle m being used, and computed by taking

$$q_n = (1 + \varepsilon_n^q) \cdot p_m, \quad \varepsilon_n^q \sim N(0, \sigma_q) \tag{6.3}$$

where ε_n^q is the error coefficient for a particular parameter and experiment, and σ_q is the assumed standard deviation for that parameter. The experiment dependent parameters used and their assumed standard deviations are given in Table 6.5. For any model parameter not included in the table the vehicle dependent value was used directly.

Table 6.5: Experiment dependent parameter error standard deviations used in simulations.

Parameter, q	Symbol	Standard deviation σ_q
Vehicle mass	m	0.10
Wheel radius	r_{w}	0.01
Rolling resistance coefficient	c_{r}	0.05
Air drag coefficient	c_{w}	0.10

6.2.3 Measurements

In addition to the errors introduced by the parameter deviations from the nominal parameters, simulated sensor noise was added to the measurements. The sensor models used for generating the noise are described in Sections 3.4.1 and 3.4.2 for the driveline sensors and the GPS, respectively.

Based on comparisons of the estimation performance using simulated and real measurement data the standard deviation σ_v of the WGN in the vehicle speed signal was set to

$$\sigma_v = 0.045 \tag{6.4}$$

which yielded a slightly higher random error in the simulation than in the on-road experiments. The engine torque signal measurement error was modeled through a parameter error describing the error in the maximum engine torque, and did not include any time varying component. The standard deviation of the parameter error is given in Table 6.4.

The simulated sensor noise from the GPS was generated as a realization of a Markov process model identified from the real experiments. The models used to generate the GPS errors for the simulations were based on all 11 experiments. The modeling approach was validated separately using only part of the available data for identification. Figure 6.6 shows a comparison of the statistical properties of the southbound experimental GPS altitude errors with a realization from a Markov process model based only on the northbound experiments, with a sampling distance $\Delta s = 10\,\mathrm{m}$. While the histograms appear similar in both cases, the full autocorrelation of the true error is not captured by the model. Changes in the number of tracked satellites have not been included in the error model. This aspect of the estimator can thus not be evaluated using these simulations. Given the importance of the GPS error behavior to the convergence and performance of the estimation method, the GPS error model is identified as an area worthy of future attention.

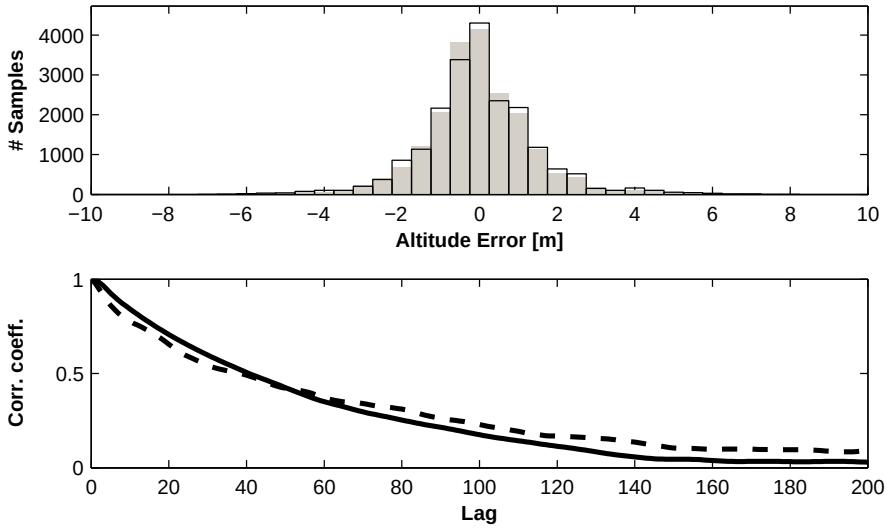

Figure 6.6: The identified GPS error model generates a similar error distribution as the one found in the validation data (top part). The model based realization is shown with a black outline, the experimental results are shown as shaded bars. The autocorrelation for large lags in the validation data (dashed line) is slightly higher than in the data from the model (solid line). This is not surprising, given the low order of the model (bottom part).

6.2.4 Reference Road Grade

To generate road grade estimates through simulations, reference road grade information for the roads to be estimated is needed. One of the motivations for this project is the present scarcity of high quality road grade information. Local road authorities in different countries often have accurate road grade information for some roads, but it is generally not complete and the EU projects in the area show that data sets from different regions are hard to combine. Commercial providers probably have the most complete coverage available today, but it is still limited to only a few countries. The commercial data are also hard to come by in an open and accessible format.

No authoritative road grade information for a large enough set of roads was available, so an alternative solution was developed. It was decided that the simulation study was to be based on road grade profiles determined by processing SRTM altitude data. Road altitude profiles were obtained by interpolating the topographic data for the locations of the nodes in the OSM data. A visualization of the SRTM data for the area where the simulation reference road grade map was created is shown in Figure 6.7.

The SRTM data are rather coarse, with a 90 m grid over Europe. They also suf-

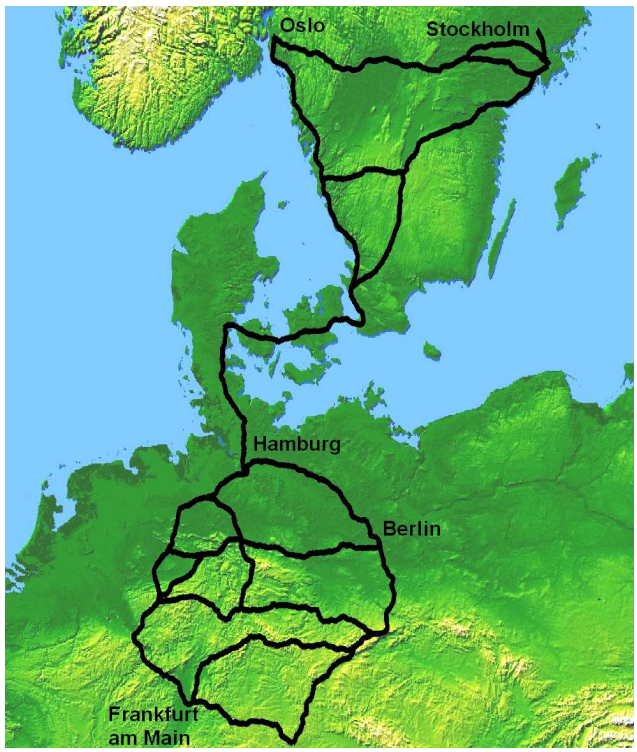

Figure 6.7: Altitude map of the road grade map generation test site based on SRTM data. Brighter hues indicate higher terrain. Reference road grades for the map creation prototype were created based on this altitude data set, interpolated for the road locations. (Courtesy NASA/JPL-Caltech.)

fer from a high noise level, and relatively low absolute accuracy. This data set is not useable as a direct estimate of road grades for control purposes. It is however possible to create a synthetic road grade profile with approximately the right amount of hills and flat sections based on the data. This was accomplished by filtering the altitude profile with a low cut-off frequency, and limiting the maximum grade, and rate of change in the grade, in a post-processing step. The artificial reference profiles generated in this way have less high frequency content than the ones obtained from on-road measurements. This makes the estimation task slightly easier, as seen in Section 6.3.1. No high quality reference road grade data for a large area were available for the study, and the described method for reference profile generation was preferred over using entirely fictional road grade profiles based only on the statistical properties of the few sections where data were available. Figure 6.8 shows a comparison of the reference road grade generated by the SRTM based procedure, and the reference obtained from on-road measurements, used throughout the thesis,

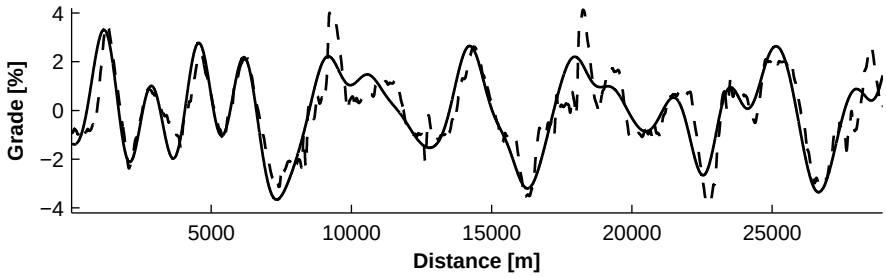

Figure 6.8: The reference road grade from the SRTM data (solid line) is compared to the reference recorded on the road (dashed line) , for the southbound E4 test site south of Södertälje. The profile generated from SRTM data is significantly smoother than the recorded reference, but they both show the same general hilliness of the road.

for a road section covered by both types of data.

6.3 Experimental Results

Two simulations studies were carried out to investigate the performance of the constant estimator over time. The results of the first study are reported in Section 6.3.1, and indicate the estimation accuracy achievable after repeated experiments, for three different reference road grade profiles. The second study expands the number of reference grade profiles to 62, and includes the construction of a road grade map. These results are reported in Section 6.3.2.

6.3.1 Estimator Convergence

The convergence of the estimated road grade to the reference profile has been studied through simulations. The road grade profile estimate and its associated RMSE were determined using an increasing number of experiments, from 1 to 100. This process was then repeated 30 times, to yield an estimate of the variations in the rate of convergence. The experiments were carried out under the conditions of both the scenarios described in Section 6.1, i.e., with and without communication between vehicles. As an illustration of the convergence of the estimates Figure 6.9 shows the RMSE achieved when using an increasing number of experiments.

The estimation performance is consistently higher in the scenario where different vehicles parameter errors were used for each experiment, than when the same parametrization was used for all experiments. The difference when GPS data is being used in the estimator, as is the case in Figure 6.9, is however rather small compared to the same difference when excluding GPS data from the estimation. This is due to the effective bias compensation from the GPS signal. The same phe-

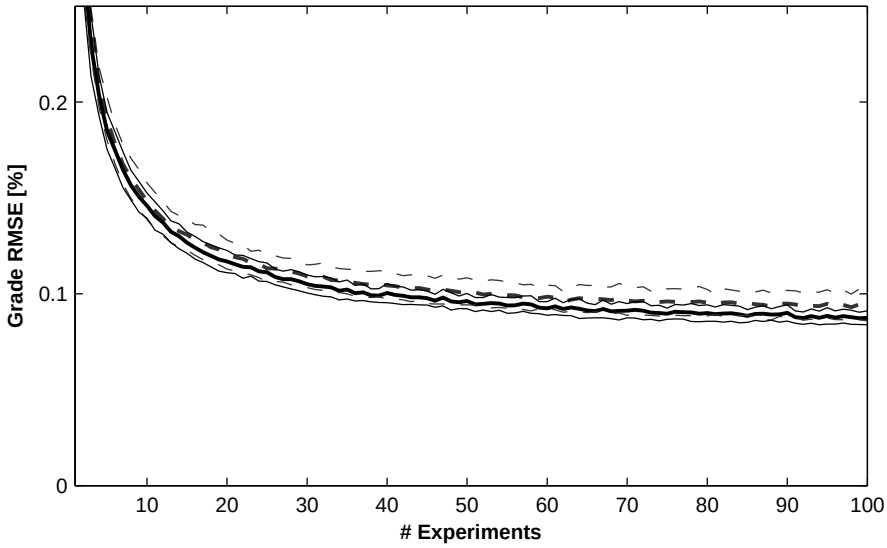

Figure 6.9: The RMSE in the estimated road grade is shown for the southbound highway section from Södertälje to Nyköping. The constant estimator has been used with an increasing number of simulation experiments. The results when only one vehicle, with a fixed set of vehicle parameter errors, was used (dashed lines), are only slightly worse than when different vehicles were used for each experiment (solid lines). The mean RMSE for 30 sets of 1–100 experiments is shown. It is flanked by narrow lines indicating the sample standard deviation over the 30 sets, for the RMSE estimates.

nomenon was also seen in the on-road experiments, as described in Section 5.4.5. The estimation performance difference is illustrated in Figure 6.10.

According to the simulation results, operating the estimator on-board a single vehicle would produce only slightly worse estimates, after a fixed number of trips, than using a system where data is shared among vehicles. It is of course likely that more experiments would be available at a given time in the communication enabled scenario. However, if convergence to around 0.1 % grade can be realized in under 100 experiments in a single vehicle, communication may be unnecessary in many applications.

The simulation results show that the properties of the reference road grade profile are important for the final value of the road grade RMSE after many experiments. The convergence is faster for the smoother road grade profile generated from SRTM data used for the road E25 from Hamburg to Berlin, than for the reference profiles measured on the roads. This is likely due to the low-pass properties of the estimator, which will lead to the removal of high frequency road grade signal content in a similar way in all experiments. There is also a noticeable difference in the

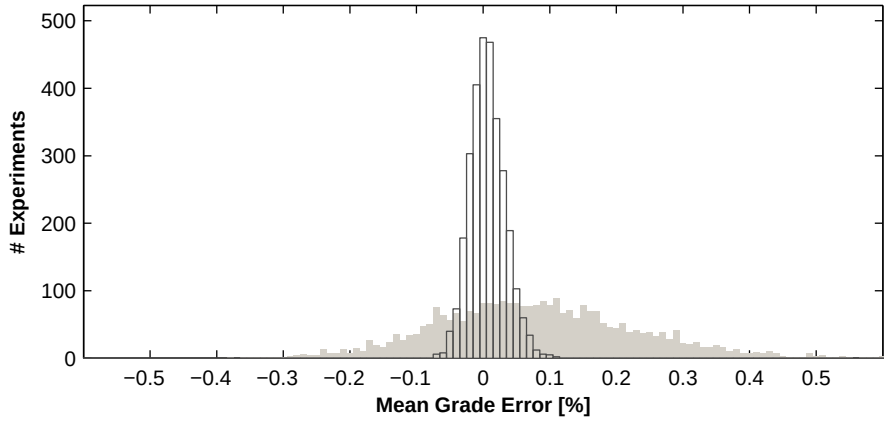

Figure 6.10: The combination of GPS and vehicle model data in the road grade estimator significantly reduces the bias in the estimates, compared to relying only on the vehicle model. The distribution of the mean grade error is shown for 3 000 simulation experiments on the Södertälje to Nyköping segment, with different error realizations for the vehicle parameters being used in each experiment. The shaded bars represent the grade bias from using only the vehicle model. The outlined bars indicate the grade bias of the output from the estimator.

estimation errors between the two reference profiles measured with the same equipment. The profile recorded on E44 between Koblenz and Trier is not estimated as precisely as the one from E4 in Sweden. Short sections of the estimated and reference profiles, for each of the three test roads, are shown in Figure 6.11.

The convergence results, as an increasing number of experiments are used for estimation, for each of the studied road segments, are shown in Figure 6.12. The decrease in the RMSE over the first few experiments approximately follows the theoretical $1/\sqrt{N}$ decline, where N is the number of included experiments. As the total error decreases the influence of correlation and systematic errors slow the convergence for the two roads based on accurate reference data. Since all simulations have been conducted with the same vehicle model, but difference reference road grades, it is clear that the properties of the reference heavily influence the behavior after many experiments. The relatively smooth reference profile created from SRTM altitude measurements yields a convergence rate very close to the theoretical one. For the other profiles the convergence rate decreases after a while, and the improvement beyond ≈ 100 experiments appears to be very small. The Koblenz–Trier segment reference profile gives the largest residual error.

The corresponding convergence of the relative altitude prediction error 1 km ahead of the current position, illustrated in Figure 6.13, shows a similar behavior. The residual RMS altitude prediction error for the Koblenz–Trier segment, after 100 experiments, is 0.68 m. The Hamburg–Berlin segment with a reference profile

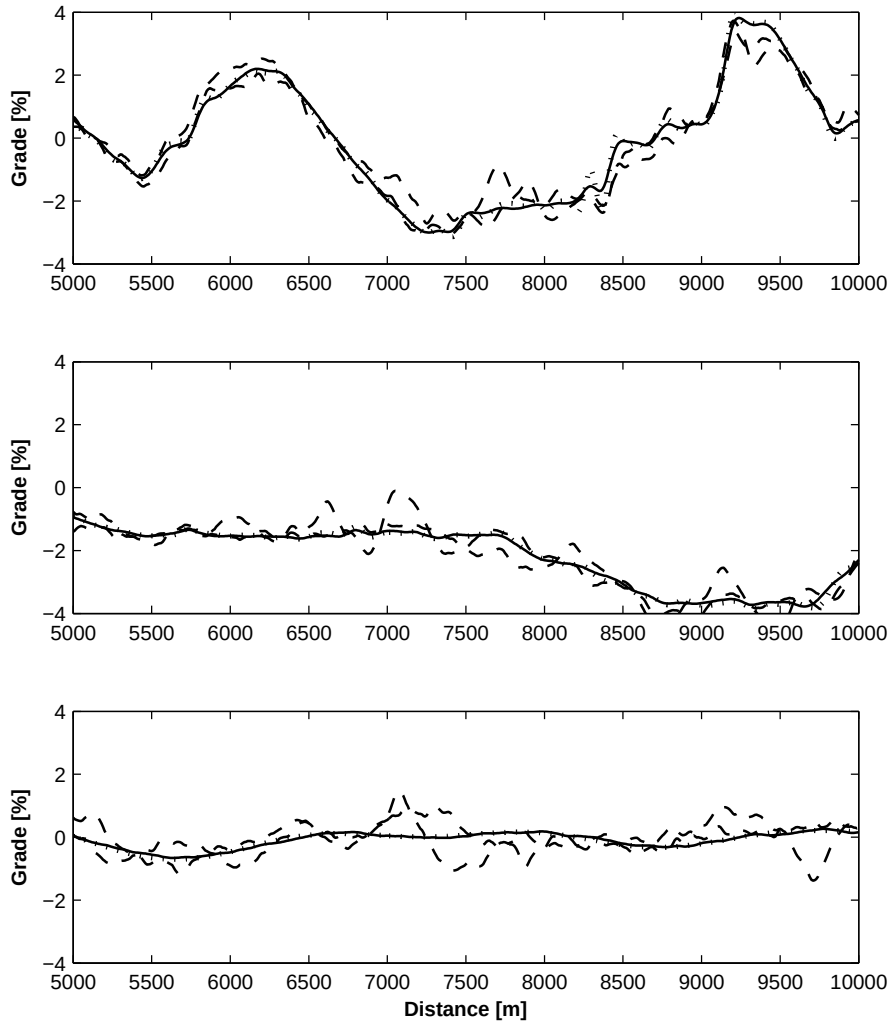

Figure 6.11: Illustration of the estimated (solid) and reference road grade profiles (dotted), after 100 experiments, for the three test road sections investigated in simulations. Results from two individual experiment are also shown for each section (dashed). The top figure shows a part of the Södertälje–Nyköping segment. The middle one presents a part of E44 between Koblenz and Trier, and the bottom figure shows a part of the Hamburg–Berlin segment.

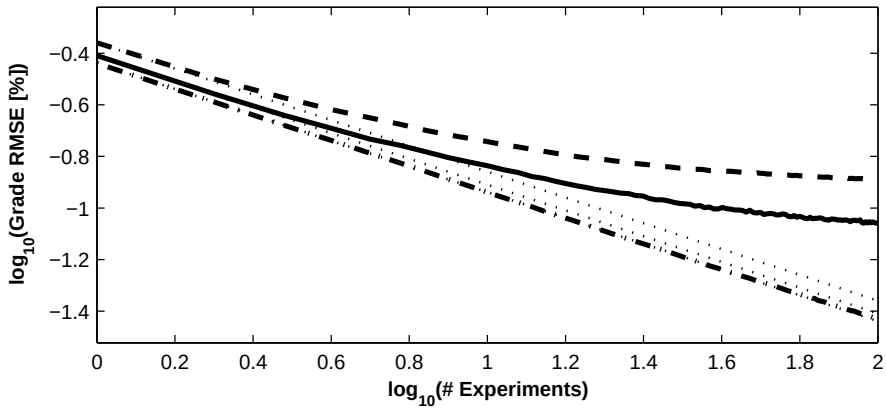

Figure 6.12: The mean RMSE between the estimated map and reference road grade profile, after an increasing number of experiments have been used is shown for three road segments; The Södertälje–Nyköping segment (solid), the Koblenz–Trier segment (dashed), and the Hamburg–Berlin segment (dash-dotted). The nominal decrease of the RMSE, for uncorrelated normally distributed estimates of a constant quantity, is a straight line with the slope $-1/2$ in the log-log diagram. Straight lines with this slope, starting at the RMSE from a single experiment, are therefore included for comparison (dotted).

created from SRTM data, has a RMS altitude prediction error of 0.17 m, that is still decreasing after 100 experiments.

The simulation study indicates that the properties of the true road grade are very important for the convergence of the estimates. There seems to be a trade-off to be made between good estimation results after only a few experiments, and the long term convergence to a low error. If the parameters of the road grade estimator are adjusted to raise its low-pass cut-off frequency, better convergence may be achieved for road profiles that contain significant energy at higher frequencies. This will on the other hand lead to larger estimation errors from sensor noise that has to be removed by averaging of data from many experiments. The range of frequencies to be considered for the reference depends mainly on the application for the estimated data.

6.3.2 Road Grade Map

The map building method, described in Section 6.1.3, was tested through experiments where simulated vehicles drove missions, between 50 and 500 km in length, on the roads of the extracted OSM data. The road grade for each mission was estimated using the constant estimator. The road grade estimates from each experiment were then added to the map.

The quality of the road grade estimates depends both on the number of vehicles

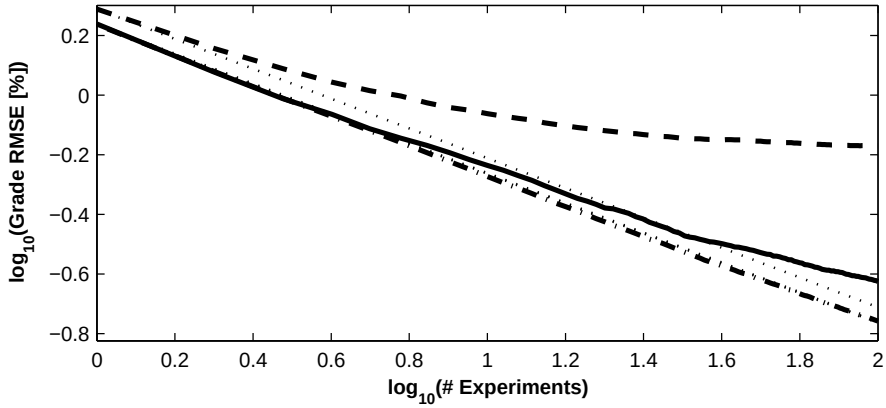

Figure 6.13: The RMS relative altitude prediction error 1 km ahead of the current vehicle position, after an increasing number of experiments have been considered, is shown for three road segments; The Södertälje–Nyköping segment (solid), the Koblenz–Trier segment (dashed), and the Hamburg-Berlin segment (dash-dotted). Straight lines, indicating the nominal error decrease, are included for comparison (dotted). The relative altitude error for the Södertälje–Nyköping segment decreases at close to the theoretical rate for a larger number of experiments than the road grade error, while the Koblenz–Trier segment convergence falls off at a similar rate for both errors.

that have driven along a particular segment, and the estimation accuracy in each experiment. Figure 6.14 shows the evolution of the estimate quality, as more experiments are included in the generated map. Results are shown for $N = 10$, 100, and 1 000 experiments. Figure 6.15 shows the number of experiments that have been used for each location on the map, when the same total number of experiments have been completed as above. The dots in the figures represent averages over 250 data points each, so that the entire map can be visualized at a zoomed out scale.

6.4 Discussion

The simulation studies indicate that the proposed estimator can successfully be used to generate high quality road grade information, based on a reasonable number of trips along major roads. The estimation results are remarkably accurate, given the low-cost sensors, simple vehicle model, and relatively large model parameter errors. The accuracy of the estimator makes it appropriate for use as a part of a system designed to generate road grade maps for vehicle control applications.

The simulation studies show similar estimator performance regardless of whether a single vehicle, or many different vehicles, are used to collect the measurements. When a single vehicle is used to collect all data, the bias in the final road grade

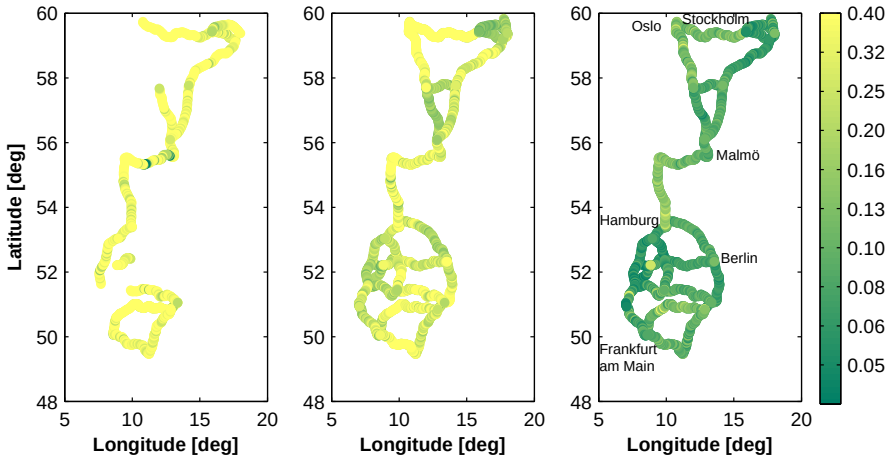

Figure 6.14: The generated road grade map accuracy is illustrated by a scatterplot with dots representing groups of 250 data points each. The RMS grade error in each group determines the color, darker dots mean more accurate road grade data. Starting from the left the figures show the data at different states of the map creation process, after $N = 10$, 100, and 1 000 profile estimates from trips between 50 and 500 km each have been added.

profile depends largely on the properties of the GPS signal. The GPS signal model used in the simulation studies yields very good bias error compensation. A real GPS receiver is likely to provide similar performance when operating under close to ideal circumstances, i.e. with few multipath errors and good satellite visibility. Unfortunately the intermittent, but important and common, GPS errors from signal reflections and loss of satellite contact are very hard to model accurately. Since these errors are not included in the GPS model used, the actual estimator performance degradation from using data collected with only one vehicle may be higher than indicated by the simulations.

The data transfer requirements for a system where estimates are shared with other vehicles through a server are considerable, but not prohibitive, using current technology. Given the observed convergence rate, a fleet of vehicles would rather quickly generate a useable map of their shared area of operation. In system with a centralized server it is easier to validate the data based on external sources, and possibly disable estimation in vehicles that produce poor results. If a centralized server is used one can also ensure that the control algorithms applied perform consistently in all vehicles, a factor that may be important for driver acceptance.

In a scenario where the vehicles on the road act as probes that send information to some other party, the ownership of that information becomes important. Whoever controls the information flow from a large number of vehicles stands to gain significant advantages from using those data. The legal and privacy concerns

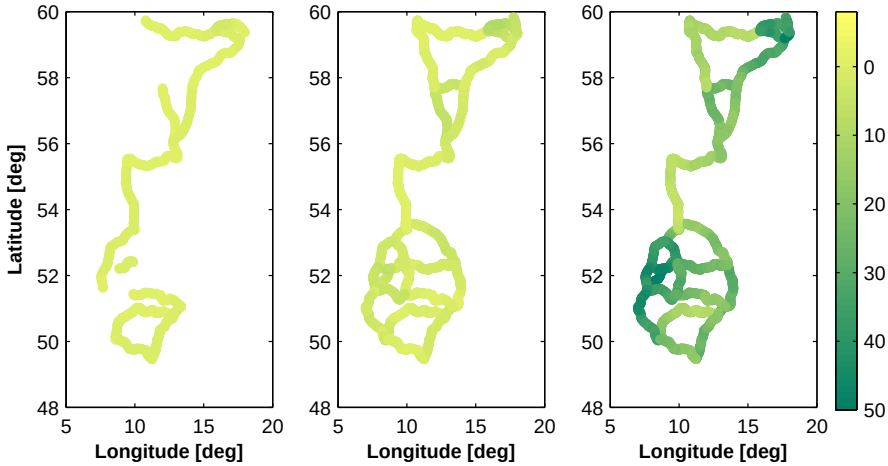

Figure 6.15: Each vehicle in the simulation study was started at a random location, and then chose a random turn direction at each highway intersection. Each trip lasted for a random distance, between 50 and 500 km. The average number of trips recorded for a group of 250 data points is indicated by the intensity of the corresponding point in the map. Roads that have not been driven are not printed, and black roads have been driven at least 50 times. Starting from the left the figures show the data at different states of the map creation process, after data from $N = 10$, 100, and 1 000 experiments have been added.

involved in large scale application of a distributed road grade estimation system are likely to be at least as challenging as the remaining technical aspects. A large fleet owner, or truck manufacturer, who deploys estimators in many vehicles, may be able to commercialize the generated road grade data. The economic benefits may even extend beyond avoiding the licensing costs associated with purchasing the same information from a provider running traditional road surveys.

Very successful online services have been built around the desire of people to share data, e.g. Wikipedia, Facebook, and Twitter. If the right tools are created, the incumbents in the mapping industry may face serious competition. Such a tool could for example give ordinary users mobile access to high quality map data at zero cost, in exchange for their recorded traces. The income for the map provider could, as in the examples above, come from targeted advertising or even donations, instead of map licenses. The current implementations in the area are too hard to use for non-enthusiasts, but that may change quickly. Using the methods proposed in this thesis, road grade information could be included in such maps. The view of Steve Coast, the founder of the OSM project is clear, in an interview he stated:

> The plan is to overtake Tele Atlas and Navteq. It's coming for them and it'll hit them hard like it did for the guys at Encyclopedia Britannica

> when Wikipedia grew. I want OSM to become the biggest mapping service in the world. (Sung, 2009)

One of the main difficulties in autonomous map creation is getting the topology of the information correct. In OSM this task is handled by a large group of volunteers, each working on a small part of the data. Attracting and keeping these volunteer manual workers is currently a key factor to the success of OSM. Attaching sensed and estimated information, such as the road grade, to the roads that are already present in the map, or even adjusting the position of the roads to increase the accuracy, can to a large degree be done by automatic methods.

While most personal navigation devices currently lack a connection to vehicle sensors, this may change as in-vehicle navigation evolves. As an example, Saab has recently announced a new system that will allow third party developers to write applications for an on-board device similar to an integrated smartphone, running the Android operating system. Vehicle signals are going to be made available through an API (Saab Press Release, 2011). In the long run, this potentially enables third parties to create the type of crowdsourced high quality digital map service envisioned above, within vehicles of different brands.

The current market leaders in the navigation data field are also involved in the development towards more user generated content. Many recently launched navigation devices contain two-way communication links, and are equipped to send automatic or user initiated map error reports and update requests back to the manufacturers. The proposed estimators may thus find application also within the production chain of established map providers. Only the future will tell if the current model for commercial map data creation will survive, or if it will be replaced by something else.

6.5 Summary

The performance of the constant grade estimator, when using multiple experiments and vehicles, has been evaluated. Both the convergence to a reference grade profile over single road segment, and the accuracy of a generated road grade map have been investigated. The presented simulations show that highly accurate road grade estimates can be obtained by using measurements from many different trips along a road section. While a large scale on-road experimental investigation of the limit of accuracy attainable by a real life system remains future work, a similar trend can be observed in the experimental data in Chapter 5.

Chapter 7

Conclusions and Future Work

> "*The most exciting phrase I hear in science, that heralds new discoveries, is not 'Eureka!' But 'That's funny'.*"
>
> Isaac Asimov

Access to stored road grade information yields significant advantages in HDV control. A system for obtaining such information using standard vehicles in regular operation has been developed and evaluated in this thesis. It has been shown through experiments that the proposed distributed road grade estimators generate results that are consistent with reference road grade profiles. The generated estimates improve when additional measurements are used to create a profile. The inclusion of data from more than one run along a road segment reduces the effects of spurious estimation errors on the road grade map. The possible performance of one of the proposed methods in a large scale application has been evaluated through simulations. This chapter details the conclusions that can be drawn from the results, and outlines avenues for future work in the area.

7.1 Conclusions

Recent advances in the development of embedded electronics, and low cost global positioning, enable new vehicle control systems that use map data to supplement traditional sensors. These systems rely on digital maps that include accurate road attributes. Recent work, by numerous authors, indicates that the road grade is an attribute of particular importance, particularly for HDV control. Using distributed estimation and crowdsourcing the necessary road grade information can be obtained by vehicles in regular operation, instead of through traditional road surveys.

Several studies show that predicting the future vehicle speed and adapting the current speed and engine output to the road ahead can significantly reduce the energy consumption of long haulage transport (Huang, 2010; Hellström et al., 2010; Terwen et al., 2004). The control signal is sensitive to road grade errors, since it is

determined based on an open loop speed prediction over a significant distance. In Chapter 2 we saw that a relative predicted altitude error on the order of 1 m or less is desirable in order to realize the potential savings. The vehicle speed can be seen as an energy buffer, and other energy buffers, such as a hybridized driveline, the pressurized air system, and engine cooling system may be used in similar ways.

In all these applications the future energy needs, and appropriate use of the energy buffer, are largely determined by the future road grade and speed profiles. Commercial providers are beginning to provide maps with road grade data. The cost for an initial map and regular updates can however be high, and the coverage is still limited. Local road grade authorities have some data on road grades, but they are not comprehensive, and it is difficult to combine databases from several regions. This leaves a need for alternative methods of obtaining road grade information. The sensor information available in modern HDVs is sufficient to obtain *rough* estimates of the *current*[1] road grade. To obtain the accurate information on future road grades required by emerging control applications, several things need to be accomplished. Estimates have to be stored in such a way that they can be recalled at the right time, and the accuracy has to be improved. Both these issues have been addressed in the thesis.

As described in Chapter 3, vehicle and road models have been developed, that link the road grade to sensor signals that are generally already available in the control network of HDVs. In Chapter 4 these models are used to design a distributed iterative scheme for creating and improving road grade maps, with three alternative road grade estimator implementations. The estimators use information about gearshifts, vehicle braking and satellite coverage to adjust to varying sensor signal uncertainties and weight the influence of new grade estimates being added to the map.

Based on the experimental results, given in Chapter 5, we can conclude that the combination of in-vehicle signals and GPS receiver derived altitude generates road grade estimates with higher and more consistent accuracy than each of the sensors taken individually. By using location information from the GPS, and storing the estimates in a map, estimates may be recalled ahead of future trips along the same road. If a vehicle is stopped in a location, which has previously been driven past, the road grade can be obtained despite the lack of input for grade estimation at that time.

The experimental results show that best of the proposed estimators generates road grade estimates with an average RMSE of 0.14 % grade for the two test road sections, based on the combination of 5 and 6 experiments respectively for each of the sections. The RMSE for the predicted relative altitude 320 m ahead is 0.47 m and the same error 1 000 m ahead of the vehicle is 1.19 m. Braking, gearshifts, and loss of satellite coverage are handled well, when they occur simultaneously in only some of the included experiments. From the simulation study in Chapter 2 we

[1] Due to the processing involved estimates are really only available for positions visited in the recent past. It is also hard to estimate the grade when standing still.

conclude that this accuracy is sufficient for e.g. predictive HDV speed control.

In the simulations in Chapter 6 the performance when using data from only one vehicle, but many experiments, is similar to that when using different vehicle in every experiments. This indicates that sharing of data between vehicles may not be necessary from an estimation accuracy standpoint. This result is mainly due to the bias compensation provided by the GPS signal. It thus depends on the signal quality of the GPS, and in many practical situations the parameter spread from using many vehicles will likely still be important. To get a definitive answer on the need for multiple vehicles a larger field study would be necessary.

From the simulation study it is clear that convergence of the estimates when using a large number of experiments depends to a large degree on the reference road grade profile. As seen in Chapter 6, the estimated road grade converges to an error close to the differences between multiple reference measurement runs, around 0.1 % RMSE. The proposed estimators have a clear low-pass characteristic, and therefore cannot accurately track a reference signal with too much energy at high frequencies. The definition of what is a high frequency depends on the parametrization of the estimators. Proper parameters should be chosen to cover the road grade signal frequencies relevant to the considered applications.

The distributed nature of two of the proposed road grade estimators make them suitable for use in community powered scenarios, where recorded data are shared between many users. The OSM project has already created a large open database with road information. If this resource is combined with automated data collection, as is described in Chapter 6, that database can be extended with high quality road grade information. The current major map data providers are also moving towards getting more information from their users. Navigation devices that communicate with both vehicle sensors and a central server can use one of the proposed estimators, and send road grade estimates back to the supplier. Therefore the proposed estimation methods can potentially lead to improved both free and commercial road grade maps. The presented work has led to several patents, and the ideas are being implemented in future generation control systems for HDVs.

7.2 Future Work

The performance of the road grade estimator developed in this thesis shows that using data from multiple runs along a road section, as a way of generating accurate road grade estimates based on standard HDV sensors is feasible. The work has also generated new questions, where additional research is proposed.

There are several ways that the current system can be expanded. Additional sensors may be added, as they are introduced in new vehicles. This would potentially increase both the accuracy and the reliability of the system. The basic ideas of the work may also be applied to estimating other attributes than the road grade. Candidate attributes include curve radii and statistics on traffic speed. These attributes are also of interest in many vehicle control applications, and many of the

same motivations as for road grade estimation apply. More refined methods of updating existing map databases based on the estimated attributes also need to be developed.

The proposed road grade estimation methods are currently tailored to, and only evaluated in, highway use. They will likely need some modifications to work well in an urban setting, with much lower average speeds and more prevalent unmodeled behavior in the driveline. There are also a number of details in the grade estimators that can likely be tuned to improve the end results. A closer look at the sensors and how they are modeled may enable their noise characteristics to be estimated and used directly in the KF, in place of the design parameters currently used. This can either be done off-line, to provide better design parameters, or on-line during operation of the estimator. Ideally this would lead to greater confidence that the grade estimator is operating in the best way possible at any given time.

The vehicle parameters used to compute road grade estimates from the sensor readings are currently fixed at their nominal values. The experimental results indicate that the error in the predicted total resistive force at a particular speed and road grade commonly reach 25–35 % of the total force. This error is mainly caused by wind, vehicle parameter errors, and variations in rolling resistance. These factors are often slow-varying compared to the road grade signal, and therefore lead to a bias in the grade estimates. The errors can be detected by comparing the GPS derived estimate to the vehicle model derived one. If adaptation of the model parameters were to be introduced, the estimation performance may be improved. This is particularly true when the GPS coverage disappears, and the bias correction provided by the merging of the sensors is lost.

Since experimental data from only three different vehicles have been available, and the total number of distinct experiments is also limited, no clear results on the distribution of parameter errors over large groups of vehicles are available. The analysis of the convergence over many experiments and evaluation of the map creation system are based on best effort models of these distributions, and it would be interesting to attempt to confirm these through a larger field test.

The final verdict on whether the data quality is good enough will eventually come from the applications where it is to be used. Many applications envisioned today depend on predictions of the future speed, and in these the ability to accurately adapt the vehicle model to current conditions is as important as the accuracy of the road grade information. This ties back to the idea of an adaptive version of the estimator described above. A vehicle using the road grade information to predict the future speed will need to have a good set of parameters describing the present total resistive force. This parameter estimate can in part be obtained based on previous road grade estimates. Using previous grade estimates to adapt model parameters may increase their accuracy, but it is important to also analyze the convergence of an estimator using such identified parameters for its updates.

Abbreviations

ADAS	Advanced driver assistance systems
CAN	Controller area network
CEP	Circle error probable
DGPS	Differential GPS
DOP	Dilution of precision
EKF	Extended Kalman filter
GDF	Geographic data files
GPS	Global positioning system
HDV	Heavy duty vehicle
INS	Inertial navigation system
ITS	Intelligent transportation systems
KF	Kalman filter
LIDAR	Light detection and ranging
OSM	OpenStreetMap
RMS	Root mean square
RMSE	Root mean square error
RTS	Rauch-Tung-Striebel
SLAM	Simultaneous localization and mapping
SRTM	Shuttle radar topography mission
WGN	White Gaussian noise

Bibliography

AASHTO. *AASHTO Green Book - A Policy on Geometric Design of Highways and Streets*. American Association of State Highway and Transportation Officials, 4th edition edition (2001).

ActMAP. Actmap final report. ActMAP delivereable to EC (2005). URL `http://www.ertico.com/assets/actmap/117v10-D12-ActMAP-final%20report.pdf`. Accessed: November 15, 2010.

J. Akerman. *Cartographies of travel and navigation*. The Kenneth Nebenzahl, Jr., lectures in the history of cartography. University of Chicago Press (2006). URL `http://books.google.co.uk/books?id=4S-UaFxGVL8C`.

A. Alam. *Optimally Fuel Efficient Speed Adaptation*. Master's thesis, Royal Institute of Technology (KTH) (2008).

A. Alam, J. Andersson, and P. Sahlholm. *Fastställande av accelerationsbeteende [Determination of acceleration behavior]*. Swedish patent SE 533 144 C2 (filed 2008*a*).

A. Alam, J. Andersson, and P. Sahlholm. *Metod, system och datorprogram för automatisk hastighetsreglering av ett motorfordon [Method, system and computer program product for automated vehicle speed control]*. Swedish patant SE 531 922 C2 (filed 2008*b*).

A. Alam, J. Andersson, and P. Sahlholm. *Determination of acceleration behaviour*. World patent WO 2010 062242 (filed 2009*a*).

A. Alam and P. Sahlholm. A method for determining an economical speed for heavy vehicles. In *15th World Congress on ITS*. New York, NY, USA (2008).

A. Alam and P. Sahlholm. *Metod och system för reglering av ett fordons hastighet i en kurva [Method and system for vehicle curve speed control]*. Swedish patent SE 533 044 C2 (filed 2008).

A. Alam, P. Sahlholm, and J. Andersson. *Method, system and computer program product for automated vehicle speed control*. World patent WO 2009 096882 (filed 2009*b*).

D. Allerton. *Principles of Flight Simulation*. Aerospace Series. John Wiley & Sons, LTD, Chichester (2009).

A. Aminpour and M. Reiner. *Method for determining the gradient of a roadway*. U.S. Patent # 5,797,109 (filed 1995).

N. Andersson. *Skapande av karta för fordonsreglering med framförhållning [Map creation for look-ahead vehicle control]*. Master's thesis, Royal Institute of Technology (KTH) (2011). In preparation.

M. Back. *Prädiktive Antriebsregelung zum energieoptimalen Betrieb von Hybridfahrzeugen*. Ph.D. thesis, Unversität Karlsruhe (TH) (2005).

H. Bae, J. Ryu, and J. Gerdes. Road grade and vehicle parameter estimation for longitudinal control using GPS. In *Proceedings of IEEE Conference on Intelligent Transportation Systems*. San Francisco, CA, USA (2001).

M. Barrett. The making of navteq maps: Onboard with the survey team. http://www.pocketgpsworld.com/making-navteq-maps-a1038.php (2008). Accessed: March 2, 2011.

J. Bassho, M. Hoemer, U. Kiencke, and T. Matsunaga. Estimation of elevation difference based on vehicle's inertial sensors. In *16th IFAC World Congress*. Prague, Czech Republic (2005).

R. Brüntrup, S. Edelkamp, S. Jabbar, and B. Scholz. Incremental map generation with GPS traces. In *Proceedings of IEEE Intelligent Transportation Systems*. Vienna, Austria (2005).

A. Carlsson, H.-C. Reuss, and G. Baumann. Implementation of a self-learning route memory for forward-looking driving. *SAE International Journal of Passenger Cars - Electronic and Electrical Systems*, 1(1): 62–70 (April 2009). URL `http://saepcelec.saejournals.org/content/1/1/62.abstract`.

R. Casino. *Method and system for obtaining road grade data*. U.S. Patent # 6,847,887 (filed 2003).

W.-K. Ching and M. K. Ng. *Markov Chains: Models, Algorithms and Applications*. International Series in Operations Research & Management Science. Springer Verlag, Berlin (2005).

EC. Galileo: signature of major contract leading to initial services in 2014. EC press release IP/10/1382 (2010). URL `http://europa.eu/rapid/pressReleasesAction.do?reference=IP/10/1382&format=HTML&aged=0&language=EN&guiLanguage=en`. Accessed: November 3, 2010.

eCoMove. Project presentation and fact sheet. eCoMove delivereable to EC (2010). URL http://www.ecomove-project.eu/assets/Documents/Deliverables/100714-DEL-D1.2-ProjectPresentationfactsheetweb.pdf. Accessed: November 3, 2010.

A. El-Rabbany. *Introduction to GPS : the global positioning system*. Artech House, Boston, 2. ed. edition (2006).

ERTICO. Its can help improve our daily lives (2010). URL http://www.ertico.com/about-ertico-its/index.html. Accessed: March 16, 2011.

H. Fathy, D. Kang, and J. Stein. Online vehicle mass estimation using recursive least squares and supervisory data extraction. In *Proceedings of American Control Conference*. Seattle, WA, USA (2008).

FeedMAP. Final feedmap specification. FeedMAP delivereable to EC (2008). URL http://www.ertico.com/assets/download/feedmap/fm111v10d33_feedmap_specification_final_457122[1].pdf. Accessed: November 25, 2010.

R. L. French. Automobile navigation in the past, present and future. In *International Symposium on Computer-Assisted Cartography*, 542–551 (1987).

A. Fröberg. *Efficient Simulation and Optimal Control for Vehicle Propulsion*. Ph.D. thesis, Linköpings universitet (2008).

E. G. Gaeke. *Road Grade Sensor*. U.S. Patent #3,752,251 (filed 1971).

J. Gonder. Route-based control of hybrid electric vehicles. In *SAE World Congress & Exhibition, April 2008*. Detroit, MI, USA (2008). 2008-01-1315.

M. Gramann, R. Helldörfer, J. Leuteritz, A. Stecher, and B. Töpfer. *Travel path inclination evaluation system for vehicle*. German patent DE4308128 (filed 1993).

F. Gustafsson. *Statistical sensor fusion*. Studentlitteratur (2010).

N. Gustafsson. *The Use of Positioning Systems for Look-Ahead Control in Vehicles*. Master's thesis, Linköpings tekniska högskola (2006).

L. Guzzella. Automobiles of the future and the role of automatic control in those systems. *Annual Reviews in Control*, 33(1): 1 – 10 (2009). URL http://www.sciencedirect.com/science/article/B6V0H-4W2V4PB-1/2/319a32f25797177faa17e156a76b8f4e.

S. Han and C. Rizos. Road slope information from GPS-derived trajectory data. *Journal of Surveying Engineering*, 125(2): 59–68 (1999).

C. Hatger and C. Brenner. Extraction of road geometry parameters from laser scanning and existing databases. In *International Archives of the Photogrammetry, Remote Sensing and Spatial Information Sciences XXXIV(Pt. 3/W13)*. International Society for Photogrammetry and Remote Sensing (2003).

E. Hellström. *Look-ahead Control of Heavy Vehicles*. Ph.D. thesis, Linköpings universitet (2010).

E. Hellström, J. Åslund, and L. Nielsen. Design of an efficient algorithm for fuel-optimal look-ahead control. *Control Engineering Practice*, 18(11): 1318 – 1327 (2010). Special Issue on Automotive Control Applications, 2008 IFAC World Congress.

W. Huang. *Design and Evaluation of a 3D Road Geometry Based Heavy Truck Fuel Optimization System*. Ph.D. thesis, Auburn University (2010).

S. Ichikawa, Y. Yokoi, S. Doki, S. Okuma, T. Naitou, T. Shiimado, and N. Miki. Novel energy management system for hybrid electric vehicles utilizing car navigation over a commuting route. In *Intelligent Vehicles Symposium, 2004 IEEE*, 161–166 (2004).

Intermap. 3d roads: Accurate road data for enhancing automotive applications | intermap (2011). URL `http://www.intermap.com/3D-Roads`. Accessed: March 1, 2011.

ISO 11898-1:2003. *Road vehicles – Controller area network (CAN) – Part 1: Data link layer and physical signalling*. ISO, Geneva, Switzerland (2003).

L. Johannesson. On energy management strategies for hybrid electric vehicles. Licentiate thesis, Chalmers tekniska högskola (2006). Series: R - Department of Signals and Systems, Chalmers University of Technology, no: R022.

L. Johannesson and B. Egardt. A novel algorithm for predictive control of parallel hybrid powertrains based on dynamic programming. In *Fifth IFAC Symposium on Advances in Automotive Control*. Monterey Coast, CA, USA (2007).

K. Johansson. *Road slope estimation with standard truck sensors*. Master's thesis, Royal Institute of Technology (KTH) (2005).

H. Kawasaki. *Apparatus and method for judging road surface gradients, and program for judging gradients*. European patent EP1271098 (filed 2002).

E. Keogh, S. Chu, D. Hart, and M. Pazzani. *Segmenting Time Series: A Survey and Novel Approach*, chapter 1, 1–21. World Scientific (2004).

U. Kiencke and L. Nielsen. *Automotive Control Systems*. Springer Verlag, Berlin (2003).

S. Kim, K. Koh, S. Boyd, and D. Gorinevsky. l_1 Trend Filtering. *SIAM Review*, 51(2): 339–360 (2009).

J. Lauffenburger, B. Bradai, A. Herbin, and M. Basset. Navigation as a virtual sensor for enhanced lighting preview control. In *IEEE Intelligent Vehicles Symposium* (2007).

D. Lemire. A better alternative to piecewise linear time series segmentation. In *SIAM Data Mining 2007* (2007).

P. Lingman and B. Schmidtbauer. Road slope and vehicle mass estimation using Kalman filtering. In *Proceedings of the 17th IAVSD Symposium*. Copenhagen, Denmark (2001).

J. Löwenau, S. Durekovic, B. Thomas, and H. Otto. The actmap to feddmap framework automatic detection and incremental updating for advanced in-vehicle applications. In *Proceedings of the 10th International Conference on AATT*. Athens, Greece (2008).

J. Löwenau, K. Gresser, D. Wisselmann, W. Richter, D. Raber, and S. Durekovic. *Advanced Microsystems for Automotive Applications 2006*, chapter Dynamic Pass Prediction - A New Driver Assistance System for Superior and Safe Overtaking, 67–77. Springer-Verlag, Berlin, Germany (2006).

J. Löwenau, P. Venhovens, and J. Bernasch. Advanced vehicle navigation applied in the BMW real time light simulation. *The Journal of Navigation*, 53: 30–41 (2000).

Y. Masumoto. *Global Positioning System*. U.S. Patent # 5,210,540 (filed 1992).

P. McBurney and P. Braisted. *Use of an altitude sensor to augment availability of GPS location fixes*. U.S. Patent # 6,055,477 (filed 1997).

M. McIntyre, T. Ghotikar, A. Vahidi, X. Song, and D. Dawson. A Two-Stage Lyapunov-Based Estimator for Estimation of Vehicle Mass and Road Grade. *Vehicular Technology, IEEE Transactions on*, 58(7): 3177–3185 (2009).

P. Misra and P. Enge. *Global positioning system : signals, measurements and performance*. Ganga-Jamuna Press, Lincoln, Mass., 2. ed. edition (2006).

NAVTEQ Press Release. *NAVTEQ Announces Industry Strategy for Map- Enhanced Advanced Driver Assistance Systems*. NAVTEQ, 425 West Randolph Street, Chicago, Illinois 60606, USA (2008). URL `http://press.navteq.com/index.php?s=4260&item=5097`. Accessed: March 16, 2011.

O. Nelles. *Method and device for determining the mass of a vehicle and road ascent by a recursive state estimation algorithm*. World patent WO 03/023334 (filed 2002).

NextMAP. Final report. NextMAP delivereable to EC (2002). URL `http://www.ertico.com/assets/download/nextmap/2_D1.zip`. Accessed: November 25, 2010.

U. Noyer, H. Mosebach, S. Karrenberg, H. Philipps, J. Rataj, and A. Bartels. Modeling freeways for digital high precision maps. In *FISITA World Automotive Congress*. Munich, Germany (2008).

G. O. Ogonda. *Recovery of the geometric road design elements using low-cost sensors: a feasibility study*. Ph.D. thesis, Universität Stuttgart (2009).

H. Ohnishi, J. Ishii, M. Kayano., and H. Katayama. A study on road slope estimation for automatic transmission control. *JSAE Review*, 21: 322–327 (2000).

OmniSTAR. About OmniSTAR worldwide DGPS service (2011). URL `http://www.omnistar.com/about.html`. Accessed: March 4, 2011.

OpenCycleMap. Opencyclemap (2010). URL `http://www.opencyclemap.org`. Accessed: November 25, 2010.

OpenStreetMap. Openstreetmap (2010). URL `http://www.openstreetmap.org`. Accessed: November 25, 2010.

OpenStreetMap Altitude. De:altitude - openstreetmap wiki (2011). URL `http://wiki.openstreetmap.org/wiki/DE:Altitude`. Accessed: March 4, 2011.

OpenStreetMap License. Openstreetmap, copyright and license (2010). URL `http://www.openstreetmap.org/copyright`. Accessed: November 25, 2010.

OpenStreetMap tag watch. Openstreetmap, tagwatch europe (2010). URL `http://tagwatch.stoecker.eu/Europe/En/index.html`. Accessed: November 12, 2010.

Oxford Technical Solutions Limited. *User Manual; Covers RT2000, RT3000 and RT4000 products*. Oxford Technical Solutions Limited, 77 Heyford Park, Upper Heyford, Oxfordshire, OX25 5HD, England (2010). URL `http://www.oxts.co.uk/downloads/rtman.pdf`. Accessed: March 16, 2011.

N. Pettersson and K. Johansson. Modelling and control of auxiliary loads in heavy vehicles. *International Journal of Control*, 79(5): 479 – 95 (2006).

Racelogic Limited. *VBOX III 100 Hz GPS Data Logger User Guide*. Racelogic Limited, Unit 10, Swan Business Centre, Osier Way, Buckingham MK18 1TB, United Kingdom (2009). URL `http://www.racelogic.co.uk/_downloads/vbox/Manuals/Data_Loggers/RLVB3_Manual\%20-\%20English.pdf`. Accessed: March 16, 2011.

H. Rauch, F. Tung, and C. Striebel. Maximum likelihood estimates of linear dynamic systems. *AIAA Journal*, 3(8): 1445 – 1450 (1965).

C. Ress, D. Balzer, A. Bracht, S. Durekovic, and J. Löwenau. Adasis protocol for advanced in-vehicle applications. In *15th World Congress on Intelligent Transport Systems*. New York, NY, USA (2008).

ROSATTE. Deliverable d1.1 state of the art (2008). URL `http://www.ertico.com/assets/pdf/DELRSTD11State-of-the-Artv1.0.pdf`. Accessed: November 3, 2010.

Saab Press Release. *World First from Saab: Saab IQon - Open Innovation in Car Infotainment*. Saab Automobile AB, 461 80, Trollhättan, Sweden (2011). URL `http://media.saab.com/press-releases/2011-03-01/world-first-saab-saab-iqon-open-innovation-car-infotainment`. Accessed: March 1, 2011.

P. Sahlholm. Improved heavy duty vehicle performance through the use of 3d map data. In *15th World Congress on Intelligent Transport Systems*. New York, NY, USA (2008).

P. Sahlholm, A. Gattami, and K. H. Johansson. Piecewise linear road grade estimation. In *SAE 2011 World Congress, accepted for publication*. Detroit, MI, USA (2011).

P. Sahlholm, H. Jansson, and K. H. Johansson. Road grade estimation results using sensor and data fusion. In *14th World Congress on Intelligent Transport Systems*. Beijing, China (2007*a*).

P. Sahlholm, H. Jansson, and K. H. Johansson. Road grade estimation for look-ahead vehicle control. In *17th IFAC World Congress*. Seoul, Korea (2008).

P. Sahlholm, H. Jansson, and E. Kozica. *Metod och anordning för estimering av lutningen för ett underlag på vilket ett fordon färdas [Method and system for esimating the inclination of a surface on which a vehicle is driving]*. Swedish patent SE 530 728 C2 (filed 2006). Revoked: Sep 2, 2010.

P. Sahlholm, H. Jansson, E. Kozica, and K. H. Johansson. A sensor and data fusion algorithm for road grade estimation. In *Fifth IFAC Symposium on Advances in Automotive Control*. Monterey Coast, CA, USA (2007*b*).

P. Sahlholm and K. H. Johansson. Road grade estimation for look-ahead vehicle control using multiple measurement runs. *Control Engineering Practice*, 18(11): 1328 – 1341 (2010*a*). Special Issue on Automotive Control Applications, 2008 IFAC World Congress.

P. Sahlholm and K. H. Johansson. Segmented road grade estimation for fuel efficient heavy duty vehicles. In *49th Conference on Decision and Control*. Atlanta, GA, USA (2010*b*).

F. Salmasi. Control strategies for hybrid electric vehicles: Evolution, classification, comparison, and future trends. *Vehicular Technology, IEEE Transactions on*, 56(5): 2393–2404 (2007).

S. Schroedl, K. Wagstaff, S. Rogers, P. Langley, and C. Wilson. Mining GPS traces for map refinement. *Data Mining and Knowledge Discovery*, 9: 59–87 (2004).

M. L. Sena. Final report, solvi - safe operation for large vehicles initiative. Technical report, Intelligent Vehicle Safety Systems Project (2008). Report # AL80 A 2008:73473.

J. Slettengren, H. Jansson, and P. Sahlholm. *Förfarande och anordning för att stödja en reglerstrategi för framförandet av ett fordon [Method and device for supporting a regulating strategy for the driving of a vehicle]*. Swedish patent SE 531 835 C2 (filed 2007).

J. Slettengren, H. Jansson, and P. Sahlholm. *Method and device for supporting a regulating strategy for the driving of a vehicle*. World patent WO 2009 072965 (filed 2008).

P. Ståhl. *Performance analysis of a road grade estimation method by means of simulation*. Master's thesis, Royal Institute of Technology (KTH) (2011). In preparation.

D. Sung. Openstreetmap - crowd sourced cartography set to re-map the world (2009). URL `http://www.pocket-lint.com/news/26612/osm-openstreetmap-interview-steve-coast\#ixzz1Bf1NQoNz`. Accessed: March 24, 2011.

T. Suzuki and T. Kanada. Measurement of vehicle motion and orientation using optical flow. In *International Conference on Intelligent Transportation Systems*, 25 –30 (1999).

Swedish Road Authorities. *Vägars och gators utformning, VGU [Road and street design]*. Vägverket, Sektion Utformning av vägar och gator, Vägverket, Butiken, SE-781 87 Borlänge, Sweden, 2004:80 edition (2004).

S. Terwen, M. Back, and V. Krebs. Predictive powertrain control for heavy duty trucks. In *Proceedings of IFAC Symposium on Advances in Automotive Control*. Salerno, Italy (2004).

K. Tin Leung, J. F. Whidborne, D. Purdy, and A. Dunoyer. A review of ground vehicle dynamic state estimations utilising GPS/INS. *Vehicle System Dynamics: International Journal of Vehicle Mechanics and Mobility*, iFirst: 1–30 (2010). URL `http://dx.doi.org/10.1080/00423110903406649`. First published on: 10 June 2010.

A. Vahidi, M. Druzhinina, A. Stefanopoulou, and H. Peng. Simultaneous mass and time-varying grade estimation for heavy-duty vehicles. In *American Control Conference*. Denver, CO, USA (2003).

A. Vahidi, A. Stefanopolou, and H. Peng. Recursive least squares with forgetting for online estimation of vehicle mass and road grade: Theory and experiments. *Journal of Vehicle System Dynamics*, 43: 31–57 (2005).

Vector Informatik. *Hardware Interfaces for CAN and LIN*. Vector Informatik GmbH, Ingersheimer Str. 24, D-70499 Stuttgart, Germany (2010). URL `http://www.vector-worldwide.com/portal/medien/cmc/datasheets/CAN_LIN_Interfaces_DataSheet_EN.pdf`. Accessed: March 16, 2011.

R. Vidal, Y. Ma, and S. Sastry. Generalized principal component analysis (GPCA). *IEEE Transactions on Pattern Analysis and Machine Intelligence*, 1945–1959 (2005).

K. Wänglund. *Evaluation of GPS Velocity and Altitude Data used for Road Grade Estimation*. Master's thesis, Royal Institute of Technology (KTH) (2009).

K. Wänglund and P. Sahlholm. Comparison of road grade estimation results based on GPS position and velocity data. In *16th World Congress on ITS*. Stockholm, Sweden (2009).

J. W. Weingarten, G. Gruener, and R. Siegwart. Probabilistic plane fitting in 3D and an application to robotic mapping. In *IEEE International Conference on Robotics and Automation*, volume 1, 927–932 Vol.1 (2004).

Wikipedia. Wikipedia wikiprojekt georeferenzierung/osm-gadget — wikipedia, the free encyclopedia (2010*a*). URL `http://de.wikipedia.org/wiki/Wikipedia:WikiProjekt_Georeferenzierung/OSM-Gadget`. Accessed: November 12, 2010.

Wikipedia. Wikipedia:wikiprojekt georeferenzierung/wikipedia-world — wikipedia, the free encyclopedia (2010*b*). URL `http://de.wikipedia.org/wiki/Wikipedia:WikiProjekt_Georeferenzierung/Wikipedia-World`. Accessed: November 12, 2010.

World Health Organization. The global burden of disease: 2004 update. Geneva (2008). URL `http://www.who.int/entity/healthinfo/global_burden_disease/GBD_report_2004update_full.pdf`. Accessed: November 3, 2010.

N. Yamada and T. Ishiguro. *Vehicle state estimation method and vehicular auxiliary brake control apparatus using the method*. U.S. Patent # 6,249,735 (filed 1999).

K. Zhang and H. Frey. Road grade estimation for on-road vehicle emission modeling using LIDAR data. In *Annual Meeting of the Air & Waste Management Association*. Minneapolis, MN, USA (2005).

Y. Zhao. *Vehicle Location and Navigation Systems*. The Artech House ITS Series. Artech House, Norwood, MA, U.S.A. (1997).

"*Författarnas lättnad överträffas nog bara av läsarens när vi nu förklarar denna lärobok i matematik för avslutad.*"

A. Persson and L.-C. Böiers, Analys i en variabel, 1990.

TRITA-EE 2011:008
ISSN 1653-5146
ISBN 978-91-7415-869-4